An Energy Based Formalism for State Estimation and Motion Control

Islam S. M. Khalil

Submitted to the Graduate School of Engineering and Natural Sciences
in partial fulfillment
of the requirements for the degree of
Doctor of Philosophy

Sabanci University

July, 2011

An Energy Based Formalism for State Estimation and Motion Control

Islam S. M. Khalil

APPROVED BY

Prof. Dr. Asif Sabanovic (Thesis Supervisor)	.....
Prof. Dr. Metin Gokasan	.....
Assoc. Prof. Dr. Kemalettin Erbatur	.....
Assoc. Prof. Dr. Mustafa Unel	.....
Assist. Prof. Dr. Hakan Erdogan	.....

DATE OF APPROVAL: **27 - 07 - 2011**

To my Mom Samia who gave me the means

and my Father

An Energy Based Formalism for State Estimation and Motion Control

Islam S. M. Khalil

Mechatronics Engineering, Ph.D. Thesis, 2011
Thesis Advisor: Prof. Asif Sabanovic

Key Words: Energy based formalism, *effort*-based state observer, systems with inaccessible state variables, motion control

Abstract

This work presents an *energy* based state estimation formalism for a class of dynamical systems with inaccessible/unknown outputs and systems at which sensor utilization is costly, impractical or measurements can not be taken. The physical interactions among most of the dynamical subsystems represented mathematically in terms of Dirac structures allow power exchange through the power ports of these subsystems. Power exchange is conceptually considered as information exchange among the dynamical subsystems and further utilized to develop a natural feedback-like information from a class of dynamical systems with inaccessible/unknown outputs. The feedback-like information is utilized in realizing state observers for this class of dynamical systems. Necessary and sufficient conditions for observability are studied. In addition, estimation error asymptotic convergence stability of the proposed *energy* based state variable observer is proved for systems with linear and nonlinear dynamics. Robustness of the asymptotic convergence stability is analyzed over a range of parameter deviations, model uncertainties and unknown initial conditions. The proposed *energy* based state estimation formalism allows realization of the motion and force control from measurements taken from a single subsystem within the entire dynamical system. This in turn allows measurements to be taken from this single subsystem, whereas the rest of the dynamical system is kept free from measurements. Experiments are conducted on dynamical systems with single input and multiple inaccessible outputs in order to verify the validity of the proposed *energy* based state estimation and control formalism.

An Energy Based Formalism for State Estimation and Motion Control

Islam S. M. Khalil

Mechatronics Engineering, Ph.D. Thesis, 2011
Thesis Advisor: Prof. Asif Sabanovic

Key Words: Energy based formalism, *effort*-based state observer, systems with inaccessible state variables, motion control

Ozet

Bu çalismada; ulasilamayan/bilinmeyen çikislara sahip olan, algilayici kullaniminin maliyetli veya elverissiz oldugu, ya da üzerinde ölçüm yapilmasi mümkün olmayan dinamik sistemler sinifi için bir enerji tabanli durum kestirim formalizmi sunulmaktadir. Dinamik alt sistemler arasindaki fiziksel etkilesimlerin matematiksel olarak dirac yapilari ile temsil edilmesi sayesinde bu alt sistemler arasindaki güç degisimlerinin güç portlari üzerinden gerçeklesmesi saglanmistir. Söz konusu güç degisimi kavramsal olarak dinamik alt sistemler arasindaki bilgi degisimi olarak düsünülmekte ve ulasilamayan/bilinmeyen çiktilara sahip olan dinamik sistemler için dogal bir geribesleme-benzeri bilgi olarak gelistirilmektedir. Geribesleme-benzeri bilgi, bu sinif dinamik sistemler için durum gözlemleyicilerinin gerçeklenmesi amaciyla kullanilmaktadir. Gözlemlenebilirlik için gerekli ve yeterli sartlar incelenmektedir. Ayrica, önerilen enerji tabanli durum degisken gözlemleyicisinin kestirim hatasinin asimtotik yakinsaklik kararliligi dogrusal olan ve dogrusal olmayan dinamiklere sahip sistemler üzerinde ispatlanmaktadir. Asimtotik yakinsaklik kararliliginin gürbüzlügü, bir takim parametre sapmalari, model belirsizlikleri ve bilinmeyen baslangiç kosullari karsisinda analiz edilmektedir. Önerilen enerji tabanli durum kestirimi formalizmi, bir dinamik sistem içerisindeki alt sistemlerden sadece biri üzerinden alinan ölçümler ile tüm sistem üzerinde hareket ve kuvvet kontrolü yapilmasini saglamaktadir. Böylece ölçümler sadece söz konusu alt sistem üzerinden yapilmakta ve dinamik sistemin geri kalan bölümleri her türlü ölçümden muaf kalabilmektedir. Önerilen enerji tabanli durum kestirimi formalizminin geçerliliginin dogrulanmasi amaciyla tek girisli ve ulasilamayan çikislara sahip çok çikisli dinamik sistemler üzerinde deneyler gerçeklestirilmistir.

Acknowledgments

I would like to express my deep and sincere gratitude to the faculty members of the school of Mechanical Engineering of Helwan University for allowing me the opportunity to commence my PhD at Sabanci University.

I am deeply grateful to Professor Sherif Wasfi, Former Dean of the Faculty of Engineering, Helwan University for his sincere support during my Ph.D. application. I have furthermore to thank Prof. Dr. Radwan A. Hassan, Prof. Abu Bakr Ibrahim, Prof. Dr. Abdelhay M. Abdelhay, Prof. Dr. Osama Mouneer Dauod and Prof. Dr. Abdelhalim Bassuony. I am grateful to all of them.

Again, I wish to thank Prof. Dr. Abdelhalim Bassuony for directing me toward the field of Mechatronics.

I warmly thanks Assist. Prof. Dr. Volkan Patoglu, for his sincere and friendly help and guidance throughout his courses. It would be fair to say that his guidance and support have been of great value in my research work. He apparently effortlessly supervised many of Sabanci University graduate students, including myself, throughout his courses so that we can conduct research on our own.

I owe my most sincere gratitude to Prof. Dr. Mustafa Unel for his support, constructive criticism, encouragement, excellent advice and detailed review during the preparation of my PhD thesis. He read this entire work and greatly helped with its content, style, and appearance.

I wish to express my sincere thanks to the anonymous reviewers for their valuable and constructive comments and suggestions to improve the quality of this Ph.D. thesis.

Despite the distance, my family was always nearby. My mother has given me her unconditional support, knowing that doing so contributed to my absence these last four years. She was strong enough to let me go easily, to believe in me, and to let slip away all those years during which we could have been closer.

This research was supported in part by grants to Sabanci University, including core funding from the Erasmus Mundus University-Grant number 132878-EM-1-2007-BE-ERA Mundus-ECW and the Yousef Jameel scholarship for the financial support.

Contents

1 Introduction **1**
- 1.1 Problem Statement . . . 2
- 1.2 Literature Review . . . 9
- 1.3 Thesis Outcomes and Contributions . . . 15
- 1.4 Possible Applications . . . 17

2 Interconnections in Dynamical Systems **19**
- 2.1 Modeling and Dirac Structure Representation . . . 19
  - 2.1.1 Basic definitions and properties . . . 19
  - 2.1.2 Energy storage elements . . . 22
  - 2.1.3 Energy dissipation elements . . . 24
  - 2.1.4 Energy domains . . . 25
- 2.2 Power Exchange . . . 27
  - 2.2.1 Power conserving interconnection . . . 27
  - 2.2.2 Lumped mass spring system example . . . 28
  - 2.2.3 Discussion . . . 29
- 2.3 Underactuated Mechanical Systems . . . 30
  - 2.3.1 Underactuated system example . . . 31

3 Natural Feedback **33**
- 3.1 Effort Feedback-Like Forces . . . 33
  - 3.1.1 Natural feedback (*effort*-force) modeling . . . 36
  - 3.1.2 Effort-force (disturbance) observer . . . 36
  - 3.1.3 Observer robustness and performance tradeoffs . . . 38
  - 3.1.4 Effort-force observer implementation . . . 39
  - 3.1.5 Results . . . 42
- 3.2 System Decoupled Representation . . . 44
  - 3.2.1 Summary and discussion . . . 46

4 State Observer for Systems with Inaccessible Outputs **48**
- 4.1 Effort based State Observer . . . 48
  - 4.1.1 Convergence stability . . . 49
  - 4.1.2 Mass-spring system example . . . 53
  - 4.1.3 Robustness analysis . . . 56
  - 4.1.4 Observer again adjustment procedure . . . 58
  - 4.1.5 Results . . . 60
  - 4.1.6 Summary and discussion . . . 63
- 4.2 Effort Based Observer for Non-linear Systems . . . 63
  - 4.2.1 Observer for Quasi-nonlinear system with linear *effort* mapping 65
  - 4.2.2 Single-link robot manipulator example . . . 67

4.2.3 Observer for Quasi-nonlinear system with nonlinear *effort* mapping . . . 71
4.2.4 Cart-pendulum example . . . 72
4.2.5 Generality of the energy based state observer formalism . . . 74
4.2.6 Summary and discussion . . . 76
4.3 Hybrid State Observers . . . 76
4.3.1 Overview . . . 76
4.3.2 Observer structure . . . 77
4.4 Effort based Observer Possible Implementations . . . 78
4.4.1 Overview . . . 78
4.4.2 Luenberger state observer . . . 78
4.4.3 High gain state observer . . . 79
4.4.4 Sliding mode state observer . . . 80
4.4.5 Summary and discussion . . . 80

5 Motion Control of Systems with Inaccessible Outputs 81
5.1 Effort Observer based Motion Control . . . 81
5.1.1 Stability margins . . . 85
5.1.2 Summary and discussion . . . 87
5.2 Effort Observer based Optimal Motion Control . . . 88
5.2.1 Set-point optimal control . . . 88
5.2.2 Tracking optimal control . . . 90
5.2.3 Results . . . 92
5.2.4 Summary and discussion . . . 95

6 Effort Force Observer based Force Control 98
6.1 Force Control and Contact Stability . . . 98
6.1.1 Modeling of force sensing . . . 98
6.1.2 Force servoing . . . 99
6.1.3 Reaction force observer based force servoing . . . 101
6.1.4 Discussion . . . 103
6.2 Effort Based Force Observer . . . 104
6.2.1 Stability and performance analysis . . . 104
6.2.2 Results . . . 108
6.2.3 Summary and discussion . . . 111

7 Effort Observer based Control of Distributed Systems 113
7.1 Optimal Model Reduction in The Hankel Norm . . . 113
7.1.1 Euler-Bernoulli beam . . . 113
7.1.2 Hankel norm approximation . . . 115
7.2 Effort based Optimal Control . . . 117
7.2.1 Effort based state observer . . . 117
7.3 Effort based control . . . 121
7.3.1 Summary and discussion . . . 123

8 Conclusion **125**

A Experimental Procedures **134**
A.1 Effort Force Estimation 134
A.2 State Estimation Experimental Setup 135

B Decoupled State Space Representation **137**
B.1 Dynamical System with 2 Degrees of Freedom 137
B.2 Dynamical System with 3 Degrees of Freedom 138

Bibliography **141**

List of Figures

1.1 Sensor associated problems. . . . 3
1.2 Root locus of system with/without force sensor ($k_e = 0 \longrightarrow 300$). . . 5
1.3 Sensor associated problems. . . . 6
1.4 Energy based state estimation formalism possible applications. . . . 9

2.1 System network representation. . . . 20
2.2 Energy storage element. . . . 22
2.3 Energy storage element interconnection. . . . 23
2.4 Energy transfer between the mass-spring. . . . 26
2.5 Dynamical system with 2 degrees of freedom. . . . 29
2.6 Block diagram representation of the dynamical system with 2 DOF. 30
2.7 Underactuated dynamical system with coupled masses via flexible and rigid links. . . . 31

3.1 Block diagram representation of the dynamical system with 3 DOF. 34
3.2 *Flow* and *effort* pairs along the dynamical system power ports. . . . 34
3.3 Block diagram representation of the dynamical system with 3 DOF. 36
3.4 *Effort*-force observer. . . . 37
3.5 *Effort*-force observer. . . . 38
3.6 Equivalent block diagram representation of the force observer. . . . 38
3.7 Observer performance stability tradeoff. . . . 40
3.8 Estimated disturbance force. . . . 42
3.9 Estimated feedback-like *effort*-force. . . . 43
3.10 *Effort*-force observer sensitivity. . . . 44

4.1 *Effort* based state observer. . . . 52
4.2 States estimation results of a dynamical subsystem with 3-Dof through measurements taken from its single input. . . . 55
4.3 States estimation results of a dynamical subsystem with 3-Dof under parameter uncertainties (25% deviation of viscous damping coefficient and masses - 50% deviation of stiffness). . . . 57
4.4 Nyquist diagrams of the input and estimation error output mappings. 59
4.5 Bode plots of the input and estimation error output mappings. . . . 60
4.6 Impulse response of the input and estimation error output mappings. 61
4.7 Estimated versus actual state variables experimental results in the absence and presence of parameter deviations from the actual ones. . 62
4.8 Estimated versus actual state variables experimental results using the *effort*-based state observer. . . . 64
4.9 Experimental result of the state estimation through the *effort*-based state observer. . . . 65

4.10 State estimation results. 68
4.11 State estimation results in the presence of different initial conditions $\Delta x_3(0) = 0.5\ rad$ and $\Delta x_4(0) = 0.1\ rad/s$. 69
4.12 State estimation results in the presence of different initial conditions $\Delta x_3(0) = -0.5\ rad$ and $\Delta x_4(0) = 0.5\ rad/s$. 70
4.13 State estimation results in the presence of different initial conditions $\Delta x_3(0) = 18\ deg$ and $\Delta x_4(0) = 3\ deg/s$. 73
4.14 State estimation results in the presence of different initial conditions $\Delta x_3(0) = 45\ deg$ and $\Delta x_4(0) = -9\ deg/s$. 74

5.1 *Effort*-based state observer based control system. 83
5.2 Experimental setup consists of a microsystems with multiple degree of freedom dynamical system. 84
5.3 Sensor based motion control versus *effort*-based state observer based motion control results to a 300 μm reference input experimental result. 85
5.4 Stability margins of the sensor versus *effort*-based control system for controlling the first non-collocated mass. 86
5.5 Stability margins of the sensor versus *effort*-based control system for controlling the second non-collocated mass. 87
5.6 Stability margins of the sensor versus *effort*-based control system for controlling the second non-collocated mass. 88
5.7 *Effort* state observer based optimal set point tracking for a dynamical subsystem with state variables that are not available for measurements (dashed-line). 90
5.8 Experimental results of optimal states regulation of a dynamical system with 3-dof (Optimal set point tracking and regulation of the third non-collocated mass to a reference position). 91
5.9 *Effort* state observer based optimal trajectory tracking for a dynamical subsystem with state variables that are not available for measurements (dashed-line). 92
5.10 Experimental setup consists of a single input attached via an energy storage element with a three degrees of freedom flexible system. . . . 93
5.11 Experimental results of optimal states regulation of a dynamical system with 3-dof (Optimal regulation of the second non-collocated mass to a reference position). 95
5.12 Experimental results of optimal states regulation of a dynamical system with 3-dof (Optimal regulation of the second non-collocated mass to a reference position). 96
5.13 Experimental results of optimal states regulation of a dynamical system with 3-dof (Optimal regulation of the second non-collocated mass to a reference position). 96
5.14 Experimental results of optimal states regulation of a dynamical system with 3-dof (Optimal regulation of the second non-collocated mass to a reference position). 97

5.15 Experimental results of optimal states regulation of a dynamical system with 3-*dof* (Optimal regulation of the first non-collocated mass to a reference position). 97

6.1 Force sensor model indicating the non-collocation added via force sensor to the end-effector 99
6.2 root locus of system with and without force sensor for $k_e = 0 \longrightarrow 300$ 100
6.3 Robot in contact with environment with force sensing and force servoing control system 101
6.4 root locus of system with force servoing 101
6.5 Force servoing control system using reaction force observer 102
6.6 Interaction force estimation experimental setup to investigate the sensitivity of the force observer in the presence of measurement noise . . 103
6.7 Signal to noise ration of the estimated interaction forces 104
6.8 *effort*-based force observer and force servoing control system 105
6.9 Frequency response of the *effort*-based force observer force control versus sensor based force control 106
6.10 Frequency response of the *effort*-based force observer force control versus sensor based force control 107
6.11 *effort*-based force observer experimental setup 108
6.12 Nyquist stability for the *effort*-based force control versus the force sensor based control for constrained *effort*-force observer gains showing larger stability margins for the sensor based force control system 109
6.13 *effort*-based force observer experimental results 110
6.14 *effort*-based force observer experimental results 111

7.1 Frequency response of the original high order system Σ with 22-state variables 117
7.2 Hankel singular values of the high order model Σ. 117
7.3 Optimal truncated model versus original system frequency response. 118
7.4 *Effort*-force based state observer for the optimal truncated model Σ_k. 119
7.5 Estimated state variables through the *effort*-based state observer versus the actual state variables simulation results. 120
7.6 Estimated state variables versus actual one. 121
7.7 Regulated versus non regulated flexible beam impulse responses. . . 122
7.8 *effort*-based optimal control result. 123
7.9 Regulated state variables. 124

A.1 *Effort*-force based state observer experiment on a micro system workstation. 135
A.2 State estimation experimental setup. 136

B.1 Dynamical system with 2 degrees of freedom. 138
B.2 Block diagram representation of the dynamical system with 3 DOF. 139

List of Tables

3.1 *effort* observer transfer functions 39

4.1 Experimental and simulation parameters 54
4.2 Simulation parameters 75

5.1 Experimental parameters 95

6.1 Experimental and simulation parameters 110

7.1 Simulation parameters 119

A.1 Experimental parameters 136

Chapter 1

Introduction

THE recent research efforts in the design of mechatronics systems have been partially devoted to the problem of how to have sensors embedded to these systems and how to overcome their associated problems. Mechanically, mechatronics systems have to be designed and manufactured such that several sensors criterions are met such as accuracy, alignment and including enough space for sensors with their associated electronic setups and complex wirings. From a control viewpoint on the other hand, sensors utilization requires considering many aspects such as their limited bandwidth, measurements noise, uncertainties, hysteresis and non-collocation problems. Therefore, it would be natural to devise observers to estimate dynamical system state variables. However, the current state observers require having measurements to be used as basis of the estimation process that in turn necessitates having at least few sensors embedded within these systems. The sensors associated problems limits the usefulness of many state variables estimation and control frameworks due to several aspects including, but not limited to, their noisy outputs, their limited bandwidth due to their physical structure and the complexity they add to the control system. It would be fair to say that, effectiveness and usefulness of state variable observers and controllers have been evaluated by their capability to handle the previously mentioned sensors associated problems. Many attempts have been proposed to overcome these problems, but few were proposed to provide a comprehensive solution for sensor problems through exploring alternatives to the undesirable, possibly unavailable, measurements. This motivates carrying out an irregular attempt by conceptually considering the control and the state variables estimation problem of a dynamical subsystem with state variables that are not available for measurements. Such conceptual consideration allows not only avoiding the problem of inaccessibility of the outputs and state variables, but also solving the numerous sensor related problems as the dynamical subsystem are assumed to have state variables that are not accessible for measurements. It follows immediately that the state estimation and the consequent control system cannot be realized due to the absence of information from these dynamical subsystems. However, the *energy* based formalism which is commonly agreed to be a very powerful tool in modeling and controlling a wide class of dynamical nonlinear systems [Ortega 2001], can be utilized to provide a comprehensive alternative in designing state variables observers for these class of dynamical subsystems with state variables and outputs which are not available for measurements. The interconnection and the power exchange between these dynamical subsystems can be utilized in the realization of natural feedback-like signals [O'Connor 2007a] which can be used as basis in designing state

variables observers and controllers for these class of dynamical subsystems. This work is concerned with utilizing the *energy* based formalism in realizing a natural feedback from these class of dynamical subsystems in terms of power exchange along the interconnection power ports of these subsystems. The work is further concerned with investigating whether it is possible to acquire such natural feedback-like signals from a dynamical subsystem in the complete absence of its state variables and outputs, then how to utilize such signal as basis in estimating state variables observers and control systems.

1.1 Problem Statement

Considerable attention has been given in the last few decades to the control problem of systems with inaccessible/unknown outputs, e.g., microsystems and micromanipulation operations are classes of systems at which sensors utilization is costly or even measurements can not be taken. Pushing, pulling and many other operations form the backbone of any micromanipulation operation. The workspace at which these operations are performed is of few millimeters or even less. However, measurements are required to be taken from this limited workspace that in turn requires utilization of sensors to obtain proper feedbacks to the control system. First, one has to think about how to have these sensors embedded to each end-effector during the design stage which represents quite an engineering problem as these sensors have to fit into a very limited workspace. Second, one has to consider the numerous problems associated with each embedded sensor within the system including, but not limited to, sensor limited bandwidth, measurement uncertainties, sensor noise and the complicated electronic setups. In addition, the additional cost due to sensor utilization increases the cost of any mechatronics system tremendously. Therefore, different control frameworks have to be developed for dynamical systems with inaccessible/unknown outputs and operations such as micro-manipulation and micro-assembly at which measurements are costly or even impractical. These applications require realization of the motion, vibration and force control in the absence of system outputs.

A question naturally arises: Can we estimate and control dynamical system states when neither of its outputs are measured or when these dynamical systems are required to be free from any attached sensors to overcome their associated problems or even when it is impractical to make measurements due to limited workspace constraints ?

It is important to note that success to reduce the number of attached sensors to a certain dynamical system is of great importance due to the numerous drawbacks associated with sensor utilization such as:

- Measurements noise:

The effect of sensor noise on the performance of a typical feedback control system is depicted in Fig. 1.1 where $C(s)$ and G(s) are the controller and plant transfer

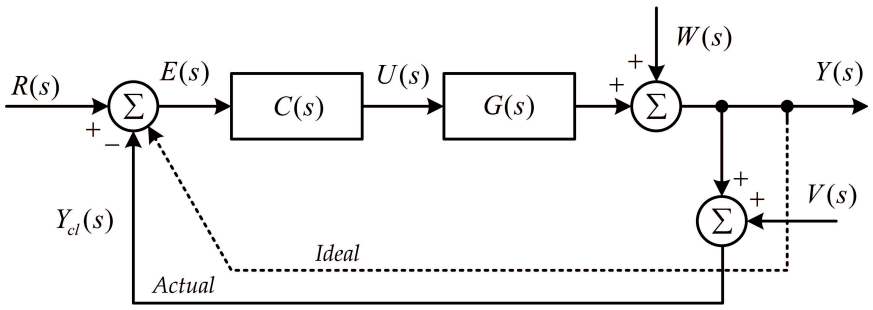

Figure 1.1: Sensor associated problems.

functions, respectively. $R(s)$, $U(s)$, $Y(s)$, $Y_{cl}(s)$, $W(s)$ and $V(s)$ are the reference input, control input, closed loop output, sensor output, disturbance input on the output and measurement noise, respectively. The output is related to the sensor noise input with the following relation,

$$Y_{cl}(s) = \frac{C(s)G(s)}{1+C(s)G(s)}R(s) + \frac{1}{1+C(s)G(s)}W(s) - \frac{C(s)G(s)}{1+C(s)G(s)}V(s) \tag{1.1}$$

the equation of error $E(s)$

$$E(s) = R(s) - Y_{cl}(s) \tag{1.2}$$

$$\begin{aligned} E(s) &= R(s) - \left[\frac{C(s)G(s)}{1+C(s)G(s)}R(s) + \frac{1}{1+C(s)G(s)}W(s) - \frac{C(s)G(s)}{1+C(s)G(s)}V(s)\right] \\ &= \frac{1}{1+C(s)G(s)}R(s) - \frac{1}{1+C(s)G(s)}W(s) + \frac{C(s)G(s)}{1+C(s)G(s)}V(s) \end{aligned}$$

it is clear from the previous equation that sensor noise input and disturbance are related with the error through the following sensitivity and complimentary sensitivity functions

$$\mathcal{S}(s) = \frac{1}{1+C(s)G(s)} = \left.\frac{Y(s)}{W(s)}\right|_{\substack{V(s)=0\\R(s)=0}} = \left.\frac{E(s)}{R(s)}\right|_{\substack{V(s)=0\\W(s)=0}} = -\left.\frac{E(s)}{W(s)}\right|_{\substack{R(s)=0\\V(s)=0}} \tag{1.3}$$

$$\mathcal{T}(s) = \frac{C(s)G(s)}{1+C(s)G(s)} = \left.\frac{Y(s)}{R(s)}\right|_{\substack{V(s)=0\\W(s)=0}} = -\left.\frac{Y(s)}{V(s)}\right|_{\substack{R(s)=0\\W(s)=0}} = \left.\frac{E(s)}{V(s)}\right|_{\substack{R(s)=0\\W(s)=0}} \tag{1.4}$$

therefore,

$$E(s) = \mathcal{S}(s)R(s) - \mathcal{S}(s)W(s) + \mathcal{T}(s)V(s) \tag{1.5}$$

Equation (1.1) along with error equation (1.2) show how sensor noise influence error between the desired input and the measured output $Y_{cl}(s)$. However, due to the sensor noise, the feedback control system depicted in system does not guarantee that the actual system output $Y(s)$ would follow the desired input. The dashed line in Fig. 1.1 represents the output that cannot be ideally fed back due to the

additional sensor noise input. Therefore, it would be natural to devise observers to estimate variables such as positions, velocities and forces rather than using sensors. Indeed, utilization of observers allow reducing the number of attached sensors to the dynamical system, in addition to estimating the inaccessible state variables. However, for a system with inaccessible outputs, all current observers can not be designed as they depend on injecting some of the dynamical system outputs onto the observer structure so as to guarantee convergence of the estimated states to the actual ones.

- Narrow bandwidth problems and frequency separation

Due to the sensor noise problem, most of the measurements especially the force and velocity measurements have to be realized through a low-pass filter. Therefore, the bandwidth of these sensors are limited by the bandwidth of the sensor noise. In addition, in order to obtain satisfactory tracking of the reference signal along with good rejection of the disturbances, we need $\mathcal{S}(s) \approx 0$ and $\mathcal{T}(s) \approx 1$.

These conditions can be satisfied by setting $\mid C(s)G(s) \mid \gg 1$. However, in order to prevent propagation of measurement noise to the error and output signals, we have to set $\mathcal{T}(s) \approx 0$ and $\mathcal{S}(s) \approx 1$. These conditions are only satisfied when $\mid C(s)G(s) \mid \ll 1$. Therefore, in order to achieve the previous objectives, there must be a frequency separation between the reference and disturbance signals on one hand and the measurement noise on the other hand, i.e., if the sensor noise bandwidth is limited with a filter with cut-off frequency ω_c, $\mid C(j\omega)G(j\omega) \mid$ has to satisfy the following constrains,

$$\mid C(j\omega)G(j\omega) \mid \gg 1 \; \forall \; \omega < \omega_c \; , \quad \mid C(j\omega)G(j\omega) \mid \ll 1 \; \forall \; \omega > \omega_c \tag{1.6}$$

- Complexity and non-collocation

It is commonly agreed that utilization of certain sensors adds an extra degree of freedom to the control system. Without any loss of generality, force sensor adds an extra degree of freedom to the control system due to its soft structure, i.e., an energy storage element and possibly energy dissipation element will exist between the actuated degree of freedom and the end-effector in contact with the environment. In order to illustrate the non-collocation problem associated with force sensor utilization, we consider a robot with single degree of freedom in contact with an environment with stiffness k_e. In order to impose the desired force on the environment, the interaction force between the end-effector and the environment has to be sensed by means of force sensor which in turn adds an extra degree of freedom to the control system. Fig. 1.2 illustrates the effect of this extra degree of freedom on the root locus of this simple force control system for different values of environmental stiffness. The extra degree of freedom shapes the root locus of the system such that the system is unstable for certain environmental stiffness as shown in Fig. 1.2-b that is not the case for the collocated control system shown in Fig. 1.2-a.

Generally, force sensors are replaced with force observers. This however requires velocity (*flow*) measurement in order to realize the force observer. For the dynamical

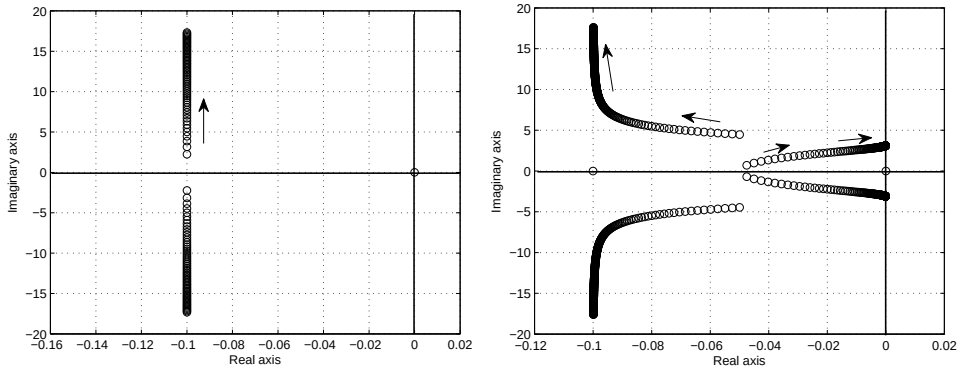

(a) collocated system (b) non-collocated system

Figure 1.2: Root locus of system with/without force sensor ($k_e = 0 \longrightarrow 300$).

system we consider in this work, velocity or *flow* information might be inaccessible or cannot be measured. Therefore, realization of the force observers and force control for this class of dynamical systems is considered in this work in the absence of force sensing and velocity or *flow* information.

- Instability

The previous sensor and measurement related problems might cause instability, e.g., due to the limited bandwidth of force sensors due to their physical structures, stable force control can be realized within a certain frequency range out of which the control system can be oscillatory and possibly unstable. Increasing this bandwidth can be achieved if the force sensor is replaced with the well-known force observer which depends on measuring the velocity (*flow* variable) of the interacting degree of freedom with the environment. This measurement, however limits the bandwidth of the force control with the *flow* variable sensor bandwidth.

- Complex electronics setup and their associated wirings

Each embedded sensor to the control system has its own electronics and associated wirings that in turn add more complexity to the overall mechatronics system.

Fig. 1.3 illustrates the previous sensor and measurement associated problems. This motivates exploring control systems which do not depend on measurements taken from dynamical systems but rather depend on some natural feedback-like signals that are going to be studied and further explored in the next sections. In the sequel, it is assumed that the dynamical system has $(n - r)$ state variables that are not available for measurement, where n and r are the dimensions of the dynamical system and dimension of the active degrees of freedom representing a subsystem from which state variables can be measured. By assuming that the $(n - r)$ are inaccessible state variables, the control system have to be realized in the absence of physical measurements. Therefore, success to realize the control system

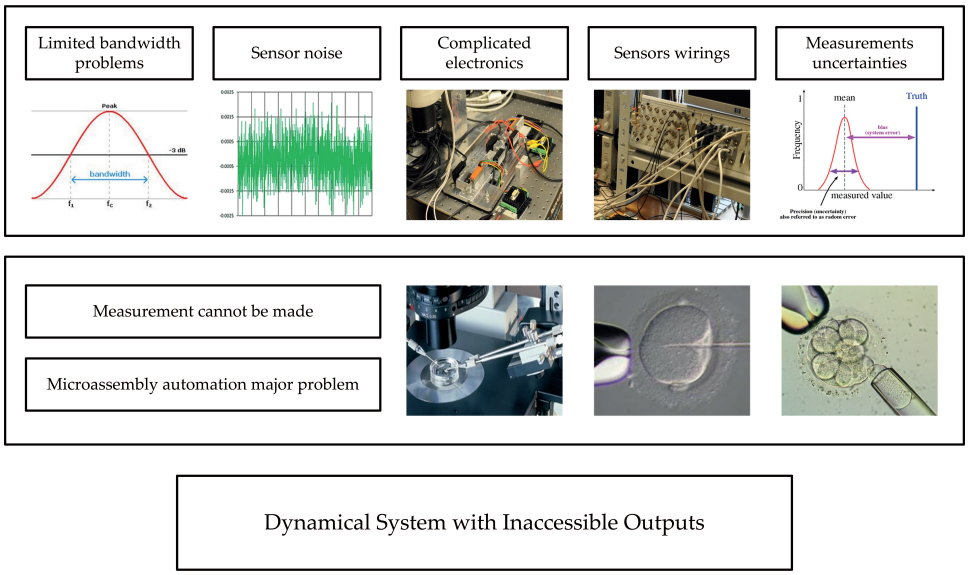

Figure 1.3: Sensor associated problems.

in the absence of these measurements allows avoiding the sensor related problems mentioned previously.

This work is concerned with developing and analyzing an *energy* based state estimation formalism along with a control framework that allows controlling motion, residual vibration and forces of a class of dynamical system with inaccessible/unknown outputs. Neither of the dynamical systems (excluding the active degrees of freedom) are accessible, model is uncertain, parameters are inaccurate and the initial conditions are not known. The previous assumptions are equivalent to keeping the dynamical system free from any attached sensors along with considering the unmodeled dynamics and parameter deviations.

At first sight, realization of the motion, vibration and force control for systems with inaccessible outputs seems impossible since one has to sense or measure some variables and use them as basis for any estimation process. If we further considered the real life problems, e.g., parameter deviations, model uncertainties and the inaccurate initial conditions, realization of the motion control for these class of dynamical system would be unrealistic. Therefore, system measurements or outputs have to be replaced with some other variables that can be used as basis for the estimation processes. The goal of this work is to study and present a control framework that enables realization of the motion control in the absence of system measurements and in the presence of parameter deviations, model inaccuracies and unknown initial conditions.

Based on the *energy* based formalism, the proposed state estimation and control framework allows realization of motion, vibration and force control for dynamical systems through measurements taken from their actuators, whereas, dynamical plants are kept free from any measurement which in turn implies that these plants

can be kept free from any attached sensors while estimating and controlling their dynamical states. In addition, the proposed *energy* based formalism presents a unique way of combining two very important criterions, namely robustness and sensorless control. The first has to be achieved in order to guarantee that control system is less sensitive to parameter variations, model uncertainties and external disturbances while the second allows eliminating all the previously mentioned drawbacks associated with sensors utilization.

The sensorless control problem of non-collocated end-effectors or points of interest along a flexible systems with inaccessible unknown outputs is addressed in this work. Flexibility, non-collocation and unavailability of system outputs make realization of the motion, vibration or the force control nearly impossible. However, it is commonly believed that dynamical systems are excited by means of at least one actuator. Availability of actuator variables enables realization of feedback-like signals in terms of power or information exchange along the *power ports* of the interconnected subsystems which build up any complex dynamical system. Strictly speaking, the *energy* based formalism allows studying complex linear and nonlinear systems by decomposing them into simpler subsystems that, upon interconnection, add up their energies to determine the full system's behavior. In this decomposition, there might exist dynamical subsystems with inaccessible state variables or outputs in interconnection with other subsystems. The *energy* based formalism allows realizing an information exchange between these subsystems regardless to the availability of their state variables and outputs for measurements. Therefore, the interconnection of a dynamical subsystem with inaccessible outputs allows realizing a natural feedback from another subsystem in terms of *flow* or *effort* variables. The nature of these variables can be specified upon the nature of the power exchange along the power ports of the interconnected subsystems. Therefore, the *energy* based formalism allows realizing a natural feedback from dynamical subsystem with inaccessible state variables or outputs providing that some *power-conserving* interconnection exist between these subsystems.

It would be natural to split the dynamics of the entire system into two subsystem, the first has state variables that are available for measurement while the second has inaccessible state variables or outputs. In the sequel, the first system is considered as the actuator or the active degrees of freedom subsystem while the second can be any subsystem with linear, nonlinear, lumped or distributed dynamics. In addition, the claim that a dynamical subsystem has inaccessible state variables is equivalent to an attempt to avoid utilization of sensors so as to avoid their associated problems and complexities. The state variables of the first subsystem has to be sufficient in realizing the incident natural feedback *effort* or *flow* variables from the second subsystem with inaccessible state variables. Then these natural feedback *effort* or *flow* variables have to be sufficient to perform regular procedures on the second subsystem with inaccessible state variables such as parameter identification, state variables estimation, motion control, active vibration suppression and force control.

Utilization of the *energy* based formalism allows using actuators as single platforms for measurement and control where the whole dynamical system is split into

two portions; actuator and plant sides. Actuator variables are available, whereas plant outputs are inaccessible. Actuator variables can be used to realize the incident feedback-like *effort* or *flow* variables due to the power exchange along the power ports of the interacting subsystems. In the absence of plant outputs, these feedback-like variables can be considered as the only available information from the plant.

Generally, control input consists of two portions. The first is an excitation control input while the second is an additional control input to suppress disturbances that assists in the attainment of robust acceleration control. Therefore, one can say without any doubt that in any event a dynamical system will be excited and the incident disturbances have to be realized then suppressed for the sake of robustness attainment. Based on the *energy* based formalism, the excitation or the interconnection means that the subsystem that imposes the excitation can impose either *flow* or *effort* variables, regardless to their nature that can be specified upon the nature of the exchanged power. The subsystem that imposes the excitation can only impose either of the power variables not both. In addition, the imposed output excitation of any of the power variables is instantaneously followed by a received input variable that belong to the dual space of the imposed output excitation variable. Therefore, whenever a subsystem with accessible state variables interacts with another subsystem with state variables that are not available for measurements, the latter would impose power variables that can be either *effort* or *flow* variables on the first subsystem.

Figure 1.4 illustrates a set of well-known dynamical systems from which measurements have to be determined in order to realize their control systems. In order to stabilize the inverted pendulum depicted in Fig. 1.4, the angular position and/or velocity of the pendulum have to be measured. However, unavailability of these measurements makes it hard to realize the control law for such system. The delta robot depicted in Fig. 1.4 consists of three kinematical chains, the combination of the constrained motion of these three chains ensures a resulting translatory degrees-of-freedom for the robot tool base. However, there exist six passive angular position and six angular velocities that have to determined in the realization of the motion control law. It is commonly believed that these angles can be obtained through the active angles of the robot by iteratively solving a set of non-linear algebraic equations representing the robot's holonomic constrains. The real-time implementation of the controller doesn't recommend the iterative solution of these equation. In addition, it is not recommended to embed a velocity or position sensor with each joint. Therefore, the delta robot depicted in Fig. 1.4 can be considered as a dynamical system with inaccessible outputs.

The flexible robot arm depicted in Fig. 1.4 was extensively studied over the last few decades. The non-minimum phase property along with the insufficient measurements and actuation are some of the challenges for the control system design of such system. Generally, a measurement can be taken from a non-collocated point and used in the realization of the control law. However, this procedure depends on the accuracy of the kinematical map that is not only complicated but also inaccurate.

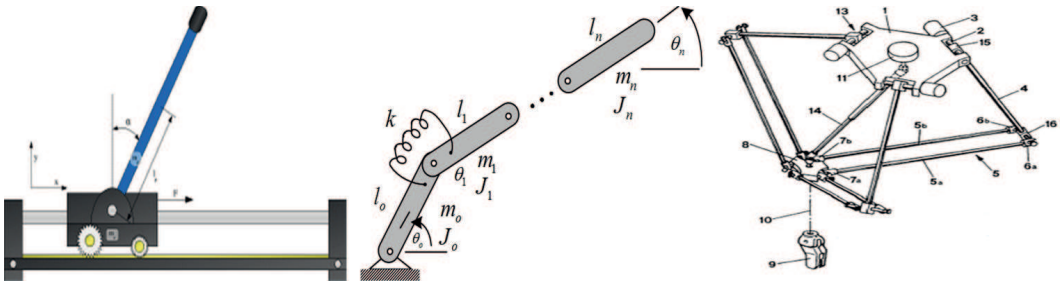

Figure 1.4: Energy based state estimation formalism possible applications.

Therefore, outputs of the flexible robot arm are considered inaccessible.

Non-linearity, non-minimum phase property, end-effector position non-collocation with the input, flexibility, model uncertainties, parameter deviations, existence of external disturbances along with the inaccessibility of system outputs are considered during the realization of the motion, vibration and force control of dynamical systems such as the ones depicted in Fig. 1.4.

1.2 Literature Review

Observer design for dynamical systems has been a long standing challenging problem in the field of motion control and system dynamics. A typical design procedure is to inject the measured states onto the observer structure so as to enforce the estimation error dynamics to be stable. Therefore, design of state observers requires the presence of at least few dynamical system states to be used as the basis of the estimation process. In other control system applications, such as the optimal control problem for a linear dynamical system with a quadratic objective function, feedback of every state variable is required that in turn restricts the usefulness of optimal control. The previous restriction motivated many authors in the last few decades to investigate the validity of realizing the optimal control when system states are inaccessible. In [Liou 1972], the authors proposed to differentiate the the optimal control law a number of times to obtain an equivalent control law based on those state variables which are measurable. In addition, it was shown that through suitable transformations, the optimal control law can be obtained in terms of the output alone. However, in the complete absence of system outputs and state variables, the previous method can not be used in the realization of the optimal control law. The high-gain observer presented by Khalil and Esfandiari shows excellent robustness properties for large enough observer gains [Esfandiari 1992, Ball 2008]. The practical difficulty is, however, the determination of proper observer gain due to the trade-off between the desired bounds on the observer error and the sensitivity to noise. An adaptation scheme was presented in [Bullinger 1997], for adjustment of the high-gain observer gain such that its advantages are retained. The trade-off between speed of state reconstruction and the immunity to measurements noise is studied in [Ahrens 2009],

and a method is proposed by switching the high-gain matrix between two values, high gain during the transient to quickly recover the state reconstruction, then once a steady state error threshold has reached, the observer gain is switched to another gain to reduce the effect of measurement noise.

The well-known Luenberger observer provides a comprehensive solution for the estimation problem where system states can be observed along with the disturbances which can be considered as state variables providing that dynamical system model is known a priori, inputs are known and outputs are accessible [Luenberger 1971, Luenberger 1964]. The Luenberger observer is a very useful tool for estimating the internal variables of the system, the main challenge is, however, the complete dependance of the mathematical model accuracy. Based on the sliding mode approach, robustness over a range of system uncertainties was enhanced by the sliding mode observer presented by Utkin in [Utkin 1992]. A key feature in the Utkin observer is the introduction of the well-known switching function in the observer to achieve a sliding mode and stable error dynamics. This switching function is claimed to result is an excellent system performance, i.e., disturbance rejection and insensitivity to parameter variations. In [Darouach 2000, Aldeen 1999], a sliding mode functional observer is introduced, including the same switching function so as to inherit the benefits of robustness and insensitivity of the conventional sliding mode observer. The sliding mode functional observer, in addition, has a lower order that is the characteristic of functional observers. Authors in [Rundell 1996], utilized sliding mode observer to estimate derivative of measured signals in the presence of unmatched disturbances by filtering discontinuities approximations of the derivatives. A non-linear extended state observer was proposed by Han [Han 1995], where the non-linear model is treated as extended state. Moreover, the non-linear model along with its derivative are assumed unknowns. Trajectory tracking controller for robots with flexible joints was presented in [Talole 2010], based on feedback linearization, an extended state observer showing robustness in the presence of model uncertainties.

The concept of functional observability and detectability was introduced in [Fernando 2010], that ascertains the ability to estimate a given linear function of the state vector using dynamical observer. Zhang proposed a functional observer for singular systems in the polynomial fraction form that requires no prerequisite impulsive mode elimination [Zhang 1990]. Necessary and sufficient conditions for the existence of disturbance decoupled functional observers for linear time-invariant systems were studied in [Hou 1999, Murdoch 1974]. A non-linear state observer was proposed by Thau and further extended by Kuo [Hou 1999]. Necessary and sufficient conditions under which nonlinear system can be transformed into an observable canonical form have been investigates in [Krener 1985, Xiao 1989]. These methods, however, do not include a systematic procedure for the construction of the observer and the gains adjustment that satisfies the sufficient conditions of the estimation error asymptotic stability. Thau's well-known inequality which relates the Lipschitz nonlinearity constant with the minimum and maximum eigenvalues of the arbitrary matrices of the error dynamics inequality, can be used in the design and selection of the observer gain vector [Thau 1973]. However, Thau's method is not straight-

forward and can be violated. Therefore, it can serve as a check after the selection of the observer gain. Another attempt was made by Raghavan [Raghavan 1994] to formulate condition for stabilizing the error dynamics, the condition however fails for some observable pairs (A, C). Similarly, a condition was proposed by Zak in [Zak 1990], which relates the singular values of the matrix $(A - LC)$ with the Lipschitz nonlinearity constant through an inequality which have to be satisfied by the observer gain vector L. Necessary and sufficient conditions for stability of the nonlinear estimation error dynamics for Lipschitz nonlinear system were proven by Rajamani [Rajamani 1998, Rajamani 1995a]. In most of these approaches, a typical procedure is to classify the nonlinearities according to the role they play in the derivative of a certain Lyapunov function candidate that is very tied up with the particular selection of the Lyapunov function, which, stemming from the linear inheritance, is systematically taken to be a quadratic function in the estimation error.

The well-known Luenberger observer can be extended to estimate disturbance signals when disturbances are treated as state variables. Therefore, the disturbance observer [Kobayashi 2007, Murakami 1993b] can be considered as a special class of the Luenberger observer. In general, disturbance observers are used for the attainment of robust acceleration control by identifying and suppressing the total mechanical load and parameter variation [Murakami 1993a, Ohnishi 1994, Ohnishi 1996]. Hori and Umeno proposed a disturbance observer with a Butterworth Q filter based on the parameterization of two degree of freedom controllers [Umeno 1991]. Adaptive robust control makes the closed-loop system robust to plant model uncertainties with better tracking performance and transient in the presence of discontinuous disturbances such as coulomb friction [Yao 1997, Yi 1999]. Model based disturbance attenuation is used to attenuate load variations and frictional forces in [Choi 1999].

The observers described above either focused on state variables observation or disturbance estimation. Few schemes, however, were developed to simultaneously estimate state variables along with disturbances. State and disturbance estimation scheme was developed in [Stein 1988, Park 1988], by differentiating the output measurement. The method is based on the singular value decomposition concept and are applicable when a rank condition between the output and disturbance matrices is satisfied. Without differentiating the outputs, rank and norm conditions have to be imposed on the unknown inputs in simultaneously estimating dynamical system state variables and disturbances [Tu 1998, Corless 1998].

The previous state observers differ in the sense of their characteristics and drawbacks, non is completely satisfactory under all headings. However, they all have a common feature. These observers depend on measuring the energy *flow* information. In other words, most of the dynamical systems are in physical contact. Energy exchange occurs along the points of interactions or the energy ports of these systems [Macchelli 2003]. The energy exchange means exchanging the *effort* and *flow* information along the energy ports of any *power-conserving* interconnected subsystems. The previously mentioned observers can be categorized as *flow*-based observers as they all depend on injecting the measured *flow* information onto the

observer structure so as to enforce asymptotic stable estimation error dynamics. However, for a class of dynamical system at which measurements cannot be made, such observers cannot be designed. Without any loss of generality, Manianna and Heikki [Savia 2009], pointed out that there exist at least two major problems that makes it difficult to automate the micromanipulation systems, namely, the poor understanding of the interaction phenomena and the difficulty of making measurements at micro scale. Therefore, the previous state observers are hard to be implemented for such applications as measurements cannot be made. In [Rakotondrabe 2009], a 2-DOF (linear and angular) positioning device is introduced based on the stick-slip motion principle, the linear and angular motions delivered to the end-effector are measured by the mean of laser interferometers which add more complicity to the system, require accurate alignments and above all they require enough space for the retroreflectors [Hung 2007, Alici 2005]. Due to the lack of space, Hwee and Bijan utilized capacitive sensors to obtain position measurements from the piezo-actuated four-bar flexure-based mechanism rather than using laser interferometry based sensing system [Liaw 2009].

The previous attempts to embed sensors with sophisticated mechatronics systems is due to the dependence of the state observers and control systems on certain measurements which are necessary for the realization of observers and controllers. To be more precise, realization of control systems and their associated observers depends on measuring the *flow* energy variables. If the power flow along the physical system interconnection or energy port is specified, one can define the nature of the *flow* and *effort* energy variables. In the case of a mass-spring system, without any loss of generality, the energy exchange between the interconnected systems can be described with the force (*effort*) and velocity (*flow*) [Macchelli 2002a, Macchelli 2002b]. Each mass integrates the force (*effort*) in order to determine its speed (*flow*), while the spring integrates the speed to determine the amount of deformation and consequently computes a force that depends on this deformation. In this case, the subsystems of the mass-spring system interact by exchanging the *effort-flow* or the generalized force-velocity information. The state observers presented so far in the literature are *flow*-based, i.e., the *flow* information is measured and injected onto their structures so as to enforce certain asymptotic error dynamics behavior. A question naturally rises, Is it possible to design state observers based on the *effort* information rather than the *flow* information which might be inaccessible. To be more precise, this work attempts to provide a feedback-like signal or a natural feedback from dynamical system with inaccessible outputs.

The natural feedback concept was first introduced by O'Connor [O'Connor 2007a, O'Connor 2007b]. The concept of natural feedback was presented and utilized to control motion and vibration of flexible structures such as lumped robots, robots with flexible arms and gantry cranes. O'Connor considered the mechanical waves that propagates back and forth between an actuator and an end boundary condition as natural feedback signals or feedback-like forces from the flexible system on the actuator. Conceptual consideration of the propagating mechanical waves as natural feedback was utilized to construct a control framework known as the *wave based*

control. The previous controller was utilized to precisely position a non-collocated point to a target position by using the actuator to launch and absorb the mechanical waves which propagate through dynamical flexible systems [O'Connor 2003]. Although the natural feedback was presented and utilized in O'Connor work, it was not fully utilized and measurement is required to be taken from the plant subsystem for the realization of the *wave based control* along with assuming that the actuator subsystem has its own controller [O'Connor 1998]. However, if the dynamical subsystem has inaccessible outputs, the *wave based control* cannot be realized since it requires measuring the position of the first non-collocated mass along the interface plane of the actuator subsystem with the dynamical subsystem. Nevertheless, the *wave based control* introduces the natural feedback concept which can be further investigated in order to provide an alternative for the inaccessible measurements.

It is worth noting that the wave based control idea is quite similar and can be studied under the framework of wave variables and scattering operators. Wave variables and scattering operators were utilized in control theory for the attainment of stable teleoperation systems in the presence of network time delay [Niemeyer 1991]. Changing the basis of the teleoperation system from power variables to wave variables that are independent of the time-delay makes the communication passive or even lossless [Anderson 1989]. On the one hand, Spong and Anderson utilized the wave variables and scattering operators in order to achieve robust stable teleoperation systems under varying transmission time-delay, on the other, O'Connor utilized the wave ideas in order to control motion and suppress residual vibration of dynamical flexible systems through a single measurement from the dynamical sub-plant. Van der Schaft [Cervera 2006] studied the composition of Dirac structures, both in power variables and in wave variables (scattering representation) to formulate equational representation of the composed Dirac structure.

Sensorless motion control was realized in [Khalil 2010a, Khalil 2009b], where the reaction torque signal is conceptually considered as a natural feedback from a flexible system with multi degree of freedom. In addition, system parameters and state variables are identified and estimated, respectively, through this natural feedback used in recursive observers in cascade. However, this recursive observer is model dependent. Therefore, it is sensitive to parameter deviations, unmodeled dynamics and unknown initial conditions due to the unavailability of any induced injected measurement which can enforce asymptotic estimation error stability [Khalil 2009a]. A similar approach was proposed in [Khalil 2009c], to control the interaction forces between a non-collocated end-effector and an environment by estimating the interaction forces through a reaction force observer and a recursive state variables observer. A sensorless motion and vibration control for flexible system was proposed in [Celebi 2010], where a quadratic energy cost function is minimized in order to minimize the energy content of the system during a motion control assignment, through a sensorless optimal control law based on the estimated states obtained using a reaction force and state observers. In [Khalil 2010c], the action reaction law of dynamics is realized at the plane of interface of an actuator subsystem with a dynamical subsystem with three degrees of freedom, then reaction forces are in-

duced in the structure of an action reaction state observer. Injection of the reaction forces guarantees the convergence of the estimates states to the actual ones. In addition, residual vibration control is realized by minimizing an energy-like performance index. In [Khalil 2011], the authors proposed an *effort*-based state observer to overcome the inaccessibility problem of dynamical system states, the *effort* information is estimated from the energy port or the interaction point of a dynamical subsystem with inaccessible state variables and an actuator subsystem. Injecting this estimated *effort* information onto the observer structure, allows enforcing the estimation error dynamics to be asymptotically stable. In addition, necessary and sufficient conditions of observability of dynamical subsystems with inaccessible states were proved. The previous observer can be considered as the first attempt to alter the dependence of all relevant existing observers on the *flow* variable space with the *effort* variable space. It was shown in [Stramigioli 2000, Macchelli 2002a], that the interactions among physical system is in feedback, i.e., interaction of the dynamical subsystems results in an exchange of power which can be represented as a product of the system input and output or the *effort* and *flow*, respectively.

In order to design state observer for dynamical subsystem with inaccessible state variables, the energy exchange along the energy ports of physical systems can be utilized in realizing a natural feedback. This natural feedback can then be used as basis of the state variables estimation process. It is worth noting that, the port-Hamiltonian formalism provides a comprehensive framework for modeling physical systems based on energy concepts, power ports and energy exchange. Much effort has been expanded in the last few decades in modeling and controlling physical system through *energy based methods* [Ortega 2001, Ortega 1999]. Starting from the port-Hamiltonian model, it is possible to identify the energetic properties that have to be controlled in order to achieve a desired interactive behavior and it is possible to build a port-Hamiltonian controller that properly regulates the robotic interface. The port-Hamiltonian formalism allows dealing with complex interactive systems, both linear and nonlinear in a very intuitive way due to its generality. In addition, the port-Hamiltonian formalism can be further utilized in order to provide a tool for designing state observers for a class of dynamical system with inaccessible state variables and outputs. The interactive components of the physical system are in feedback. Therefore, there exist a natural feedback from a dynamical subsystem with inaccessible outputs that can be determined form another subsystem with accessible outputs by making use of the energy exchange along the system energy ports [van der Shaft 2002].

The central idea behind the utilization of the port-Hamiltonian formalism in designing state observers for dynamical subsystems with inaccessible state variables is based on breaking down any complex system into simpler subsystems. The interconnections, namely the exchange of information or energy (*effort* and *flow*), takes place along the system power ports. Therefore, we can conceptually consider the incident information from a subsystem with inaccessible state variable as a natural feedback. This natural feedback will occur whenever physical systems interacts, interaction is nothing but an energy exchange. Therefore, if a dynamical subsystem

has inaccessible state variables, due to its interaction with other subsystems, an energy exchange will occur along the energy ports which in turn results in a natural feedback that can be determined from those subsystems which have accessible state variables.

It can be easily shown that, all of the relevant existing state observers are *flow* based observers. In general, for any physical system, there exist *flow* variables space and its dual space, namely the *effort* variables space [Macchelli 2002a]. Indeed, one cannot specify the nature of the *effort* and *flow* variables spaces unless the power exchange along the energy ports is specified, e.g., the space of currents is the dual space of voltages if the power exchanged through the energy ports is electrical. Similarly, the space of generalized forces is the dual space of the generalized velocities if the power exchange through the energy ports is mechanical [Macchelli 2002b]. The current state observers mentioned in this literature review depends on the availability of the *flow* energy information. For the case at which mechanical power is exchanged through the energy ports of the physical system, the *flow* information is the generalized velocity. Therefore, these observers can be classified as *flow* based observers. Similar to the *energy* based formalism that has been introduced for modeling and control [Ortega 2001], the *energy* based formalism can be extended to state observers. The *energy* based formalism would allow state observers to fall under one of the following categories, *flow* or *effort*-based state observers. All current state observers are *flow*-based, therefore, they require the dynamical system to have accessible state variables or outputs. On the other hand, considering that observers can be designed based on the *effort* variables, allows designing state observer whenever the *flow* variables are not accessible. This will not only allow designing of state observer for dynamical subsystem with inaccessible state variables, but also will allow control systems to overcome the numerous drawbacks and limitations associated with sensor utilization. These limitations and drawbacks are commonly believed to constrain the performance of any control system and motivated many authors to study the several control system tradeoffs.

1.3 Thesis Outcomes and Contributions

One of the fundamental concepts in science and engineering practice is energy, where it is common to model and view dynamical systems as energy transformation devices. The main contribution of this thesis is to extend the *energy* based formalism which has been used in control and modeling to assist designing state observers for dynamical systems with inaccessible state variables. The energy based formalism would result into a classification for state observers, namely *flow* and *effort*-based state observers. The proposed *effort*-based state observer would definitely provide a solution for the control problem of dynamical subsystem with inaccessible state variables. Unlike the current *flow*-based state observer which requires the presence of system outputs or state variables, the *effort*-based state observer dose not require the availability of system outputs, it is rather standing on the idea of energy

exchange between the interacting dynamical subsystem through the system energy ports. The proposed *effort*-based state observer inherits the benefits of the current *flow* state observer, on the one hand. It does not require availability of dynamical system outputs, on the other. Jeffrey and Khalil proposed to switch the observer gain matrix values in order to reduce sensitivity to output measurements noise while achieving fast reconstruction of the estimated states [Ahrens 2009]. A similar idea was also included in [Mayne 1997] by Goodwin. These simple examples along with the previous literature review illustrate how many researchers attempted to solve the tradeoffs between state estimation reconstruction speed and sensitivity to measurements noise. In other words, the proposed *energy* based formalism would allow to increase the gain of certain observer with less sensitivity to measurement noise due to the less dependency on system state variables and outputs measurements. To be more precise, the proposed state variables observer *energy* based formalism allows inheriting the benefits proved by numerous researchers throughout the last decades, along with providing a unique solution for the inaccessible state variables or outputs. In this work, necessary and sufficient conditions for asymptotic stability convergence of the estimation error for the *effort*-based state observer are investigated and proven for a general class of systems with linear and nonlinear dynamics. A hybrid state observer is introduced and the error dynamics is analyzed in order to investigate the contribution of the injected *effort* variables on the overall estimation error dynamics.

Necessary and sufficient conditions for observability of dynamical subsystem with inaccessible outputs and state variables are proven and a correlation between these conditions and the *energy* based formalism is studied. The proposed *energy* based state observer formalism allows enhancing the tradeoffs between robustness, performance and measurements noise sensitivity. This claim was proven experimentally, by applying many control techniques on a dynamical system with multi degrees of freedom and inaccessible state variables and outputs, including optimal control, vibration control, force and impedance control.

Robustness of the proposed *effort*-based state observer to parameter deviations, model uncertainties and unknown initial conditions are investigated. In addition, procedures of the observer gain adjustment are developed in order to facilitate practical implementation of this observer which represents a powerful tool whenever dynamical subsystem states or outputs are inaccessible or cannot be measured or the sensor associated noise and problems are required to be completely avoided.

The author of this thesis believe that one of the most important applications of the proposed *energy* based state observer formalism is microsystems and micromanipulation operations. Automation of such applications is commonly agreed to be blocked by the fact that, measurements cannot be made due to the tiny workspace at which operations have to be conducted. Nevertheless, simulations and experimental results were conducted on dynamical system with finite and infinite dimensions with linear and nonlinear dynamics in order to demonstrate the validity and generality of the proposed *energy* based state estimation formalism in motion control theory.

1.4 Possible Applications

The following applications are believed to be applicable for implementation using the proposed *energy* based state estimation formalism. Experimental results are conducted and included throughout the thesis to verify the validity of the proposed *energy* based state variables estimation formalism in assisting the following applications.

- ***Effort based observers***

The *energy* based formalism allows inheriting most of the useful properties of most of the relevant existing state observer including, but not limited to, sliding mode observer and high-gain observer. These observers have superior performance under a satisfactory range of parameter deviation, model uncertainties and unknown initial conditions, their usefulness however is limited with the sensor noise. Therefore, the proposed *energy* based formalism allows inheriting their useful properties along with avoiding the limitations associated with sensors utilization.

- ***Vibration control***

Usefulness of light structures in control systems is limited with their ever lasting vibration even due to the simplest manoeuvre and the difficulty of making measurements. Although, many works have been proposed in the vibration control literature concerning with the active vibration suppression of light flexible structures, the sensor related problems and the measurement uncertainties are yet, not solved. The *energy* based state estimation formalism, however provides a comprehensive solution for the vibration control problem as it provides estimates of the full observable state variables of a dynamical subsystem required to be actively vibration suppressed.

- ***Force control***

The *energy* based force observer proposed outlined in this work can be used as an alternative to both force sensor and the well-known reaction force observer. Therefore, the energy or the *effort*-based force observer would allow realizing the force control without measuring interaction forces of a robot end-effector with the environment, in addition it does not require measuring the *flow* variable of the degree of freedom that interacts with the environment as in the case of the reaction force observer.

- ***Distributed Systems Control***

The *energy* based state estimation framework can be implemented on systems with distributed dynamics such as flexible robot manipulators and flexible shafts. This requires determination of the optimal reduced order model in the Hankel norm in order to utilize the *energy* based state estimation formalism in estimating the dynamical states of these systems from measurements taken from their active degrees of freedom subsystems.

- ***Optimal control***

The proposed *energy* based state variables estimation framework allows estimating the full observerable state variables of a dynamical subsystem. This in turns allows realizing the optimal linear control system as its usefulness is dependent on the presence of each and every state variable.

- ***Microsystems and Micromanipulation***

The proposed *energy* based state variables estimation formalism can assist in automating microsystems and micromanipulation operations which are commonly agreed to be blocked by two facts, one of which is the limited capabilities of making measurements.

Chapter 2

Interconnections in Dynamical Systems

ENERGY exchange is one of the most fundamental concepts that has been used to view, model and control complex physical systems by decomposing these systems into simpler subsystems. Due to the interconnection between these subsystems which happened to be in feedback, energy exchange in terms of input and output or *flow* and *effort* occurs among the interconnected subsystems through the what's called system energy ports. The purpose of this chapter is to briefly introduce the *energy*-based formalism in modeling and control of dynamical systems so as to extend this formalism to design state observers and sensorless controllers. Naturally, the *energy* based formalism will lead to a natural feedback-like signals which can be used as basis for the design and construction of *energy* based state observers.

2.1 Modeling and Dirac Structure Representation

2.1.1 Basic definitions and properties

A dynamical system is a mathematical entity that describes a particular dynamical relation between a set of input and a set of output signals. Strictly speaking, in order to define a dynamical system it is necessary to specify: a time domain τ, an input manifold υ, a set of admissible input functions υ_f such that $\upsilon : \tau \to \upsilon$, a state manifold χ and an output manifold $\mathcal{Y}$. A continuous-time dynamical system Σ is given by the sets $\tau \equiv \mathbb{R}, \upsilon, \upsilon_f, \chi$ and $\mathcal{Y}$, by a state transition function $f : \chi \times \upsilon \times \tau \to T\chi$, such that

$$\dot{x} = f(x(t), u(t), t) \tag{2.1}$$

which has a unique solution for every initial state $x_0 \in \chi$ and admissible input function $u : \tau \to \upsilon$, $\upsilon \in \upsilon_f$, and by an output function $g : \chi \times \upsilon \times \tau \to \mathcal{Y}$, such that

$$y = g(x(t), u(t), t) \tag{2.2}$$

Now, it makes sense to write a dynamical system representation with as $\Sigma := (\tau, \upsilon, \upsilon_f, \chi, \mathcal{Y}, f, g)$. From the previous definition, a set of dynamical systems $\Sigma_i, i = 1, \ldots, n$ elaborate an information flow received as input and results in another information flow as output, based on the input and the initial states as depicted in Fig. 2.1. These systems are interconnected if the output information flow of one of these systems becomes the input of the other. Consider a simple mass-spring system with mass m, stiffness k and deformation q in the spring.

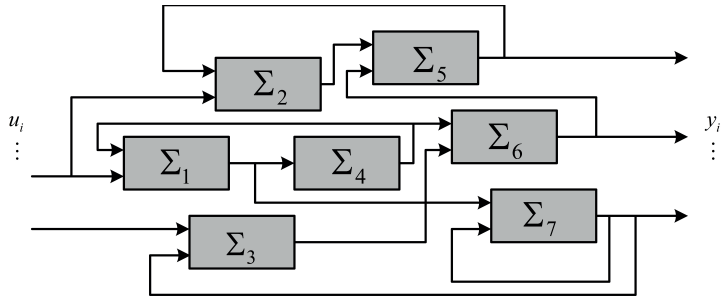

Figure 2.1: System network representation.

According to the previous definitions, the mass-spring system can be represented by two subsystems, namely the mass subsystem Σ_m and the spring subsystem Σ_s. These two systems can be modeled as follows

$$\Sigma_m : \dot{p} = F \quad , \quad y = \frac{p}{m} \quad ; \quad \Sigma_s : \dot{q} = v \quad , \quad y = -kq \tag{2.3}$$

where, p, F, and v are the mass momentum, spring force and mass velocity, respectively. It can be easily shown that the output of spring subsystem is the input to the mass subsystem, similarly the output of the mass subsystem is the input to the spring subsystem. Strictly speaking, the subsystem interconnection is in feedback. The mass integrates the force in order to determine its own velocity, whereas the spring subsystem integrates the velocity in order to determine its own deformation and upon this deformation a force is generated according to (2.3). Therefore, it would be fair to say that the mass-spring subsystems interact by exchanging the generalized force and generalized velocity information.

To be more precise, we consider an n-dimensional linear space $\mathcal{F}$, a linear function on the vector space $\mathcal{F}$ is $e : \mathcal{F} \to \mathbb{R}$. $\varepsilon := \mathcal{F}^*$ is the dual space of the linear space $\mathcal{F}$. The product space $\mathcal{F} \times \varepsilon$ is defined as a space of power variables. For each $f \in \mathcal{F}$ and $e \in \varepsilon$ the power variable can be expressed using the duality product $\mathrm{P} =< e, f >$ [van der Shaft 2002, der Schaft 2002]. In the mass-spring system example, if $\mathcal{F}$ is a space of generalized forces, then its dual space ε is the space of generalized velocities, consequently, the duality product space $< e, f >$ defines the mechanical power exchanged upon the interaction of the two subsystem defined in (2.3). Generally, the velocity variables are called *flows*, whereas the force variables are called *efforts*. For a set of dynamical subsystems in interconnection such as the previous mass-spring system, the *flows* and *efforts* are nothing but the inputs and outputs for each of these dynamical subsystems. The output of the spring subsystem is *effort* or the generalized force which acts as an input to the mass subsystem, the mass subsystem by its turn integrates this force to determine its own *flow* or generalized velocity. The velocity of the mass acts as an input to the spring subsystem, which integrates this velocity to determine its own deformation then the generalized force. A better understanding of the behavior of the mass subsystem and spring subsystem can be obtained by considering the distinction between the energy storage elements and the energy dissipation elements. In the sequel, mass-like elements, spring-like elements

and energy dissipation-like elements are considered as the basic elements which can be used to model the more complex physical systems. Therefore, behavior of each is categorized into energy storage elements and energy dissipation elements, and studied in details in the following subsection of this chapter.

The previous definitions indicate that the mass subsystem behaves in a dual way with respect to the spring subsystem. Input and output of the mass subsystem are the *effort* or generalized force and *flow* or generalized velocity, respectively. Inputs and outputs of the spring subsystem are, however, the *flow* or generalized velocity and *effort* or generalized force, respectively.

It is worth noting that it is not possible to impose both *flow* and *effort* to any given physical system. For the dynamical system we consider so far, it is not possible to impose both force and velocity at a time. Considering the space of power variable ($\mathcal{F} \times \varepsilon$) and the symmetric bilinear form $<<(f_1, e_1), (f_2, e_2)>>:=< e_1, f_2 > + < e_2, f_1 >$, the Dirac structure of $\mathcal{F}$ is a linear subspace $\mathbb{D} \subset \mathcal{F} \times \varepsilon$ such that $\mathbb{D} = \mathbb{D}^{\perp}$. The fact that, $dim(\mathbb{D}) = dim(\mathcal{F})$ indicates that it is not possible for any interconnection to impose both *effort* and *flow* variables. Based on this observation, a natural feedback can be obtained from the interconnected dynamical subsystems. Whenever a dynamical subsystem imposes an *effort* on another subsystem, *flow* will be received by the subsystem which imposed the *effort*. Similarly, due to the duality behavior of the interconnected dynamical subsystem, if the other dynamical subsystem is subjected to an *effort*, it would result in a *flow* as output.

We can conclude that, *information can always be obtained from a dynamical subsystem even if its outputs and state variables are inaccessible, providing that it is interconnected with other dynamical subsystem and efforts or flows are imposed on this dynamical subsystem with inaccessible outputs or state variables.*

- **Definition 2.1 (Natural Feedback)**

Consider a set of dynamical systems $\{\Sigma_i$ where $i = 1, \ldots, n\}$; composed out of subsystems with inaccessible state variables and outputs, and subsystems with accessible state variables. A natural feedback [O'Connor 2007b] can be obtained from the dynamical subsystem with inaccessible state variables and outputs providing that the following conditions are satisfied:

1. The set of dynamical systems are physically interconnected;
2. The interconnection is *power-conserving*;
3. *Effort* or *flow* is imposed by at least one of the dynamical subsystems of the set Σ_i.

The natural feedback can be either *flow* or *effort* information. For the mass-spring system we consider, if one of its subsystems has inaccessible outputs or state variables, an incident natural feedback can be obtained from the other. The state variable of the mass subsystem can be the mass momentum (p), whereas the state

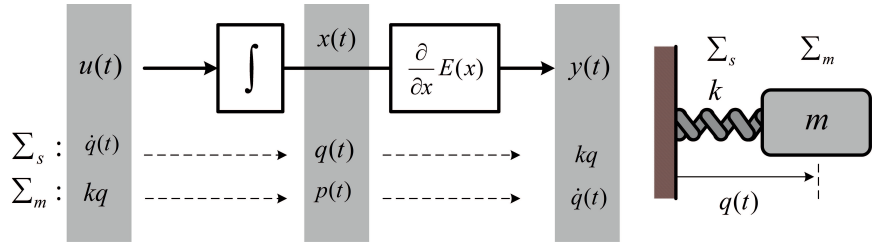

Figure 2.2: Energy storage element.

variable of the spring is the spring deformation (q). Conceptually considering that the state of the mass subsystem is inaccessible, due to the interconnection between these two subsystems, the *flow* (velocity) of the mass is acting as an input to the spring subsystem. Therefore, despite of the fact that state of the mass subsystem is not accessible conceptually, there exist a natural feedback, namely the *flow* information, from the mass subsystem on the spring subsystem. In the next chapters, the idea of natural feedback will be used in order to design *energy* based state observers for dynamical system with inaccessible outputs and state variables.

In order to formulate a comprehensive understanding of the *energy* based formalism that is going to be used extensively in the subsequent sections, the basic elements which can be used in building up any complex physical system are analyzed. Such elements include energy storage elements such as masses, springs, capacitors and inductors, energy dissipation elements such as dampers and resistors.

2.1.2 Energy storage elements

Energy storage elements are characterized with the ability of storing energy within their elastic elements. every energy storage element has to be characterized by: an input $u(t)$, an output signal $y(t)$, a state variable $x(t)$ and a scaler energy function $E(x)$, with the following mathematical representation,

$$\dot{x}(t) = u(t) \quad , \quad y(t) = \frac{\partial}{\partial x} E(x) \tag{2.4}$$

which indicates that an energy storage element has an integral representation as depicted in Fig. 2.2. However, the only distinction between the different energy storage elements is the nature of input and output, i.e., energy storage elements outputs and inputs differ in the sense of being described with *effort* or *flow* variables. Mass is an energy storage element, its state variable is the mass momentum, input is the force and its output is the mass velocity. For the mass element, the *effort* of the spring is the input which is integrated by the mass to provide the momentum, then the output *flow* (velocity) is obtained by differentiating the kinetic energy scaler function with respect to the momentum. The spring, on the other hand, is an energy storage element which has a dual behavior to the mass. Its state variable is the spring deformation, its input is the velocity while its output is force. The spring is subjected to a *flow* input, i.e., velocity. In order to determine the amount

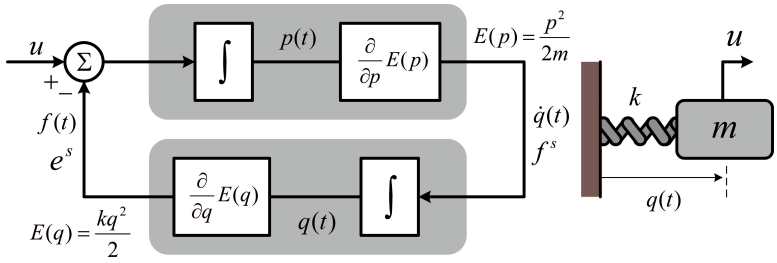

Figure 2.3: Energy storage element interconnection.

of deformation the spring integrates this velocity input (*flow*) and then determine the force output (*effort*) by differentiating the potential energy with respect to the deformation. Fig. 2.2 illustrates the block diagram representation of the mass and spring energy storage elements, whereas the interconnection between the mass and spring energy storage elements is depicted in Fig. 2.3 at which the duality nature of the interconnection is clear. The *effort* which is the output of the spring energy storage element is the input to the mass energy storage element. Similarly, the *flow* which is the output of the mass energy storage element is the input of the spring energy storage element. It should be clear from Fig. 2.3 that the interconnection is in feedback. This will be further used in the realization of a natural feedback from dynamical subsystems with inaccessible state variables and outputs.

To be more precise, the potential energy stored in the spring element can be represented by the Hamiltonian energy function $H^s(q) = \frac{1}{2}kq^2$. Therefore, (2.4) can be expressed as

$$\dot{q} = f^s \quad , \quad e^s = \frac{d}{dq}H^s(q) \tag{2.5}$$

the mass Hamiltonian energy function on the other hand is $H^m(p) = \frac{1}{2m}p^2$. Similarly, (2.4) can be shown as

$$\dot{p} = f^m \quad , \quad e^m = \frac{d}{dp}H^m(p) \tag{2.6}$$

the previous energy storage elements are connected via the following Dirac structure

$$f^s = e^m = y \quad , \quad f^m = -e^s + u \tag{2.7}$$

through the previous Dirac structure, (2.5) and (2.6) can be expressed as

$$\begin{bmatrix} \dot{q} \\ \dot{p} \end{bmatrix} = \begin{bmatrix} 0 & 1 \\ -1 & 0 \end{bmatrix} \begin{bmatrix} \frac{\partial}{\partial q}H(q,p) \\ \frac{\partial}{\partial p}H(q,p) \end{bmatrix} + \begin{bmatrix} 0 \\ 1 \end{bmatrix} u \tag{2.8}$$

$$y = \begin{bmatrix} 0 & 1 \end{bmatrix} \begin{bmatrix} \frac{\partial}{\partial q}H(q,p) \\ \frac{\partial}{\partial p}H(q,p) \end{bmatrix} \tag{2.9}$$

It is worth noting that the previous interacting energy storage elements belong to different energy sub-domains. The mass energy storage element belongs to the

mechanical kinetic sub-domain, whereas the spring energy storage element belongs to the mechanical potential sub-domain. Nevertheless, information exchange occurs upon the interaction defined through the Dirac structure (2.7) regardless to the nature of the energy sub-domains to which the interacting elements belong. In general, energy storage elements falls under two categories, passive and active energy storage elements, the first is discussed in details in this section while the second is equivalent to position feedback controller.

2.1.3 Energy dissipation elements

Energy dissipation elements such as dampers and resistors models the irreversible phenomena of conservation of energy and can be represented by a statical relationship between the *flow* and the *effort* depending on whether the system is admittance or impedance type, i.e., admittance type energy storage elements can be written as $f = Y(e)$, whereas the impedance type energy storage element can be expressed as $e = Z(f)$ providing the $Z(f)f \leq 0$ and $eY(e) \leq 0$ holds, which indicate the dissipative behavior of the energy dissipation elements.

Considering the previous mass-spring system described by (2.8), presence of an energy dissipation element would result in adding another extra energy port to the Dirac structure (2.7). Adding a damper element with viscous damping coefficient c to the mass-spring system with the constitutive relation $e^d = cf^d$ changes the Dirac structure to

$$f^s = e^m = y \quad , \quad f^m = e^s - e^d + u \tag{2.10}$$

the spring-mass-damper system therefore can be shown as

$$\begin{bmatrix} \dot{q} \\ \dot{p} \end{bmatrix} = \left(\begin{bmatrix} 0 & 1 \\ -1 & 0 \end{bmatrix} - \begin{bmatrix} 0 & 0 \\ 0 & c \end{bmatrix} \right) \begin{bmatrix} \frac{\partial}{\partial q} H(q,p) \\ \frac{\partial}{\partial p} H(q,p) \end{bmatrix} + \begin{bmatrix} 0 \\ 1 \end{bmatrix} u \tag{2.11}$$

$$y = \begin{bmatrix} 0 & 1 \end{bmatrix} \begin{bmatrix} \frac{\partial}{\partial q} H(q,p) \\ \frac{\partial}{\partial p} H(q,p) \end{bmatrix} \tag{2.12}$$

(2.8) and (2.11) can be rewritten using the following compact notation

$$\dot{\mathrm{x}} = [J(\mathrm{x}) - R(\mathrm{x})] \frac{\partial}{\partial \mathrm{x}} H + G(\mathrm{x}) u \ , \ y = G(\mathrm{x})^{\mathrm{T}} \frac{\partial}{\partial \mathrm{x}} H \tag{2.13}$$

where $J(\mathrm{x}) \in \mathbb{R}^{2\times 2}$ is the interconnection skew symmetric matrix and $R(\mathrm{x}) \in \mathbb{R}^{2\times 2}$ is the damping matrix. It should be clear from (2.8) and (2.11) that the interconnection matrix is derived upon the definition of the Dirac structures (2.7) and (2.10), respectively. In general, for dynamical system with n-dimension, the interconnection matrix is $J(\mathrm{x}) \in \mathbb{R}^{n\times n}$ encodes all the *power-conserving* interconnections among the energy ports of the system, whereas the damping matrix $R(\mathrm{x}) \in \mathbb{R}^{n\times n}$ encodes all the ports which are terminated with energy dissipative elements.

The previous mass-spring-damper example illustrates the power or information exchange between physical elements from similar energy domain, i.e., the mechanical power, through continuous conversions between the kinetic energy and potential

energy of the mass and spring elements, respectively. Therefore, the Hamiltonian energy function ($H(q,p)$) in (2.8) and (2.11) is the sum of the kinetic and potential energies of the interacting elements. (2.8) and (2.11) illustrates how the *flow* and *effort* variables are getting exchanged in the absence and presence of power dissipation and external input u. Similar to the energy storage elements, dissipation elements fall under two categories, passive dissipative elements and active dissipative elements, the first is discussed in details in this section while the second is equivalent to the velocity feedback controllers. Therefore, these basic (energy storage, dissipation and transformation elements) elements can model both the dynamical system and their controllers.

2.1.4 Energy domains

The energy domain we considered so far is mechanical which consists of mechanical potential and mechanical kinetic energy sub-domains. The mass and spring energy storage elements store kinetic and potential energy, respectively. Rather than the mechanical energy domain, there exists several domains such as the electromagnetic domain which consists of the electrical and magnetic sub-domains, and the hydraulic energy domain which consists of the kinetic and potential energy sub-domains. The mechatronics systems we consider in this work are composed of several physical elements which belong to different energetic domains. Nevertheless, the previous argument is still valid, regardless to the energy domain to which each mechatronics systems elements belong. Therefore, it would be fair to say that the mass-spring-damper system we considered so far is fairly general especially when we consider the analogy which exists between this mechanical and electrical systems. Fig. 2.4-a illustrates the oscillatory impulse response of the mass-spring system due to the energy transfer between the mass and spring energy storage elements in the absence of dissipation element, while in the presence of a dissipation element, the sinusoidal function is decaying exponentially due to the energy loss in the damper as depicted in Fig.2.4-b.

The previous mass-spring-damper system is an example of the energy interaction between elements which belong to the same energy domain. On the other hand, the DC motor, for instance, includes physical elements which belong to different energy domains, namely the electromagnetic and mechanical energy domains which consist of storage elements such as the inductor and the rotary inertia that belong to the electrical and mechanical energy domains, respectively.

The DC motor also consists of energy dissipative elements such as the resistance and the viscous friction that belong to the electrical and mechanical energy domains as well. The state variable of the rotor inertia is its momentum, while the state variable of the inductor is its current. Therefore, the *flow* and *effort* pairs through the energy ports between the electrical and mechanical energy domains are the (voltage and current) and (force and velocity), respectively. Then many other energy ports can be added to model the interaction with the environment and ports can be terminated with energy dissipation elements. Nevertheless, the energy exchange

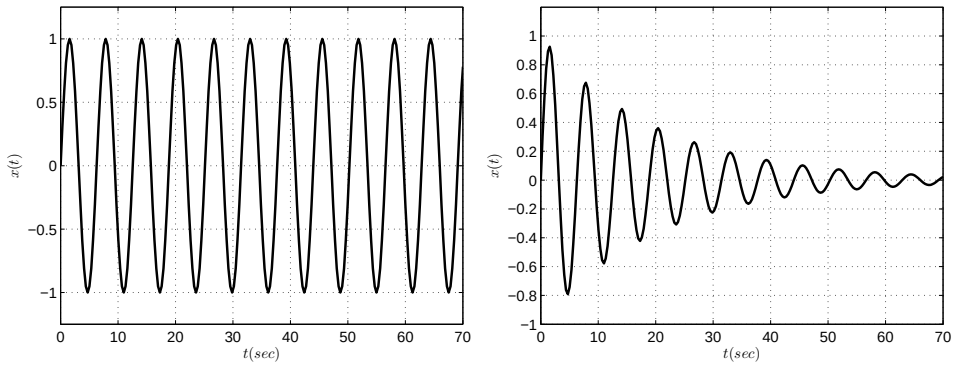

(a) Absence of energy dissipation element (b) Presence of energy dissipation element

Figure 2.4: Energy transfer between the mass-spring.

occurs among the different element of the physical system whenever they interact. Therefore, for any complex physical system, every element that belongs to a specific energy sub-domain with specific nature such as dissipation, transformation or storage has its on *flow-effort* pair and power port through which it can interact with the environment and other elements.

To be more precise, the previous DC motor example shows how interactions between elements which belong to different energy domains result in an exchange of power and mapping between the *effort* and *flow* variables of each energy port. Since the incoming power is equal to the outgoing power, the incoming electrical power is equal to the outgoing mechanical power

$$P_{ele} = e_{ele} f_{ele} = e_{mec} f_{mec} = P_{mec} \tag{2.14}$$

the incoming *flow* is mapped to the outgoing *effort* and the incoming *effort* is mapped to the outgoing *flow*. This can be better presented if the interaction matrix $(J(x))$ is driven based on the Dirac structure of each energy port. The Hamiltonian energy function can be expressed as follows

$$H(p, \phi) = \frac{1}{2}\frac{p^2}{I} + \frac{1}{2}\frac{\phi^2}{L} \tag{2.15}$$

where, I and L are the rotary inertia and inductance of the DC motor, respectively. p and ϕ are their associated momentum and flux, respectively. Therefore, (2.13) can be expressed as

$$\begin{bmatrix} \dot{p} \\ \dot{\phi} \end{bmatrix} = \left(\begin{bmatrix} 0 & K \\ -K & 0 \end{bmatrix} - \begin{bmatrix} c & 0 \\ 0 & R \end{bmatrix} \right) \begin{bmatrix} \frac{\partial}{\partial q} H(p, \phi) \\ \frac{\partial}{\partial \phi} H(p, \phi) \end{bmatrix} + \begin{bmatrix} 0 \\ 1 \end{bmatrix} u \tag{2.16}$$

$$J(\mathrm{x}) = \begin{bmatrix} 0 & K \\ -K & 0 \end{bmatrix}, \; R(\mathrm{x}) = \begin{bmatrix} c & 0 \\ 0 & R \end{bmatrix}$$

where c and R are the coefficients of the mechanical and electrical dissipative elements associated with the DC motor. K is the torque constant which control the mapping between the input *flow* and output *effort* and input *effort* and output *flow*.

The interaction matrix of (2.16) indicates that the input electrical *flow* is mapped into output mechanical *effort*, while the input electrical *effort* is mapped into output mechanical *flow*. In other but equivalent words, the torque is related to the current through the torque constant and due to the *power-conserving* property, the remaining *flow* and *effort* variables are relating the e.m.f and the angular velocity. Therefore, the *power-conserving* interconnected structure has the property of exchanging and mapping the *flow* and *effort* variables through their different energy ports. This in turn inspires the idea of having a natural feedback from interacting dynamical subsystems which have inaccessible state variables or outputs. Then use this natural feedback as basis for the states estimation process and further designing controllers for such systems.

2.2 Power Exchange

2.2.1 Power conserving interconnection

It was shown in section 2.1.1 that a Dirac structure $\mathbb{D}$ on $\mathcal{F} \times \mathcal{F}^*$ is a subspace $\mathbb{D} \subset \mathcal{F} \times \mathcal{F}^*$ such that $\mathbb{D} = \mathbb{D}^{\perp}$. Therefore, it follows that the *effort-flow* pair $< e \mid f >= 0$ for all $(f, e) \in \mathbb{D}$, and hence any Dirac structure is *power-conserving*. In addition, if $\mathcal{F} \in \mathbb{R}^n$, then any Dirac structure $\mathbb{D} \subset \mathcal{F} \times \mathcal{F}^*$ satisfies $dim(\mathbb{D}) = dim(\mathcal{F})$.

This reveals a very important property for the realization of a natural feedback from dynamical systems with inaccessible state variables or outputs. If a dynamical system with inaccessible state variables is in physical contact with another dynamical system from the same energy domain. The *effort-flow* pair along the energy port between these two systems can be used in the realization of a natural feedback from the first system on the second. Strictly speaking, even in the absence of one of the dynamical systems state variables and outputs, due to the *power-conserving* interconnection between the dynamical subsystems of the same energy domain, the power flow along the energy port that models the interaction would ensure the presence of a natural feedback from one system on the other.

On the other hand, if the dynamical interconnected subsystems are from different energy domains, the previous argument holds, except that the *flow* and *effort* variables will be mapped from one energy domain to another as it was explained in 2.1.4, since the Dirac structure is *power-conserving* and the $dim(\mathbb{D}) = dim(\mathcal{F})$, this can be shown by considering the following *effort-flow* pairs $(f_1, e_1), (f_2, e_2) \in \mathbb{D}$, this implies that $(f_1 + f_2, e_1 + e_2) \in \mathbb{D}$ and since the Dirac structure is *power-conserving*, then for every $(f, e) \in \mathbb{D}$,

$$< e, f >= 0 \tag{2.17}$$

therefore,

$$< e_1 + e_2, f_1 + f_2 >=< e_1, f_2 > + < e_2, f_1 > + < e_1, f_1 > + < e_2, f_2 >= 0 \quad (2.18)$$

which can be written in the following symmetric bilinear form,

$$<< (f_1, e_1), (f_2, e_2) >>= 0 \quad (2.19)$$

Then, $\mathbb{D} \subset \mathbb{D}^{\perp}$ and $dim(\mathbb{D}) = dim(\mathcal{F}) = n$, then $\mathbb{D} = \mathbb{D}^{\perp}$. Since the dimension of the Dirac structure is equal to the dimension of the linear space $\mathcal{F}$, the *effort-flow* pair cannot be imposed at the same time.

A spring subsystem is imposing an *effort* (generalized force) on the mass subsystem while receiving a *flow* (generalized velocity). Similarly, the mass subsystem has a dual behavior, it imposes *flow* (generalized velocity) and receives *effort* (generalized force). Due to the *power-conserving* interconnection the power is getting transformed between kinetic and potential mechanical sub-domains, indefinitely. By the same token, the *power-conserving* property along with the ideal transformation assumptions, the two ports that models the interaction between the electrical and mechanical elements of the DC motor are behaving in a similar way except that the electrical variables are mapped into the mechanical ones. The input *flow* (current) and *effort* (voltage) are mapped into output *effort* (generalized force) and *flow* (generalized velocity). In either ports, only one power variable can be imposed at a time. Therefore, there exists a continuous information flow along the interacting dynamical subsystem regardless to their energy domains or sub-domains.

Van der Schaft [Cervera 2006] proposed an equivalent Dirac structure matrix representation that is going to be used in the sequel. The Dirac structure $\mathbb{D} \in \mathcal{F} \times \mathcal{F}^*$ with $dim(\mathcal{F}) = n$ can be represented as

$$\mathbb{D} = \{(f, e) \in \mathcal{F} \times \varepsilon \mid Ff + Ee = 0\} \quad (2.20)$$

where F and E are $n \times n$ matrices s.t,

$$\begin{aligned} EF^{\mathrm{T}} + FE^{\mathrm{T}} &= 0 \\ rank[F] &= n \end{aligned} \quad (2.21)$$

2.2.2 Lumped mass spring system example

Considering a flexible mechanical system with 2 degrees of freedom and single input u and flexible element with stiffness k as depicted in Fig. 2.5. The state variables are (x_i, p_i), the position and momentum of each degree of freedom, $i = 1, 2$.

The total energy of the system can be written using the Hamiltonian energy function as

$$H(x, p) = \frac{1}{2}\frac{p_1^2}{m_1} + \frac{1}{2}\frac{p_2^2}{m_2} + \frac{1}{2}k(x_2 - x_1)^2 \quad (2.22)$$

which represent total energy stored within the masses and spring energy storage elements of the dynamical system. It can be easily shown using the previous analysis of section 2.1.2 that the power variables through the energy port between the

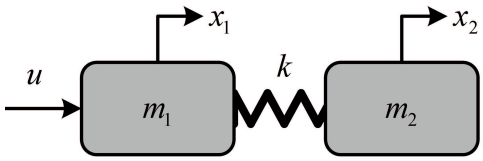

Figure 2.5: Dynamical system with 2 degrees of freedom.

mass (m_1) and spring subsystems are the *effort* (input forces) and *flow* (1^{st} mass velocity). Similarly, the power variables of the energy port between the second mass and the spring subsystems are the *effort* (spring force) and *flow* (2^{nd} mass velocity). Using (2.13) the system dynamical equations can be written as follows.

$$\begin{bmatrix} \dot{x}_1 \\ \dot{p}_1 \\ \dot{x}_2 \\ \dot{p}_2 \end{bmatrix} = \begin{bmatrix} 0 & 1 & 0 & 0 \\ -1 & 0 & 0 & 0 \\ 0 & 0 & 0 & 1 \\ 0 & 0 & -1 & 0 \end{bmatrix} \begin{bmatrix} \frac{\partial}{\partial x_1} H(x,p) \\ \frac{\partial}{\partial p_1} H(x,p) \\ \frac{\partial}{\partial x_2} H(x,p) \\ \frac{\partial}{\partial p_2} H(x,p) \end{bmatrix} + \begin{bmatrix} 0 \\ 1 \\ 0 \\ 0 \end{bmatrix} u \tag{2.23}$$

The previous *effort-flow* analysis can be directly interpreted from the skew-symmetric interaction matrix of (2.23). In addition, the *power-conserving* property can be investigated through (2.20) and (2.21) as E and F are,

$$E = \begin{bmatrix} 0 & 1 & 0 & 0 & 0 & 0 \\ -1 & 0 & 0 & 0 & 0 & 0 \\ 0 & 0 & 0 & 1 & 0 & 0 \\ 0 & 0 & -1 & 0 & 0 & 0 \\ 0 & -1 & 0 & 0 & 1 & 0 \\ 0 & 0 & 0 & -1 & 0 & 1 \end{bmatrix}, \quad F = \begin{bmatrix} 1 & 0 & 0 & 0 & 0 & 0 \\ 0 & 1 & 0 & 0 & 1 & 0 \\ 0 & 0 & 1 & 0 & 0 & 0 \\ 0 & 0 & 0 & 1 & 0 & 1 \\ 0 & 0 & 0 & 0 & 0 & 0 \\ 0 & 0 & 0 & 0 & 0 & 0 \end{bmatrix} \tag{2.24}$$

then, it can be easily verified that $EF^{\mathrm{T}} + FE^{\mathrm{T}} = 0$ and $rank[F] = n$. As shown in Fig. 2.6, the interconnection of the different energy storage elements is in feedback, regardless to the nature of the physical elements and the energy domains to which they belong, i.e., if a DC motor is connected to the system depicted in Fig. 2.5, the interconnection would still be in feedback regardless to the mapping between the *effort-flow* pair from the electromagnetic to mechanical energy domains.

2.2.3 Discussion

Interconnection between different elements of any dynamical system is in feedback. Due to the fact that, such interconnection is described by Dirac structures which is equivalent to a *power-conserving* interconnection, along with the fact that the dimension of the Dirac structure itself is equal to the dimension of the *effort* variable space or its dual space, we can conclude that power is getting exchanged through the

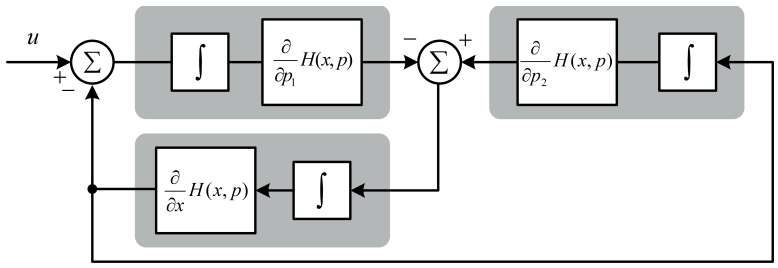

Figure 2.6: Block diagram representation of the dynamical system with 2 DOF.

energy ports of the interconnected elements from particular energy domain or subdomain to another. In addition, imposing both *effort* and *flow* through power ports cannot be realized. Therefore, through every power port between the interconnected dynamical elements, if an input *effort* is imposed, an output *flow* would be received. The problem we consider is related to realizing a feedback-like signal from dynamical system with inaccessible outputs and state variables. It should be clear from the previous argument that, if such system is interconnected with other elements, upon the *power-conserving* interconnection between this system and those elements, a natural feedback can be realized which is either a *flow* or *effort* variable.

2.3 Underactuated Mechanical Systems

Underactuated mechanical systems have fewer control inputs than degrees of freedom and arise in several applications including, but not limited to, flexible robot arms, undersea robots and mobile robots. The Lagrangian dynamics of these systems can be expressed as follows,

$$\frac{d}{dt}\frac{\partial \mathcal{L}}{\partial \dot{q}} - \frac{\partial \mathcal{L}}{\partial q} = F(q)u \tag{2.25}$$

where $u \in \mathbb{R}^m$ is the control input vector and $F(q) \in \mathbb{R}^{n\times m}$ is a non-square matrix with $m < n$ and full column rank $\forall q$ which denotes that the number of control inputs is less than the degrees of freedom n. $q \in \mathbb{R}^n$ is a vector of generalized coordinates. The equations of motion for the underactuated mechanical system (2.25) can be expressed as

$$M(q)\ddot{q} + C(q,\dot{q})\dot{q} + g(q) = \mathbf{F}(q)u \tag{2.26}$$

for a suitable partition of the system, the vector q can be written as $q^{\mathrm{T}} = (q_a, q_i)$, where $q_a \in \mathbb{R}^{n-m}$ and $q_i \in \mathbb{R}^m$, therefore we may write (2.26) as

$$\begin{aligned} M_{11}\ddot{q}_a + M_{12}\ddot{q}_i + h_1(q_a,\dot{q}_a,q_i,\dot{q}_i) + \phi_1(q_a,q_i) &= F(q_a,q_i)u \\ M_{12}\ddot{q}_a + M_{22}\ddot{q}_i + h_1(q_a,\dot{q}_a,q_i,\dot{q}_i) + \phi_2(q_a,q_i) &= 0 \end{aligned} \tag{2.27}$$

where $h_i(q,\dot{q})$ and $C(q,\dot{q})$ include Coriolis and centrifugal terms, whereas $\phi_i(q)$ and $g(q)$ contain the term derived from the potential energy such as the elastic generalized forces and the gravitational forces. It can be easily shown that upon the

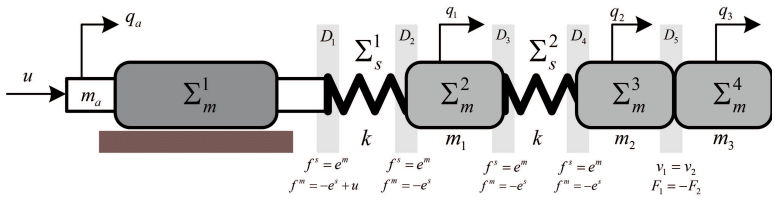

Figure 2.7: Underactuated dynamical system with coupled masses via flexible and rigid links.

power-conserving interconnections among the power ports of the system (2.26). It is important to note that, in the case of underactuated systems, the interconnection can happen between physical elements not only from the same energetic domains but also from the same type. So far, we have analyzed the case at which different elements from different energetic domains and sub-domains interact. yet, interconnection between coupled masses, for instance, is not analyzed. The underactuated systems may have coupled masses or inertias few of which are actuated.

Consider l masses $m_1, m_2, \ldots, m_l$ that are rigidly linked to each other. Such system can be described by the following system,

$$\dot{p}_i = F_i \ , \ v_i = \frac{p_i}{m_i} \ , \ i = 1, 2, \ldots, l \tag{2.28}$$

for simplicity, we assume that $l = 2$, therefore we can write

$$F_1 = -F_2 \ , \ v_1 = v_2 \tag{2.29}$$

this yields the following system

$$\begin{bmatrix} \dot{p}_1 \\ \dot{p}_2 \end{bmatrix} = \begin{bmatrix} 1 \\ -1 \end{bmatrix} \ , \ \begin{bmatrix} 1 & -1 \end{bmatrix} \begin{bmatrix} \frac{p_1}{m_1} \\ \frac{p_2}{m_2} \end{bmatrix} = 0 \tag{2.30}$$

this is not the case when the underactuated masses or the degrees of freedom are interconnected via different energy storage element such as linear springs. From (2.30), the *effort* and *flow* pair can be determined and further extended to systems of the form (2.26).

2.3.1 Underactuated system example

Consider the underactuated dynamical system depicted in Fig. 2.7, it consists of three degrees of freedom, one of which is active. The first and second masses are connected to each other and with the single active degree of freedom via spring energy storage elements. The last mass, however, is rigidly linked with the second mass. As shown in Fig. 2.7, in the absence of energy dissipation elements, the Dirac structure of the *power-conserving* interconnections between the underactuated system physical elements are describing how the power variables are getting exchanged along the systems power ports.

The net force acting on the first mass energy storage element Σ_m^a is getting integrated my the mass Σ_m^1 to result in its momentum. This momentum is used in integrating the scaler energy function of the element Σ_m^1 to result in a velocity input to the first spring energy storage element Σ_s^1 which also receives a velocity flow from the second mass energy storage element Σ_m^2. The difference between these two velocities is integrated by the spring energy storage element Σ_s^1 to determine its own deflection then the resulting force which acts on both the mass energy storage elements Σ_m^1 and Σ_m^2. Similarly, the second spring energy storage element Σ_s^2 receives velocities generated at the second and third masses energy storage elements, Σ_m^1 and Σ_m^2, respectively. Then Σ_s^2 integrates these velocities difference to determine its own deflection. The generated force at Σ_s^2 is then generated by integrating the stored potential energy in Σ_m^1 with respect to the determined deflection obtained through the previous integration process. The generated force at the spring energy storage element Σ_s^2 is then integrated by the mass energy storage element Σ_m^3 to determine its own momentum which is then used in the determination of its own velocity through differentiating the scaler kinetic energy function of Σ_m^3 with respect to this momentum. Due to the rigid link between the energy storage elements Σ_m^3 and Σ_m^4, their velocities are similar and they are both constrained with the $\dot{p}_2 + \dot{p}_3 = 0$. In the presence of energy dissipation elements along the dynamical system depicted in Fig. 2.7, the power ports have to terminated with dampers or energy dissipation elements in general.

The previous example indicates how the underactuated elements interact among each other. Input is only supplied to the first Dirac structure $\mathbb{D}_1$, then upon the *power-conserving* interconnections between the different elements of the system, *flow* and *effort* power variables are getting exchanged indefinitely. It is worth noting that the underactuated system depicted in Fig. 2.7 can be used to represent or approximate more complicated systems with continuous dynamics and infinite modes such as flexible robot arms and manipulators.

Chapter 3

Natural Feedback

FEEDBACK is a key element in the realization of control systems and state variables observers. Therefore, the presence of measurements in terms of state variables and outputs is a must since these measurements have to be used as basis for the estimation process in order to enforce specific estimation error dynamics. The class of dynamical system we consider, however, has inaccessible state variables and outputs. Thus realization of their state observers and controllers have to rely on some different alternatives, namely, natural feedbacks or feedback-like signals [O'Connor 2003] which can be determined in the absence of these systems state variables or outputs.

In the previous section, it was shown that that the *power-conserving* interconnection is in feedback form. Therefore, having a dynamical system with inaccessible state variables interconnected with other elements with accessible outputs would allow realization of an incident natural feedback from these system. Providing that the interconnection is *power-conserving* and at least one degree of freedom imposes either *flow* or *effort* variables into any of the system power ports. In the sequel, we will show that a natural feedback-like signal can be determined from these class of dynamical systems from measurements taken from other elements that are in *power-conserving* interconnection with these systems.

3.1 Effort Feedback-Like Forces

Consider a dynamical system with three degrees of freedom, composed of three masses m_i, $i = 1, 2, 3$, linked by elastic springs with stiffness k_l, $l = 1, 2$, and subjected to a single input u which is collocated with the first degree of freedom as depicted in Fig. 3.1. The state variables are the positions and momentum of each degree of freedom x_i and p_i, respectively. The Hamiltonian of this system is

$$H(x,p) = \frac{1}{2}\frac{p_1^2}{m_1} + \frac{1}{2}\frac{p_2^2}{m_2} + \frac{1}{2}\frac{p_3^2}{m_3} + \frac{1}{2}k_1(x_2 - x_1)^2 + \frac{1}{2}k_2(x_3 - x_2)^2 \tag{3.1}$$

which is the total energy stored within the energy storage elements of the dynamical system. The interconnection along the system energy ports can be interpreted through the dynamical motion equation. The power variables through the power port between the first mass and spring are the input *effort* (input and spring forces) and output *flow* (1^{st} mass velocity). Similarly, the power variables through the power port between the second mass and springs are the input *effort* (spring forces)

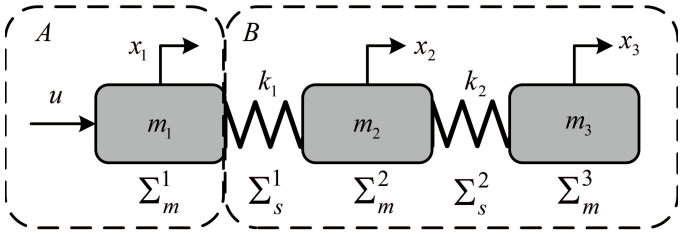

Figure 3.1: Block diagram representation of the dynamical system with 3 DOF.

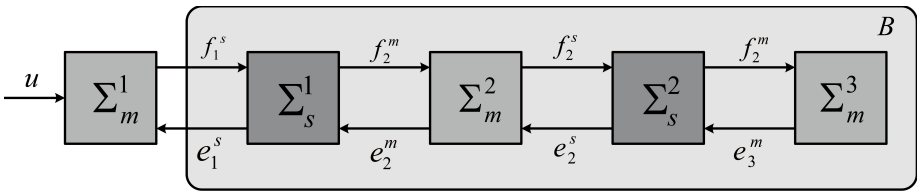

Figure 3.2: *Flow* and *effort* pairs along the dynamical system power ports.

and output *flow* (2^{nd} mass velocity). Finally, the power variables through the power port of the last mass and second spring are the input *effort* (spring force) and output *flow* ($3rd$ mass velocity). The power variables through the energy ports of the system are shown in Fig. 3.2 at which the *effort* and *flow* variables are acting as input and outputs of for the different elements of the dynamical system.

$$\begin{bmatrix} \dot{x}_1 \\ \dot{p}_1 \\ \dot{x}_2 \\ \dot{p}_2 \\ \dot{x}_3 \\ \dot{p}_3 \end{bmatrix} = \begin{bmatrix} 0 & 1 & 0 & 0 & 0 & 0 \\ -1 & 0 & 0 & 0 & 0 & 0 \\ 0 & 0 & 0 & 1 & 0 & 0 \\ 0 & 0 & -1 & 0 & 1 & 0 \\ 0 & 0 & 0 & -1 & 0 & 1 \\ 0 & 0 & 0 & 0 & -1 & 0 \end{bmatrix} \begin{bmatrix} \frac{\partial}{\partial x_1} H(x,p) \\ \frac{\partial}{\partial p_1} H(x,p) \\ \frac{\partial}{\partial x_2} H(x,p) \\ \frac{\partial}{\partial p_2} H(x,p) \\ \frac{\partial}{\partial x_3} H(x,p) \\ \frac{\partial}{\partial p_3} H(x,p) \end{bmatrix} + \begin{bmatrix} 0 \\ 1 \\ 0 \\ 0 \\ 0 \\ 0 \end{bmatrix} u \tag{3.2}$$

The energies stored in each mass and spring storage element are,

$$E_1 = \frac{1}{2}\frac{p_1^2}{m_1}\ ,\ E_2 = \frac{1}{2}\frac{p_2^2}{m_2}\ ,\ E_3 = \frac{1}{2}\frac{p_3^2}{m_3}\ ,\ E_1 = \frac{1}{2}k_1\Delta x_{12}^2\ ,\ E_2 = \frac{1}{2}k_2\Delta x_{23}^2 \tag{3.3}$$

where Δx_{12} and Δx_{23} are the elongations in the first and second springs, respectively.

By conceptually considering that the dynamical system starting from the first spring to the last non-collocated mass has state variables and outputs that are not available for measurements, labeled with (B) as depicted in Fig. 3.1. Due to the *power-conserving* interconnection between the first mass and first spring energy storage elements, even in the absence of states and variables of the system B, we can realize a natural feedback from system B, namely the *effort*-force. The energy storage element A imposes *flow* input (velocity) on the first element of system B, the

spring integrates the velocity to determine the amount of deflection which is then used in computing the corresponding amount of stored potential energy, eventually, the spring or system B imposes a natural feedback or *effort*-(force) on system A. Therefore, if states variables of system A are utilized in order to determine this natural feedback *effort*-force, we would be able to realize a natural feedback from the dynamical system B even in the absence of its state variables and outputs. This natural feedback *effort*-force is instantaneous, it occurs whenever system A imposes *flow* input on system B. As shown in Fig. 3.2, in every *power-conserving* port, information exchange occurs between the interconnected elements. The presentation depicted in Fig. 3.2 illustrates that, upon the interaction of the dynamical subsystem B with the subsystem Σ_m^1, a natural feedback would always exist in terms of *effort* or *flow* variables along the power port of the interconnected subsystems.

It is worth noting that the current analysis holds for wide range of dynamical systems with linear and nonlinear dynamics, thus it would be fair to say that the current *energy* based formalism is fairly general. Simply, we have to split the dynamical system into two portion, the first portion with inaccessible state variable and the second with accessible state variables or outputs. As soon as the dynamical system is partitioned, the Dirac structure which describes the *power-conserving* interconnection has to be specified. This can be done through the kernel/image representation of the Dirac structure explained in the previous chapter. The kernel/image representation of the system (3.2) is,

$$F = \begin{bmatrix} 1 & 0 & 0 & 0 & 0 & 0 & 0 \\ 0 & 1 & 0 & 0 & 0 & 0 & 1 \\ 0 & 0 & 1 & 0 & 0 & 0 & 0 \\ 0 & 0 & 0 & 1 & 0 & 0 & 0 \\ 0 & 0 & 0 & 0 & 1 & 0 & 0 \\ 0 & 0 & 0 & 0 & 0 & 1 & 0 \\ 0 & 0 & 0 & 0 & 0 & 0 & 0 \end{bmatrix}, \quad E = \begin{bmatrix} 0 & 1 & 0 & 0 & 0 & 0 & 0 \\ -1 & 0 & 0 & 0 & 0 & 0 & 0 \\ 0 & 0 & 0 & 1 & 0 & 0 & 0 \\ 0 & 0 & -1 & 0 & 1 & 0 & 0 \\ 0 & 0 & 0 & -1 & 0 & 1 & 0 \\ 0 & 0 & 0 & 0 & -1 & 0 & 0 \\ 0 & -1 & 0 & 0 & 0 & 0 & 1 \end{bmatrix} \tag{3.4}$$

then, it can be easily verified that $EF^{\mathrm{T}} + FE^{\mathrm{T}} = 0$ and $rank[F] = n$. The importance of specifying the Dirac structure of the *power-conserving* interconnections among system (3.2) is to understand the interaction between systems A and B, or the interconnection between the dynamical system with inaccessible states with the other with accessible state variables. However, the previous kernel/image Dirac structure representation is showing the whole interconnections among the various elements of system (3.2).

The *effort* and *flow* pairs of the dynamical system (3.1) are depicted in Fig. 3.3, it can be easily shown through Fig. 3.3 that the interconnections of system (3.2) elements are in feedback. Therefore, the natural feedback *effort*-force can be realized through subsystem A state variables or subsystem Σ_m^1 in the representation depicted in Fig. 3.2. In the sequel, the first active degree of freedom will be used to model the actuator, whereas the rest of the multi-degree of freedom system would

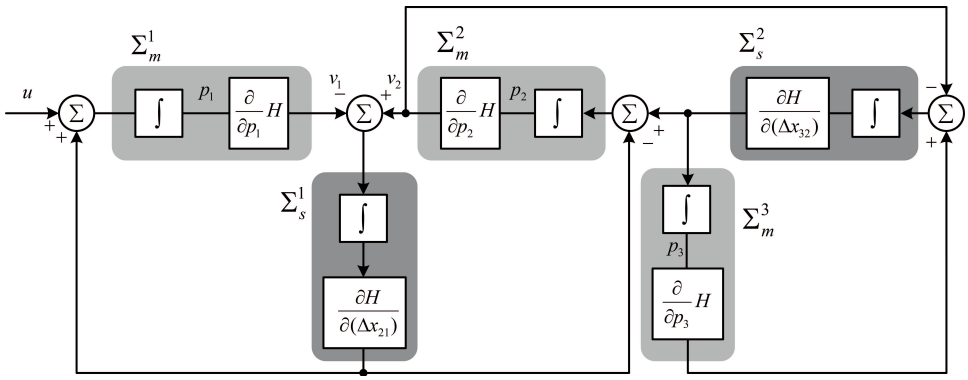

Figure 3.3: Block diagram representation of the dynamical system with 3 DOF.

represent a dynamical system with inaccessible state variables or outputs. It is commonly believed that the a special class of the well-known Luenberger observer can be used in the estimation of the incident natural feedback *effort*-force, namely disturbance and reaction force observers. In addition, conceptually considering the natural feedback *effort*-force as disturbance, would allow utilization of few solid techniques for disturbance decoupling from the literature [Hao 2007].

3.1.1 Natural feedback (*effort*-force) modeling

Since the *effort*-force (e) is a function of time, it can be therefore approximated by a polynomial with the proper order k [Ohnishi 1996],

$$\frac{d^k}{dt^k}e(t) = 0 \tag{3.5}$$

if the *effort*-force is approximated by a step function, the order of the polynomial (3.5) is $k = 1$, and if approximated by a ramp function, the order of the polynomial is $k = 2$, similarly, a parabolic approximation of the *effort*-force requires the order of the polynomial to be $k = 3$, and so forth.

It will be shown in the upcoming subsections that the approximation of the *effort*-force affects, both the performance and robustness of the estimation process, selecting a higher order polynomial to model the *effort*-force would require designing observers with higher order which induces certain amount of phase lag that might affect the estimation process if it was not considered properly.

3.1.2 Effort-force (disturbance) observer

The incident natural feedback (*effort*-force) from the dynamical system B can be determined from system A or Σ_m^1 state variables and inputs, namely the *flow* (velocity) and supplied input u,

$$\begin{aligned} e_o &= u - P_n^{-1}(v - n) \\ &= (P^{-1} - P_n^{-1})v + e + P_n^{-1}n \end{aligned} \tag{3.6}$$

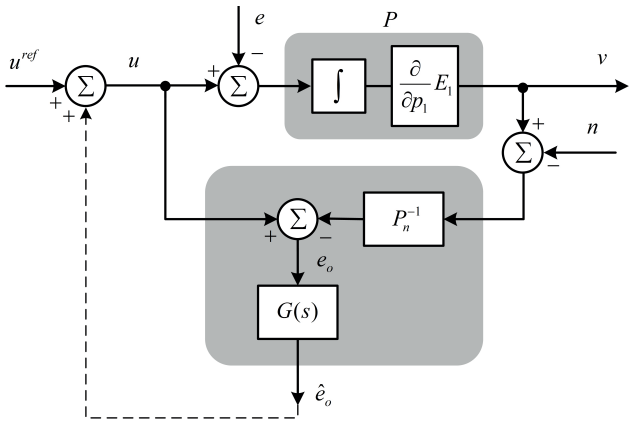

Figure 3.4: *Effort*-force observer.

where, P_n is the nominal model of the plant P, n is the measurement input noise. Due to the presence of differentiators in the inverse plant dynamics, the *effort*-force has to be determined through a low-pass filter $G(s)$,

$$\widehat{e}_o = G(s)e_o \tag{3.7}$$

where the bandwidth of the filter (3.7) is limited by the sensor noise bandwidth. The order of the low-pass filter associated with the *effort*-force observer depends on the degree of the polynomial that models the *effort*-force. It can be easily shown that there exist a tradeoff between stability and performance during the estimation of the *effort*-force through (3.7). The higher the order, the better performance and ability to realize the nominal system for various types of plants. However, stability is deteriorated due to the increase of the induced phase lag. Therefore, the bandwidth of the observer is limited to the bandwidth of the sensor noise while its order depends on the dynamical system.

The *effort*-force observer illustrated in Fig. 3.4 has to be oriented within the power port of the interacting system as it utilizes the outgoing *flow* variable in order to estimate the incoming *effort* variable. The nature of the *effort-flow* pair can be specified upon the definition of the power transformed through the power port. For the dynamical system depicted in Fig. 3.3, mechanical power is transformed through the power port, therefore the *effort-flow* pair represent the generalized force and velocity, respectively.

In general, the previous observer is implemented for the attainment of robust motion control by estimating the disturbance forces/torques at robots joint spaces and using them in the realization of an additional control inputs to suppress the unknown disturbance inputs.

The *effort*-force observer is illustrated in Fig. 3.5 in order to estimate the estimated incident *effort*-force from the dynamical subsystem B on the subsystem Σ_m^1. As shown in Fig. 3.5, the *effort* observer utilizes the available *flow* variable along with the input of the subsystem Σ_m^1 in order to estimate the *effort* feedback-like

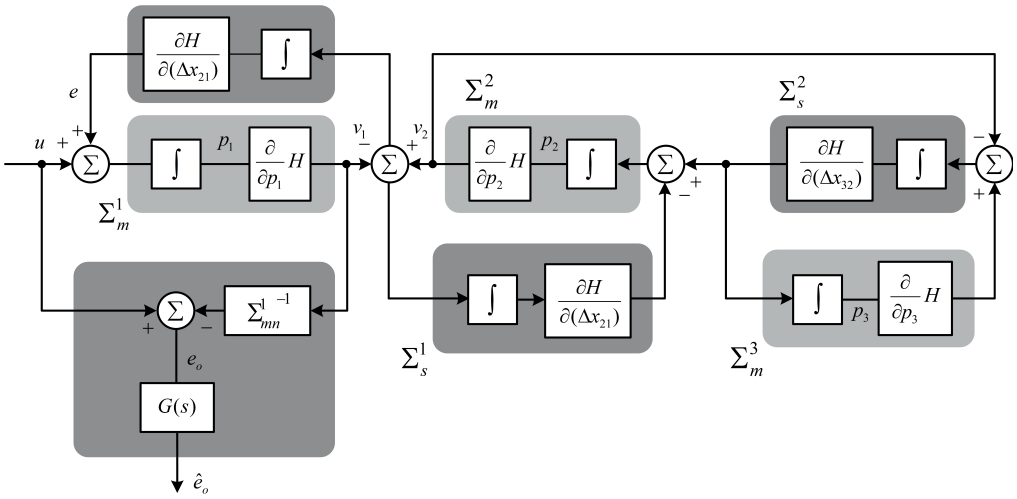

Figure 3.5: *Effort*-force observer.

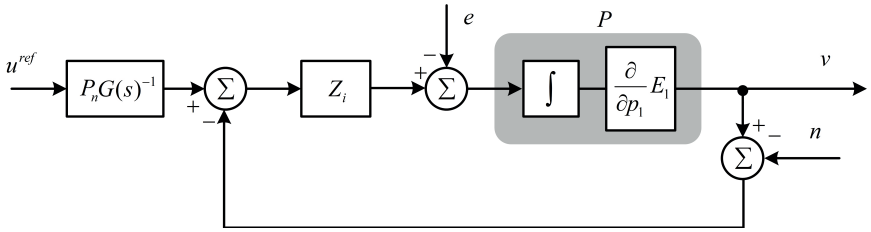

Figure 3.6: Equivalent block diagram representation of the force observer.

force from the dynamical subsystem B which is conceptually assumed to have state variables that are not accessible for measurements.

3.1.3 Observer robustness and performance tradeoffs

In order to understand the tradeoffs between stability and performance of the observer (3.7), we consider that the estimated *effort*-force is fed back to provide an additional input. Therefore, the overall input u^{ref},

$$u^{ref} = u + G(s)e_o \tag{3.8}$$

then, it can be shown that observer (3.7) along with the modified input (3.8) can be represented by the system depicted in Fig. 3.6, This can be shown by rewriting u in terms of u^{ref} and $\widehat{e}_o$ as follows

$$u = \frac{G(s)}{1 - G(s)} P_n^{-1} \big(G(s)^{-1} P_n u^{ref} - y + n \big)$$

and Z_i is

$$Z_i(s) = \frac{G(s)}{1 - G(s)} P_n^{-1} \tag{3.9}$$

Table 3.1: *effort* observer transfer functions

$Z_0(s)$	$\frac{G_0(s)}{1-G_0(s)}P_n^{-1}$	$G_0(s)$	$\frac{g_1}{s+g_1}s^2$
$Z_1(s)$	$\frac{G_1(s)}{1-G_1(s)}P_n^{-1}$	$G_1(s)$	$\frac{g_2}{s^2+g_1s+g_2}s^2$
$Z_2(s)$	$\frac{G_2(s)}{1-G_2(s)}P_n^{-1}$	$G_2(s)$	$\frac{g_2s+g_3}{s^3+g_1s^2+g_2s+g_3}s^2$
$Z_3(s)$	$\frac{G_3(s)}{1-G_3(s)}P_n^{-1}$	$G_3(s)$	$\frac{g_2s^2+g_3s+g_4}{s^4+g_1s^3+g_2s^2+g_3s+g_4}s^2$

where the subscript i is used to indicate the order of the filter associated with the observer. In order to study the tradeoffs between the observer stability and performance, the nominal plant is modeled with a double integrator plant ($\frac{1}{s^2}$). The filters associated with the transfer function (3.9) are included in Table. 3.1 in order to analyze the effect of utilizing higher order filters during the estimation of the *effort*-force. The observer scaler gains has to be selected such that $g_i \in \mathbb{R}^+$.

The phase and gain diagrams of the transfer function (3.9) for the filters included in Table. 3.1 are depicted in Fig. 3.7. It can be easily concluded from the phase diagram that at the low-frequency range, the phase of $Z(s)$ lags by $\pi/2$ due to the increased order of the filter $G(s)$ associated with $Z(s)$. Since the objective of realizing a natural feedback-like force from dynamical systems which have inaccessible state variables and outputs, is to utilize this feedback-like force as basis to design state observers and controllers for these class of dynamical systems, the phase lag associated with the observer can deteriorate the upcoming observers and controllers that are going to be designed based on this feedback-like force or estimated *effort*-force. Therefore, the tradeoffs between the performance of the *effort*-force observer and its stability has to be considered such that the phase lag induced during the estimation process does not affect the subsequent processes that are going to be explained in the upcoming sections. The gains of the *effort*-observer have to be selected such that the observer bandwidth doesn't exceed the bandwidth of the sensor noise, the order of the observer on the other hand has to be selected according to the order of each particular dynamical system. Nevertheless, a higher order observer might cause instability due to the induced phase lag.

3.1.4 Effort-force observer implementation

Due to the presence of uncertainties and parameter deviations over the dynamical model of the plant P or Σ_m^1 over which the *effort*-force observer is implemented, the estimated *effort*-force is coupled with many other terms, namely the parameter deviation induced disturbances. Without any loss of generality, plant P or Σ_m^1 in general represents the actuator dynamics. Therefore, it can be shown that the estimated *effort*-force is coupled with the actuator force ripple and self-varied mass forces [Ohnishi 1996]. These two forces are coupled with the estimated *effort*-force due to the deviation between the actuator force constant and mass nominal values and their actual values. These nominal values are utilized in the structure of the observer (3.7) due its dependence on the nominal plant that is known beforehand

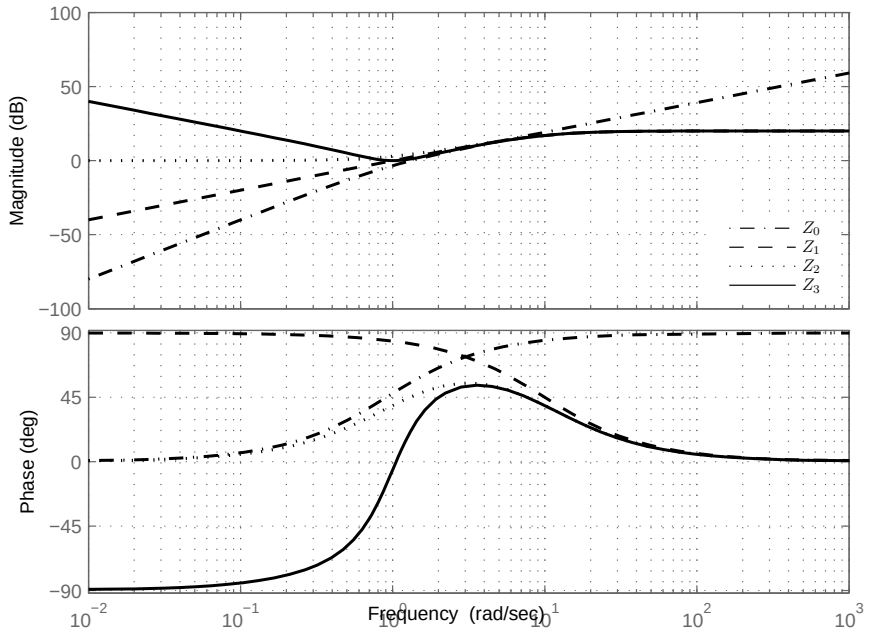

Figure 3.7: Observer performance stability tradeoff.

up to a certain level. The actuator force ripple is the product of the reference input current and the deviation over the force constant, while the self-varied mass force is the product of the actuator acceleration and the deviation over the actuator mass. Therefore, if the deviation between the actual and nominal values of the force constant and mass are known, the estimated *effort*-force can be decoupled out of the total estimated disturbance or force obtained through (3.7). A parameter identification procedure can be carried out in order to determine the deviation between the nominal and actual parameters, then the estimated deviation can be incorporated in the previous observer in order to decouple the *effort*-force.

Considering the interaction between an actuator and a dynamical system with inaccessible outputs and state variables. The actuator reference current i^{ref} and velocity $\dot{x}_a$ are available. The deviation between the actuator torque constant and mass actual values and their nominal values are $\Delta k_f = k_f - k_{fn}$ and $\Delta m_a = m_m - m_{mn}$, respectively. Therefore, the actuator induced disturbance force d_{par} which can be estimated through the disturbance observer is composed out of the actuator force ripple and self-varied mass, $\Delta k_f i_a$ and $\Delta m_a \ddot{x}_a$, respectively.

$$d_{par} = \Delta k_f i_a - \Delta m_a \ddot{x}_a \tag{3.10}$$

The actuator parameter deviations from the actual values are obviously inherent properties of the actuator, their values are independent to the system with which

the actuator interacts. Therefore, one can determine the parameters deviation using (3.10) through a parameter identification experimental procedure at which the actuator has to perform any arbitrary manoeuvre in the absence of any interconnection with the plant so as to allow the disturbance observer to provide an estimate $\widehat{d}_{par}$ for d_{par} [Khalil 2010b]. The actuator reference current, acceleration and parameter deviation induced disturbance during this arbitrary motion manoeuvre have to be recorded and considered as vectors of data points with length equal to r, $\underline{i}_m \in \mathbb{R}^{1\times r}$, $\underline{\ddot{x}}_m \in \mathbb{R}^{1\times r}$ and $\underline{\widehat{d}}_{par} \in \mathbb{R}^{1\times r}$, respectively. The previous vectors can be utilized in formulating the following over-determined systems

$$\begin{bmatrix} \triangle k_f & -\triangle m_m \end{bmatrix}_{1\times 2} \begin{bmatrix} \underline{i}_m \\ \underline{\ddot{x}}_m \end{bmatrix}_{2\times r} = \begin{bmatrix} \underline{\widehat{d}}_{par} \end{bmatrix} \tag{3.11}$$

$$\mathbf{H} \triangleq \begin{bmatrix} \underline{i}_m & \underline{\ddot{x}}_m \end{bmatrix}^{\mathrm{T}}$$

$$\begin{bmatrix} \widehat{\triangle k_t} & -\widehat{\triangle m_m} \end{bmatrix} = \mathbf{H}^{\dagger}\left[\underline{\widehat{d}}_{par}\right] = [\mathbf{H}^{\mathrm{T}}\mathbf{H}]^{-1}\mathbf{H}^{\mathrm{T}}\left[\underline{\widehat{d}}_{par}\right] \tag{3.12}$$

$\widehat{\triangle k_t}$ and $\widehat{\triangle m_m}$ are the optimum coefficients that minimize the norm square of errors of the over-determined equations set (3.12), $\mathbf{H}^{\dagger}$ is the pseudo inverse of $\mathbf{H}$. The parameter deviation induced disturbance can be determined through an observer similar to (3.7),

$$\begin{aligned} \widehat{d}_{par} &= \frac{g_{par}}{s+g_{par}}[g_{par}m_{mn}\dot{x}_m + i_m k_{fn}] - g_{par}m_{mn}\dot{x}_m \\ &= \frac{g_{par}}{s+g_{par}}[i_m k_{fn} - s m_{mn}\dot{x}_m] = \frac{g_{par}}{s+g_{par}} d_{par} \end{aligned} \tag{3.13}$$

where $g_{par} \in \mathbb{R}^+$ is the cut-off frequency of the low-pass filter associated with observer (3.13). Once the actuator or system P parameter deviations are identified through the previous procedure or any other parameter identification method, the estimated *effort*-force can be decoupled out of the total disturbance force. The following observer can be used in order to estimate the total incident disturbances on plant P,

$$\begin{aligned} \widehat{d} &= \frac{g_{dist}}{s+g_{dist}}[g_{dist}m_{mn}\dot{x}_m + i_m k_{fn}] - g_{dist}m_{mn}\dot{x}_m \\ &= \frac{g_{dist}}{s+g_{dist}}[i_m k_{fn} - s m_{mn}\dot{x}_m] = \frac{g_{dist}}{s+g_{dist}} d \end{aligned} \tag{3.14}$$

$g_{dist} \in \mathbb{R}^+$ is the cut-off frequency of the low-pass filter associated with observer (3.14), then the identified parameters obtained through (3.12) are used in order to decouple the feedback-like force or the *effort*-force estimate $\widehat{e}$ out of the estimated disturbance force $\widehat{d}$,

$$\widehat{e} = \frac{g_{eff}}{s+g_{eff}}[g_{eff}\widehat{\Delta m_m}\dot{x}_m + i_m\widehat{\Delta k_f} + \widehat{d}] - g_{eff}\widehat{\Delta m_m}\dot{x}_m \tag{3.15}$$

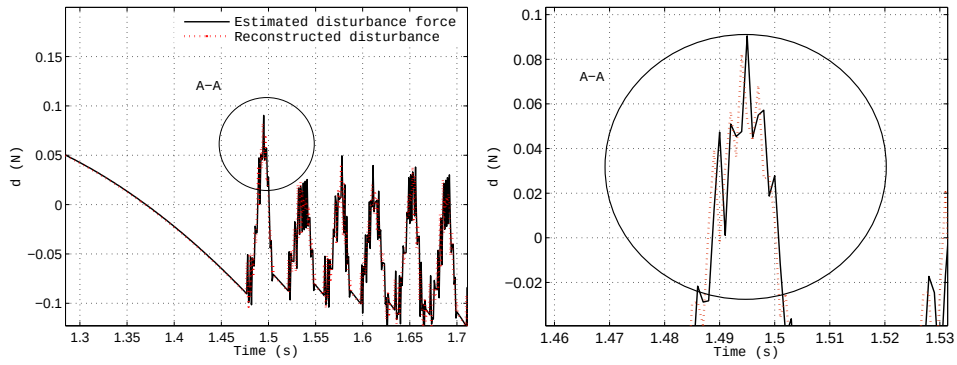

(a) estimated vs reconstructed disturbance force using the identified parameters

(b) magnified plot

Figure 3.8: Estimated disturbance force.

$g_{eff} \in \mathbb{R}^+$ is the cut-off frequency of the low-pass filter associated with *effort*-force observer.

It is worth noting that the difference between observer (3.13) and (3.14) is not only the scaler cut-off frequency gains, observer (3.13) is implemented in the absence of interconnection between a plant and the actuator or system P in order to estimate the parameter deviation induced disturbance force so as to use it in (3.12), on the other hand, observer (3.14) is used to estimate the total disturbance force which includes the parameter deviation induced disturbance along with the feedback-like *effort*-force in the presence of normal interconnection between the actuator subsystem or system P and the dynamical system with inaccessible state variables or outputs.

3.1.5 Results

In this section, experimental results are included in order to illustrate how the feedback-like *effort*-force can be estimated through the *effort*-force observer (3.15). The experimental setup consists of a linear motor from which a single measurement can be taken, namely its position through a linear position encoder with 1μm resolution. The linear actuator is interconnected via a flexible element with a linear mass-spring system with three degrees of freedom. Firstly, the linear actuator parameter deviation have to be identified through (3.12) and (3.13) in order to decouple the actuator force ripple and self-varied mass forces from the estimated interconnection forces.

Experimentally, the actuator has to perform an off-line arbitrarily motion manoeuvre in the absence of any interconnection, meanwhile vectors of actuator supplied reference current input, acceleration and estimated parameter deviation induced disturbances have to be recorded. These vectors are used in realizing the over-determined set of equations (3.12). The estimated parameter deviation in-

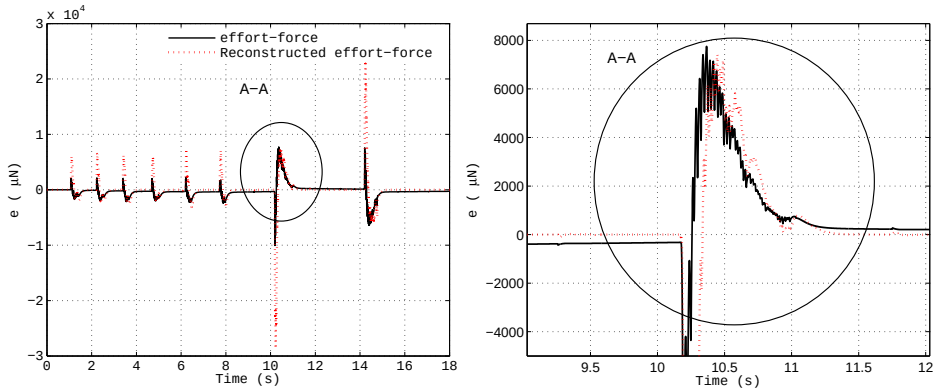

(a) estimated vs actual *effort*-force (b) magnified plot

Figure 3.9: Estimated feedback-like *effort*-force.

duced disturbance forces are plotted against the reconstructed ones through the estimated parameters obtained through (3.12) as shown in Fig. 3.8. The estimated parameters are utilized in (3.15) in order to decouple the feedback-like *effort*-force from the actuator force ripple and self-varied mass forces. The estimated *effort*-force is illustrated in Fig. 3.9 versus the actual *effort*-force. The estimated one is obtained from measurements taken from the actuator, whereas the actual one is determined through measurements taken from both the actuator and the interconnected dynamical system along with the knowledge of the interconnected system parameters and the mathematical expression which model the interconnection, namely the Dirac structure. Therefore, in the absence of these information, the estimated *effort*-force can be conceptually considered as a natural feedback from the interconnected dynamical system to the actuator.

In order to further examine the sensitivity of the *effort*-force observer to micron scale interconnection forces, since a possible application of this work is oriented toward microsystems and micromanipulation applications at which measurements cannot be made or states are inaccessible, an additional experiment is performed by allowing a single degree of freedom robot to interact with a flexible environment (biological cell) with $1mm$ diameter. The estimated *effort*-force obtained through (3.15) is illustrated in Fig. 3.10-a and Fig. 3.10-b. The sensitivity of the observer is relying on the sensitivity of the position or velocity sensor utilized in the realization of (3.15). In this experiment, a position sensor is utilized with 1μm resolution then the velocity signal is obtained by differentiation through a low-pass filter with a proper cut-off frequency that is limited with the sensor noise. Therefore, it can be concluded from Fig. 3.10 that the *effort*-force observer sensitivity is defined by the sensitivity of the position or velocity sensor. In addition, the observer can be utilized in applications at which the interconnection forces are of micron scale. As shown in Fig. 3.10, the *effort*-force observer is able to sense the peak forces that occur up on the interaction between a single degree of freedom robot end-effector and

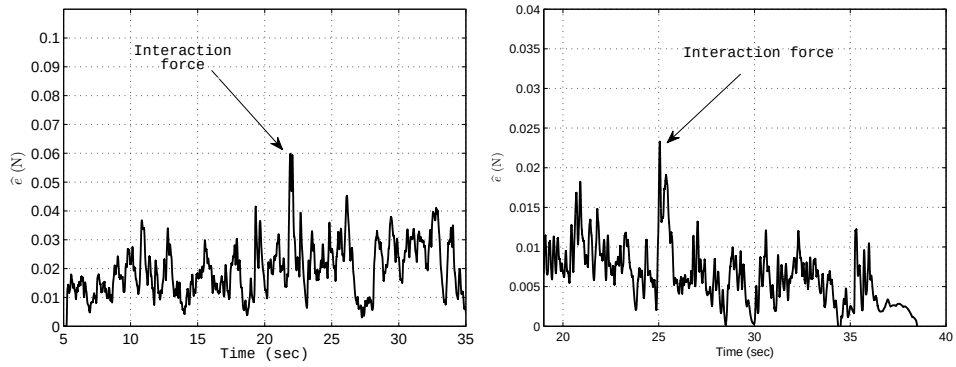

(a) (b)

Figure 3.10: *Effort*-force observer sensitivity.

a flexible biological cell. Such experiments are commonly conducted for biological cell characterization and cell manipulation. More details about the experimental procedures included in this chapter can be found in Appendix A along with the experimental parameters and setup description.

3.2 System Decoupled Representation

Since we are seeking a natural feedback-like signal which happened to be a power variable in terms of *flow* or *effort* variable that can be specified upon the nature of the power being exchanged between the physical elements of the system, the system have to represented such that we can decouple the entire system into two subsystems, the first is the one from which state variables can be measured, whereas the second has state variables that are not accessible for measurements. In addition, we are seeking a presentation which reveals the feedback-like signal or the *effort* feedback-like force between these two interconnected subsystems.

Considering a plant with $(n-r)$ state variables x_i^p, that are not available for measurements and the remaining r state variables x_l^a, are available for measurement, where $i = r+1, \ldots, n-r$ and $l = 1, \ldots, r$. So far we have been considering the phase space with state variables (x, p) in order to illustrate the *power-conserving* interconnection among different systems, in order to be consistent with the relevant existing state observers in the literature, we are going to use the state space variables $(x, \dot{x})$. Dynamics of this system is described by

$$\begin{aligned} \dot{\mathrm{x}} &= \mathrm{A}\mathrm{x} + \mathrm{B}u \\ \mathrm{y} &= \mathrm{C}\mathrm{x} + \mathrm{D}u \end{aligned} \tag{3.16}$$

where $\mathrm{x} = [x_i^p \mid x_l^a] \in \mathrm{R}^n$ and $\mathrm{y} \in \mathrm{R}^m$ are the state and measurement vectors, respectively. A, B, C and D are the system matrix, distribution vector of input, observation column vector and feed forward matrix with the appropriate dimensions,

respectively. In order to represent the state space equation (3.16) such that available state and non available state variables are separated in addition to revealing the *effort* feedback-like forces between the interacting systems, it can be shown that the state space equation (3.16) can be written as

$$\begin{bmatrix} \dot{\mathrm{x}}^a \\ -- \\ \dot{\mathrm{x}}^p \end{bmatrix} = \left[\begin{array}{c|c} \mathrm{A}^a & \emptyset \\ -- & -- \\ \emptyset & \emptyset \end{array}\right] \begin{bmatrix} \mathrm{x}^a \\ -- \\ \mathrm{x}^p \end{bmatrix} + \left[\begin{array}{c|c} \emptyset & \emptyset \\ -- & -- \\ \emptyset & \mathrm{A}^p \end{array}\right] \begin{bmatrix} \mathrm{x}^a \\ -- \\ \mathrm{x}^p \end{bmatrix} + \begin{bmatrix} \mathrm{B}^a \\ -- \\ \emptyset \end{bmatrix} u + \left[\begin{pmatrix} \emptyset \\ -- \\ \mathrm{B}^p \end{pmatrix} + \begin{pmatrix} \mathrm{B}^{eff} \\ -- \\ \emptyset \end{pmatrix} \right] e(\mathrm{x^a}, \mathrm{x^p}) \tag{3.17}$$

Therefore, the state equation of the dynamical system (3.16) can be represented as,

$$\dot{\mathrm{x}}^a = \mathrm{A}^a \mathrm{x}^a + \mathrm{B}^a u + \mathrm{B}^{eff} e(\mathrm{x^a}, \mathrm{x^p}) \tag{3.18}$$

$$\dot{\mathrm{x}}^p = \mathrm{A}^p \mathrm{x}^p + \mathrm{B}^p e(\mathrm{x^a}, \mathrm{x^p}) \tag{3.19}$$

where, $\mathrm{A}^a \in \mathrm{R}^{r\times r}$ and $\mathrm{A}^p \in \mathrm{R}^{(n-r)\times(n-r)}$ are the system matrices of the dynamical subsystems with accessible and inaccessible state variables, respectively. $\mathrm{B}^a \in \mathrm{R}^{r\times 1}$, $\mathrm{B}^{eff} \in \mathrm{R}^{r\times 1}$ and $\mathrm{B}^p \in \mathrm{R}^{(n-r)\times 1}$ are the distribution vector of the input $u \in \mathrm{R}^{1\times 1}$, distribution vector of the *effort*-force $e(\mathrm{x^a}, \mathrm{x^p})$ for system (3.18) and (3.19) with the proper dimensions, respectively. It is worth noting that putting the state space equation (3.16) in the form (3.17) requires defining the Dirac structure of the interconnection between dynamical subsystems with and without accessible state variables for measurements. Appendix B includes a detailed derivation of (3.17) from the state space representation (3.16).

The purpose of putting the state space equation in the form (3.18) and (3.19) is to reveal the *effort*-force that is conceptually considered as a feedback-like signal from system (3.19) which has inaccessible state variables (x_i^p) on system (3.18) which has accessible state variables (x_l^a). It was shown in the previous chapter that, the *effort*-force can be estimated from system (3.18) through the *effort*-force observer.

we further consider a dynamical system with Quasi-nonlinear dynamics of the form

$$\dot{\mathrm{x}} = \mathrm{A}\mathrm{x} + \mathrm{B}u + \Phi(\mathrm{x}, u) \tag{3.20}$$

where $\Phi(\mathrm{x}, u)$ is a Lipschitz nonlinearity with a Lipschitz constant $\gamma \in \mathrm{R}^+$, i.e.,

$$\| \Phi(\mathrm{x}, u) - \Phi(\widehat{\mathrm{x}}, u) \|_2 \ \leq \ \gamma \| \mathrm{x} - \widehat{\mathrm{x}} \|_2 \tag{3.21}$$

it can be shown that system (3.20) have the following partitioned form,

$$\begin{bmatrix} \dot{\mathrm{x}}^a \\ -- \\ \dot{\mathrm{x}}^p \end{bmatrix} = \left[\begin{array}{c|c} \mathrm{A}^a & \emptyset \\ -- & -- \\ \emptyset & \emptyset \end{array}\right] \begin{bmatrix} \mathrm{x}^a \\ -- \\ \mathrm{x}^p \end{bmatrix} + \left[\begin{array}{c|c} \emptyset & \emptyset \\ -- & -- \\ \emptyset & \mathrm{A}^p \end{array}\right] \begin{bmatrix} \mathrm{x}^a \\ -- \\ \mathrm{x}^p \end{bmatrix} + \begin{bmatrix} \mathrm{B}^a \\ -- \\ \emptyset \end{bmatrix} u$$

$$+\left[\begin{pmatrix}\emptyset\\--\\ \mathrm{B}^{p}\end{pmatrix}+\begin{pmatrix}\mathrm{B}^{eff}\\--\\ \emptyset\end{pmatrix}\right]e(\mathrm{x}^{\mathrm{a}},\mathrm{x}^{\mathrm{p}})+\begin{bmatrix}\emptyset\\--\\ \Phi(\mathrm{x},u)\end{bmatrix} \tag{3.22}$$

through which we can partition the dynamical subsystem with accessible state variable for measurement from the dynamical subsystem with state variables that cannot be measured along with revealing the natural feedback-like signal or *effort*-force between these two dynamical subsystems. The *effort* feedback-like force in the representation (3.17) has a linear function of the dynamical state variables of the system (3.16), whereas the feedback-like *effort*-force of the representation (3.22) may or may not be nonlinear function of the state variables of the dynamical system (3.20) depending on the Dirac structure representation of the *power-conserving* interconnection of the two subsystems.

3.2.1 Summary and discussion

In the absence of a certain dynamical systems state variables and outputs, the *power-conserving* interconnection of these systems with other elements can be utilized in order to realize a natural feedback-like signals, namely the *effort*-forces or their dual variables. Nevertheless, this *effort* does not have to be force, its specific nature can be defined up to the nature of the power being transferred or transformed through certain power port.

This *effort* variable is conceptually considered as a natural feedback as it can be determined from the power port of the interconnected systems in the complete absence of one of the interconnected systems state variables, outputs and even mathematical model.

Along the power ports of the *power-conserving* interconnections, *effort*-force observers can be designed in order to estimate the instantaneous incident natural feedback-like forces. Issues such as the order of the observer and its robustness versus performance tradeoffs were investigated. The order of the observer is based on the polynomial order that models the *effort*-force. However, the induced phase lag due to the utilization of higher order observer would result in instability. It was shown using the gain and phase diagram that a phase lag of $\pi/2$ is induced when a forth order third order observer is utilized. Therefore, the enhanced performance of the observer comes with the cost of instability if their tradeoff is not properly considered.

In general, the estimated *effort*-force is coupled with parameter deviation induced forces such as the force ripple and self-varied mass force due to the dependence of the *effort*-force observer on a nominal plant with nominal parameters that differ from their actual ones. A parameter deviation identification procedure is proposed and its effectiveness was demonstrated with few experimental results. In addition, sensitivity of the *effort*-force observer for micron-scale forces was experimentally evaluated as one of the possible potential applications of the proposed *energy* based state observer formalism is microsystems or micromanipulation operations at which

sensor utilization is problematic. All experiments included in this chapters are explained in more details in Appendix A.

Eventually, it was shown that the dynamical system can be partitioned into two dynamical subsystems, one of which has state variables which are not available for measurement while the second has state variables which are accessible for measurements. In addition, this presentation reveals the natural feedback-like *effort*-force from the first subsystem on the second.

Chapter 4

State Observer for Systems with Inaccessible Outputs

SINCE the innovative work of Luenberger, many state variables observers were proposed based on different approaches that make them different in their estimation robustness to dynamical model uncertainties, unknown initial conditions, parameter deviations and presence of disturbances. Regardless to the different approaches these observer are based on, the estimation error is enforced to asymptotically converge to zero by injecting the measured outputs or the available state variables onto their structures then designing and selecting the observer gains accordingly such that the desired estimation error dynamics is accomplished. In the absence of the dynamical system state variables, we have to make a distinction between the *flow*-based state observers and *effort*-based state observers. A quick and careful look at the state observers literature would allow us to realize that all the proposed state observers are *flow*-based. They depend on the availability of the dynamical system state variables or outputs, for the space of state variables, the *flow*-variables are velocities. This chapter is however, concerned with altering the unavailable *flow* variables with the *effort* feedback-like forces in designing state observers for situations in which *flow* variables or dynamical system states are not available for measurement.

4.1 Effort based State Observer

Considering a plant with $(n-r)$ state variables x_i^p, that are not available for measurements and the remaining r state variables x_l^a, are available for measurement, where $i = 1, \ldots, n-r$ and $l = 1, \ldots, r$. So far we have been considering the phase space with the variables (x, p) in order to illustrate the *power-conserving* interconnection among different systems. In order to be consistent with the relevant existing state observers in the literature, we are going to use the state space variables $(x, \dot{x})$. Dynamics of this system is described by

$$\begin{aligned} \dot{\mathrm{x}} &= \mathrm{A}\mathrm{x} + \mathrm{B}u \\ \mathrm{y} &= \mathrm{C}\mathrm{x} + \mathrm{D}u \end{aligned} \tag{4.1}$$

where $\mathrm{x} = [x_i^p \mid x_l^a] \in \mathrm{R}^n$ and $\mathrm{y} \in \mathrm{R}^m$ are the state and measurement vectors, respectively. A, B, C and D are the system matrix, distribution vector of input, observation column vector and feedforward matrix with the appropriate dimensions,

respectively. It was shown in the previous Chapter that the state space realization (4.1) can be partitioned and expressed in the following form,

$$\left[\begin{array}{c}\dot{\mathrm{x}}^a\\ --\\ \dot{\mathrm{x}}^p\end{array}\right]=\left[\begin{array}{c|c}\mathrm{A}^a & \emptyset\\ -- & --\\ \emptyset & \emptyset\end{array}\right]\left[\begin{array}{c}\mathrm{x}^a\\ --\\ \mathrm{x}^p\end{array}\right]+\left[\begin{array}{c|c}\emptyset & \emptyset\\ -- & --\\ \emptyset & \mathrm{A}^p\end{array}\right]\left[\begin{array}{c}\mathrm{x}^a\\ --\\ \mathrm{x}^p\end{array}\right]+\left[\begin{array}{c}\mathrm{B}^a\\ --\\ \emptyset\end{array}\right]u$$
$$+\left[\left(\begin{array}{c}\emptyset\\ --\\ \mathrm{B}^p\end{array}\right)+\left(\begin{array}{c}\mathrm{B}^{eff}\\ --\\ \emptyset\end{array}\right)\right]e(\mathrm{x^a},\mathrm{x^p}) \tag{4.2}$$

$$\dot{\mathrm{x}}^a=\mathrm{A}^a\mathrm{x}^a+\mathrm{B}^a u+\mathrm{B}^{eff}e(\mathrm{x^a},\mathrm{x^p}) \tag{4.3}$$

$$\dot{\mathrm{x}}^p=\mathrm{A}^p\mathrm{x}^p+\mathrm{B}^p e(\mathrm{x^a},\mathrm{x^p}) \tag{4.4}$$

where, $\mathrm{A}^a\in\mathrm{R}^{r\times r}$ and $\mathrm{A}^p\in\mathrm{R}^{(n-r)\times(n-r)}$ are the system matrices of the dynamical subsystems with accessible and inaccessible state variables, respectively. $\mathrm{B}^a\in\mathrm{R}^{r\times 1}$, $\mathrm{B}^{eff}\in\mathrm{R}^{r\times 1}$ and $\mathrm{B}^p\in\mathrm{R}^{(n-r)\times 1}$ are the distribution vector of the input $u\in\mathrm{R}^{1\times 1}$ and distribution vector of the *effort*-force $e(\mathrm{x^a},\mathrm{x^p})$ with the proper dimensions, respectively. It would be natural to devise a state observer of the following form,

$$\left[\begin{array}{c}\dot{\mathrm{x}}^a\\ --\\ \dot{\widehat{\mathrm{x}}}^p\end{array}\right]=\left[\begin{array}{c|c}\mathrm{A}^a & \emptyset\\ -- & --\\ \emptyset & \emptyset\end{array}\right]\left[\begin{array}{c}\mathrm{x}^a\\ --\\ \widehat{\mathrm{x}}^p\end{array}\right]+\left[\begin{array}{c|c}\emptyset & \emptyset\\ -- & --\\ \emptyset & \mathrm{A}^p\end{array}\right]\left[\begin{array}{c}\mathrm{x}^a\\ --\\ \widehat{\mathrm{x}}^p\end{array}\right]+\left[\begin{array}{c}\mathrm{B}^a\\ --\\ \emptyset\end{array}\right]u$$
$$+\left[\left(\begin{array}{c}\emptyset\\ --\\ \mathrm{B}^p\end{array}\right)+\left(\begin{array}{c}\mathrm{B}^{eff}\\ --\\ \emptyset\end{array}\right)\right]e(\mathrm{x^a},\mathrm{x^p})+\mathrm{M}[\widehat{e}(u,\mathrm{x}^a)-e(\mathrm{x}^a,\widehat{\mathrm{x}}^p)] \tag{4.5}$$

to estimate the state variables x^p of the subsystem (4.3) with state variables that are not available for measurements, based on the available state variables x^a. $\mathrm{M}\in\mathrm{R}^{n\times 1}$ is the *effort*-based state observer (4.5) vector gain. $e(.)$ is a function that ca be derived based on the *power-conserving* interconnection between the dynamical subsystems with and without accessible state variables for measurements, denoted with the superscript a and p, respectively. $\widehat{e}(u,\mathrm{x}^a)$ is the estimated feedback-like *effort*-force through the accessible variable of the subsystem denoted with a, $e(\mathrm{x}^a,\widehat{\mathrm{x}}^p)$ is the reconstructed feedback-like *effort*-force using the estimated state variables $\widehat{\mathrm{x}}^\mathrm{p}$ and the available state variables from the subsystem a.

4.1.1 Convergence stability

In order to estimate the state variables of the dynamical system (4.3) in the absence of its state variables, we have to inject the natural feedback-like force or the *effort*-force $e(\mathrm{x}^a,\mathrm{x}^p)$ onto the observer structure so as to achieve the desired estimation error asymptotic convergence stability. Therefore, this feedback-like force has to be

estimated first through the *effort*-force observer outlined in the previous chapter. The *effort*-based state observer can be expressed as follows

$$\dot{\widehat{\mathrm{x}}} = \mathrm{A}\widehat{\mathrm{x}} + \mathrm{B}u + \mathrm{M}\big(\widehat{e}(u, \mathrm{x}^a) - e(\mathrm{x}^{\mathrm{a}}, \widehat{\mathrm{x}}^p)\big) \tag{4.6}$$

$$\widehat{e}(u, \mathrm{x}^a) = \frac{g_{eff}}{s + g_{eff}}[g_{eff}\widehat{\Delta m_a}\dot{x}_a + i_a\widehat{\Delta k_f} + \widehat{d}] - g_{eff}\widehat{\Delta m_a}\dot{x}_a \tag{4.7}$$

$$\widehat{d} = \frac{g_{dist}}{s + g_{dist}}[g_{dist}m_{an}\dot{x}_m + i_a k_{fn}] - g_{dist}m_{an}\dot{x}_a \tag{4.8}$$

Here we assumed that the state space equation (4.3) is modeling an actuator, without any loss of generality. $\widehat{e}(u, \dot{x}_a)$ is the estimated *effort*-force that is determined through the *effort*-force observers (4.7) and (4.8) as it was outlined in the previous chapter. $e(\mathrm{x}^{\mathrm{a}}, \widehat{\mathrm{x}}^p)$ is the model based *effort*-force which depends on the estimated states and the available ones. $\mathrm{M} \in \mathrm{R}^{n\times 1}$ is *effort*-based state observer gain vector.

In order to study the estimation error dynamics, we have to define the Dirac structure that describes the interconnection between the dynamical subsystems (4.3) and (4.4). If the Dirac structure of the interconnection between these systems is described with

$$f^s = e^m = y \quad , \quad f^m = e^s - e^d + u \tag{4.9}$$

the interaction matrix can be driven from the port-Hamiltonian representation,

$$\begin{bmatrix} \dot{x} \\ \dot{p} \end{bmatrix} = \left(\begin{bmatrix} 0 & 1 \\ -1 & 0 \end{bmatrix} - \begin{bmatrix} 0 & 0 \\ 0 & c \end{bmatrix}\right) \begin{bmatrix} \frac{\partial}{\partial x}H(x,p) \\ \frac{\partial}{\partial p}H(x,p) \end{bmatrix} + \begin{bmatrix} 0 \\ 1 \end{bmatrix} u \tag{4.10}$$

Therefore, the *effort*-force represented using the state space variables instead of the phase space variable can be written as

$$e(\mathrm{x}^a, \mathrm{x}^p) = c(\dot{x}^a - \dot{x}_i^p) + k(x^a - x_i^p) \tag{4.11}$$

where, the index i refers to the degree of freedom of the dynamical subsystem (4.4) which interact with the dynamical subsystem (4.3). Ideally, the estimated feedback-like *effort*-force $\widehat{e}(u, \dot{x}_a)$ would converge to the actual one $e(\mathrm{x}^a, \mathrm{x}^p)$ in finite time through proper design of the *effort*-force observers (4.7) and (4.8),

$$\widehat{e}(u, \mathrm{x}^a) \longmapsto e(\mathrm{x}^a, \mathrm{x}^p) \tag{4.12}$$

To be more precise, the estimated *effort*-force is perturbed with the estimation error over the *effort*-force $\Delta e(\mathrm{x}^a, \mathrm{x}^p)$. According to the *effort*-force observer structure described in the previous chapter or through (4.7), it can be shown that the perturbation over the estimated *effort*-force is $\big(1 - G(s)\big)\Delta e(\mathrm{x}^a, \mathrm{x}^p)$. Therefore,

$$\widehat{e}(u, \mathrm{x}^a) = e(\mathrm{x}^a, \mathrm{x}^p) + \big(1 - G(s)\big)\Delta e(\mathrm{x}^a, \mathrm{x}^p) \tag{4.13}$$

as it was shown in the previous chapter, $G(s)$ is the sensitivity function to the sensor noise, while $(1 - G(s))$ is the sensitivity function to the perturbation over the

estimated *effort*-force. (4.13) indicates that the estimated *effort*-force will eventually converge to the actual one.

Now, the estimation error $\mathrm{e} = \mathrm{x} - \widehat{\mathrm{x}}$ can be computed, using (4.11) along with (4.12) or (4.13), the *effort*-based state observer can be rewritten as

$$\begin{aligned} \dot{\widehat{\mathrm{x}}} &= \mathrm{A}\widehat{\mathrm{x}} + \mathrm{B}u + \mathrm{M}\big(\widehat{e}(u, \mathrm{x}^a) - e(\mathrm{x}^a, \widehat{\mathrm{x}}^p)\big) \\ &= \mathrm{A}\widehat{\mathrm{x}} + \mathrm{B}u + \mathrm{M}\big(e(\mathrm{x}^a, \mathrm{x}^p) - e(\mathrm{x}^a, \widehat{\mathrm{x}}^p) - \big(1 - G(s)\big)\Delta e(\mathrm{x}^a, \mathrm{x}^p)\big) \end{aligned} \tag{4.14}$$

subtracting (4.14) from (4.1), we obtain the following error dynamical equation

$$\begin{aligned} \dot{\mathrm{e}} &= \mathrm{A}\mathrm{e} - \mathrm{M}\big(e(\mathrm{x}^{\mathrm{a}}, \mathrm{x}^p) - e(\mathrm{x}^{\mathrm{a}}, \widehat{\mathrm{x}}^p)\big) \\ &= \mathrm{A}\mathrm{e} - \mathrm{M}\big(c(\dot{x}^a - \dot{x}_i^p) + k(x^a - x_i^p) - c(\dot{x}^a - \dot{\widehat{x}}_i^p) - k(x^a - \widehat{x}_i^p))\big) \\ &= \mathrm{A}\mathrm{e} - \mathrm{M}\big(c\dot{\widehat{x}}_i^p - c\dot{x}_i^p + k\widehat{x}_i^p - kx_i^p\big) \end{aligned} \tag{4.15}$$

therefore, the error dynamics can be expressed as

$$\dot{\mathrm{e}} = \mathrm{A}\mathrm{e} + \mathrm{M}\big[c\dot{e}_i^p + ke_i^p\big] \tag{4.16}$$

where $e_i^p = x_i^p - \widehat{x}_i^p$ and $\dot{e}_i^p = \dot{x}_i^p - \dot{\widehat{x}}_i^p$, which can be expressed as

$$e_i^p = \Big[\underbrace{0 \quad \cdots \quad 0}_{r} \quad \underbrace{l_1 \quad 0 \quad \ldots \quad 0}_{n-r}\Big]\mathrm{e} = \mathrm{L}_1\mathrm{e} \tag{4.17}$$

similarly,

$$\dot{e}_i^p = \Big[\underbrace{0 \quad \cdots \quad 0}_{r} \quad \underbrace{l_2 \quad 0 \quad \ldots \quad 0}_{n-r}\Big]\dot{\mathrm{e}} = \mathrm{L}_2\mathrm{e} \tag{4.18}$$

where $\mathrm{L}_1 \in \mathrm{R}^{1\times n}$ and $\mathrm{L}_2 \in \mathrm{R}^{1\times n}$, $l_1 = l_2 = 1$ with the index $(r+i)$ and $(r+i+1)$ along the vector L_1 and L_2, respectively. Using (4.17) and (4.18) in (4.16) we obtain

$$\dot{\mathrm{e}} = \mathrm{A}\mathrm{e} + \mathrm{M}\big[c\mathrm{L}_2\mathrm{e} + k\mathrm{L}_1\mathrm{e}\big] = \mathrm{A}\mathrm{e} + \mathrm{M}\big[c\mathrm{L}_2 + k\mathrm{L}_1\big]\mathrm{e} = \mathrm{A}\mathrm{e} + \mathrm{M}\mathrm{Z}\mathrm{e} \tag{4.19}$$

rearranging the previous terms, the estimation error dynamics can be written as follows

$$\dot{\mathrm{e}} = \big(\mathrm{A} + \mathrm{M}\mathrm{Z}\big)\mathrm{e} = \mathcal{A}\mathrm{e} \tag{4.20}$$

where $\mathrm{I} \in \mathbb{R}^{n\times n}$ is the identity matrix, $\mathrm{M} \in \mathbb{R}^{n\times 1}$, $\mathrm{Z} \in \mathbb{R}^{1\times n}$. (4.20) indicates that the estimation error will vanish if the matrix $\big(\mathrm{A} + \mathrm{M}\mathrm{Z}\big) \in \mathbb{R}^{n\times n}$ is Hurwitz. Therefore, the *effort*-based state observer vector gain vector (M) has to be selected such that $\big(\mathrm{A} + \mathrm{M}\mathrm{Z}\big)$ is Hurwitz which can be achieved through a regular pole placement procedure upon the required behavior of the observer, in general, M has to be selected such that the observer is at least twice faster than the control system.

The *effort*-based observer gain vector can be determined by direct substitution of the desired dominant observer poles in,

$$|s\mathrm{I} - \big(\mathrm{A} + \mathrm{M}\mathrm{Z}\big)| = (s - \mu_1)\ldots(s - \mu_n) \tag{4.21}$$

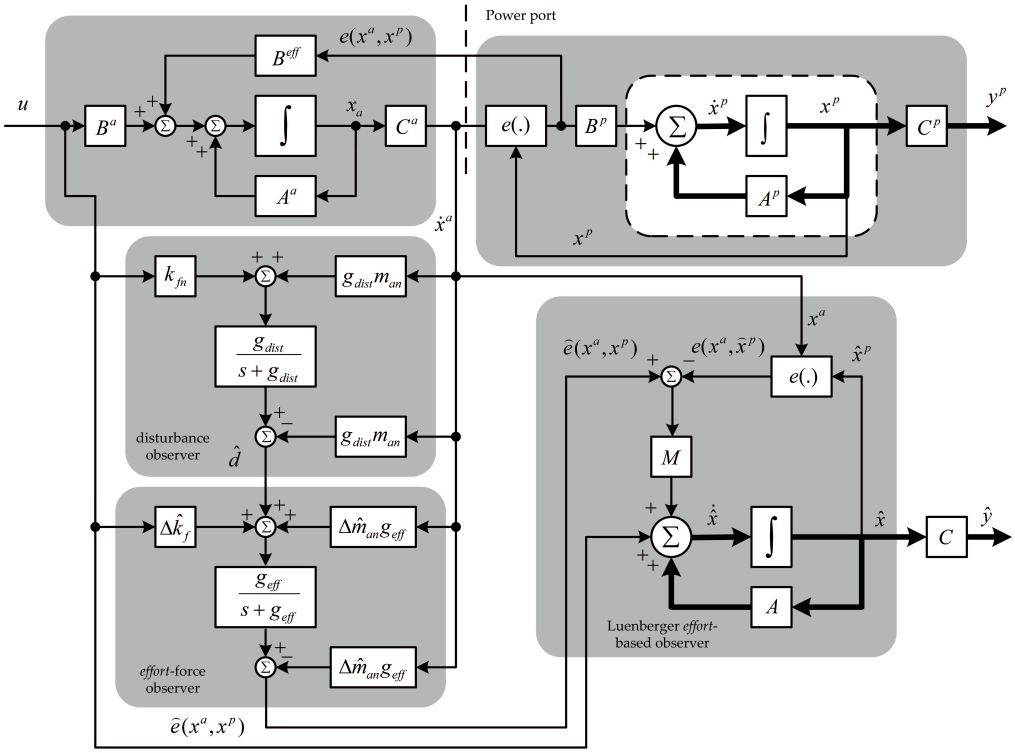

Figure 4.1: *Effort* based state observer.

where $|sI - (A + MZ)|$ is the desired characteristic polynomial and $\mu_1, \ldots, \mu_n$ are the desired observer poles.

The *effort*-based state observer which consists of three observer in cascade is depicted in Fig. 4.1, the disturbance force observer, the *effort*-force observer and a Luenberger *effort*-based like state observer. Therefore, the overall *effort*-based state observer has at least three degrees of freedom as the estimated state variables depends on the gains of each observer associated with the overall *effort*-based state observer. As shown in Fig. 4.1, the *effort*-based state observer starts by estimating the feedback-like *effort*-force along with the parameter deviation induced forces. Then the *effort*-force is decoupled out of these forces and injected onto a Luenberger-like *effort*-based state observer. The associated gains with the *effort*-based state observer depicted in Fig. 4.1 are at least, the scaler gains $g_{dist} \in \mathrm{R}^+$, $g_{eff} \in \mathrm{R}^m$ and the gain vector $\mathrm{M} \in \mathbb{R}^{n\times 1}$ associated with the disturbance force, *effort*-force and the Luenberger-like *effort*-based state observer, respectively. This is due to the utilization of first order filters within the *effort*-force observers.

First order observer are utilized in the *effort*-based state observer, therefore a single scaler observer gain is associated with the *effort*-force observer and the disturbance observer. If higher order observers are used to estimate the *effort*-force when its is modeled with a higher order polynomial, the number of scaler gains will be larger depending on the order of each observer associated with the overall

effort-based state observer.

The function $e(.)$ depicted in Fig. 4.1 depends on the definition of the Dirac structure. Therefore, the error dynamics cannot be determined unless the Dirac structure is defined. Nevertheless, this is not a problem at all and does not constrain or limit the efficiency of the analysis as the interconnections between dynamical systems described by the *power-conserving* Dirac structures are limited to few models that are going to be discussed in details in the upcoming subsection of this chapter with linear and nonlinear dynamics.

It is worth noting that due to the structure of the *effort*-based state observer, each of its observers induces a specific amount of phase lag which contributes in increasing the convergence time of the estimated state to the actual ones. Therefore, stability margins have to be studied in terms of phase and gain margins in order to analyze sensitivity of the *effort*-based state observer to the parameter deviations and the induced phase lag due to its cascaded structure.

4.1.2 Mass-spring system example

Consider a flexible lumped mass spring system with three degrees of freedom ($n-r=3$), non of its state variables are accessible. The system is non-collocated with an actuator via an energy storage element and energy dissipation element with stiffness k and viscous damping coefficient c, respectively. Therefore, the Dirac structure representation of the *power-conserving* interconnection between the dynamical subsystems with inaccessible and accessible state variables for measurement is,

$$f^s = e^m = y \quad , \quad f^m = e^s - e^d + u$$

therefore, the state space representation which decouples the state variables of the subsystems with and without available state variables for measurements is

$$\begin{bmatrix} \dot{\mathrm{x}}^a \\ -- \\ \dot{\mathrm{x}}^p \end{bmatrix} = \left[\begin{array}{c|c} \mathrm{A}^a & \emptyset \\ -- & -- \\ \emptyset & \emptyset \end{array}\right] \begin{bmatrix} \mathrm{x}^a \\ -- \\ \mathrm{x}^p \end{bmatrix} + \left[\begin{array}{c|c} \emptyset & \emptyset \\ -- & -- \\ \emptyset & \mathrm{A}^p \end{array}\right] \begin{bmatrix} \mathrm{x}^a \\ -- \\ \mathrm{x}^p \end{bmatrix} + \begin{bmatrix} \mathrm{B}^a \\ -- \\ \emptyset \end{bmatrix} u$$

$$+ \left[\begin{pmatrix} \emptyset \\ -- \\ \mathrm{B}^p \end{pmatrix} + \begin{pmatrix} \mathrm{B}^{eff} \\ -- \\ \emptyset \end{pmatrix} \right] e(\mathrm{x}^a, \mathrm{x}^p)$$

or

$$\dot{\mathrm{x}}^a = \begin{bmatrix} 0 & 1 \\ 0 & 0 \end{bmatrix} \mathrm{x}^a + \begin{bmatrix} 0 \\ \frac{k_f}{m_a} \end{bmatrix} i_a + \begin{bmatrix} 0 \\ -\frac{1}{m_a} \end{bmatrix} e(\mathrm{x}^a, \mathrm{x}^p) \tag{4.22}$$

Table 4.1: Experimental and simulation parameters

Actuator force constant	k_{fn}	6.43	N/A
Actuator Nominal mass	m_{an}	0.059	kg
Lumped masses	$m_{1,2,3}$	0.019	kg
Identified spring constants	$k_{1,2,3}$	503.96	N/m
Identified viscous damping coefficients	$c_{1,2,3}$	0.262	Ns/m
Effort-force observer gain	g_{eff}	628	rad/s
Disturbance observer gain	g_{dist}	628	rad/s
Low-pass filter gain	g_l	1000	rad/s
Sampling time	T_s	1	ms

$$\dot{\mathrm{x}}^p = \begin{bmatrix} 0 & 1 & 0 & 0 & 0 & 0 \\ \frac{-k}{m_1} & \frac{-c}{m_1} & \frac{k}{m_1} & \frac{c}{m_1} & 0 & 0 \\ 0 & 0 & 0 & 1 & 0 & 0 \\ \frac{k}{m_2} & \frac{c}{m_2} & \frac{-2k}{m_2} & \frac{-2c}{m_2} & \frac{k}{m_2} & \frac{c}{m_2} \\ 0 & 0 & 0 & 0 & 0 & 1 \\ 0 & 0 & \frac{k}{m_3} & \frac{c}{m_3} & \frac{-k}{m_3} & \frac{-c}{m_3} \end{bmatrix} \mathrm{x}^p + \begin{bmatrix} 0 \\ \frac{1}{m_1} \\ 0 \\ 0 \\ 0 \\ 0 \end{bmatrix} e(\mathrm{x}^{\mathrm{a}}, \mathrm{x}^p) \tag{4.23}$$

Table. 4.1 includes the numerical parameters of (4.22) and (4.23). If matrix $\big(\mathrm{A} + \mathrm{MZ}\big)$ was stable, the estimation error will converge to zero for any initial error vector e(0), i.e., the subsystem states $\widehat{\mathrm{x}}^p(t)$ will converge to $\mathrm{x}^p(t)$ regardless to the initial value of the estimated and actual states $\widehat{\mathrm{x}}^p(0)$ and $\mathrm{x}^p(0)$, respectively.

Assuming that the dominant poles of $\big(\mathrm{A} + \mathrm{MZ}\big)$ are required to be placed at $(-0.5 \pm 1j)$ in the left-half plane which is twice faster than system (4.1) poles. Therefore, the state observer gain vector can be shown to be [17.9635 2.0113 12.4557 $-$ 0.0885 0.8429 $-$ 0.1570 $-$ 10.3876 3.6523]. The previous observer gains can be obtained by directly substituting the desired dominant observer poles in (4.21). The estimated states versus the actual ones are depicted in Fig. 4.2 where the transient time of the estimated states to the actual ones is due to the phase lag induced by each observer associated with the overall *effort*-based state observer. Therefore, the transient time can be shortened by adjusting the observer scaler and vector gains, values of the observer gains are included in Table. 4.1.

In order to investigate sensitivity of the outlined state observer to parameter uncertainties used in (4.22), we consider parameter uncertainties. Therefore, the state observer can be written as

$$\dot{\widehat{\mathrm{x}}} = \mathbf{A}\widehat{\mathrm{x}} + \mathbf{B}u + \mathrm{M}\big(e(u, \mathrm{x}^a) - e(\mathrm{x}^{\mathrm{a}}, \widehat{\mathrm{x}}^p)\big) \tag{4.24}$$

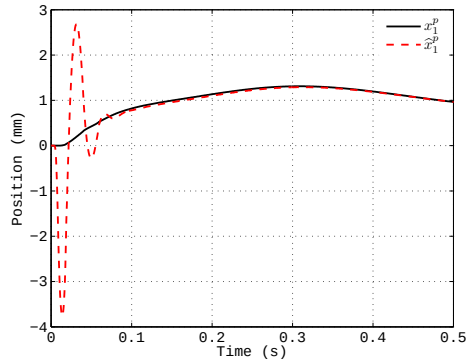

(a) x_p^1 vs. $\widehat{\mathrm{x}}_1^p$ (1^{st} mass position)

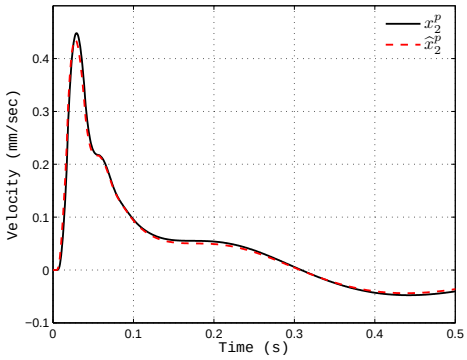

(b) x_p^3 vs. $\widehat{\mathrm{x}}_3^p$ (1^{st} mass velocity)

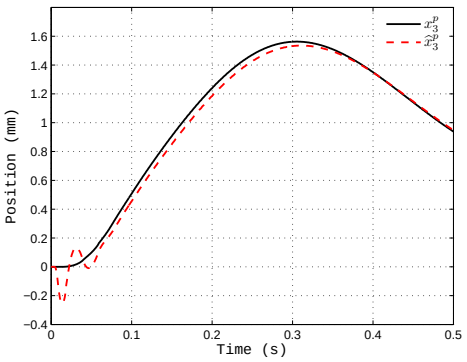

(c) x_5^p vs. $\widehat{\mathrm{x}}_p^5$ (2^{nd} mass position)

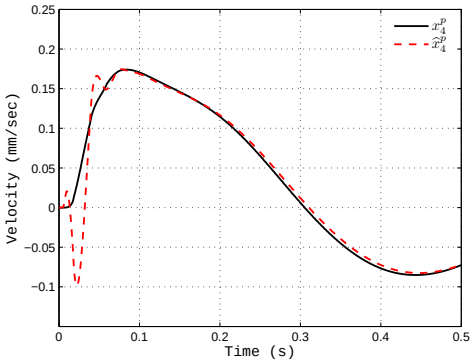

(d) x_p^2 vs. $\widehat{\mathrm{x}}_2^p$ (2^{nd} mass velocity)

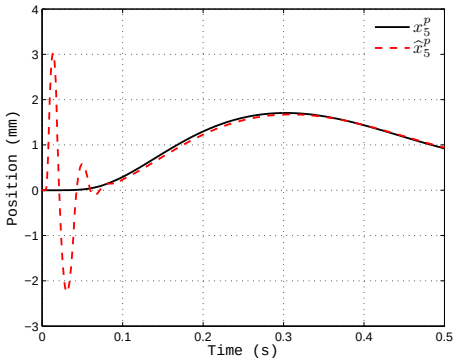

(e) x_4^p vs. $\widehat{\mathrm{x}}_p^4$ (3^{rd} mass position)

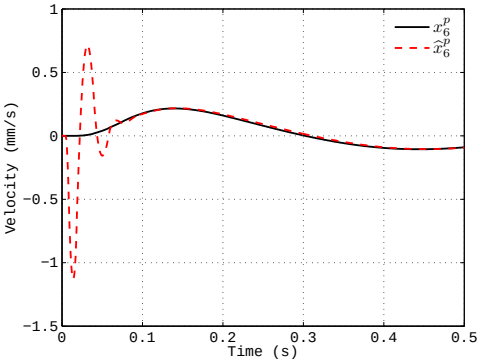

(f) x_p^6 vs. $\widehat{\mathrm{x}}_6^p$ (3^{rd} mass velocity)

Figure 4.2: States estimation results of a dynamical subsystem with 3-Dof through measurements taken from its single input.

$$\begin{aligned} \mathbf{A} &= \mathrm{A} + \Delta\mathrm{A} \\ \mathbf{B} &= \mathrm{B} + \Delta\mathrm{B} \end{aligned} \tag{4.25}$$

ΔA and ΔB represent deviation of the system parameters from the nominal ones. **A** and **B** are the perturbed system matrix and input vector, respectively. In the previous example we assume that the nominal stiffness differs from the actual one with 50% while nominal masses and viscous damping coefficients differ from the actual ones with 25%. The dominant poles of the observer are required to be placed in the same location as the previous test. Fig. 4.3 illustrates the estimated states versus the actual ones when parameter uncertainties are considered. Thus, the proposed observer can be used even if the identified system parameters are uncertain. Similar to Fig. 4.2, Fig. 4.3 illustrates that state observer accuracy and response depend entirely on the disturbance and reaction force observers. Thus, depending on the amount of phase lag each low-pass filter induces. This in turn implies that accuracy and response time of the outlined state observer can be improved by adjusting the cut-off frequencies of these force observers. It can be shown from Fig. 4.3 that in the presence of parameter deviations, the convergence time of the state variables is increased. Therefore, it is crucial to study robustness of the outlined *effort*-based state observer so as to understand its performance under certain conditions. Although the results depicted in Fig. 4.3 are obtained in the presence of parameter deviation, stability margins have to be studied to indicate how much the observer can tolerate with both parameter uncertainties and induced phase lags.

4.1.3 Robustness analysis

Robustness of the *effort*-based state observer is a key issue that has to be addressed in order to anticipate its performance in the presence of parameter deviation, unknown initial conditions, model uncertainties and external disturbances [Bor-Sen 1989]. In order to study the robustness of the *effort*-based state observer we consider the outlined dynamical system with three degrees of freedom ($n-r=3$) interconnected with another system with single degree of freedom ($r=1$) via a spring energy storage element and energy dissipation element. Considering the transfer functions between the input u and the estimation error vector e. Then by some algebraic manipulations and block diagram algebra we can derive the transfer functions between the input u and each scaler estimation error e_i where $i=1,\ldots,n-r$ that is equal to the degree of the dynamical subsystem with inaccessible or not available state variables for measurement.

The mappings between the input and the estimation error output e_i includes the dynamics of the control system, the plant and the *effort*-based state observer. Robustness of the observer depends on few issues such as model uncertainty, unknown initial conditions and parameter deviations. Therefore, if we examined the gain margins of the these mappings we can conclude whether the *effort*-based state observer can withstand greater deviations in its parameters before becoming unstable in closed loop. On the other hand, due to the structure of the *effort*-based state

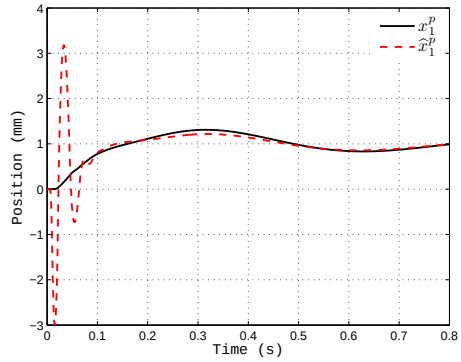

(a) x_p^1 vs. $\hat{x}_1^p$ (1^{st} mass position)

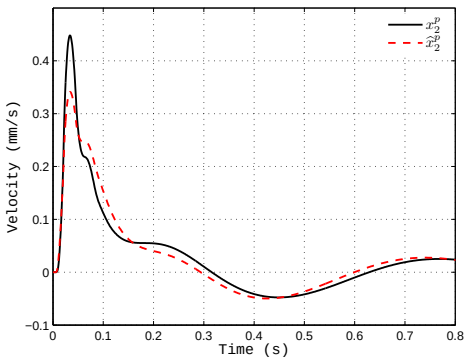

(b) x_p^3 vs. $\hat{x}_3^p$ (1^{st} mass velocity)

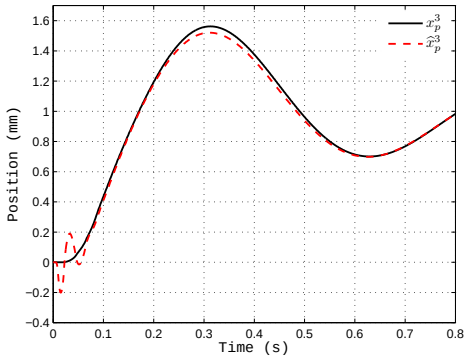

(c) x_5^p vs. $\hat{x}_p^5$ (2^{nd} mass position)

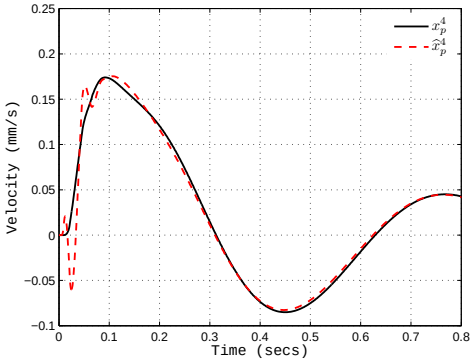

(d) x_p^2 vs. $\hat{x}_2^p$ (2^{nd} mass velocity)

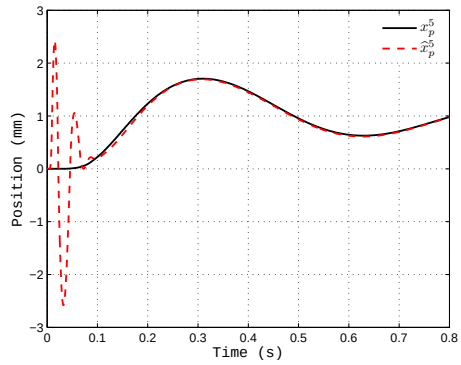

(e) x_4^p vs. $\hat{x}_p^4$ (3^{rd} mass position)

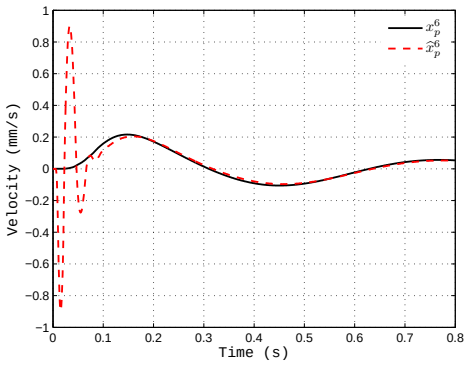

(f) x_p^6 vs. $\hat{x}_6^p$ (3^{rd} mass velocity)

Figure 4.3: States estimation results of a dynamical subsystem with 3-Dof under parameter uncertainties (25% deviation of viscous damping coefficient and masses - 50% deviation of stiffness).

observer, each single observer induces certain amount of phase lag into the system open loop. Therefore, it would be natural to examine the input and estimation errors mappings phase margins in order to provide a measure for system tolerance to the induced *effort* observer phase lag before making the closed loop system unstable. The gain and phase margin for the input and estimation errors mappings are included in Fig. 4.4 and Fig. 4.5 through the Nyquist and frequency response plots.

It can be shown from these analysis and the illustrated results that the phase and gain margins of the mapping between the input and the estimation error between the actual first mass position and its position estimate are $Gm = 23.2\ dB$ and $Pm = 97.8\ deg$, respectively as depicted in Fig. 4.4-a and 4.5-a. For the input and estimation error of the fourth state (first non-collocated mass velocity) mapping, the gain and phase margins are $Gm = 37.5\ dB$ and $Pm = 97.8\ deg$, respectively as depicted in Fig. 4.4-b and 4.5-b. Similarly, the mapping between the input and the estimation error of the second mass position and its estimate has gain and phase margins of $Gm = 28.4\ dB$ and $Pm = 74.8\ deg$, respectively as depicted in Fig. 4.4-c and 4.5-c. The gain and phase margins for the input and estimation error of the actual second mass velocity and its estimate are $Gm = 44\ dB$ and $Pm = 97.8\ deg$, respectively as depicted in Fig. 4.4-d and 4.5-d.

The gain and phase margins of the input and estimation error mappings illustrates that the estimation error has a satisfactory stability margins for both the deviation in the parameters used to construct the *effort*-based state observer in terms of gain margin, and has satisfactory tolerance to the induced phase lag by the observer in terms of phase margin. We further illustrate a time domain representation of the error dynamics in Fig. 4.6. An impulse input is induced to the system as the input, then it can be shown from Fig. 4.6 that the estimation error converges to zero in finite time.

The previous analysis and results are obtained for the *effort*-based state observer gains and plant parameters included in Table. 4.1. The indicated stability margins of the *effort*-based state observer explain its robustness to the parameter deviation in terms of the perturbed matrices $\mathbf{A}$ and $\mathbf{B}$, the simulation and experimental results of the *effort*-based state observer performance in the presence of parameter deviations are illustrated in Fig. 4.3 and Fig. 4.7, respectively.

4.1.4 Observer again adjustment procedure

Adjusting the scaler and vector gains of the *effort*-based state observer requires considering the tradeoffs between stability and performance of the observer. Firstly, the dynamical models and the interconnection among the dynamical systems have to be investigated in order to decide about the order of the polynomial that represents the feedback-like *effort*-force. Secondly, the observer relies on measurements taken from a dynamical subsystem with accessible state variables in order to estimate state variables of another subsystem with inaccessible state variables and outputs. Therefore, for these measurements, position or velocity sensors might be utilized.

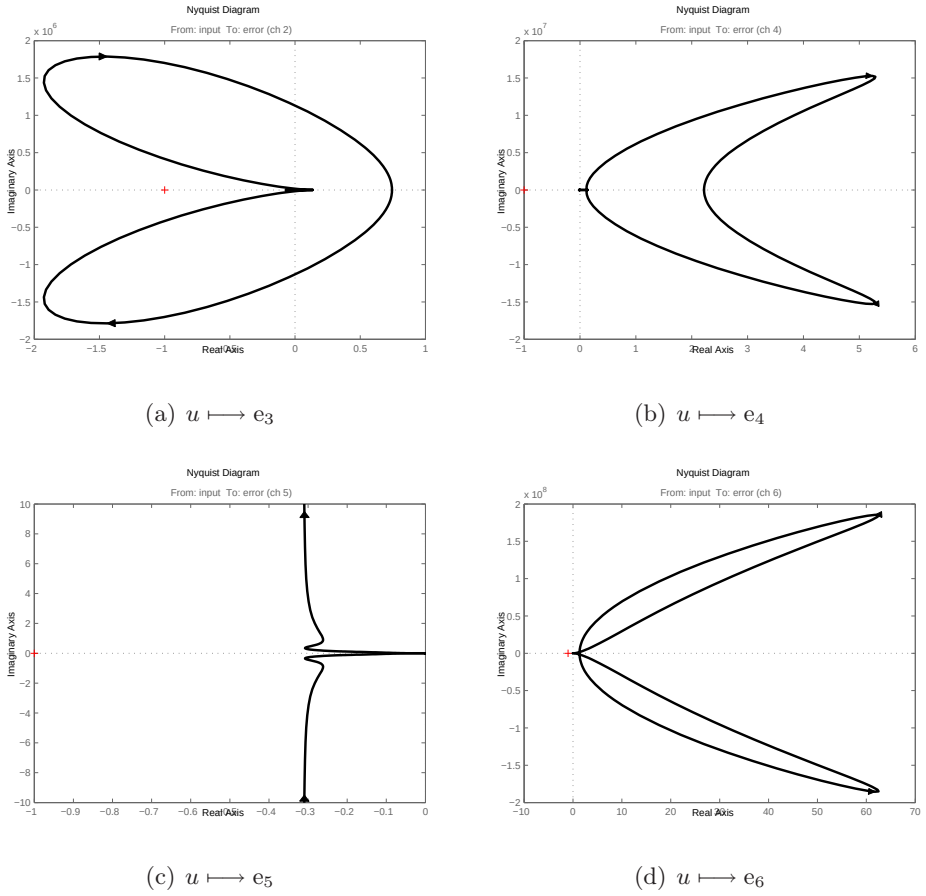

(a) $u \longmapsto e_3$ (b) $u \longmapsto e_4$

(c) $u \longmapsto e_5$ (d) $u \longmapsto e_6$

Figure 4.4: Nyquist diagrams of the input and estimation error output mappings.

The bandwidth of the sensor noise has to be determined since this bandwidth will be considered as a constrain during the selection of the observer scaler gains or the cut-off frequencies. As soon as the first and second points are considered, the feedback-like *effort*-force along with the parameter induced disturbance forces can be estimated through an observer with the proper gains and order depending on the order of the polynomial that models the *effort*-force and the sensor noise bandwidth.

The feedback-like *effort*-force has to be decoupled from the other force components induced due to the dependence of these observer on nominal plants and parameters. Therefore, an off-line parameter deviation identification experimental procedure has to be carried out in order to determine the parameter deviations then use them in the realization of the *effort*-force observer. Again, the order and gains of this observer have to be selected and limited with the model of the *effort*-force and the sensor noise bandwidth, respectively.

Based on the model of each dynamical system (so far, we considered systems with linear dynamics, in the upcoming sections, more general system are going to be considered) a Luenberger-like *effort*-based state observer has to be designed then

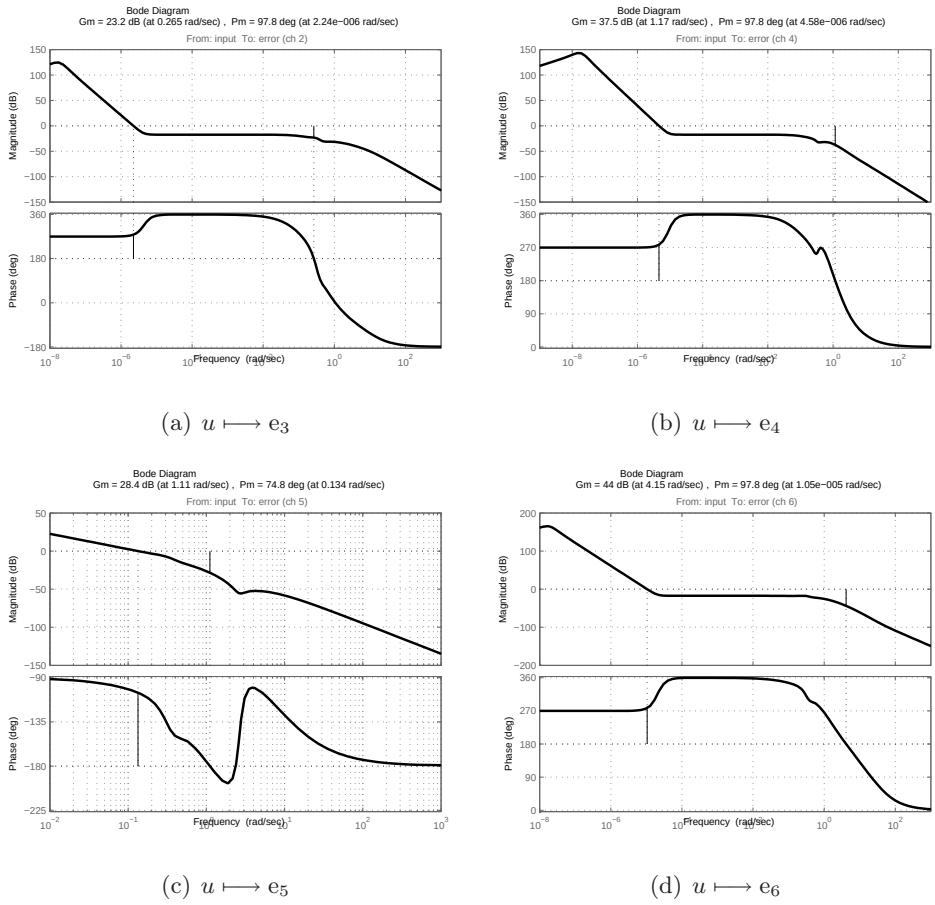

(a) $u \longmapsto e_3$ (b) $u \longmapsto e_4$

(c) $u \longmapsto e_5$ (d) $u \longmapsto e_6$

Figure 4.5: Bode plots of the input and estimation error output mappings.

the observer vector gain can be determined by directly substituting the desired observer dominant poles in (4.21). Unfortunately, a reduced order observer cannot be realized due to the absence of the state variables and the dependence of the *effort*-based state observer on the feedback-like *effort*-forces. Nevertheless, the robustness and the performance showed by the outlined error dynamics and analysis indicate effectiveness of the observer in estimating the state variables of dynamical systems with inaccessible state variables and outputs even in the presence of parameter deviations and model uncertainties.

4.1.5 Results

An experimental setup similar system to the one described in (4.1.2) is utilized in order to experimentally verify the validity of the outlined *effort*-based state observer with the same experimental parameters included in Table. 4.1. Experimentally, a similar *effort*-based state observer like the one depicted in Fig. 4.1 is utilized in estimating the state variables of the dynamical system with 3-DOF and inaccessible

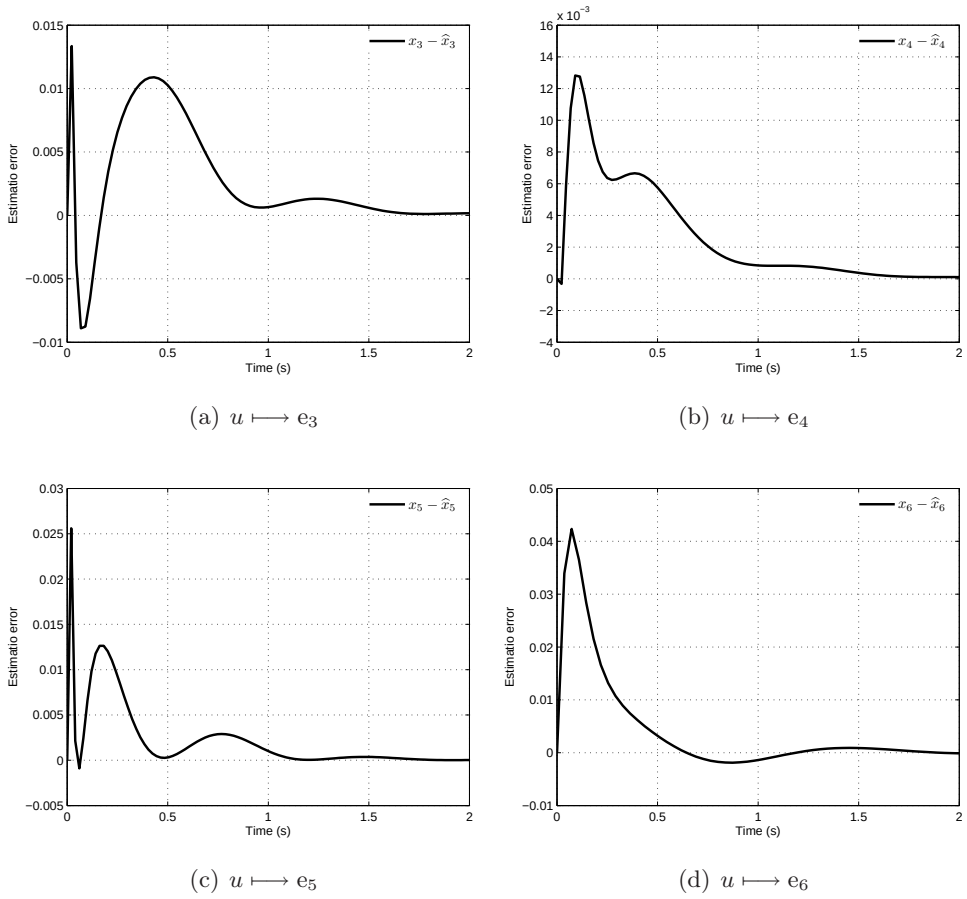

(a) $u \longmapsto \mathrm{e}_3$ (b) $u \longmapsto \mathrm{e}_4$

(c) $u \longmapsto \mathrm{e}_5$ (d) $u \longmapsto \mathrm{e}_6$

Figure 4.6: Impulse response of the input and estimation error output mappings.

state variables. The experimental setup is explained in Appendix A with more details. The experimental results of the state variables estimation are illustrated in Fig. 4.7-a-c-e. The experimental result of the state estimation process in the presence of parameters uncertainties (10% deviation of viscous damping coefficient and masses - 20% deviation of stiffness) are illustrated in Fig. 4.7-b-d-f.

Due to the abrupt oscillations of the non-collocated masses, the observer poorly estimated the transient response and allowed the estimated states to converge in the steady state. This is due to the order of the *effort*-force observer associated with the *effort*-based state observer. Increasing the order of the disturbance and *effort*-force observers would allow modeling the incident *effort*-forces accurately but with the cost of decreased phase margins due to the induced phase lags by the higher order observers.

In order to illustrate the effect of the disturbance or force observers sensitivity functions on the performance of the *effort*-based state observer, abrupt changes in the actual responses of each degree of freedom are avoided. In other words, the oscillatory response by the induced excitation is avoided. Fig. 4.8 illustrates the

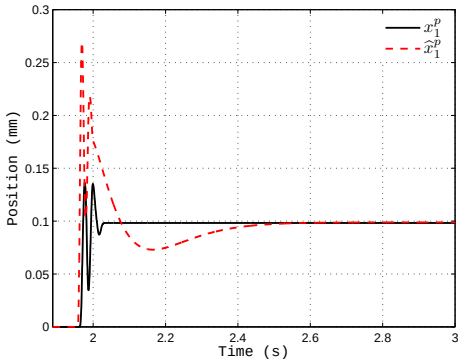

(a) x_p^1 vs. $\widehat{x}_1^p$ (1^{st} mass position)

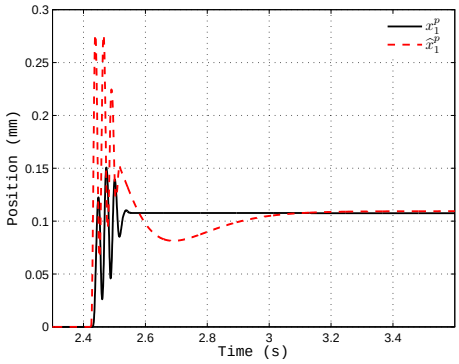

(b) x_p^3 vs. $\widehat{x}_3^p$ (with parameter deviation)

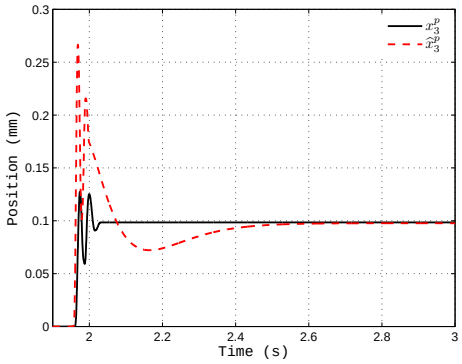

(c) x_5^p vs. $\widehat{x}_p^5$ (2^{nd} mass position)

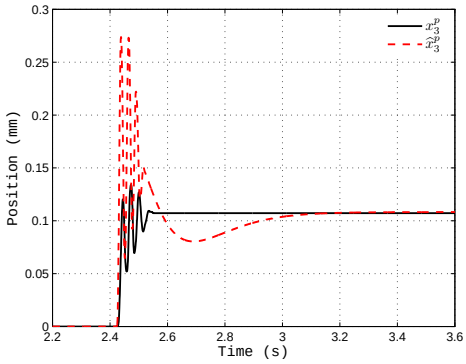

(d) x_p^2 vs. $\widehat{x}_2^p$ (with parameter deviation)

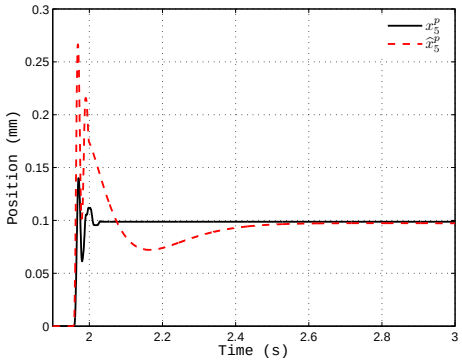

(e) x_4^p vs. $\widehat{x}_p^4$ (3^{rd} mass position)

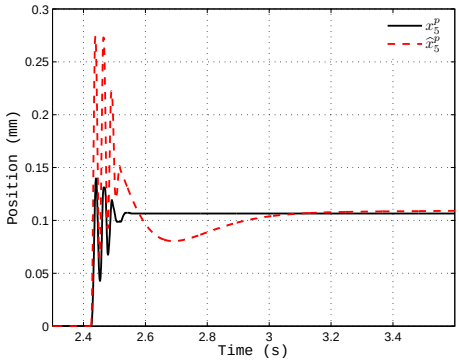

(f) x_p^6 vs. $\widehat{x}_6^p$ (with parameter deviation)

Figure 4.7: Estimated versus actual state variables experimental results in the absence and presence of parameter deviations from the actual ones.

response of the subsystem along with the estimated states. In this case, the *effort*-based state observer provides satisfactory estimation results in both transient and steady state since each of the three observers is properly functioning. Whereas, in Fig. 4.7 the disturbance observer was not able to estimate the actual *effort*-forces since the excitation was beyond its sensitivity function. Fig. 4.8-e-f illustrates the position and velocity tracking errors between actual and estimated states of the first non-collocated mass of the flexible dynamical subsystem.

In order to illustrate the performance of the *effort*-based state observer in estimating state variables of the same dynamical subsystem when it undergoes arbitrary motion with higher frequencies, the system was excited to undergo the arbitrary motions maneuvers depicted in Fig. 4.9. As it is illustrated, the performance of the *effort*-based state observer is satisfactory which indicates that each single observer within the overall *effort*-based state observer is designed properly.

4.1.6 Summary and discussion

It was shown that systems with linear dynamics of the form (4.1) can be written such that the feedback-like *effort*-forces from a subsystem with inaccessible state variables is revealed. The *effort*-forces are conceptually considered as feedback-like forces and injected onto an observer structure in order to enforce asymptotic estimation error dynamics. The obtained error dynamics proved that, if the matrix $\big(\mathrm{A}+\mathrm{MZ}\big)$ was stable, the estimation error will converge to zero for any initial error vector $\mathrm{e}(0)$, i.e., the subsystem states $\widehat{\mathrm{x}}^p(t)$ will converge to $\mathrm{x}^p(t)$ regardless to the initial value of the estimated and actual states $\widehat{\mathrm{x}}^p(0)$ and $\mathrm{x}^p(0)$, respectively.

Necessary and sufficient conditions for observability of state variable of these class of dynamical system with inaccessible outputs were driven. It was shown that for a dynamical system with linear dynamics, the system matrix has to have distinct eigenvalues if the states of any of its dynamical subsystems have to be estimated in the absence of its state variables and outputs.

Robustness of the outlined state observer is studied and experimentally evaluated for a range of parameter deviations and uncertainties. In addition, a gain adjustment procedure for designing the *effort*-based state observer is explained in details based on the tradeoffs between performance and robustness. Performance in terms of accuracy of modeling the exact *effort*-forces through higher order observers and fast construction of the state variables by increasing the observer gains, on the one hand. Robustness in terms of stability margins which are affected by the induced phase lag by the higher order observer and bandwidth limitation due to the sensor noise bandwidth, on the other.

4.2 Effort Based Observer for Non-linear Systems

The *energy* based state estimation formalism is general and can be extended for a wide class of dynamical systems with linear and nonlinear dynamics. Therefore, in the sequel, possibility of extending the previous *effort*-based state observer for more

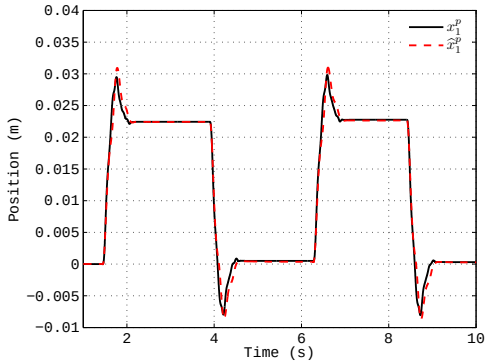

(a) x_1^p vs. $\widehat{x}_p^1$ (1^{st} mass position)

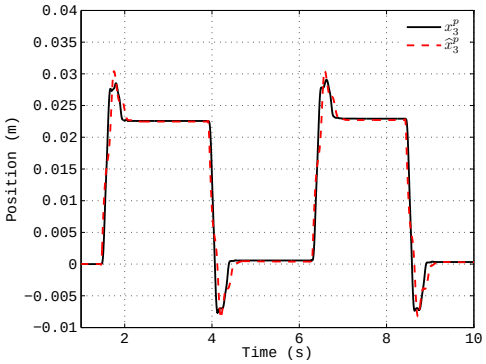

(b) x_3^p vs. $\widehat{x}_3^p$ (2^{nd} mass position)

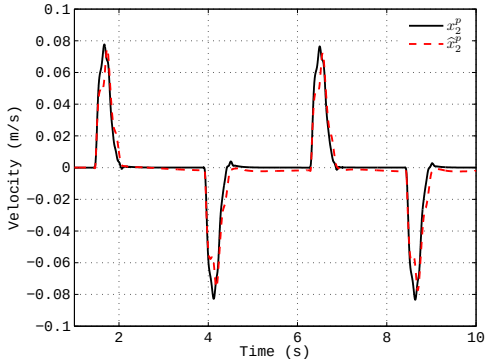

(c) x_p^2 vs. $\widehat{x}_2^p$ (1^{st} mass velocity)

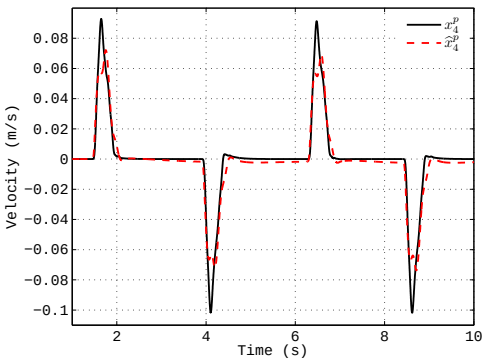

(d) x_4^p vs. $\widehat{x}_4^p$ (2^{nd} mass velocity)

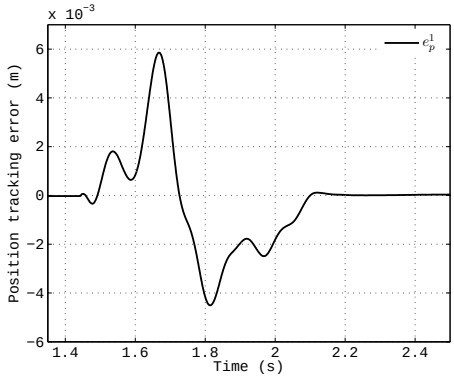

(e) position estimation error

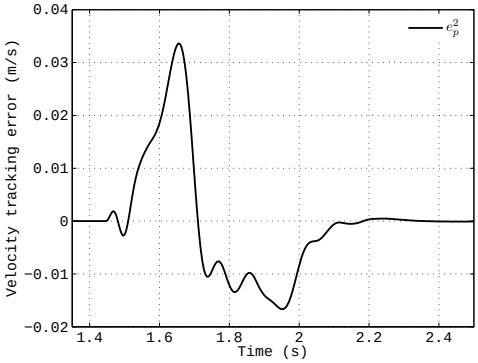

(f) velocity estimation error

Figure 4.8: Estimated versus actual state variables experimental results using the *effort*-based state observer.

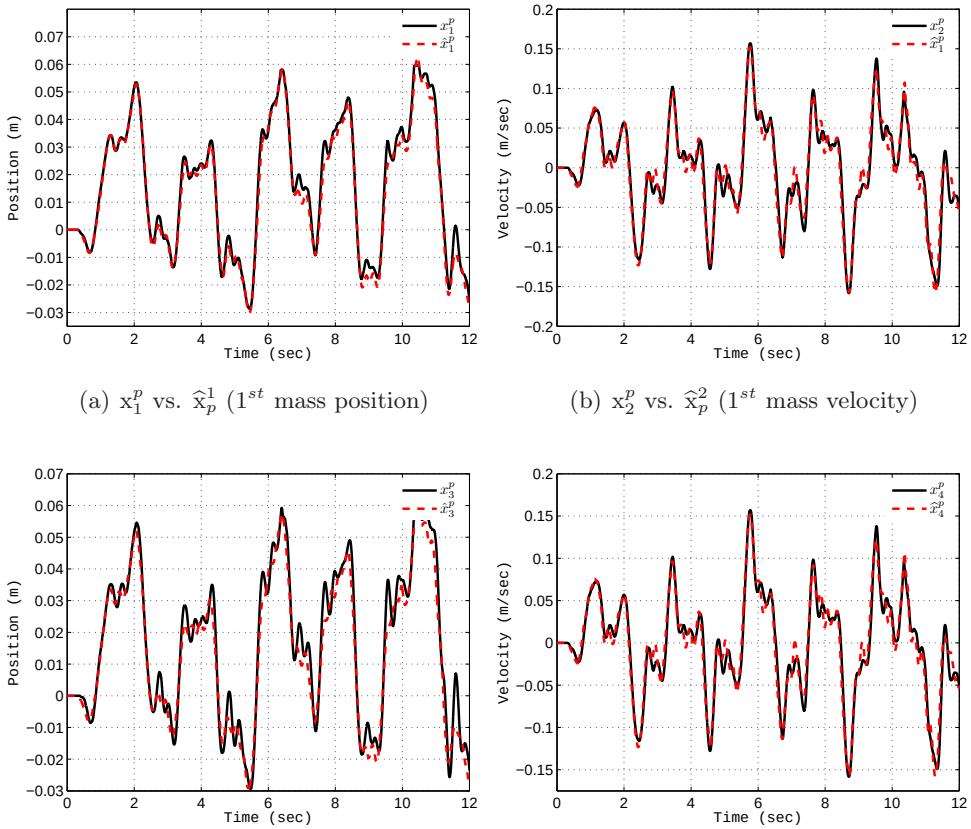

(a) x_1^p vs. $\widehat{\mathrm{x}}_p^1$ (1^{st} mass position)

(b) x_2^p vs. $\widehat{\mathrm{x}}_p^2$ (1^{st} mass velocity)

(c) x_3^p vs. $\widehat{\mathrm{x}}_p^3$ (2^{nd} mass position)

(d) x_1^p vs. $\widehat{\mathrm{x}}_p^4$ (2^{nd} mass velocity)

Figure 4.9: Experimental result of the state estimation through the *effort*-based state observer.

general systems with nonlinear dynamics is investigated. Similarly, estimation error stability is studied along with the robustness of the estimation process.

4.2.1 Observer for Quasi-nonlinear system with linear *effort* mapping

Considering the class of nonlinear dynamical system described by,

$$\dot{\mathrm{x}} = \mathrm{A}\mathrm{x} + \mathrm{B}u + \Phi(\mathrm{x}, u) \tag{4.26}$$

where $\Phi(\mathrm{x}, u)$ is a Lipschitz nonlinearity with a Lipschitz constant $\gamma \in \mathrm{R}^+$, i.e.,

$$\| \Phi(\mathrm{x}, u) - \Phi(\widehat{\mathrm{x}}, u) \|_2 \;\leq\; \gamma \, \| \mathrm{x} - \widehat{\mathrm{x}} \|_2 \tag{4.27}$$

we assume that the *effort* mapping is linear. The *effort*-based state observer for the system (4.26) is,

$$\dot{\widehat{\mathrm{x}}} = \mathrm{A}\widehat{\mathrm{x}} + \mathrm{B}u + \Phi(\widehat{\mathrm{x}}, u) + \mathrm{M}\big(\widehat{e}(u, \mathrm{x}^a) - e(\mathrm{x}^a, \widehat{\mathrm{x}}^p)\big) \tag{4.28}$$

we further assume that the Dirac structure is described by,

$$f^s = e^m = y \quad , \quad f^m = e^s - e^d + u$$

The estimation error dynamics can be shown to be given by,

$$\dot{\mathrm{e}} = \mathrm{A}(\mathrm{x} - \widehat{\mathrm{x}}) + \Phi(\mathrm{x}, u) - \Phi(\widehat{\mathrm{x}}, u) - \mathrm{M}\big[\widehat{e}(u, \mathrm{x}^a) - e(\mathrm{x}^{\mathrm{a}}, \widehat{\mathrm{x}}^p)\big] \tag{4.29}$$

$$= \mathrm{Ae} + \Phi(\mathrm{x}, u) - \Phi(\widehat{\mathrm{x}}, u) - \mathrm{M}\big[e(\mathrm{x}^a, \mathrm{x}^p) - e(\mathrm{x}^a, \widehat{\mathrm{x}}^p) - \big(1 - G(s)\big)\Delta e(\mathrm{x}^a, \mathrm{x}^p)\big]$$

According to the interconnection along the power-port defined by the Dirac structure, the error dynamics can be written as

$$\dot{\mathrm{e}} = \mathrm{Ae} + \mathrm{M}\big[c\mathrm{L}_2 + k\mathrm{L}_1\big]\mathrm{e} + \Phi(\mathrm{x}, u) - \Phi(\widehat{\mathrm{x}}, u) \tag{4.30}$$

therefore, the error dynamics is

$$\dot{\mathrm{e}} = \big(\mathrm{A} + \mathrm{M}\big[c\mathrm{L}_2 + k\mathrm{L}_1\big]\big)\mathrm{e} + \Phi(\mathrm{x}, u) - \Phi(\widehat{\mathrm{x}}, u) \tag{4.31}$$

For exponential stability of the error dynamics, $\big(\mathrm{A}+\mathrm{M}\big[c\mathrm{L}_2+k\mathrm{L}_1\big]\big) < 0$ and $\Phi(\mathrm{x}, u) - \Phi(\widehat{\mathrm{x}}, u) = 0$ have to be satisfied. By considering the following Lyapunov function

$$V = \mathrm{e}^{\mathrm{T}} P \mathrm{e} \tag{4.32}$$

where $P = P^T$ and $P > 0$, the time derivative of (4.32) is,

$$\dot{V} = \big(\mathrm{e}^{\mathrm{T}}\mathcal{A}^{\mathrm{T}} + \big[\Phi(\mathrm{x}, u) - \Phi(\widehat{\mathrm{x}}, u)\big]^{\mathrm{T}}\big)P\mathrm{e} + \mathrm{e}^{\mathrm{T}}P\big(\mathcal{A}\mathrm{e} + \big[\Phi(\mathrm{x}, u) - \Phi(\widehat{\mathrm{x}}, u)\big]\big) \tag{4.33}$$

$$= \mathrm{e}^{\mathrm{T}}\mathcal{A}^{\mathrm{T}}P\mathrm{e} + \big[\Phi(\mathrm{x}, u) - \Phi(\widehat{\mathrm{x}}, u)\big]^{\mathrm{T}}P\mathrm{e} + \mathrm{e}^{\mathrm{T}}P\mathcal{A}\mathrm{e} + \mathrm{e}^{\mathrm{T}}P\big[\Phi(\mathrm{x}, u) - \Phi(\widehat{\mathrm{x}}, u)\big]$$

where

$$\mathcal{A} = \mathrm{A} + \mathrm{M}\big[c\mathrm{L}_2 + k\mathrm{L}_1\big]$$

since

$$\dot{V} = \mathrm{e}^{\mathrm{T}}\big[\mathcal{A}^{\mathrm{T}}P + P\mathcal{A}\big]\mathrm{e} + 2\mathrm{e}^{\mathrm{T}}P\big[\Phi(\mathrm{x}, u) - \Phi(\widehat{\mathrm{x}}, u)\big] \tag{4.34}$$

using (4.27) we obtain

$$2\mathrm{e}^{\mathrm{T}}P\big[\Phi(\mathrm{x}, u) - \Phi(\widehat{\mathrm{x}}, u)\big] \leq 2\gamma \parallel P\mathrm{e} \parallel \parallel \mathrm{e} \parallel \tag{4.35}$$

we further define $a \triangleq 2\gamma \parallel P\mathrm{e} \parallel$ and $b \triangleq \parallel \mathrm{e} \parallel$, then with the algebraic relation $ab \leq \frac{a^2}{4} + b^2$ [Rajamani 1995b], (4.35) can be written as follows

$$2\mathrm{e}^{\mathrm{T}}P\big[\Phi(\mathrm{x}, u) - \Phi(\widehat{\mathrm{x}}, u)\big] \leq \gamma^2\mathrm{e}^{\mathrm{T}}P^{\mathrm{T}}P\mathrm{e} + \mathrm{e}^{\mathrm{T}}\mathrm{e} \tag{4.36}$$

then it can be shown that (4.34) is,

$$\dot{V} = \mathrm{e}^{\mathrm{T}}\big[\mathcal{A}^{\mathrm{T}}P + P\mathcal{A}\big]\mathrm{e} + \gamma^2\mathrm{e}^{\mathrm{T}}P^{\mathrm{T}}P\mathrm{e} + \mathrm{e}^{\mathrm{T}}\mathrm{e} \tag{4.37}$$

$$= \mathrm{e}^{\mathrm{T}}\big[\mathcal{A}^{\mathrm{T}}P + P\mathcal{A} + \gamma^2P^{\mathrm{T}}P + \mathrm{I}\big]\mathrm{e}$$

Therefore, the following inequality has to be satisfied in order to make the Lyapunov function candidate (4.32) negative definite,

$$\mathcal{A}^{\mathrm{T}}P + P\mathcal{A} + \gamma^2 P^{\mathrm{T}}P + \mathrm{I} < 0 \tag{4.38}$$

or equivalently,

$$\mathrm{A}^{\mathrm{T}} + \left[c\mathrm{L}_2 + k\mathrm{L}_1\right]^{\mathrm{T}}\mathrm{M}^{\mathrm{T}}P + P\mathrm{M}\left[c\mathrm{L}_2 + k\mathrm{L}_1\right] + P\mathrm{A} + \mathrm{I} + \gamma^2 P^{\mathrm{T}}P < 0$$

the previous inequalities can be represented using the following Linear matrix inequality through the Schur complement,

$$A - BD^{-1}C < 0 \;\;,\;\; D > 0 \quad \Leftrightarrow \quad \begin{bmatrix} A & B \\ C & D \end{bmatrix} < 0 \tag{4.39}$$

therefore, the previous inequalities can be represented as,

$$\begin{bmatrix} \mathcal{A}^{\mathrm{T}}P + P\mathcal{A} + \mathrm{I} & P^{\mathrm{T}} \\ P & -\frac{1}{\gamma^2}\mathrm{I} \end{bmatrix} < 0 \tag{4.40}$$

and in satisfying the previous inequality we have to search for the *effort*-based state observer vector gain M and the positive definite matrix P such that (4.40) is satisfied. In general, the previous matrix inequality can be used to find the maximum Lipschitz constant for which asymptotic stability of the error dynamics is guaranteed [Rajamani 1995a].

4.2.2 Single-link robot manipulator example

Considering a single-link robot manipulator with flexible joint with torsional spring constant k, the dynamical model of this system is [Perla 2005],

$$J\ddot{\theta}_m - k(\theta_l - \theta_m) = u \tag{4.41}$$

$$I\ddot{\theta}_l + Mgl\sin\theta_l + k(\theta_l - \theta_m) = 0 \tag{4.42}$$

where I and J are the inertias of the actuator and the robot single-link, respectively. θ_m and θ_l are the positions of the actuator and link, M, l and g are the link mass, length and gravitational constant, respectively. For the previous dynamical system we can use an *effort*-based state observer of the form (4.28). Similar to the linear case, the *effort*-force observer has to be designed in order to estimate the feedback-like force or the *effort*-force $k(\theta_l - \theta_m)$ from (4.41). The *effort*-based state observer vector gain has to be selected such that the linear matric inequality (4.40) is satisfied. The state space representation of the dynamical system (4.41) and (4.42) is,

$$\begin{bmatrix} \dot{x}_1 \\ \dot{x}_2 \\ \dot{x}_3 \\ \dot{x}_4 \end{bmatrix} = \begin{bmatrix} 0 & 1 & 0 & 0 \\ -\frac{k}{J} & 0 & \frac{k}{J} & 0 \\ 0 & 0 & 0 & 1 \\ \frac{k}{I} & 0 & -\frac{k}{I} & 0 \end{bmatrix} \begin{bmatrix} x_1 \\ x_2 \\ x_3 \\ x_4 \end{bmatrix} + \begin{bmatrix} 0 \\ \frac{1}{J} \\ 0 \\ 0 \end{bmatrix} u + \begin{bmatrix} 0 \\ 0 \\ 0 \\ -\frac{Mgl}{I}\sin(x_3) \end{bmatrix} \tag{4.43}$$

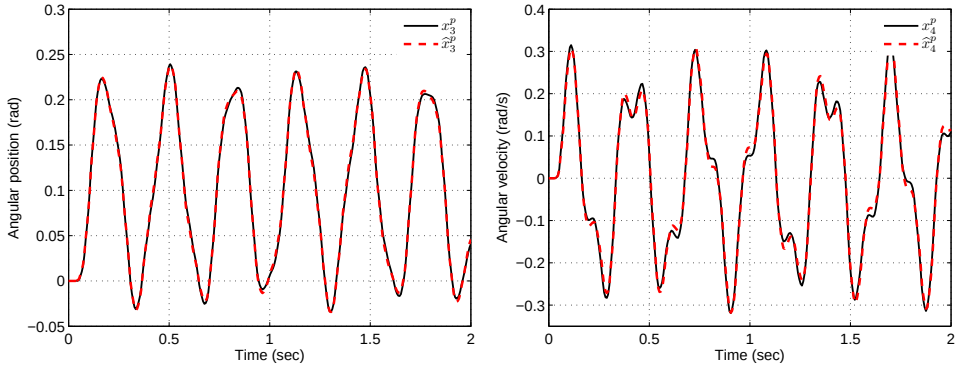

(a) estimated vs actual link position (b) estimated vs actual link angular velocity

Figure 4.10: State estimation results.

in order to further proceed in designing the *effort*-based state observer, we have to put (4.43) in the standard form shown in section 4.1, at which the state variables that are available for measurement can be separated from those that cannot be measured, in addition to revealing the *effort* feedback-like force between their subsystems upon the Dirac structure representation of the *power-conserving* interconnection,

$$f^s = e^m = y \quad , \quad f^m = -e^s + u$$

we obtain,

$$\begin{bmatrix} \dot{\mathrm{x}}^a \\ -- \\ \dot{\mathrm{x}}^p \end{bmatrix} = \left[\begin{array}{c|c} \mathrm{A}^a & \emptyset \\ -- & -- \\ \emptyset & \emptyset \end{array}\right] \begin{bmatrix} \mathrm{x}^a \\ -- \\ \mathrm{x}^p \end{bmatrix} + \left[\begin{array}{c|c} \emptyset & \emptyset \\ -- & -- \\ \emptyset & \mathrm{A}^p \end{array}\right] \begin{bmatrix} \mathrm{x}^a \\ -- \\ \mathrm{x}^p \end{bmatrix} + \begin{bmatrix} \mathrm{B}^a \\ -- \\ \emptyset \end{bmatrix} u$$

$$+ \left[\begin{pmatrix} \emptyset \\ -- \\ \mathrm{B}^p \end{pmatrix} + \begin{pmatrix} \mathrm{B}^{eff} \\ -- \\ \emptyset \end{pmatrix} \right] e(\mathrm{x}^a, \mathrm{x}^p) + \begin{bmatrix} \emptyset \\ -- \\ \Phi(\mathrm{x}, u) \end{bmatrix}$$

therefore,

$$\begin{bmatrix} \dot{x}_1^a \\ \dot{x}_2^a \end{bmatrix} = \begin{bmatrix} 0 & 1 \\ 0 & 0 \end{bmatrix} \begin{bmatrix} x_1^p \\ x_2^p \end{bmatrix} + \begin{bmatrix} 0 \\ 1/J \end{bmatrix} u^a + \begin{bmatrix} 0 \\ 1/J \end{bmatrix} e(\mathrm{x}^a, \mathrm{x}^p) \tag{4.44}$$

$$\begin{bmatrix} \dot{x}_1^p \\ \dot{x}_2^p \end{bmatrix} = \begin{bmatrix} 0 & 1 \\ 0 & 0 \end{bmatrix} \begin{bmatrix} x_1^p \\ x_2^p \end{bmatrix} + \begin{bmatrix} 0 \\ -\frac{1}{I} \end{bmatrix} e(\mathrm{x}^a, \mathrm{x}^p) + \begin{bmatrix} 0 \\ -\frac{Mgl}{I} \sin(x_{p1}) \end{bmatrix} \tag{4.45}$$

From the partitioned representation of the system we can determine the feedback-like *effort*-force from the dynamical subsystem with accessible state variables (4.44) in order to design the *effort*-based state observer to estimate the states of the nonlinear

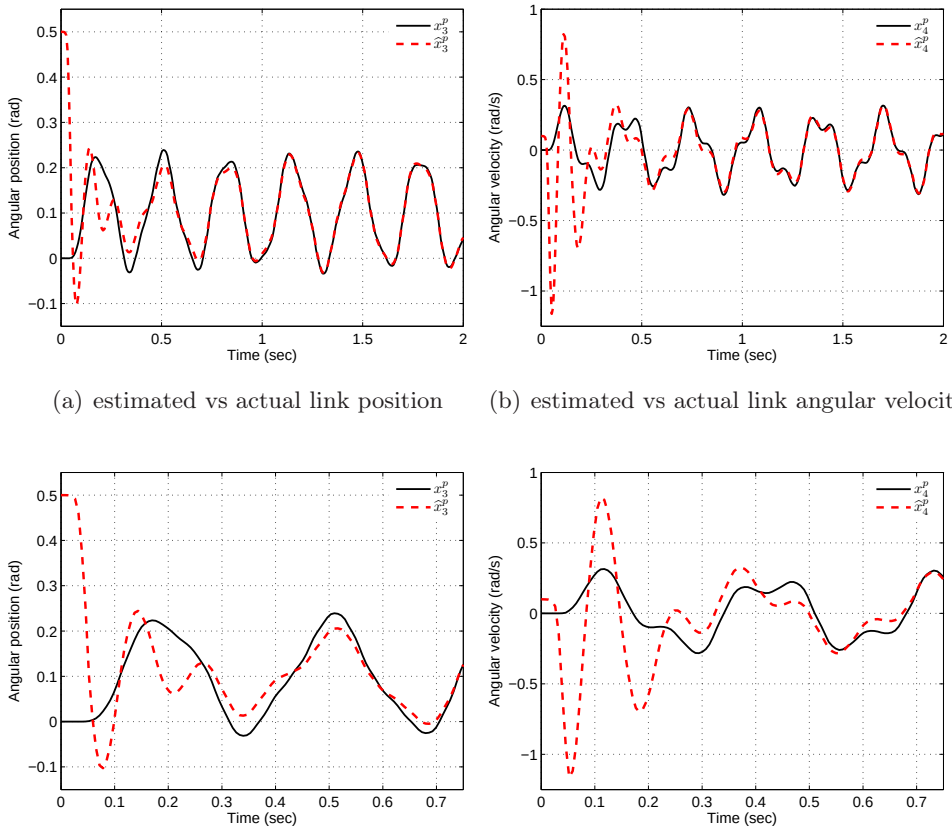

(a) estimated vs actual link position (b) estimated vs actual link angular velocity

(c) magnified plot (d) magnified plot

Figure 4.11: State estimation results in the presence of different initial conditions $\Delta x_3(0) = 0.5\ rad$ and $\Delta x_4(0) = 0.1\ rad/s$.

dynamical subsystem with inaccessible state variables (4.45). Therefore, an *effort*-force observer has to be designed to estimate $e(\mathrm{x}^{\mathrm{a}}, \mathrm{x}^{p})$ using (4.44). As soon as the *effort*-force is estimated, we can design *effort*-based state observer of the form (4.28). Fig. 4.10 illustrates the simulation results of the *effort*-based state observer for the single-link robot manipulator after selecting the observer vector gain M such that the linear matrix inequality (4.40) is satisfied.

In order to further examine the robustness of the *effort*-based state observer, we consider a deviation in the initial conditions of the actual and estimated states. A deviation of 0.5 rad and 0.1 rad/s is added to the estimated angular position and velocity of the single-link manipulator. The simulation results depicted in Fig. 4.11 illustrates how the estimated states converge to the actual ones even in the presence of different initial conditions. Similarly, in Fig. 4.12 illustrates the simulation states estimation results when the deviation between the initial estimated states and actual ones are $-0.5\ rad$ and $0.5\ rad/s$ for the single-link manipulator angular position and angular velocity, respectively. Again the depicted results show satisfactory

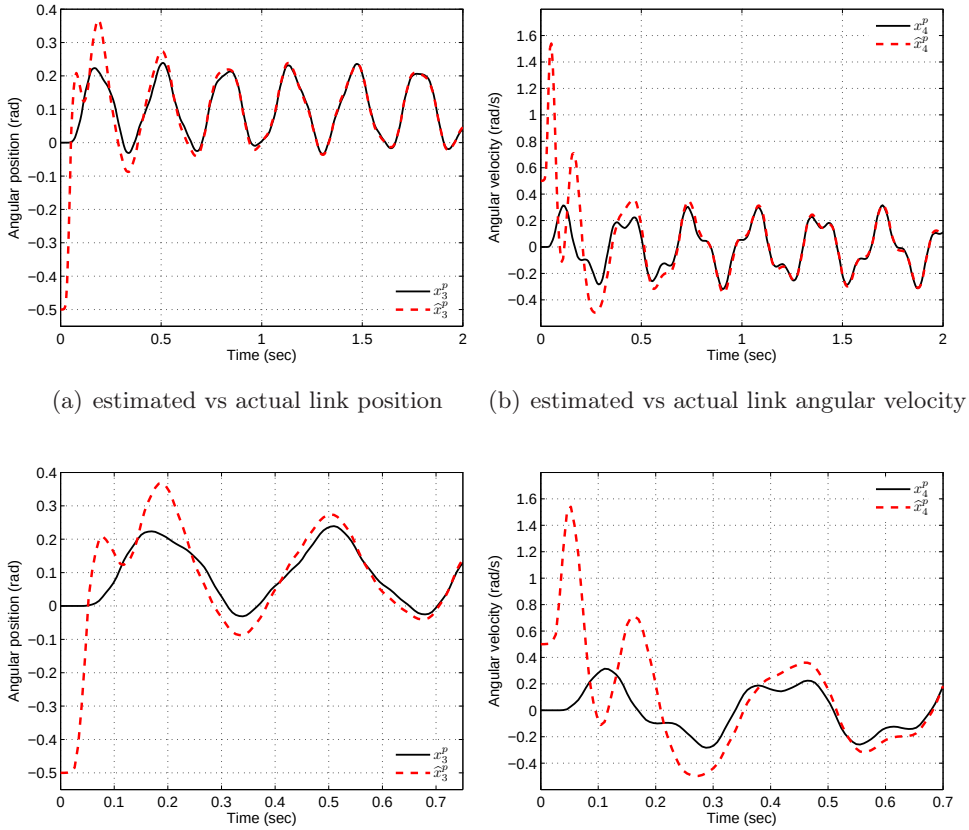

(a) estimated vs actual link position

(b) estimated vs actual link angular velocity

(c) magnified plot

(d) magnified plot

Figure 4.12: State estimation results in the presence of different initial conditions $\Delta x_3(0) = -0.5\ rad$ and $\Delta x_4(0) = 0.5\ rad/s$.

robustness of the observer performance for unknown initial conditions. It is worth noting that using the depicted parameters in Table. 4.2 along with selecting the symmetric positive definite matrix P as unity with the proper dimension, the *energy* based state observer gain vector of $[0.51 \quad 0.01 \quad -0.301 \quad 0.1]$ would satisfy the inequality (4.40). This gain vector along with the scaler gains included in Table. 4.2 are utilized throughout the simulations outlined in this section.

It is commonly agreed that the linear matric inequality can be used in the determination of the vector M such that the Lipschitz constant is maximized, i.e., maximizing the Lipschitz constant can be set as a performance index for an optimization problem constrained with the linear matrix inequality (4.40). This indicates that better results and larger range of robustness and estimation stability can be obtained when the observer gain vector is obtained throughout an optimization procedure.

4.2.3 Observer for Quasi-nonlinear system with nonlinear *effort* mapping

Consider the same dynamical system described by (4.26) except that the interconnection between its dynamical subsystem with inaccessible state variables and another subsystem with accessible state variables is described by a nonlinear function, i.e., the *effort*-force is nonlinear. The *effort*-based state observer in this case can be expressed as follows,

$$\dot{\widehat{\mathrm{x}}} = \mathrm{A}\widehat{\mathrm{x}} + \mathrm{B}u + \Phi(\widehat{\mathrm{x}}, u) + \mathrm{M}\big(e(\mathrm{x}) - e(\widehat{\mathrm{x}})\big) \tag{4.46}$$

here $\Phi(\mathrm{x}, u)$ and $e(\mathrm{x})$ are Lipschitz nonlinearities with Lipschitz constants $\gamma \in \mathrm{R}^+$ and $\beta \in \mathrm{R}^+$, respectively, i.e.,

$$\begin{aligned} \parallel \Phi(\mathrm{x}, u) - \Phi(\widehat{\mathrm{x}}, u) \parallel_2 &\leq \gamma \parallel \mathrm{x} - \widehat{\mathrm{x}} \parallel_2 \\ \parallel e(\mathrm{x}) - e(\widehat{\mathrm{x}}) \parallel_2 &\leq \beta \parallel \mathrm{x} - \widehat{\mathrm{x}} \parallel_2 \end{aligned} \tag{4.47}$$

subtracting (4.26) and (4.46), we obtain the following error dynamics

$$\dot{\mathrm{e}} = \mathrm{A}(\mathrm{x} - \widehat{\mathrm{x}}) + \Phi(\mathrm{x}, u) - \Phi(\widehat{\mathrm{x}}, u) - \mathrm{M}\big(e(\mathrm{x}) - e(\widehat{\mathrm{x}})\big) \tag{4.48}$$

we further define the following Lyapunov function $V = \mathrm{e}^{\mathrm{T}} P \mathrm{e}$ with the same symmetric positive matric P, its time derivative is $\dot{V} = \dot{\mathrm{e}}^{\mathrm{T}} P \mathrm{e} + \mathrm{e}^{\mathrm{T}} P \dot{\mathrm{e}}$ therefore,

$$\dot{V} = \mathrm{e}^{\mathrm{T}}(A^{\mathrm{T}}P + PA)\mathrm{e} + 2\mathrm{e}^{\mathrm{T}} P\big(\Phi(\mathrm{x}, u) - \Phi(\widehat{\mathrm{x}}, u)\big) - 2\mathrm{e}^{\mathrm{T}} P\mathrm{M}\big(e(\mathrm{x}) - e(\widehat{\mathrm{x}})\big) \tag{4.49}$$

it can be shown that

$$2\mathrm{e}^{\mathrm{T}} P\big[\Phi(\mathrm{x}, u) - \Phi(\widehat{\mathrm{x}}, u)\big] \leq 2\gamma \parallel P\mathrm{e} \parallel\parallel \mathrm{e} \parallel \tag{4.50}$$

$$2\mathrm{e}^{\mathrm{T}} P\mathrm{M}\big[e(\mathrm{x}) - e(\widehat{\mathrm{x}})\big] \leq 2\beta \parallel P\mathrm{Me} \parallel\parallel \mathrm{e} \parallel \tag{4.51}$$

therefore,

$$2\mathrm{e}^{\mathrm{T}} P\big[\Phi(\mathrm{x}, u) - \Phi(\widehat{\mathrm{x}}, u)\big] \leq \gamma^2 \mathrm{e}^{\mathrm{T}} P^{\mathrm{T}} P\mathrm{Ae} + \mathrm{e}^{\mathrm{T}}\mathrm{e} \tag{4.52}$$

$$2\mathrm{e}^{\mathrm{T}} P\mathrm{M}\big[e(\mathrm{x}) - e(\widehat{\mathrm{x}})\big] \leq \beta^2 \mathrm{e}^{\mathrm{T}} (P\mathrm{M})^{\mathrm{T}} P\mathrm{Me} + \mathrm{e}^{\mathrm{T}}\mathrm{e} \tag{4.53}$$

using (4.52) and (4.53) in (4.49) we obtain

$$\dot{V} = e^{\mathrm{T}}\big[\mathrm{A}^{\mathrm{T}}P + P\mathrm{A} + \gamma^2 PP - \beta^2 \mathrm{M}^{\mathrm{T}} P^{\mathrm{T}} PM\big]e \tag{4.54}$$

then the following inequality has to be satisfied in order to make the Lyapunov function negative definite

$$\mathrm{A}^{\mathrm{T}}P + P\mathrm{A} + \gamma^2 PP - \beta^2 \mathrm{M}^{\mathrm{T}} P^{\mathrm{T}} P\mathrm{M} < 0 \tag{4.55}$$

Similar to (4.40) the previous inequality can be represented using the Schur complement (4.39) as a linear matrix inequality [Zhu 2002].

4.2.4 Cart-pendulum example

Considering a cart-inverted pendulum system in order to illustrate the validity of the outlined *energy* based state observer for this class of nonlinear dynamical system with nonlinear *effort* feedback-like force. The dynamic equations of this system are [Utkin 1999],

$$(M+m)\ddot{x} + ml\ddot{\theta}\cos\theta - ml\dot{\theta}^2\sin\theta = u \tag{4.56}$$

$$\frac{4}{3}ml\ddot{\theta} + m\ddot{x}\cos\theta - mg\sin\theta = 0 \tag{4.57}$$

M and m are the masses of the cart and the inverted pendulum, respectively. l is the distance from the center of gravity of the link to its attachment point. x represents the coordinate of the cart on the horizontal axis, θ is the rotational angle of the inverted pendulum. u is the input control force. It can be easily shown from the previous model that the interconnection between the cart and the inverted pendulum is governed by a nonlinear function. Therefore, we attempt to estimate the inaccessible state variables of the inverted pendulum using the *energy* based state observer (4.46). Firstly, we have to represent the previous model in the standard partitioned state space representation in order to reveal the incident feedback-like *effort*-force,

$$\begin{bmatrix} \dot{x}_1^a \\ \dot{x}_2^a \end{bmatrix} = \begin{bmatrix} 0 & 1 \\ 0 & 0 \end{bmatrix} \begin{bmatrix} x_1^p \\ x_2^p \end{bmatrix} + \begin{bmatrix} 0 \\ \frac{4}{3k} \end{bmatrix} u + \begin{bmatrix} 0 \\ \frac{m}{k} \end{bmatrix} e(\mathrm{x}^a, \mathrm{x}^p) \tag{4.58}$$

$$k = \frac{4}{3}(M+m) - m\cos^2\theta$$

it can be shown that the incident feedback-like *effort*-force can be expressed as follows

$$e(\mathrm{x}^a, \mathrm{x}^p) = \frac{4}{3}l\dot{\theta}^2\sin\theta - g\cos\theta\sin\theta \tag{4.59}$$

which can be estimated using the *effort*-force observer that can be implemented on system (4.58). The estimated *effort*-force can then be injected onto the *energy* based state observer (4.46) to estimate the inaccessible state variables and outputs of the pendulum subsystem (angular position and velocity). The *energy* based state observer gain vector has to be selected such that the inequality (4.55) is satisfied. Therefore, the problem of designing a state observer for this class of dynamical system is equivalent to the search problem of a vector M and a positive symmetric definite matrix P that satisfy (4.55) assuming that the scaler gains associated with the *effort*-force and disturbance observers are properly determined such that the estimated *effort*-force converges to the actual *effort*-force with minimum amount of phase lag such that the overall robustness of the observer is preserved.

The simulation results of the previous example are illustrated in Fig. 4.13 at which the actual angular position and velocity of the pendulum are plotted versus the estimated ones. The simulation result is obtained in the presence of 18 deg and 3 deg/s difference between the actual and estimated initial conditions in order to

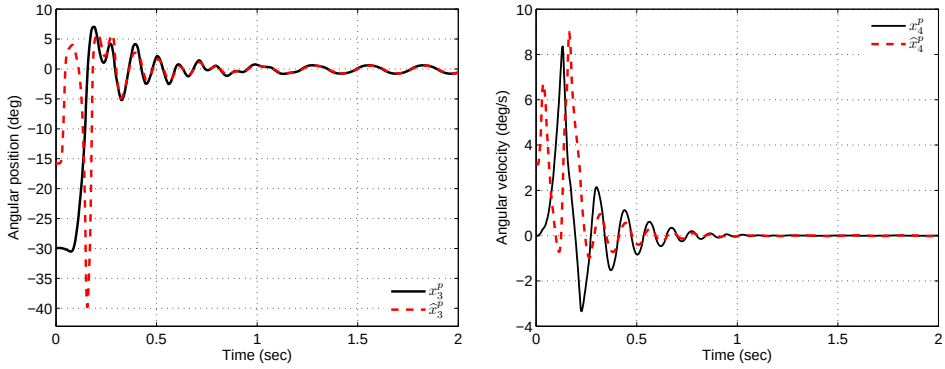

(a) estimated vs actual pendulum angular position

(b) estimated vs actual pendulum velocity

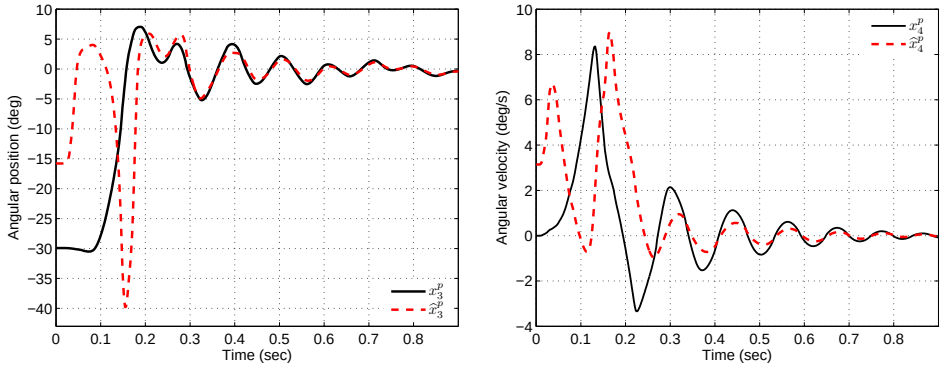

(c) magnified plot

(d) magnified plot

Figure 4.13: State estimation results in the presence of different initial conditions $\Delta x_3(0) = 18\ deg$ and $\Delta x_4(0) = 3\ deg/s$.

examine the robustness of the *energy* based state observer for unknown initial conditions. Fig. 4.14 illustrates a similar simulation result with more severe deviation in the initial conditions in order to further examine the robustness of the outlined state observer. The induced deviation in the initial conditions are 45 deg and $-9\ deg/s$ for the angular initial position and angular initial velocity, respectively. As shown in Fig. 4.14 the estimated states converge after some transient to the actual ones in approximately 0.5 s.

The previous observer is fairly general as it can be implemented on more general forms of nonlinear dynamical systems if certain necessary and sufficient conditions for transforming the more general form of nonlinear system into the Quasi-nonlinear forms we considered so far, are satisfied. In the upcoming subsection, the generality of the *effort*-based state observer formalism is studied.

It is worth noting that using the depicted parameters in Table. 4.2 along with selecting the symmetric positive definite matrix P as unity with the proper dimen-

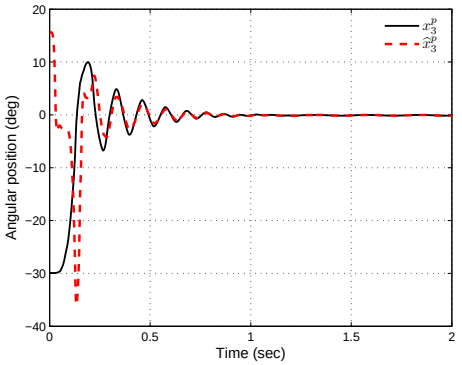

(a) estimated vs actual pendulum position

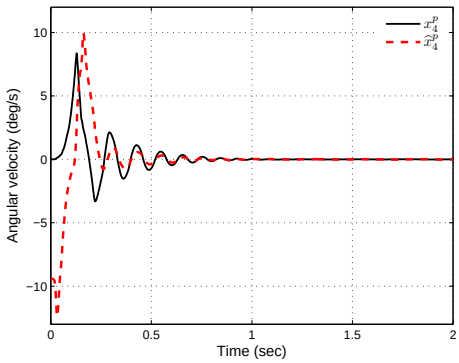

(b) estimated vs actual pendulum angular velocity

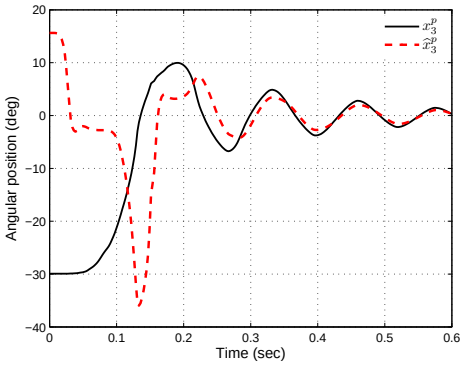

(c) magnified plot

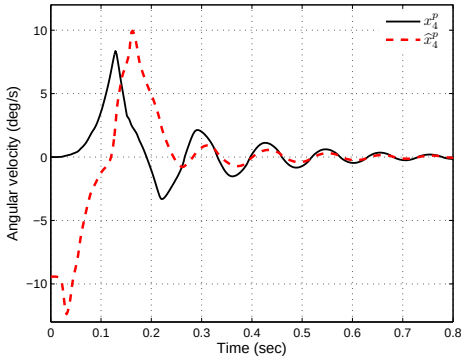

(d) magnified plot

Figure 4.14: State estimation results in the presence of different initial conditions $\Delta x_3(0) = 45\ deg$ and $\Delta x_4(0) = -9\ deg/s$.

sion, the *effort*-based state observer gain vector of [0.1 0.1 0.2 0.1] would satisfy the inequality (4.55). This gain vector along with the scaler gains included in Table. 4.2 are utilized throughout the simulations outlined in this subsection.

4.2.5 Generality of the energy based state observer formalism

Considering a class of nonlinear dynamical systems of the form

$$\dot{x} = f(x,u) \quad , \quad y = h(x) \tag{4.60}$$

where $x \in \mathbb{R}^n$ and $y \in \mathbb{R}^p$ are the states and output vectors respectively. $h : \mathbb{R}^n \mapsto \mathbb{R}$ and $f : \mathbb{R}^n \mapsto \mathbb{R}^n$ are smooth function and vector field, respectively. The

Table 4.2: Simulation parameters

Single-link manipulator	**Parameters**	**Value**	**Unit**
torsional stiffness	k	100	$N.m$
motor inertia	J	0.019	kg
single-link inertia	I	503.96	N/m
gravity constant	g	9.8	m/s^2
link length	L	1.0	m
Cart-inverted pendulum	**Parameters**	**Value**	**Unit**
cart mass	M	1.0	kg
pendulum mass	m	1.0	kg
distance from center of gravity to joint	l	1.0	m
effort-observer gain	g^{eff}	628	rad/s
disturbance force observer gain	g^{dist}	628	rad/s

observability matrix of system (4.60) is,

$$\mathcal{O} = \begin{bmatrix} dh \\ d(L_f h) \\ d(L_f L_f h) \\ \vdots \end{bmatrix} \tag{4.61}$$

where $L_f h$ is the Lie derivative of h with respect to f and can be determined by the following dot product

$$L_f h =< dh, f >= \nabla h.f \tag{4.62}$$

the Jacobian matrix of the transformation T can be expressed as [Hermann 1977],

$$\frac{\partial T}{\partial z} = \left[(ad^0 f, \frac{\partial T}{\partial z_1}), (ad^1 f, \frac{\partial T}{\partial z_1}), (ad^2 f, \frac{\partial T}{\partial z_1})\right] \tag{4.63}$$

where $\frac{\partial T}{\partial z_1}$ is the last column of $\mathcal{O}^{-1}$. Applying the transformation matrix T on system (4.60) we obtain

$$\dot{z} = \mathbf{A}z + \Phi(z, u) \tag{4.64}$$

It should be clear that system (4.64) is similar to the systems we have considered so far throughout this chapter. Therefore, it would be far to say that the class of dynamical system we considered and the proposed *effort*-based state observer for, are fairly general.

4.2.6 Summary and discussion

In order to estimate state variables of dynamical subsystem which does not have any accessible outputs, the *effort*-forces along the *power-conserving* power ports of this system can be conceptually considered as natural feedbacks that can be utilized as basis in the design and realization of the what's called *effort*-based state observers. Due to the dependence of the *effort*-forces on the Dirac structure of the interconnected subsystems, observability is based on the availability of this *effort* variables rather than the outputs. Therefore, necessary and sufficient conditions for observability are derived and it was shown that in order to observe the states of a dynamical subsystem with inaccessible outputs, the *effort*-forces can be conceptually considered as input and the system is observable from the input and *effort*-force pair providing that its eigenvalues are distinct.

The stability of the estimation error dynamics is studied and derived for systems with linear dynamics, Quasi-nonlinear dynamics and for different cases at which the *effort*-feedback-like forces are governed by linear and nonlinear functions. For the systems with linear dynamics necessary and sufficient conditions for the exponential asymptotic stability of the estimation error dynamics are derived. For systems with Quasi-nonlinear dynamics, necessary and sufficient conditions for asymptotic estimation error stability are derived in terms of linear matrix inequalities. These inequalities can be considered as constrains for an optimization problem at which the objective is to maximize the Lipschitz constant in order to obtain the optimum *effort*-based state observer gain vector that provides asymptotic stability of the estimation error for larger range of robustness and estimation stability.

4.3 Hybrid State Observers

4.3.1 Overview

It is often the case that, few state variables of the dynamical system are available for measurement. In this case, the available system outputs can be used along with the estimated feedback-like *effort*-forces in order to realize hybrid state observers or observers at which the estimation error dynamics is enforced to be asymptotically stable by both the measured *flow* variables and the incident feedback-like *effort* variables. Indeed, if the observability pair of a dynamical system is full ranked and its state variables are available for measurement, state observers can be designed and the observer poles can be placed in any desired location within the complex plane. Therefore, it is intuitively clear that in the presence of few measurement from an observable dynamical system, injecting the estimated *effort*-forces onto the observer structure to realize a hybrid state observer would not affect the convergence rate of the state variable reconstruction. However, presence of the feedback-like *effort*-forces allows investigating possibilities of designing reduced order state observers when few measurements are available for measurement.

4.3.2 Observer structure

Consider the linear time-invariant system (4.1), that can be written in the standard form (4.3) and (4.4), here we relax our previous constrains about the inaccessibility of the dynamical system (4.4) state variables. Therefore, we assume that their exist $(n-r-l)$ state variables that can be measured from the dynamical system (4.4). Due to the availability of system state variables along with the natural feedback-like *effort*-force, it would be natural to devise state observer of the following form

$$\dot{\widehat{\mathrm{x}}} = \mathrm{A}\widehat{\mathrm{x}} + \mathrm{B}u + \lambda \mathrm{L}(y - \widehat{y}) + (1-\lambda)\mathrm{M}\big(\widehat{e}(u, \mathrm{x}^a) - e(\mathrm{x}^{\mathrm{a}}, \widehat{\mathrm{x}}^p)\big) \tag{4.65}$$

where $\lambda \in \mathbb{R}^+$ is a small positive parameter ($0< \lambda <1$). The function $e(.)$ can be determined upon the Dirac structure interconnection definition of the interconnected systems (4.3) and (4.4). Here, the reconstruction of the estimated states is performed through the injected *flow* and *effort* based estimation error. When state variables are available for measurement, we can set $\lambda = 1$, whereas in the absence of system (4.4) state variables we can set $\lambda = 0$. In order to study the error dynamics of the Hybrid observer (4.65), the Dirac structure interconnection has to be defined. We assume that the interconnection between systems (4.3) and (4.4) can be modeled with a spring energy storage element and an energy dissipation element. The Dirac structure therefore is

$$f^s = e^m = y \quad , \quad f^m = e^s - e^d + u \tag{4.66}$$

now, we can write the estimation error $\widetilde{\mathrm{x}}$ dynamics

$$\dot{\widetilde{\mathrm{x}}} = A\widetilde{\mathrm{x}} + \lambda \mathbf{L}(C\widetilde{\mathrm{x}} - C\widetilde{\mathrm{x}}) - (1-\lambda)\mathrm{M}(c\dot{\widetilde{x}}_i^p + k\widetilde{x}_i^p) \tag{4.67}$$

where i is the index for the degree of freedom at which the *power-conserving* interconnection occur between the dynamical subsystems with and without accessible state variables for measurements. It can be shown that,

$$\widetilde{x}_i^p = \Big[\underbrace{0 \ \cdots \ 0}_{r} \ \ \underbrace{l_1 \ 0 \ \ldots \ 0}_{n-r}\Big]\mathrm{e} = \mathrm{L}_1\widetilde{\mathrm{x}} \tag{4.68}$$

similarly,

$$\dot{\widetilde{x}}_i^p = \Big[\underbrace{0 \ \cdots \ 0}_{r} \ \ \underbrace{l_2 \ 0 \ \ldots \ 0}_{n-r}\Big]\dot{\mathrm{e}} = \mathrm{L}_2\widetilde{\mathrm{x}} \tag{4.69}$$

where $\mathrm{L}_1 \in \mathrm{R}^{1\times n}$ and $\mathrm{L}_2 \in \mathrm{R}^{1\times n}$, $l_1 = l_2 = 1$ with the index $(r+i)$ and $(r+i+1)$ along the vector L_1 and L_2, respectively. therefore,

$$\dot{\widetilde{\mathrm{x}}} = (A - \lambda \mathbf{L}C)\widetilde{\mathrm{x}} + (1-\lambda)\mathrm{M}\big(c\mathrm{L}_2 + k\mathrm{L}_2\big)\widetilde{\mathrm{x}} \tag{4.70}$$

rearranging the terms, we obtain the following estimation error dynamics

$$\dot{\widetilde{\mathrm{x}}} = \big[(A - \lambda \mathbf{L}C) + (1-\lambda)\mathrm{M}\big(c\mathrm{L}_2 + k\mathrm{L}_2\big)\big]\widetilde{\mathrm{x}} \tag{4.71}$$

If the matrix $\big[(A - \lambda \mathbf{L}C) + (1-\lambda)\mathrm{M}\big(c\mathrm{L}_2 + k\mathrm{L}_2\big)\big]$ was stable, the estimation error will converge to zero for any initial error vector $\widetilde{\mathrm{x}}(0)$, i.e., the estimated states $\widehat{\mathrm{x}}$ will converge to x regardless to the initial value of the estimated and actual states $\widehat{\mathrm{x}}(0)$ and $\mathrm{x}(0)$, respectively.

4.4 Effort based Observer Possible Implementations

4.4.1 Overview

By a careful look at the literature survey of the relevant existing state variables observers, we can conclude that they can be categorized as *flow*-based state observers. Their structure depends on injecting all the possible measured *flow* variables or their integrals onto their structures in order to enforce certain error dynamical behavior. These observer have different structures and consequently different robustness to many aspects such as estimation robustness to unknown initial conditions, model uncertainties and parameter deviations. For instant, the sliding mode state observer was claimed to result in superb system performance in terms of insensitivity to parameter deviations and complete rejection of disturbances. This observer can be, indeed categorized as a *flow*-based state observer as the *flow* variables have to be measured and injected onto its structure. A question naturally rises, is it possible to benefit from the different structures of the relevant existing state observers which commonly agreed to have superb performances when the *flow* are altered with the *effort* variables. briefly, we will consider few well-known observers and examine how to turn them from *flow*-based into *effort*-based state observers.

4.4.2 Luenberger state observer

The well known Luenberger state observer has the following form

$$\dot{\widehat{\mathrm{x}}} = A\widehat{\mathrm{x}} + Bu + L(\mathrm{Y} - \widehat{\mathrm{Y}}) \tag{4.72}$$

Where L is the observer gain matrix which has to be selected such that the matrix $(A - LC)$ is Hurwitz. It was shown throughout this chapter that the previous structure can be preserved while altering the unavailable outputs and state variables Y with the natural feedback *effort*-forces e. However, the error dynamics turned out to be nontrivial. In other words, the error dynamics has a form that depends on the definition of the Dirac structure of the interconnection between the dynamical subsystem with accessible state variables and the other with inaccessible state variables. Nevertheless, it can be easily shown that the interconnection between dynamical systems in terms of Dirac structures is limited to few models. All these models are studied in this chapter in the previous sections with explicit derivations of the error dynamics.

Strictly speaking, if the Dirac structure defines the interconnection in terms of an energy storage element with energy storage function $\frac{1}{2}kx^2$, stable error dynamics can be obtained if the matrix $(\mathrm{A}+k\mathrm{M}L)$ is Hurwitz. Similarly, if the Dirac structure describe the interconnection in terms of an energy storage element along with the constitutive relation $e = z(f) = cf$, then stable error dynamics can be obtained if the matrix $\mathrm{A}+\mathrm{M}\left[c\mathrm{L}_2+k\mathrm{L}_1\right]$ is Hurwitz. Therefore, the class of observers represented in the Luenberger form can be simply altered to be *effort*-based when states or outputs of a dynamical subsystem are not available for measurement.

The previous observer structure based on the *effort* variable was examined throughout this chapter and showed satisfactory robustness in terms of unknown initial condition and model uncertainties using experiments and simulation results

4.4.3 High gain state observer

Many mechanical systems can be represented by the following form

$$\dot{x}_1 = x_2 \quad , \quad \dot{x}_2 = f(x_1, x_2, u) \quad , \quad y = x_1 \tag{4.73}$$

the high-gain observer for such system is,

$$\dot{\widehat{x}}_1 = \widehat{x}_2 + \frac{k_1}{\varepsilon}(y - \widehat{y}) \quad , \quad \dot{\widehat{x}}_2 = \frac{k_2}{\varepsilon^2}(y - \widehat{y}) \quad , \quad \widehat{y} = \widehat{x}_1 \tag{4.74}$$

where $\varepsilon \in \mathbb{R}^+$ is a small positive parameter ($0< \varepsilon <1$), $k_1 \in \mathbb{R}^+$ and $k_2 \in \mathbb{R}^+$ are positive constants that must be chosen such that,

$$\begin{bmatrix} -k_1 & 1 \\ -k_2 & 0 \end{bmatrix} < 0$$

under the previous condition and the transformation ($\widetilde{z}_1 = \widetilde{x}_1$, $\widetilde{z}_2 = \varepsilon \widetilde{x}_2$), the estimation error $\widetilde{x} = x - \widehat{x}$ dynamics can be seen as

$$\varepsilon \dot{\widetilde{z}} = A\widetilde{z} + \varepsilon^2 B f(\widetilde{z}_1, \widetilde{z}_2, u) \quad , \quad B = [0 \;\; 1]^{\mathrm{T}} \tag{4.75}$$

Ideally, it can be easily shown from the error dynamics that the gains of the observer should be selected large enough to achieve convergence of the estimated states to the actual ones. However, benefits of the previous observer are limited due to the associated sensor noise ζ with the measured output y, Therefore, the observer has to be written as

$$\dot{\widehat{x}}_1 = \widehat{x}_2 + \frac{k_1}{\varepsilon}((y+\zeta) - \widehat{y}) \;,\; \dot{\widehat{x}}_2 = \frac{k_2}{\varepsilon^2}((y+\zeta) - \widehat{y}) = \frac{k_2}{\varepsilon^2}(y - \widehat{y}) + \frac{k_2}{\varepsilon^2}\zeta \;,\; \widehat{y} = \widehat{x}_1 \tag{4.76}$$

which indicates that the inevitable sensor noise will propagate to the estimated state variables. Although, a switching gain approach was proposed in [Ahrens 2009] which allows using high gain when the estimation error is large for fast reconstruction at the cost of larger measurement noise error, and when the output error becomes small the observer gains is switched to smaller values to balance the error due to model uncertainty and measurement noise. we further consider solving the problem by altering the *flow* variables measurements with the natural feedback *effort*-forces.

It should be at least intuitively clear that the noise associated with the estimated feedback-like *effort*-forces is much less than the noise associated with the measured *flow* variables. Therefore, the *flow*-based high gain observer performance can be enhanced if the *flow* variables are altered with the *effort* variables. However, the main application for this procedure is when measurements cannot be made from a dynamical subsystem.

4.4.4 Sliding mode state observer

For a system with linear time invariant dynamics, the sliding mode state observer can be expressed as,

$$\dot{\mathrm{x}} = A\mathrm{x} + Bu + Lv(\widehat{x}_1 - x_1) \tag{4.77}$$

here, the output $y = x_1$ and $L \in \mathbb{R}^n$ is an observer gain vector, $v : R \longmapsto R$ is a nonlinear function of the first state measured error. Therefore, the error $\mathrm{e} = \widehat{\mathrm{x}} - \mathrm{x}$ dynamics is

$$\dot{\mathrm{x}} = A\mathrm{e} + Lv(\widehat{x}_1 - x_1) = A\mathrm{e} + Lv(e_1) \tag{4.78}$$

we define the sliding mode switching function $\sigma \triangleq e_1 = \widehat{x}_1 - x_1$, to attain the sliding mode $\sigma\dot{\sigma} < 0$ for all x, to ensure that, we can select $v(\sigma) = Msgn(\sigma)$, where $M > \max\{|a_{11}e_1 + A_{12}\mathrm{e}_2|\}$. e_2 is the estimation error vector not including the first state estimation error. Similarly, in the absence of the *flow* variable measurements or their integrals for a dynamical subsystem, we can simply alter these variables with the *effort* variables.

4.4.5 Summary and discussion

The superb performance of the *flow*-based state observers such as sliding mode and high gain observers can be preserved if the *flow* variables are altered with the *effort* variables. This can be performed when dynamical subsystem states are inaccessible or cannot be measured for certain reasons. Possibility or altering the *flow* variables to *effort* variable for the Luenberger state observer was studied in details and validated with experimental results. The stability margins of the *effort*-based state observer were investigated and showed satisfactory tolerances for both parameter deviation and induced observers phase lags in terms of gain and phase margins.

The noise amplification and noise propagation on the estimated states problems associated with the high gain state observer can be avoided if the *effort* variables are utilized instead of the measured *flow* variables. This, however, needs to be verified both theoretically and experimentally.

Chapter 5

Motion Control of Systems with Inaccessible Outputs

IT is often the case that, sensors have to be embedded with any dynamical plant in order to realize the feedback control system. However, there exist systems at which making measurement is problematic or even measurements cannot be made at all. Microsystems and micromanipulation are applications at which measurements are problematic due to the limited workspace at which specific operation has to be performed. It is commonly agreed, as well that making measurements for these applications prevent them from getting automated [Savia 2009]. Therefore, motion in micro scale is considered along with the presence of flexibility and non-collocation. In the sequel, the *energy* based state observer is realized in order to estimate state variables of a dynamical system that is conceptually considered to have inaccessible state variables or outputs.

5.1 Effort Observer based Motion Control

The *effort*-based state observer structure consists of three observers in cascade, the disturbance force observer, the *effort*-force observer and the Luenberger *effort*-based state observer. Each of these observer induces certain amount of phase lag which has to be considered when the *effort*-based state observer is utilized in realizing control systems as shown in Fig. 5.1. In general, the *effort*-based state observer has to be twice faster than the control system regardless to the amount of phase lag induced by each single observer within the overall *effort*-based state observer.

As shown in Fig. 5.1, the *effort*-based state observer makes all the observable state variables of the dynamical system available. Therefore, the state feedback control can be realized. Most importantly, the optimal linear control law requires measuring or estimating each and every state variable. However, in practice it is difficult to measure every state variable, and thus the optimal control is not widely accepted. Therefore, in the upcoming section we will show how to realize the optimal control law through the *effort*-based state observer. For a linear time invariant system, the *effort*-based state observer based control system can be expressed as follows,

$$\dot{\mathrm{x}} = A\mathrm{x} - B\mathrm{K}\hat{\mathrm{x}} + B\mathrm{K}\mathrm{x} - B\mathrm{K}\mathrm{x} \tag{5.1}$$

here, we assumed that an *effort*-based state observer state feedback controller is

utilized with control matrix gain K, it can be shown that

$$\dot{\mathrm{x}} = (A - B\mathrm{K})\mathrm{x} + B\mathrm{K}\mathrm{e} \tag{5.2}$$

it has been shown in the previous chapter that, if the Dirac structure between the two interconnected subsystems, one of which has state variables with inaccessible state variables, was defined as,

$$f^s = e^m = y \quad , \quad f^m = e^s - e^d + u \tag{5.3}$$

then the estimation error dynamics can be shown expressed as,

$$\dot{\mathrm{e}} = \big[A + \mathrm{M}\big(c\mathrm{L}_2 + k\mathrm{L}_1\big)\big]\mathrm{e} = \mathcal{A}\mathrm{e} \tag{5.4}$$

which is, along with (5.2) can be written in the following matrix form,

$$\left[\begin{array}{c} \dot{\mathrm{x}} \\ -- \\ \dot{\mathrm{e}} \end{array}\right] = \left[\begin{array}{c|c} A - B\mathrm{K} & B\mathrm{K} \\ -- & - - - - - - - \\ \emptyset & A + \mathrm{M}\big(c\mathrm{L}_2 + k\mathrm{L}_1\big) \end{array}\right] \left[\begin{array}{c} \mathrm{x} \\ -- \\ \mathrm{e} \end{array}\right]$$

which describes the *effort*-based state observer based control system dynamics, its characteristic equation is of the following form,

$$\left|\begin{array}{cc} s\mathrm{I} - A + B\mathrm{K} & -B\mathrm{K} \\ \emptyset & s\mathrm{I} - \mathrm{A} - \mathrm{M}\big(c\mathrm{L}_2 + k\mathrm{L}_1\big) \end{array}\right| = \emptyset \tag{5.5}$$

or equivalently,

$$\mid s\mathrm{I} - A + B\mathrm{K} \mid\mid s\mathrm{I} - A - \mathrm{M}\big(c\mathrm{L}_2 + k\mathrm{L}_1\big) \mid = \emptyset$$

the previous characteristic equation indicates that the pole placement of the control system and the pole placement of the observer are independent of each other. In addition, we have to derive the transfer function of the *effort*-based state observer based control system in order to achieve stability of the entire system through the controller and observer gains. The dynamical equation of the *effort*-based state observer based on (5.3) is,

$$\dot{\widehat{\mathrm{x}}} = \big(A - B\mathrm{K} - \mathrm{M}(k\mathrm{L}_1 + c\mathrm{L}_2)\big)\widehat{\mathrm{x}} - \mathrm{M}\big(k\mathrm{L}_1 + c\mathrm{L}_2\big)\mathrm{x} \tag{5.6}$$

by taking the Laplace transform of (5.6), assuming zero initial conditions, we obtain the following expression for $\widehat{\mathrm{X}}(s)$,

$$\widehat{\mathrm{X}}(s) = -\big[s\mathrm{I} - A + B\mathrm{K} + \mathrm{M}(k\mathrm{L}_1 + c\mathrm{L}_2)\big]^{-1}\mathrm{M}(k\mathrm{L}_1 + c\mathrm{L}_2)\mathrm{X}(s) \tag{5.7}$$

therefore, the transfer function of the *effort*-based state observer based control system when a feedback controller is utilized is,

$$\frac{\mathrm{U}(s)}{\mathrm{X}(s)} = \mathrm{K}\big[s\mathrm{I} - A + B\mathrm{K} + \mathrm{M}(k\mathrm{L}_1 + c\mathrm{L}_2)\big]^{-1}\mathrm{M}(k\mathrm{L}_1 + c\mathrm{L}_2) \tag{5.8}$$

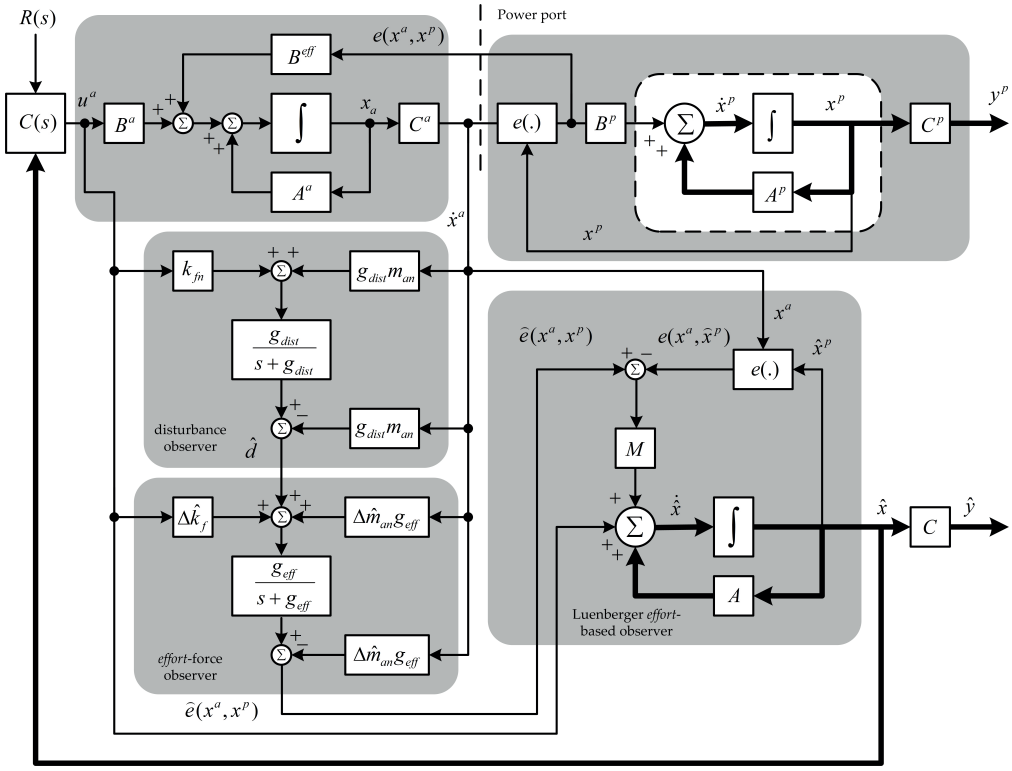

Figure 5.1: *Effort*-based state observer based control system.

which has to be stable through the state feedback gain matrix K and the *effort*-based state observer gain vector M. Here, the other *effort*-based state observer gains are assumed to be selected such that the convergence of the disturbance and *effort*-force observers is fast enough such that the estimated *effort*-force converges to the actual one, this in turn allows realizing the simple transfer function (5.8) without including the other observer dynamics.

In order to realize the control system from the estimated states obtained through the *effort*-based state observer, we consider a dynamical system with 3 degrees of freedom ($n - r = 3$), non of its states are available for measurements. This system is attached via an spring energy storage element to another subsystem, namely an actuator from which a single measurement can be determined. This measurement can be either the actuator position or velocity. The reference supplied reference current to the actuator is also known and used in the realization of the *effort*-force observer. The dynamical system with inaccessible outputs consists of three degrees of freedom connected to each other via spring energy storage elements as shown in the experimental setup depicted in Fig. 5.2. Firstly, the *effort*-based state observer is realized and its optimum vector gain is determined along with its scaler gains. As soon as the *effort*-based state observer is realized, it would be natural to devise a motion control law to position any of the non-collocated masses along the dynamical system of the form

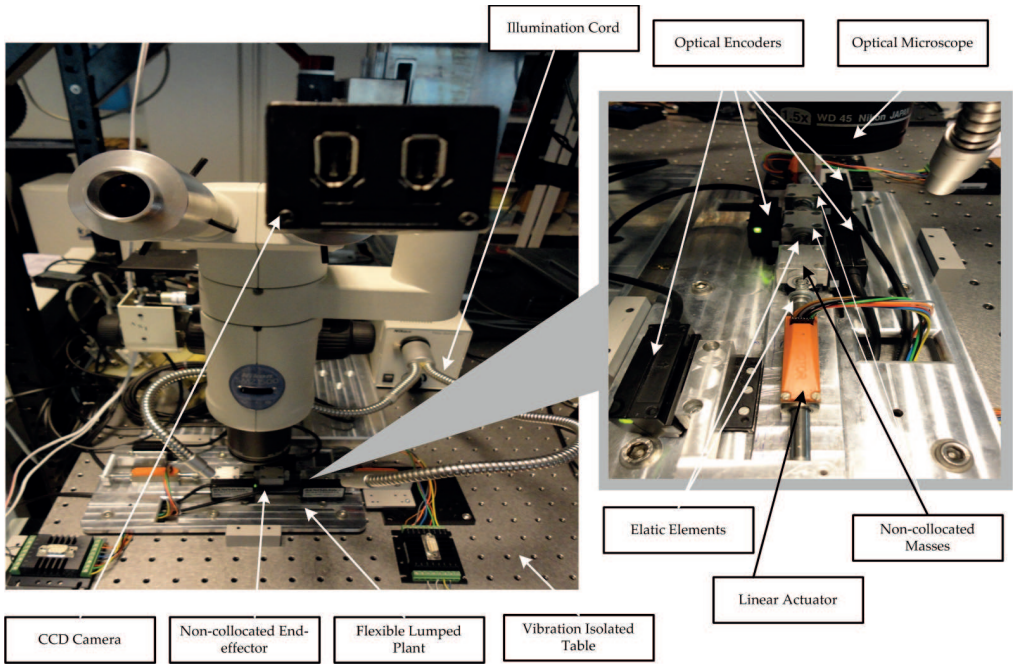

Figure 5.2: Experimental setup consists of a microsystems with multiple degree of freedom dynamical system.

$$u = -\mathrm{K}\widehat{\mathrm{x}} + \frac{1}{k_{fn}}\widehat{d} \tag{5.9}$$

where the first term is a regulating input based on the estimated states ($\widehat{\mathrm{x}}$) obtained through the *effort*-based state observer, the second term is a disturbance suppression control input for the attaintment of robustness. The state feedback gain vector K can be determined through a regular pole placement procedure. k_{fn} is the nominal actuator force constant. Such controller can be used to precisely position any of the non-collocated points along the 3 degree of freedom flexible system to a target position based on the estimated feedback-like *effort*-force rather than having many sensors attached to the system.

The experimental results of controlling the second non-collocated mass along the 3 degree of freedom system through the control input (5.9) for both measurements and estimation based control. Measurements are used in the realization of the controller (5.9) and compared when the estimated states obtained through the *effort*-based state observer are used instead of the actual measurements. Similarly, the control result of the third non-collocated mass is depicted in Fig. 5.3-b for a reference input of 300 μm. It can be easily shown that for the same controller gains and initial conditions, the *effort*-based state estimation and control is more oscillatory than the measurement based controller during the transient period. The oscillatory response of the estimation based control result is due to the dependence of the *effort*-based state observer on consecutive number of observers at which the *effort*-force has to be accurately modeled and estimated. The illustrated results indicates that the

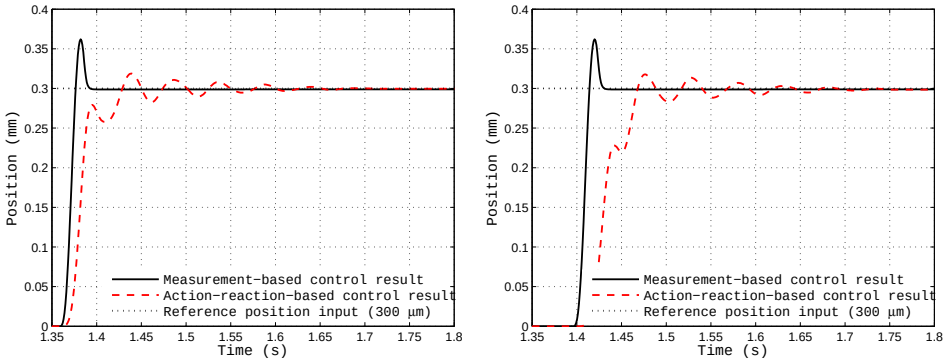

(a) second non-collocated mass position control (b) third non-collocated mass position control

Figure 5.3: Sensor based motion control versus *effort*-based state observer based motion control results to a 300 μm reference input experimental result.

estimated *effort*-force converge to the actual ones in the steady state not in the transient. Therefore, a higher order *effort*-observer has to be used in order to better model and estimate the *effort*-force during both transient and steady state.

5.1.1 Stability margins

Indeed, we have to examine the stability margins of the control system especially when the feedback control system is realized through the estimated states obtained by the *effort*-based state observer. The previous experimental results depicted in Fig. 5.3 illustrate both performances of the sensor based controller versus the *effort*-based state observer based controller for the same controller gains and experimental parameters. As shown in Fig. 5.3, the performance of the sensor based controller is much better in the sense of settling time, whereas the *effort*-based state observer based controller exhibits oscillatory response for the same controller gains. Therefore, stability margins have to be analyzed. It is at least intuitively clear that due to the structure of the *effort*-based state observer, certain amount of phase lag is added to the control system. The *effort*-based state observer consists of three observers in cascade, a disturbance force observer, an *effort*-force observer and a Luenberger-like *effort*-based state observer. Each of these observer induces certain amount of phase lag into the open loop transfer function which affects the overall stability of the closed loop system. Therefore, the key feature in examining the stability of the *effort*-based state observer based control system is its phase margin.

Considering the same dynamical system at which the experiments are performed which consists of three degrees of freedom and attached to an actuator via a spring energy storage element. Here, due to the non-collocated nature of this system and its single input multiple output structure, we have to examine the difference for each degree of freedom individually. Fig. 5.4 illustrates the phase and gain margin for the sensor and *effort*-based state observer based control system. The phase margin

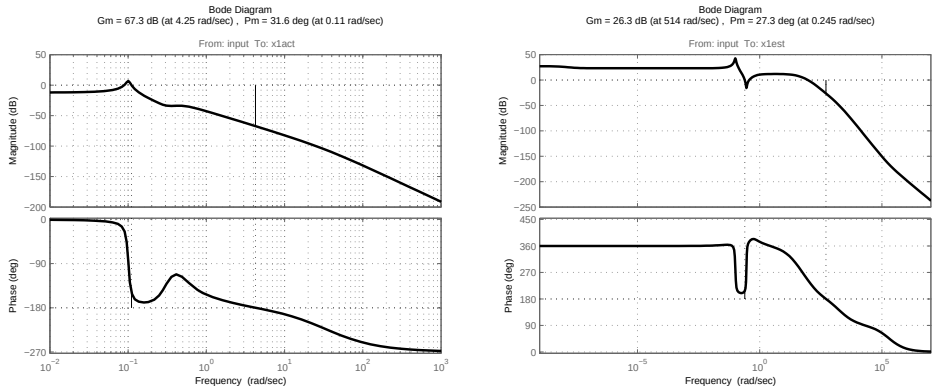

(a) $PM = 31\ deg$ (b) $PM = 27\ deg$

Figure 5.4: Stability margins of the sensor versus *effort*-based control system for controlling the first non-collocated mass.

of the sensor based control system is 31 *deg* while the *effort*-based state observer based control system has a phase margin of 27 *deg*. This indicates that the sensor based control has better stability over the *effort*-based observer based controller. This also explains the experimental behavior illustrated in Fig. 5.3 at which the *effort*-based control system is closer to instability while the sensor based controller is more stable due to its higher phase margin.

We have to further examine stability of the second non-collocated mass. Due to the non-collocation and the presence of more energy storage elements between the input and the second mass the system is naturally expected to be more unstable. Fig. 5.5 illustrates the stability margins when control system is required to position the second non-collocated mass. The phase margin of the sensor based control system is dropped to $PM = 14\ deg$ while the phase margin of the *effort*-based state observer based control system becomes $PM = 8.2\ deg$ and indeed such mass became harder to control.

Similarly, when the third non-collated mass of the dynamical system is required to be positioned, more energy storage elements would be trapped between the input and the sensor location. The phase margin of the sensor based control system in this case turned out to be 12 *deg* and for the *effort*-based state observer based controller is 3.8 *deg*. Therefore, the *effort*-based controller of the third non-collocated mass is very close to instability not only because of the phase lag induced by the *effort*-based state observer but also because of the non-collocated nature of this point from the control input.

It can be easily concluded that the *effort*-based state observer induces certain amount of phase lag into the control which can cause instability and poor performance in comparison to the sensor based controller. This also explains one important tradeoff for the outlined observer, i.e., the accuracy of estimation can be enhanced by increasing the order of each observer associated with the overall *effort*-based

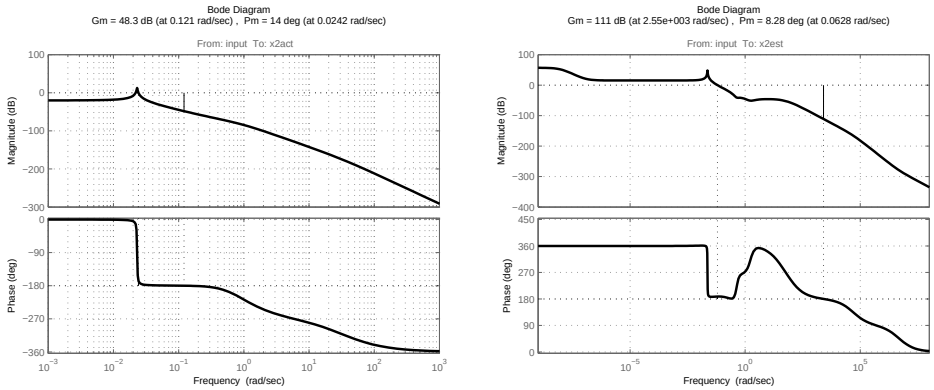

(a) $PM = 14\ deg$ (b) $PM = 8.2\ deg$

Figure 5.5: Stability margins of the sensor versus *effort*-based control system for controlling the second non-collocated mass.

state observer but with the cost of stability as the induced phase lag would increase and result in less phase margin for the control system. It is also worth noting that the decreased stability margins from the first non-collocated mass to the third non-collocated is due to the migration of the virtual sensor (*effort*-based state observer) along the system from one collocated point to another. This result in decreasing the number of zeros of the closed loop transfer functions which results in instability. In other words, for the control result depicted in Fig. 5.4 the system has few zeros that stabilize the system, whereas, the system depicted in Fig. 5.5 has fewer zeros and the system in Fig. 5.6 has no zeros. Therefore, migrating the sensor along the system toward the last non-collocated point has a tendency toward instability.

5.1.2 Summary and discussion

Due to the structure of the *effort*-based state observer at which there exists three observers in cascade. The phase lag induced by each affects the stability of the control system when the estimated states obtained through the *effort*-based state observer are used to realize the feedback control system. It was shown that the phase margin of the sensor based control system is larger than the *effort*-based state observer based controller. Experimentally, this was also shown in Fig. 5.3 where the sensor based controller has shorter settling time over the observer based controller which exhibits oscillatory response for the same controller gains. This indicates that the *effort*-based state observer has to be designed properly such that the induced phase lag does not deteriorate the performance or possibly result in instability.

It was also shown that the control system can be designed independently to the design of the *effort*-based state observer as the characteristic equation of the *effort*-based observer based control system (5.5) consists of poles due to the pole placement control design that are independent of the poles due to the observer design. In

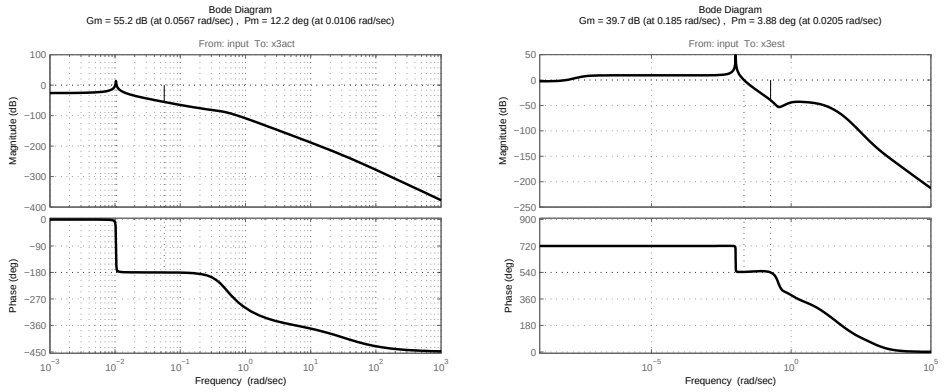

(a) $PM = 12\ deg$ (b) $PM = 3.8\ deg$

Figure 5.6: Stability margins of the sensor versus *effort*-based control system for controlling the second non-collocated mass.

addition, the transfer function of the *effort*-based state observer for certain Dirac structure representation was derived without considering the dynamics of the *effort*-force observer and the disturbance force observers for simplicity.

5.2 Effort Observer based Optimal Motion Control

The optimal linear control laws require the measurement of each and every state variable. However, in practice it is difficult to measure every state variable, and thus the optimal control is not widely accepted. However, the *effort*-based state observer can be utilized in order to provide every unavailable state variable for measurement as discussed in the previous section.

5.2.1 Set-point optimal control

Assuming that certain process is described by the following state equation

$$\dot{\mathbf{x}}(t) = \mathbf{a}(\mathbf{x}(t), \mathbf{u}(t), t) \tag{5.10}$$

which can be written in terms of the estimated states obtained through the following *effort*-based state observer

$$\dot{\widehat{\mathbf{x}}} = \mathbf{a}(\widehat{\mathrm{x}}(t), \mathrm{u}(t), t) + \mathrm{M}\big(\widehat{e}(u, \mathrm{x}^a) - e(\mathrm{x}^{\mathrm{a}}, \widehat{\mathrm{x}}^p)\big) \tag{5.11}$$

or

$$\dot{\widehat{z}} = \mathbf{A}\widehat{z} + \Phi(\widehat{\mathrm{z}}, u) + \mathrm{M}\big(\widehat{e}(u, \mathrm{z}^a) - e(\mathrm{z}^{\mathrm{a}}, \widehat{\mathrm{z}}^p)\big) \tag{5.12}$$

as follows

$$\dot{\widehat{\mathbf{x}}}(t) = \mathbf{a}(\widehat{\mathbf{x}}(t), \mathbf{u}(t), t) \tag{5.13}$$

which has to be controlled to minimize the performance measure

$$\mathbf{J} = h(\widehat{\mathbf{x}}(t_f), t_f) + \int_{t_0}^{t_f} g(\widehat{\mathbf{x}}(\tau), \mathbf{u}(\tau), \tau) d\tau, \tag{5.14}$$

where h and g are specified function, t_0 and t_f are fixed, and τ is the dummy variable on integration. It can be shown that the optimal *effort*-observer based control law can be determined by solving the following Hamilton-Jacobi equation

$$\mathbf{J}_t^*(\widehat{\mathbf{x}}(t), t) + \mathscr{H}\big(\widehat{\mathbf{x}}(t), \mathbf{u}^*(\widehat{\mathbf{x}}(t), J_x^*, t), J_{\mathrm{x}}^*, t\big) = 0 \tag{5.15}$$

$$\mathscr{H}(\widehat{\mathbf{x}}(t), u(t), J_{\mathrm{x}}^*, t) \triangleq g(\widehat{\mathbf{x}}(t), u(t), t) + J_{\mathrm{x}}^{*T}\big[\mathbf{a}(\widehat{\mathbf{x}}(t), \mathbf{u}(t), t)\big] \tag{5.16}$$

For a linear plant dynamics and quadratic performance criteria, (5.13) and (5.14) can be expressed as

$$\dot{\mathbf{x}}(t) = \mathbf{A}\mathbf{x}(t) + \mathbf{B}\mathbf{u}(t) \tag{5.17}$$

$$\mathbf{J} = \frac{1}{2}\widehat{\mathbf{x}}^{\mathrm{T}}(t_f)\mathbf{H}\widehat{\mathbf{x}}(t_f) + \int_{t_0}^{t_f} \frac{1}{2}\big[\widehat{\mathbf{x}}^{\mathrm{T}}(t)\mathbf{Q}\widehat{\mathbf{x}}(t) + \mathbf{u}^{\mathrm{T}}(t)\mathbf{R}\mathbf{u}(t)\big] dt \tag{5.18}$$

$\mathbf{H} = \mathbf{H}^{\mathrm{T}}$, $\mathbf{H} \geq 0$ and $\mathbf{Q} = \mathbf{Q}^{\mathrm{T}}$, $\mathbf{Q} \geq 0$ are real symmetric positive semi-definite matrices, $\mathbf{R} = \mathbf{R}^{\mathrm{T}}$, $\mathbf{R} > 0$ is a real symmetric positive definite matrix. We first formulate the Hamiltonian [Sussmann 1997]:

$$\begin{aligned} \mathscr{H}(\widehat{\mathbf{x}}(t), u(t), J_{\mathrm{x}}^*, t) \;=\; & \frac{1}{2}\widehat{\mathbf{x}}^{\mathrm{T}}(t)\mathbf{Q}\widehat{\mathbf{x}}(t) + \frac{1}{2}\mathbf{u}^{\mathrm{T}}(t)\mathbf{R}\mathbf{u}(t) \\ & + \mathbf{J}_t^{*\mathrm{T}}(\widehat{\mathbf{x}}(t), t)\big[\mathbf{A}\mathbf{x}(t) + \mathbf{B}\mathbf{u}(t)\big] \end{aligned} \tag{5.19}$$

A necessary condition for $\mathbf{u}(t)$ to minimize $\mathscr{H}$ is that $\frac{\partial \mathscr{H}}{\partial u} = 0$; thus

$$\frac{\partial \mathscr{H}}{\partial \mathbf{u}}(\mathbf{x}(t), \mathbf{u}(t), J_{\mathbf{x}}^*, t) = \mathbf{R}\mathbf{u}^*(t) + \mathbf{B}^{\mathrm{T}}\mathbf{J}_{\mathrm{x}}^*(\widehat{\mathbf{x}}(t), t) = 0 \tag{5.20}$$

solving (5.20) for $\mathbf{u}^*(t)$ gives

$$\begin{aligned} \mathbf{u}^*(t) \;&=\; -\mathbf{R}^{-1}\mathbf{B}^{\mathrm{T}}\mathbf{J}_{\mathrm{x}}^*(\widehat{\mathbf{x}}(t), t) \\ &=\; -\mathbf{R}^{-1}\mathbf{B}^{\mathrm{T}}\mathbf{K}\widehat{\mathbf{x}}(t) \end{aligned} \tag{5.21}$$

$$\dot{\mathbf{K}} + \mathbf{Q} - \mathbf{K}\mathbf{B}\mathbf{R}^{-1}\mathbf{B}^{\mathrm{T}}\mathbf{K} + \mathbf{K}\mathbf{A} + \mathbf{A}^{\mathrm{T}}\mathbf{K} = 0 \tag{5.22}$$

which is the optimal state feedback control law that depends on the estimated states $\widehat{\mathbf{x}}(t)$ obtained through the *effort*-based state observer (5.11). The set point tracking optimal controller is illustrated in Fig. 5.7. Actuator variables are used as inputs to the *effort* observers (DOB), then feedback-like *effort*-force is estimated using the *effort*-force observer (EFO). Eventually, *effort*-force is injected onto the Luenberger-like *effort*-based observer structure so as to guarantee convergence of the estimated states to the actual ones.

The optimal minimum energy optimal control results are illustrated in Fig. 5.8. The phase portrait shows the behavior of the third non-collocated mass states when

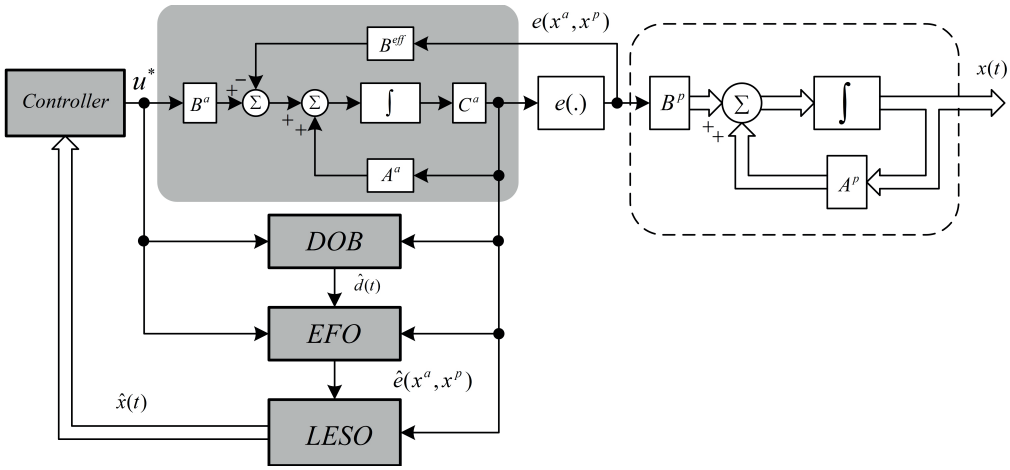

Figure 5.7: *Effort* state observer based optimal set point tracking for a dynamical subsystem with state variables that are not available for measurements (dashed-line).

effort-based state observer based optimal controller in Fig. 5.8-a-b, at which the third non-collocated mass is positioned to a reference target. In Fig. 5.8, the third non-collocated mass is regulated to the origin through the same *effort*-based state observer based optimal controller. The phase portraits illustrate that the third mass is regulated with minimum residual vibration when the optimal controller is implemented. In addition, non of the system states are fed back to the controller which in turn demonstrates the validity of realizing the optimal control system when measurements/output are inaccessible or unknown.

5.2.2 Tracking optimal control

In order to generalize the pervious results, the performance measure to be minimized is

$$\mathbf{J} = \frac{1}{2}[\widehat{\mathbf{x}}(t_f) - \mathbf{r}(t_f)]^{\mathrm{T}}\mathbf{H}[\widehat{\mathbf{x}}(t_f) - \mathbf{r}(t_f)] + \int_{t_0}^{t_f} \frac{1}{2}\big[(\widehat{\mathbf{x}}(t) - \mathbf{r}(t))^{\mathrm{T}}\mathbf{Q}(\mathbf{x}(t) - \mathbf{r}(t)) + \mathbf{u}^{\mathrm{T}}(t)\mathbf{R}\mathbf{u}(t)\big]dt \tag{5.23}$$

where $\mathbf{r}(t)$ is the desired reference value of the state vector. $\mathbf{H}$ and $\mathbf{Q}$ are real symmetric positive semi-definite matrices, and $\mathbf{R}$ is a real symmetric positive definite matrix [Kirk 1970]. The Hamiltonian can therefore be written as

$$\begin{aligned}\mathscr{H}(\widehat{\mathbf{x}}(t), \mathbf{u}(t), \widehat{\mathbf{p}}(t), t) \;=\; & \frac{1}{2} \parallel \widehat{\mathbf{x}}(t) - \mathbf{r}(t) \parallel^2_{\mathbf{Q}} + \frac{1}{2} \parallel \mathbf{u}(t) \parallel^2_{\mathbf{R}} \\ & + \widehat{\mathbf{p}}^{\mathrm{T}}(t)\mathbf{A}\widehat{\mathbf{x}}(t) + \widehat{\mathbf{p}}^{\mathrm{T}}(t)\mathbf{B}\mathbf{u}(t)\end{aligned} \tag{5.24}$$

$\widehat{\mathbf{p}}(t)$ is the estimate of costate vector with the following costate equation

$$\dot{\widehat{\mathbf{p}}}^*(t) = -\frac{\partial \mathscr{H}}{\partial \mathbf{u}} = -\mathbf{Q}\widehat{\mathbf{x}}(t) - \mathbf{A}\widehat{\mathbf{p}}(t) + \mathbf{Q}\mathbf{r}(t) \tag{5.25}$$

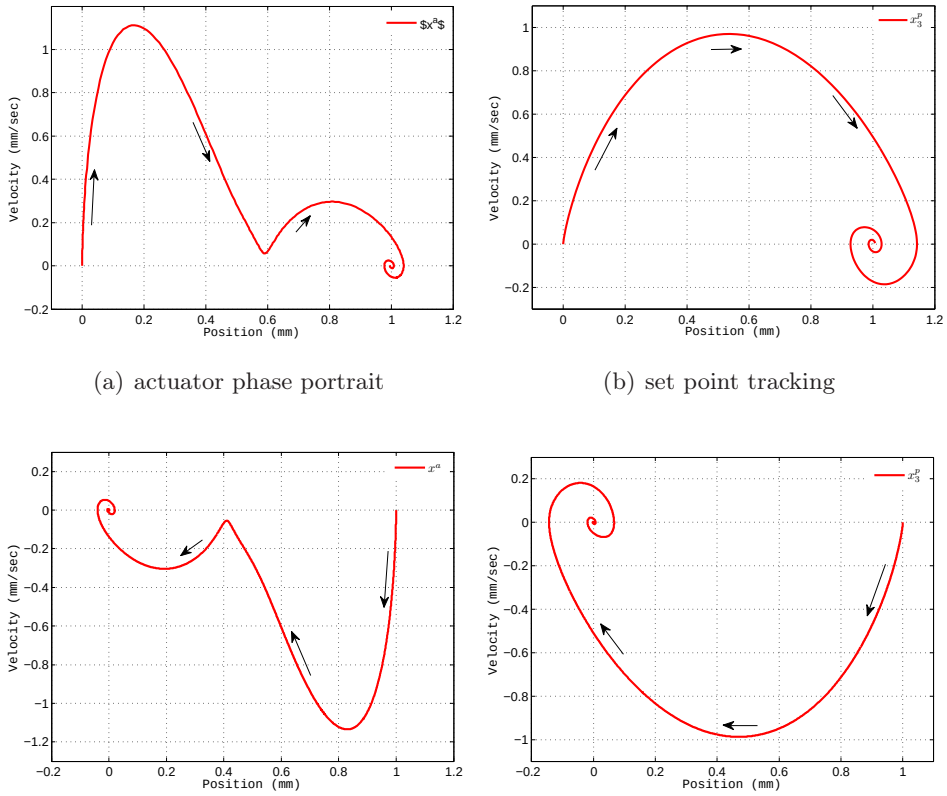

(a) actuator phase portrait

(b) set point tracking

(c) actuator phase portrait

(d) regulation

Figure 5.8: Experimental results of optimal states regulation of a dynamical system with 3-*dof* (Optimal set point tracking and regulation of the third non-collocated mass to a reference position).

the following must be satisfied

$$\frac{\partial \mathscr{H}}{\partial \mathbf{u}} = \mathbf{R}\mathbf{u}^*(t) + \mathbf{B}\widehat{\mathbf{p}}^*(t) = 0 \tag{5.26}$$

therefore,

$$\mathbf{u}^*(t) = -\mathbf{R}^{-1}\mathbf{B}\widehat{\mathbf{p}}^*(t) \tag{5.27}$$

Substituting (5.20) in the state equation yields the estimated state and costate matrix equation

$$\begin{bmatrix} \dot{\widehat{\mathbf{x}}}^*(t) \\ -- \\ \dot{\widehat{\mathbf{p}}}^*(t) \end{bmatrix} = \left[\begin{array}{c|c} \mathbf{A} & -\mathbf{B}\mathbf{R}^{-1}\mathbf{B}^{\mathrm{T}} \\ -- & --- \\ -\mathbf{Q} & -\mathbf{A}^{\mathrm{T}} \end{array}\right] \begin{bmatrix} \widehat{\mathbf{x}}^*(t) \\ -- \\ \widehat{\mathbf{p}}^*(t) \end{bmatrix} + \begin{bmatrix} 0 \\ -- \\ \mathbf{Q}\mathbf{r}(t) \end{bmatrix} \tag{5.28}$$

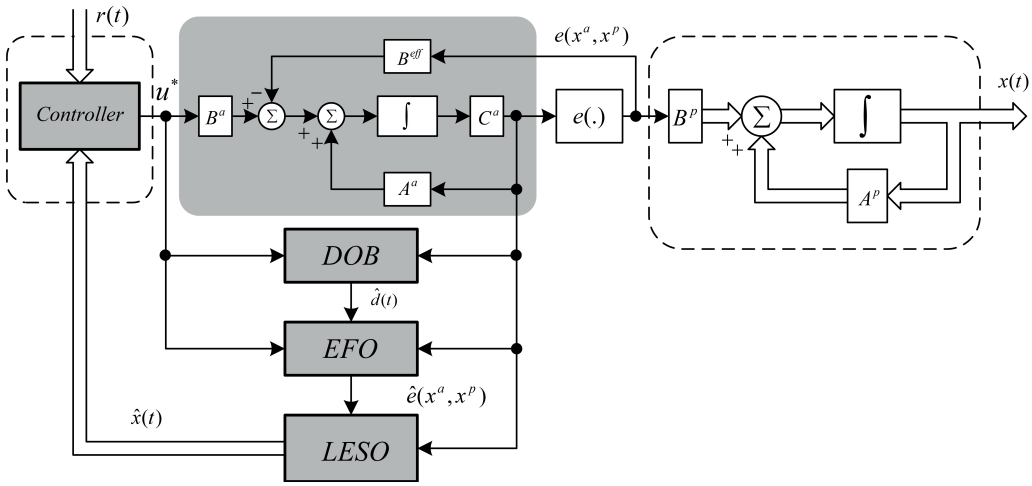

Figure 5.9: *Effort* state observer based optimal trajectory tracking for a dynamical subsystem with state variables that are not available for measurements (dashed-line).

the solution of (5.21) is

$$\begin{bmatrix} \mathbf{x}^*(t_f) \\ --- \\ \mathbf{p}^*(t_f) \end{bmatrix} = \varphi(t_f, t) \begin{bmatrix} \mathbf{x}^*(t) \\ --- \\ \mathbf{p}^*(t) \end{bmatrix} + \int_t^{t_f} \varphi(t_f, \tau) \begin{bmatrix} 0 \\ --- \\ \mathbf{Q}\mathbf{r}(\tau) \end{bmatrix} d\tau \tag{5.29}$$

where $\varphi(t_f, t)$ is the transition matrix of (5.28) and the optimal control law can be expressed as

$$\mathbf{u}^*(t) = -\mathbf{R}^{-1}\mathbf{B}^{\mathrm{T}}\mathbf{K}\widehat{\mathbf{x}}(t) - \mathbf{R}^{-1}\mathbf{B}^{\mathrm{T}}\widehat{\mathbf{s}}(t) \tag{5.30}$$

$$\dot{\mathbf{K}} = -\mathbf{K}\mathbf{A} - \mathbf{A}^{\mathrm{T}}\mathbf{K} - \mathbf{Q} + \mathbf{K}\mathbf{B}\mathbf{R}^{-1}\mathbf{B}^{\mathrm{T}}\mathbf{K} \tag{5.31}$$

$$\dot{\mathbf{s}} = -[\mathbf{A}^{\mathrm{T}} - \mathbf{K}\mathbf{B}\mathbf{R}^{-1}]\mathbf{s} + \mathbf{Q}\mathbf{r}(t) \tag{5.32}$$

The previous controller guarantees that system (5.17) will track a time varying reference trajectory $\mathbf{r}(t)$ in the absence of all system outputs. Fig. 5.9 illustrates the *effort*-based state observer based optimal tracking controller for systems with inaccessible/unknown outputs. As shown in Fig. 5.9, non of the plant state variable are required to be measured in the realization of the optimal control law (5.30), the *effort* feedback-like force is instead used in the realization of the *effort*-based state observer which provides full estimates of the plant state variables. Then the optimal control law is implemented based on these estimated states.

5.2.3 Results

In order to verify the validity of the control system, experiments are conducted on a single input (A) multiple outputs flexible dynamical system with four degrees of freedom (P) like the one depicted in Fig. 5.10. The flexible plant (P) is conceptually

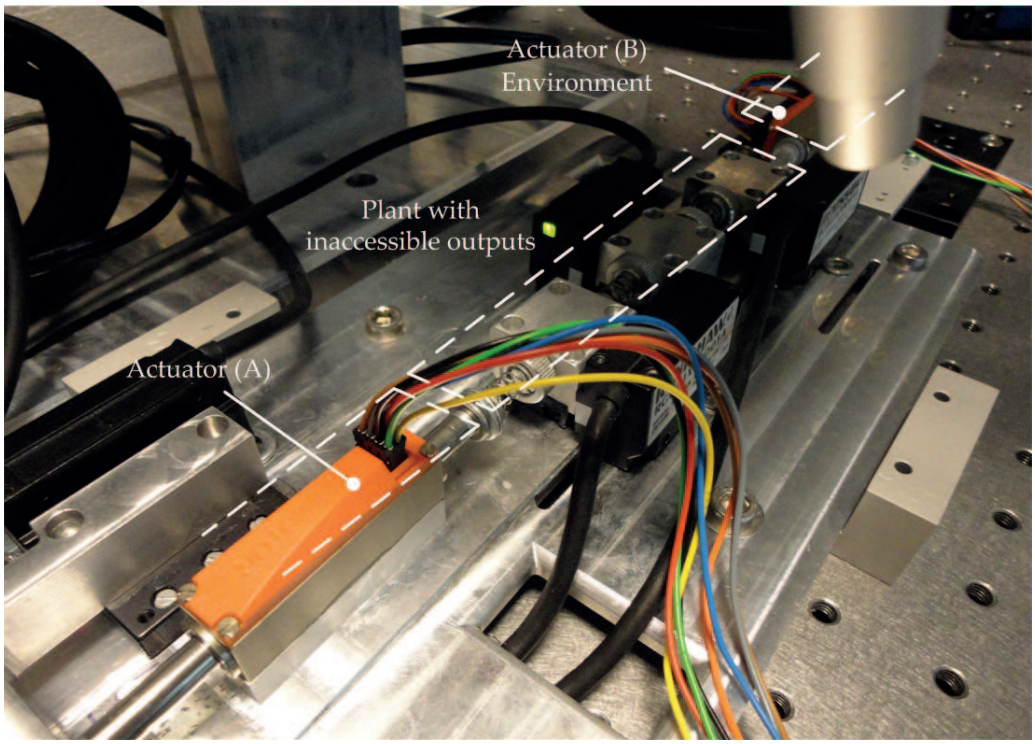

Figure 5.10: Experimental setup consists of a single input attached via an energy storage element with a three degrees of freedom flexible system.

considered to have inaccessible state variables or outputs in order to examine the validity of the outlined *effort* state observer based optimal control system. The encoder attached to each degree of freedom are used for the sake of verification through comparing the estimated state variables with the actual measured ones, each has resolution of 1 μm. Experiments are performed on a lumped system due to the simplicity and accuracy of the measurement since each lumped degree of freedom can easily has its own encoder, whereas a kinematical map is required to be used if experiments were to conducted on a distributed system such as a flexible robot arm or shaft.

The *effort*-force observers gains were set to 628 rad/s, whereas the Luenberger-like *effort*-based state observer gain vector is selected such that observer (5.4) becomes twice faster than the control system. However, before selecting the proper gains of the state observer (5.11), the observability condition of this class of dynamical systems has to be checked. The eigenvalues of the system matrix (A) have to be distinct in order to design *effort*-based state observers of the form (5.11). It can be easily shown that the system matrix for the dynamical system depicted in Fig. 5.10 under the assumption that contacts between the lumped masses and their slides are smooth enough that its behavior can be can be accurately governed with a linear

model in the neighborhood of a given operating point.

$$\mathrm{A} = \begin{bmatrix} 0 & 1 & 0 & 0 & 0 & 0 & 0 & 0 \\ -a & -b & a & b & 0 & 0 & 0 & 0 \\ 0 & 0 & 0 & 1 & 0 & 0 & 0 & 0 \\ d & e & -2d & -2e & d & e & 0 & 0 \\ 0 & 0 & 0 & 0 & 0 & 1 & 0 & 0 \\ 0 & 0 & f & g & -2f & -2g & f & g \\ 0 & 0 & 0 & 0 & 0 & 0 & 0 & 1 \\ 0 & 0 & 0 & 0 & h & r & -h & -r \end{bmatrix} \tag{5.33}$$

$$a \triangleq \frac{k}{m_a}\ ,\ b \triangleq \frac{c}{m_a}\ ,\ d \triangleq \frac{k}{m_1}\ ,\ e \triangleq \frac{c}{m_1}$$

$$f \triangleq \frac{k}{m_2}\ ,\ g \triangleq \frac{c}{m_2}\ ,\ h \triangleq \frac{k}{m_3}\ ,\ r \triangleq \frac{c}{m_3}$$

where, c and k are the viscous damping coefficient and spring stiffness, respectively, that can be identified. Therefore, using these identified parameters along with the given ones from Table. 5.1, eigenvalues of the dynamical system turned out to be distinct. The following observer vector gain was utilized through the whole experiment which can be obtained though directly direct substitution of the desired observer poles in the characteristic equation of the *effort*-based state observer,

$$\mathrm{M} = [0.3 \quad 0.1 \quad 0.3 \quad 0.3 \quad 0.1 \quad 0.2 \quad 3 \quad 3]'$$

An identity regulation matrix (R) was used in the performance index (5.18), the diagonal entries of the matrix (Q) were selected such that the first term of the performance index integrand represents both potential and kinetic energy of the plant. Therefore, (5.18) represents the energy trapped in the system along with energy induced by the controller. The optimal state feedback vector gains (K)

$$\mathrm{K} = [10.03 \quad 2.12 \quad 6.75 \quad 1.43 \quad 6.55 \quad 1.43 \quad 6.45 \quad 1.42]'$$

The experimental results of the regulation control law (5.13) are depicted in Fig. 5.11, the phase portrait shown in Fig. 5.11-a illustrates the behavior of the first non-collocated mass while Fig. 5.11-b illustrates the second mass phase portrait to the optimal control law (5.21) which is used to regulate the second non-collocated mass to a pre-specified reference. The phase portraits show that the second non-collocated mass is positioned with minimum residual vibration. Similarly, the phase portrait for the second and first non-collocated masses are illustrated in Fig. 5.12 for different target position reference. The previous phase portraits indicate that the even in the absence of the plant outputs, an optimal control law can be realized.

In Fig. 5.13 and Fig. 5.14 the optimal regulating control law regulates the system to the origin with minimum residual vibration of the non-collocated masses. The previous experimental results indicates that the *effort*-based optimal regulating

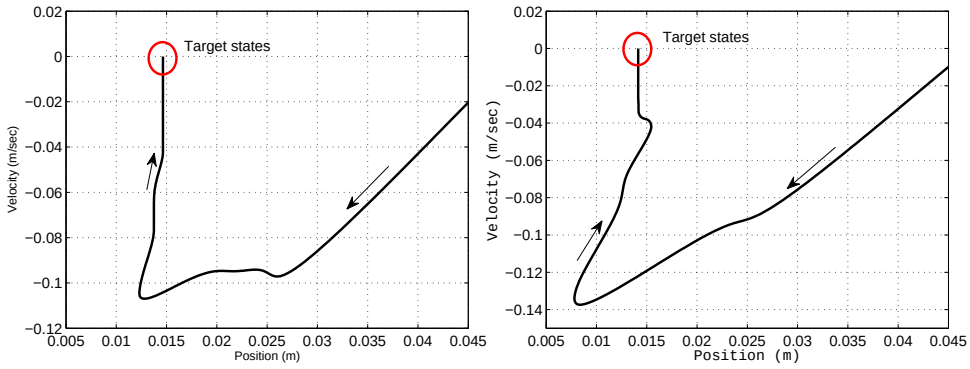

(a) 1^{st} non-collocated mass phase portrait (b) 2^{nd} non-collocated mass phase portrait

Figure 5.11: Experimental results of optimal states regulation of a dynamical system with 3-*dof* (Optimal regulation of the second non-collocated mass to a reference position).

Table 5.1: Experimental parameters

Actuator force constant	k_{fn}	6.43	N/A
Actuator Nominal mass	m_{an}	0.059	kg
Lumped masses	$m_{1,2,3}$	0.019	kg
Force observer gain	g_{reac}	628	rad/s
Disturbance observer gain	g_{dist}	628	rad/s
Sampling time	T_s	1	ms

control law is able to precisely position some non-collocated point along the flexible system to a target position with minimum residual vibration. Similarly, the *effort*-based state observer based optimal control law is utilized to regulate the first non-collocated mass to a target position while taking out the residual vibrations of the entire dynamical system as depicted in Fig. 5.15.

5.2.4 Summary and discussion

Motion control can be realized even in the complete absence of a dynamical subsystem state variables or outputs. The *effort*-based state observer is used in order to realize the incident *effort*-forces which are used as basis of estimating the states of this subsystem. Due to the presence of the estimated *effort*-forces along with the estimated states, it was natural to devise controller of the form (5.1). Possibility to realize the optimal motion control is also investigated and the optimal motion control law which minimizes the energy content along the energy storage elements of the dynamical system is realized in the complete absence of a dynamical subsystem

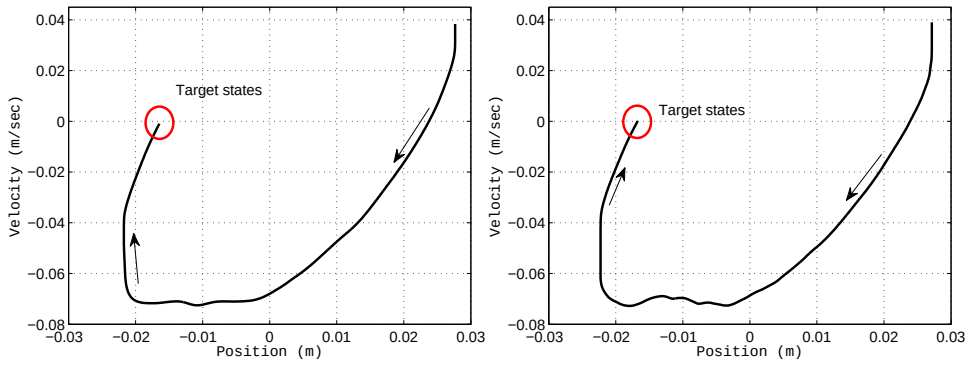

(a) 1^{st} non-collocated mass phase portrait (b) 2^{nd} non-collocated mass phase portrait

Figure 5.12: Experimental results of optimal states regulation of a dynamical system with 3-*dof* (Optimal regulation of the second non-collocated mass to a reference position).

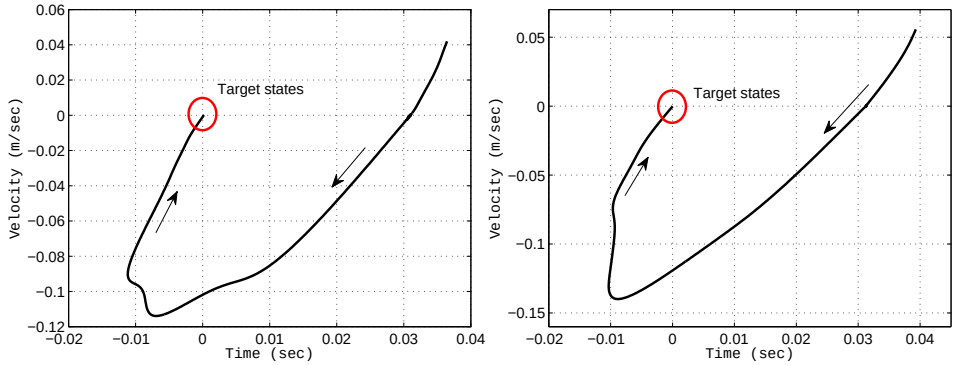

(a) 1^{st} non-collocated mass phase portrait (b) 2^{nd} non-collocated mass phase portrait

Figure 5.13: Experimental results of optimal states regulation of a dynamical system with 3-*dof* (Optimal regulation of the second non-collocated mass to a reference position).

state variables or outputs.

The experimental results conducted on a multi-degree of freedom flexible system verified the validity of the outlined control system where controllers of the form (5.9) and (5.21) are experimentally evaluated based on the *effort*-based state observer. The experimental implementation of the control law (5.9) is conducted using both the estimated and the actual measured states. Performance of the estimated based one was oscillatory during the transient due to the insufficient order of the *effort*-force observer utilized within the *effort*-based state observer. Nevertheless, the steady state response is satisfactory and better results can be obtained by increas-

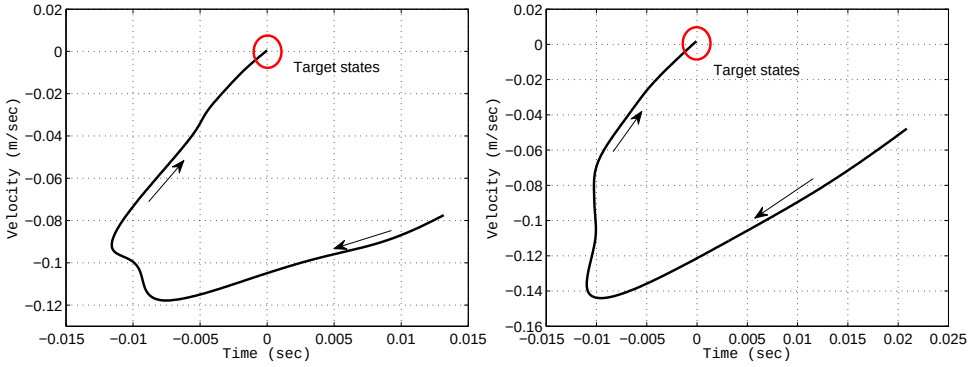

(a) 1^{st} non-collocated mass phase portrait (b) 2^{nd} non-collocated mass phase portrait

Figure 5.14: Experimental results of optimal states regulation of a dynamical system with 3-*dof* (Optimal regulation of the second non-collocated mass to a reference position).

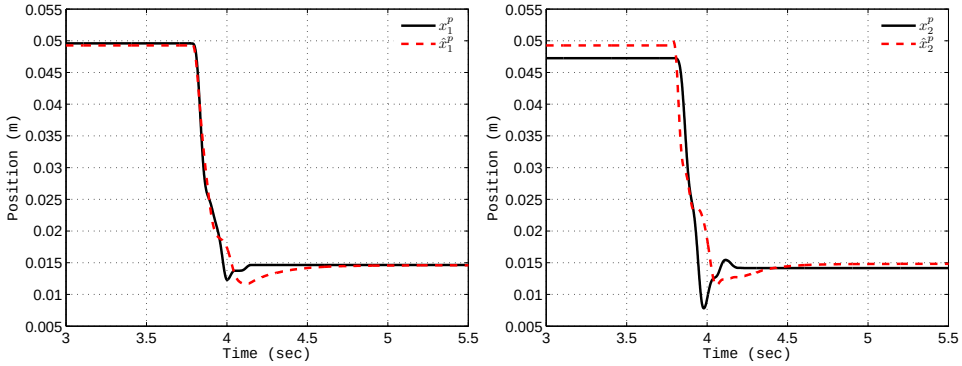

(a) 1^{st} non-collocated mass vs. its estimate (b) 2^{nd} non-collocated mass vs. its estimate

Figure 5.15: Experimental results of optimal states regulation of a dynamical system with 3-*dof* (Optimal regulation of the first non-collocated mass to a reference position).

ing the order of the associated *effort* observers with the overall *effort*-based state observer. In addition, due to the availability of both the estimated states and the estimated *effort*-forces it was natural to devise controller with two inputs, the first is a regulating control input while the second is for the attaintment of robustness.

Chapter 6

Effort Force Observer based Force Control

THE aim of force control is to impose the desired force on the environment regardless to its characteristic. In general, force sensors are utilized in order to sense the interaction forces between robots and their surrounding environment. Unfortunately, force measurement is commonly agreed to be problematic. Instability, measurement noise, complicity and non-collocation are some of these problems associated with force sensors. In the sequel, an *energy* based force observer is introduced in order to provide a natural alternative to force sensors. Based on the *energy* formalism studied through out this work, we attempt to design an *energy* based force observer in order to assist in avoiding the associated problems with force sensors. The work presented in this chapter allows realizing the force control from dynamical system with inaccessible state variables and outputs by designing a force observer that doesn't depend on the availability of the system state variables and outputs but rather on the feedback-like *effort*-forces which can be estimated and used as basis in designing force observers and controllers.

6.1 Force Control and Contact Stability

The main challenge in the force control problem is to maintain stability whenever the robot manipulator were to interact with relatively stiff environments. The cause of this instability is due to the increase of the equivalent position gain of the control system by the environmental stiffness matrix. This would results in a highly under damped or possibly unstable system if the velocity gain is not chosen based on the control system position gain along with the large environmental stiffness. In addition to this contact stability issue, presence of force sensor adds an extra degree of freedom, measurement noise and limited bandwidth that result in instability [Katsura 2006]-[Bazaei 2011]. In this section, force sensor and the contact stability are modeled and further investigated.

6.1.1 Modeling of force sensing

Contact between a robot end-effector with single degree of freedom and an environment in the presence of force sensing is illustrated in Fig. 6.1, where m and m_s are the masses of the robot end-effector and the force sensor respectively. k_s, k_e and D_e

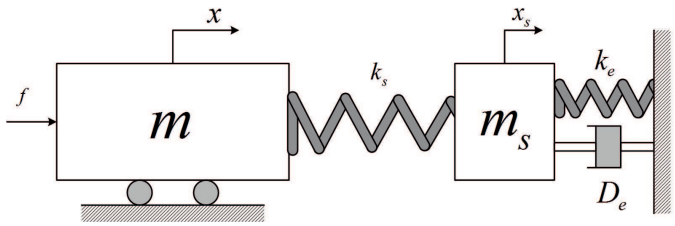

Figure 6.1: Force sensor model indicating the non-collocation added via force sensor to the end-effector

are force sensor stiffness, environmental stiffness and the environment viscous damping coefficient, respectively. x and x_s are the positions of the robot end-effector and the force sensor, respectively. The following motion equations describe the contact mechanism depicted in Fig. 6.1

$$m\ddot{x} + k_s(x - x_s) + f_{dist_1} = f \tag{6.1}$$

$$m_s\ddot{x}_s - k_s(x - x_s) + f_{dist_2} = -f_{ext} \tag{6.2}$$

$$f^{ext} = z_e x_s \tag{6.3}$$

where z_e is the environmental impedance. f_{dist_1}, f_{dist_2} and f^{ext} are the disturbance forces on the first and second system degrees of freedom and the interaction force with the environment, respectively. In a regular force servoing problem the control system is designed such that the robot end-effector exerts a force f_{ext} that is equal to the desired force reference f^{des}. It is worth noting that in the previous example the environment is assumed stationary therefore its acceleration is not included among the previous motion equations. In addition, the environmental impedance can be modeled with either an energy storage element or energy dissipation elements or both. Therefore, in the presence of a force sensor, an extra degree of freedom is added to the system. In addition, the previous model shows that the end-effector is non-collocated via an energy storage element with stiffness k_s due to the soft structure of the force/torque sensor. The root locus of the system when the force sensor is attached to the robot end-effector is depicted in Fig. 6.2-b, whereas, Fig. 6.2 illustrates the root locus of the same system in the absence of force sensor. In both cases, the root locus is plotted for different values of the environmental stiffness gain k_e. It can be easily shown from Fig. 6.2 that adding a force sensor to the dynamical model of the system affects stability of the system dramatically. Controlling a collocated point is much easier then a non-collocated point along the dynamical system as it can be shown from Fig. 6.2.

6.1.2 Force servoing

In order to impose the desired force on the environment, the force measurement taken through a force sensor has to be used to realize the motion control system as depicted in Fig. 6.3. However, due to the force measurement nature at which the

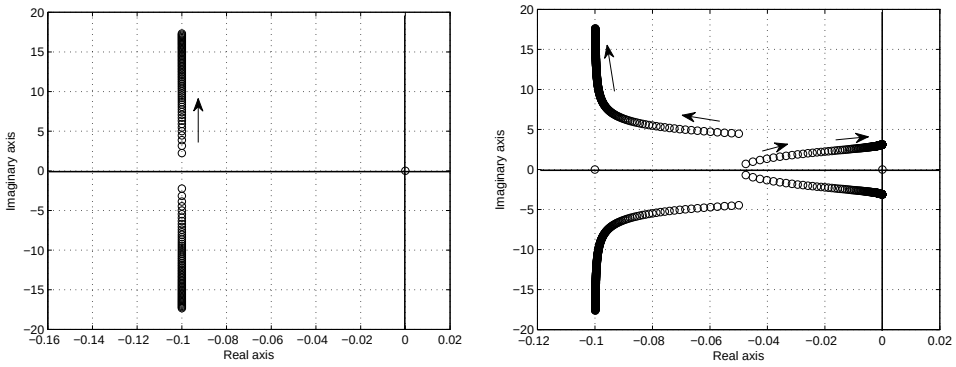

(a) collocated system (b) non-collocated system

Figure 6.2: root locus of system with and without force sensor for $k_e = 0 \longrightarrow 300$

strain is measured and amplified along with the noise v^s, the actual interaction force with the environment cannot be precisely measured. In Fig. 6.3, k_v and k_p are the velocity feedback gain and proportional gains, respectively. k_r is the reaction force feedback gain [Katsura 2005]. Due to the presence of noise in the force measurement. The force response of the force control system can be expressed as follows

$$\frac{f^{ext}_{ref}(s)}{f^{ref}(s)} = \frac{k_p k_f (k_e + sD_e)}{s(ms + k_v)(m_s s^2 + k_s + z_e) + k_s k_r (ms^2 + z_e) + k_p k_s (k_e + sD_e)} \tag{6.4}$$

$$\frac{f^{ext}_{n}(s)}{V^s(s)} = \frac{k_p k_f (k_e + sD_e)}{s(ms + k_v)(m_s s^2 + k_s + z_e) + k_s k_r (ms^2 + z_e) - k_p k_s (k_e + sD_e)} \tag{6.5}$$

The previous transfer functions describe the force response for both the reference and force sensor noise inputs, respectively. Therefore, the total response of the system can be written as a superposition of the reference input response $f^{ext}_{ref}(s)$ and the noise input response $f^{ext}_{n}(s)$

$$f^{ext} = f^{ext}_{ref}(s) + f^{ext}_{n}(s) \tag{6.6}$$

The previous equations indicate the effect of the force sensor noise on the desired force response. In addition, the force control parameters (k_v) and (k_p) have to be selected such that the characteristic equation of the transfer function (6.4) is stable. This can be easily done by using the denominator of (6.4) to formulate the Routh Hurwitz array and determine the gains such that stability is achieved according to the Routh Hurwitz stability criterion. The root locus of the force servoing system described by (6.4) is illustrated in Fig. 6.4 for different values of environmental stiffness (k_e) and velocity feedback gain (k_v). In general, environmental stiffness and the velocity feedback gain are of great importance for any force control problem since the cause of instability is that the environmental stiffness matrix increases the equivalent position gain of the control system. Therefore, the velocity gain has to

be chosen to be chosen not only based on the position gain but also on the large environmental stiffness. Otherwise the resulting system will be highly under damped and possibly unstable.

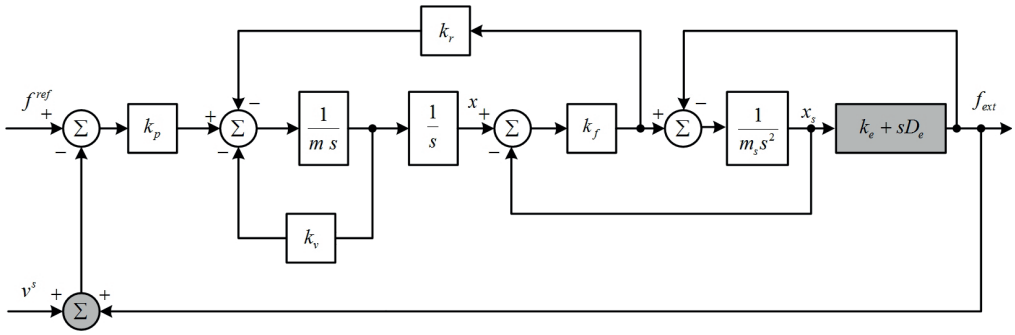

Figure 6.3: Robot in contact with environment with force sensing and force servoing control system

6.1.3 Reaction force observer based force servoing

In order to avoid majority of the previously outlined force sensor problems such as the non-collocation, sensor noise, limited bandwidth and complicity, many researchers proposed reaction force observers in order to estimate the interaction forces with the environment through other measurements rather then the force measurement, namely the *flow* variable of the degree of freedom which interacts with the environment. The reaction force observer based force control system is depicted in Fig. 6.5. It can be easily shown that the interaction force with the environment f^{ext} is realized through the *flow* variable measurement $\dot{x}_2$ of the degree of freedom

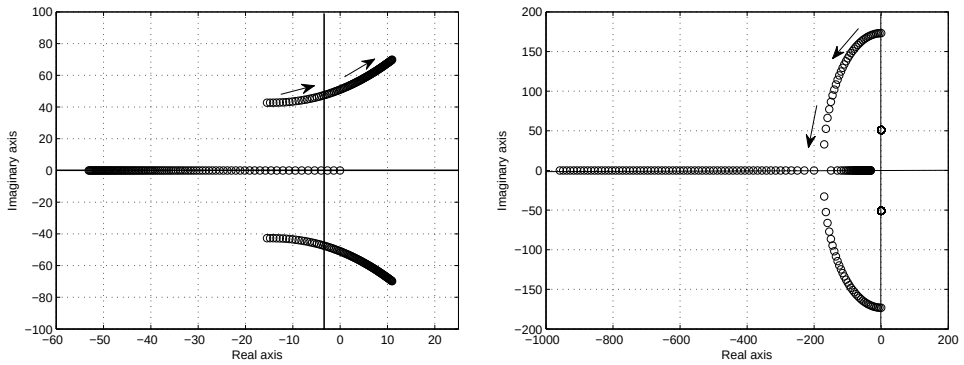

(a) $k_r = 1 \longrightarrow 10000$ (b) $k_v = 1 \longrightarrow 2000$

Figure 6.4: root locus of system with force servoing

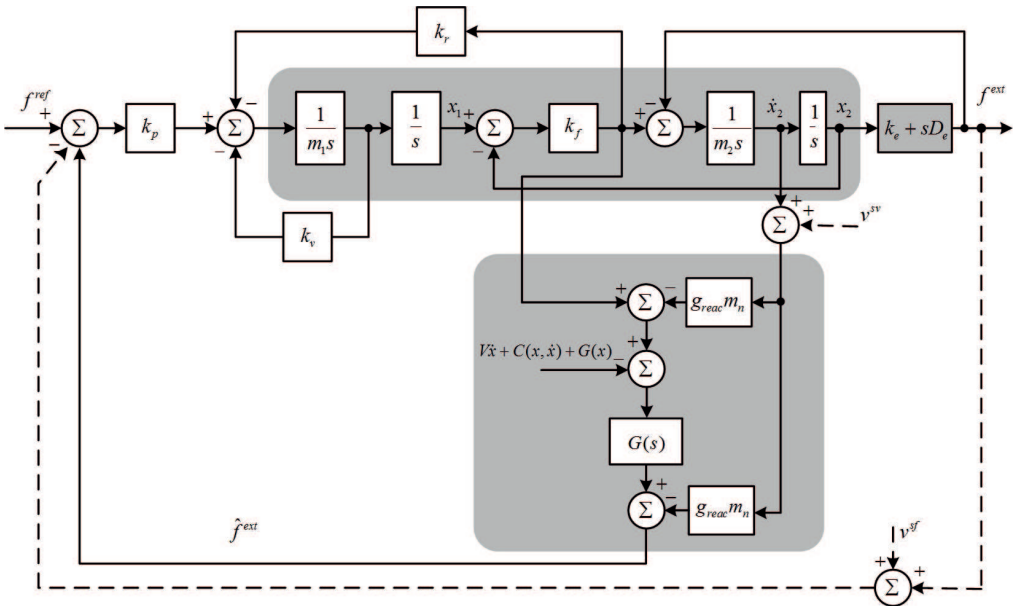

Figure 6.5: Force servoing control system using reaction force observer

which interacts with the environment.

$$\widehat{f}^{ext} = \frac{g_{reac}}{s + g_{reac}} \left(I_a^{ref} k_{tn} + g_{reac} m_{2n} \dot{x}_2 - \mathrm{V}\dot{x}_2 - C(x_2, \dot{x}_2) - G(x) \right) - g_{reac} m_{2n} \dot{x}_2 \quad (6.7)$$

m_{2n} and k_{tn} are the nominal inertia/mass and torque/force constants. The interaction force with the environment is observed through a low-pass filter with a cut-off frequency $g_{reac} \in \mathrm{R}^+$. $G(s)$ is the low-pass filter associated with the reaction force observer. The reaction force observer spares the force control system from the noise associated with the force sensor v^{sf}. However, it didn't spare the control system from the noise v^{sv} associated with the sensor utilized to measure $\dot{x}_2$. It is intuitively clear that the noise associated with the velocity measurement is much less than the noise associated with the force sensing. Nevertheless, the noise associated with the *flow* variable measurement limits the sensitivity of the reaction force observer in estimating micro scale interaction forces. Fig. 6.6 illustrates a micro system experimental setup designed to manipulate micro objects. In order to investigate the effect of the *flow* variable measurement noise on the sensitivity of the reaction force observer, we investigate the interaction of an end-effector (needle with 50 nm diameter) with a Biological cell in order to study whether the amplitude to noise ration of the detected interaction force allows further utilization of the detected estimated signal in further analysis.

Although the reaction force observer was able to estimate the interaction forces within micro scale accuracy as shown in Fig. 6.7, the signal to noise ration in the depicted two experimental results are 1.585 and 1.3 as shown in Fig. 6.7-a and Fig. 6.7-b, respectively. This is due to the dependence of the reaction force observer on the *flow* variable measurement which can be considered relatively as problematic and

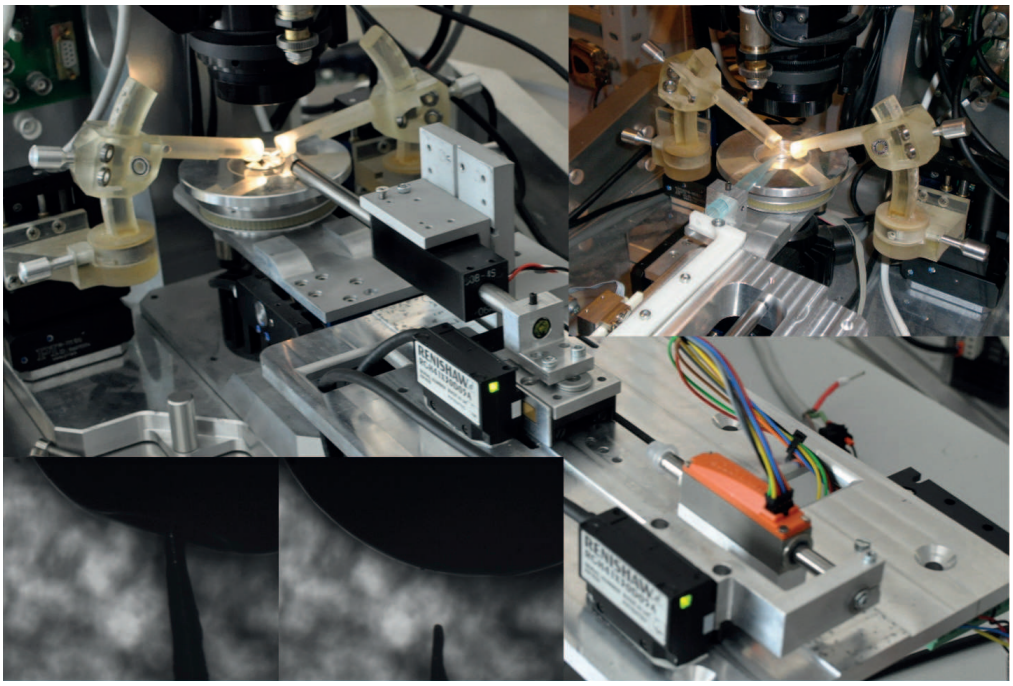

Figure 6.6: Interaction force estimation experimental setup to investigate the sensitivity of the force observer in the presence of measurement noise

undesirable as the force measurement. Practically, the *flow* variables measurements are realized through a low-pass filters in order to attenuate the noise associated with the direct differentiation of the position sensors signals. On the one hand, this can be useful due to the fact that noise generally belongs to a different frequency range. On the other, obtaining the *flow* variable through a low-pass filter limits the bandwidth of the control system which might cause instability.

In addition, the class of dynamical systems we consider have inaccessible state variables, i.e., x_2 and $\dot{x}_2$ are not available for measurement. Therefore, we attempt to expand the *energy* based state observer formalism to estimate the interaction forces with the environment in the absence of x_2 and $\dot{x}_2$. In fact, the previous reaction force observer is *flow* based, it depends on measuring the *flow* variables of the interacting degree of freedom with the environment and using it in realizing the reaction force observer (6.7).

6.1.4 Discussion

Realization of the interaction force with the environment through force observer can be realized through measuring the *flow* variable of the degree of freedom which interacts with the environment. Although this procedure would spare the control system from force sensing, the force sensing is altered with the *flow* variable measurement. In applications such as characterization of Biological cell properties, the signal to noise ratio of the estimated interaction forces is very close to unity as it was verified

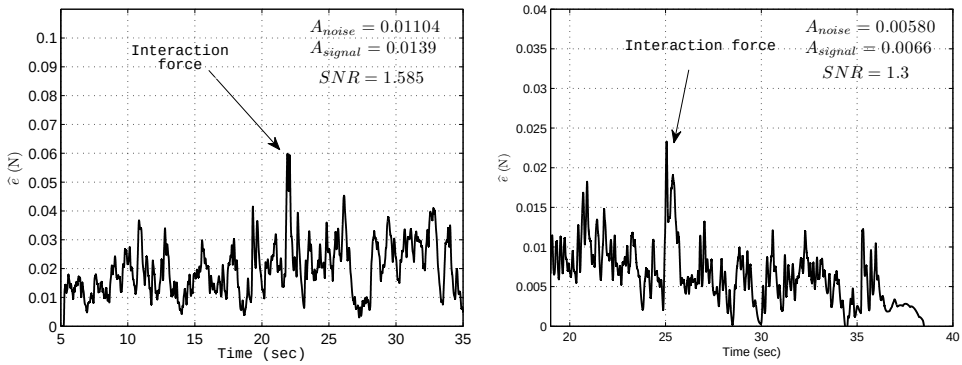

(a) interaction force experiment A (b) interaction force experiment B

Figure 6.7: Signal to noise ration of the estimated interaction forces

experimentally. Changing the cut-off frequency associated with the force observer in order to attenuate the effect of the measurement noise would limit the bandwidth of the force observer and the force control system.

6.2 Effort Based Force Observer

The *energy* based formalism studied in this work allows estimating state variables of a dynamical subsystem with inaccessible state variables and outputs as it was explained in the previous sections, i.e., the degree of freedom which interacts with the environment can be conceptually considered as a dynamical system with inaccessible state variables and outputs then its power port with some other subsystem can be used in the realization of a natural feedback-like *effort*-force which can be used as basis of the force estimation process.

First, a typical *effort*-based state observer has to be designed in order to estimate the *flow* variable of the interacting degree of freedom with the environment. As soon as the *flow* of the interacting degree of freedom with the environment is determined through the *effort*-based state observer, a typical reaction force observer can be used based on the estimated *flow* variables rather than the measured one. Fig. 6.8 illustrates the structure of the *effort*-based force observer which consists of a typical *effort*-based state observer along with a reaction force observer. From Fig. 6.8, one can conclude that the *effort*-force observer allows estimating the interacting forces between the robot non-collocated end-effector and the environment in the complete absence of measurements from this end-effector.

6.2.1 Stability and performance analysis

Bandwidth is one of the most important issues which cause instability during a force control task with a stiff environment. The structure of the force sensor limits its

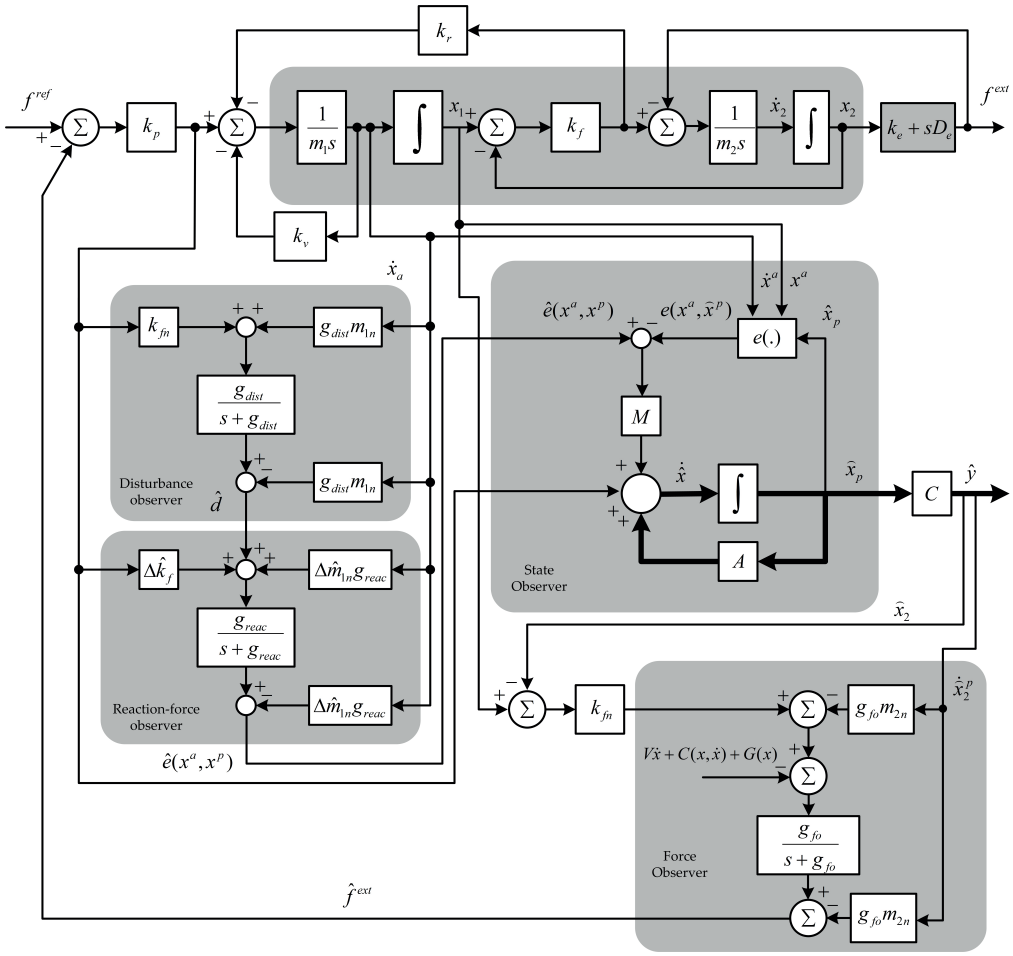

Figure 6.8: *effort*-based force observer and force servoing control system

bandwidth. Therefore, the *effort*-based force observer is expected to have a larger bandwidth than the force control which based on force sensor. However, we first assume that the force sensor has enough bandwidth in order to compare its ideal performance with the *effort*-based force observer. As shown in Fig. 6.8, the force control system is realized through the estimated force obtained through the *effort*-based force observer. We first compare the magnitude frequency response for the cases at which the feedback is obtained through force sensor and the *effort*-based force observer.

comparison between the frequency response of the sensor based force control with the frequency response of the *effort*-based force control is depicted in Fig. 6.9 for different values of the *effort*-based force observer gains (g_{eff}) and (g_{fo}). The frequency response comparisons are depicted in Fig. 6.9 and Fig. 6.10. It can be shown from the frequency response analysis that at ($g_{eff} = 628.3\ rad/sec$) and ($g_{fo} = 628.3\ rad/sec$) both the frequency responses of the force sensor based control and *effort*-based observer based control have perfect match over a satisfactory

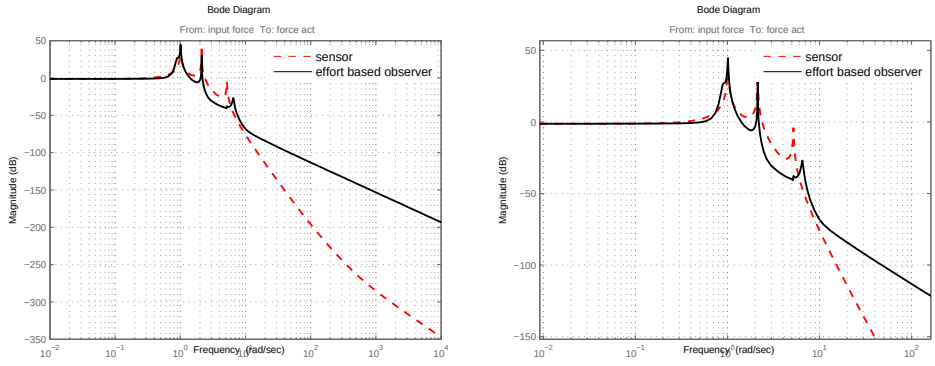

(a) $g_{eff} = 6.28\ rad/sec$, $g_{fo} = 6.28\ rad/sec$ (b) magnified plot

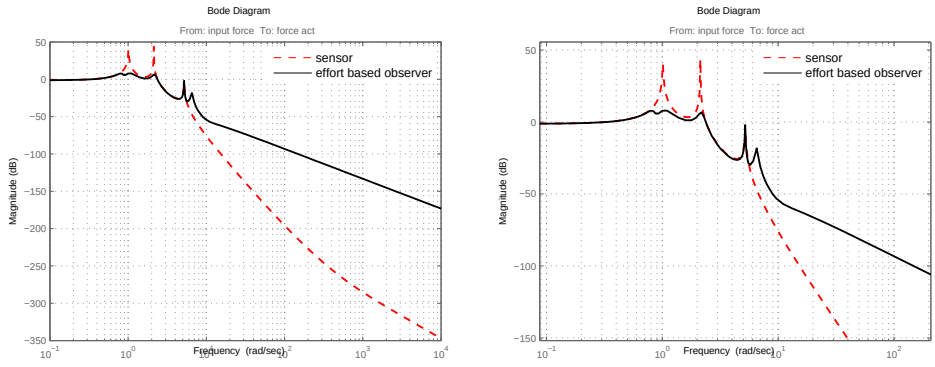

(c) $g_{eff} = 62.83\ rad/sec$, $g_{fo} = 62.83\ rad/sec$ (d) magnified plot

Figure 6.9: Frequency response of the *effort*-based force observer force control versus sensor based force control

frequency range.

The depicted results are obtained for a dynamical system with three degrees of freedom in contact with an environment (B) with varying impedance (z_e). The dynamical system has a single input (A) from which measurements are taken, whereas the 3 degree of freedom dynamical system and the environment are free from any attached sensor like the dynamical system depicted in Fig. 6.11. It can be shown from Fig. 6.10-c that the *effort*-based force observer has a similar frequency response to the ideal force sensor. Therefore, the force control can be realized through the outlined *effort*-based force observer. Advantages of the *effort*-based force control over the force sensor and reaction force observer based force controllers should now be obvious. The first requires having force sensor attached to the robot end effector while the second requires measuring the *flow* variable of the end-effector in contact with the environment. The *effort*-based force observer, however, keeps the robot end effector free from force sensor and it doesn't require measuring the *flow* variable of the end-effector.

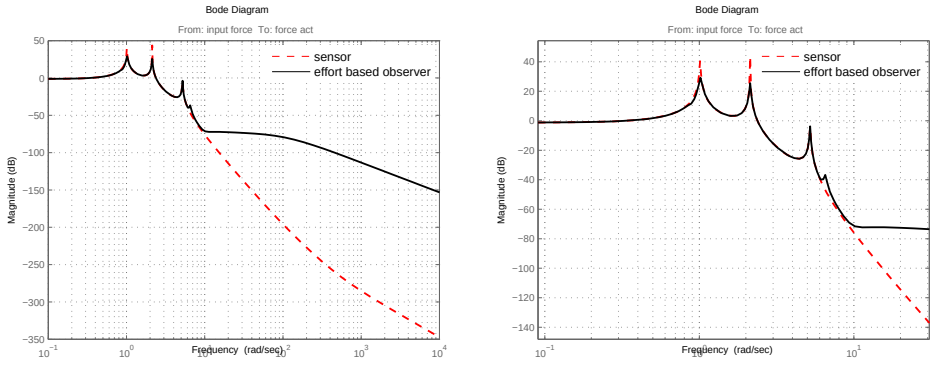

(a) $g_{eff} = 628.3\ rad/sec$, $g_{fo} = 628.3\ rad/sec$ (b) magnified plot

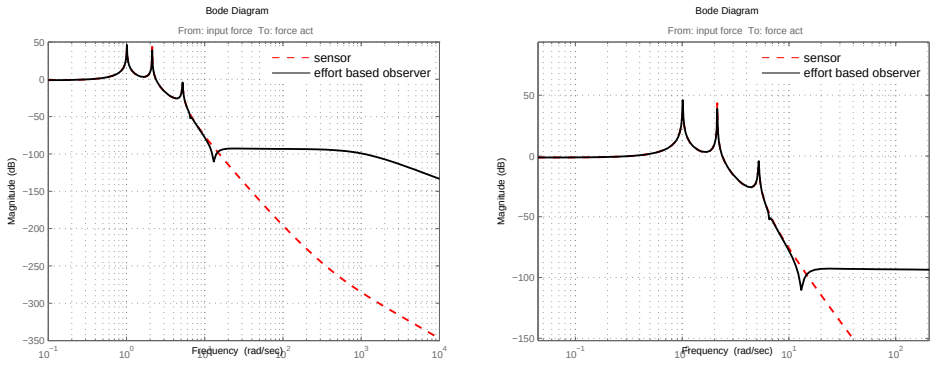

(c) $g_{eff} = 6283.1\ rad/sec$, $g_{fo} = 6283.1\ rad/sec$ (d) magnified plot

Figure 6.10: Frequency response of the *effort*-based force observer force control versus sensor based force control

The previous frequency response comparisons indicated that tuning or increasing the cut-off frequencies of the low-pass filters associated with each observer included within the overall *effort*-based force observer makes the frequency response magnitude similar to the sensor based controller. In practice, however, increasing these cut-off frequencies comes with the cost of increasing the effect of the measurement noise. Although the proposed *energy* based formalism allows realization of the force control and the full dynamical states with minimum amount of measurement. Nevertheless, considering that the measurement utilized to realize the *effort*-based force observer is corrupted with sensor noise would give more insight and allows utilization of the outlined *energy* based formalism in the filed of state estimation and force observers. Therefore, we limit the increase of the cut-off frequency according to the sensor noise bandwidth and rather than using the gains ($g_{eff} = 628.3\ rad/sec$) and ($g_{fo} = 628.3\ rad/sec$) which provide superior response as illustrated in Fig. 6.10-c, we limit both of these gains to ($g_{eff} = 314\ rad/sec$) and ($g_{fo} = 125\ rad/sec$) in order to guarantee that the sensor noise is attenuated. Fig. 6.12 indicates the Nyquist

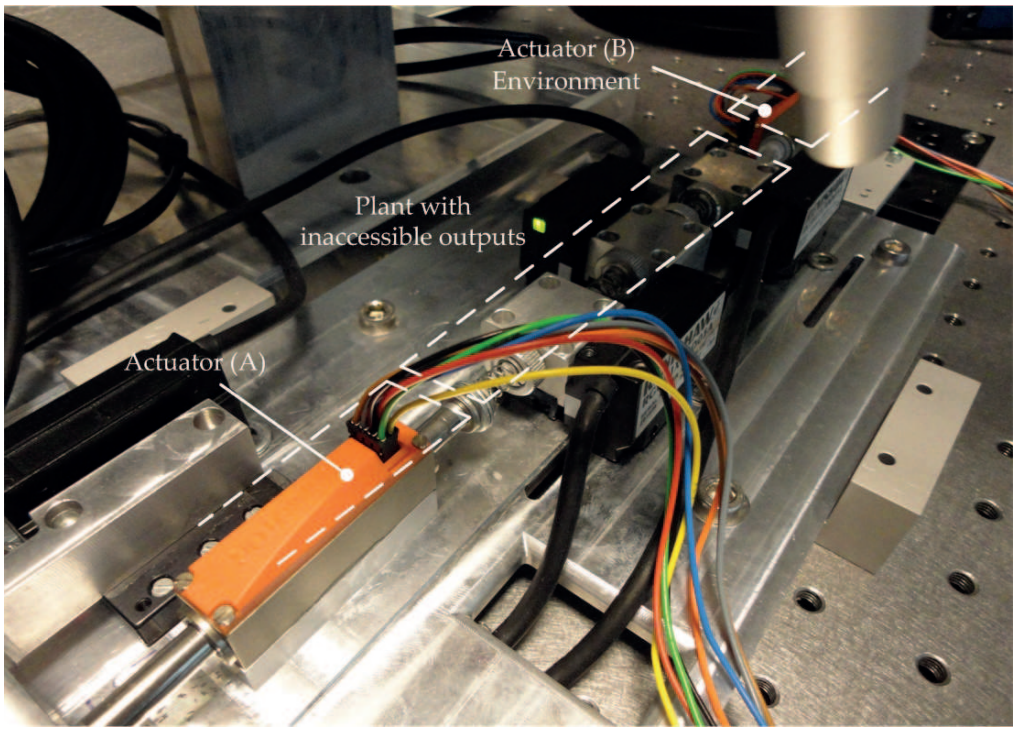

Figure 6.11: *effort*-based force observer experimental setup

stability plots for the *effort*-based state observer based force control and force sensor based control. Due to the limited observer scaler gains, the phase margin of the force observer controller is higher than the *effort*-based observer based controller. Therefore, for these particular *effort*-based observer gains the sensor based force control is more stable than the *effort*-based force controller.

The difference between the gain margins of these two force control systems is 1.3 *deg* which is acceptable especially when we consider the numerous advantages of the *effort*-based force controller and its dependency on minimum amount of measurements from the dynamical system. It is worth noting that due to the physical structure of the force sensor, its bandwidth is limited, thus the bandwidth of the *effort*-based force observer is larger and better in the sense or robustness attainment during contact with stiff environment.

6.2.2 Results

The experimental validation of the *effort*-based force observer is conducted on a dynamical system like the one depicted in Fig. 6.11. Experimental parameters are included in Table. 6.1. Instead of mounting several environments in order to examine different impedances, a linear actuator is mounted in contact with the non-collocated end-effector of the dynamical system depicted in Fig. 6.11. This allows varying the impedance from soft to hard environment without altering the environment. The dynamical system has three degrees of freedom and non of its state variables are

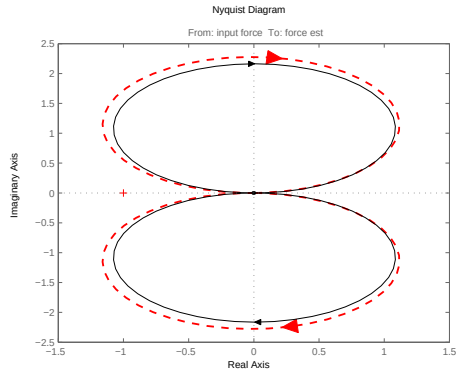

(a) $g_{eff} = 628.3\ rad/sec$, $g_{fo} = 628.3\ rad/sec$

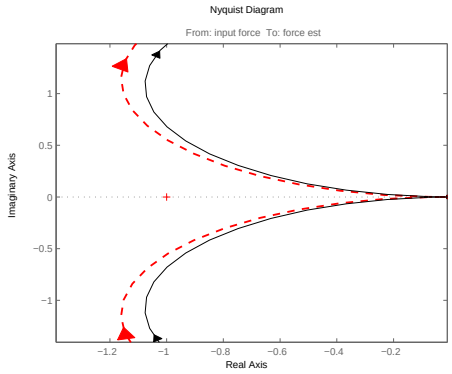

(b) magnified plot

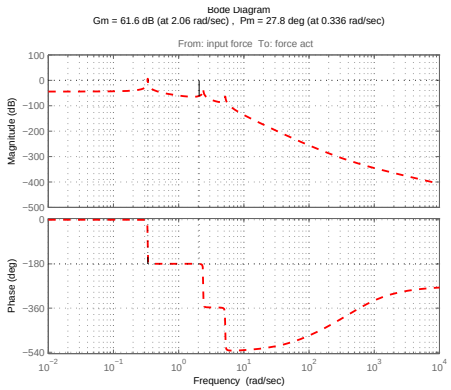

(c) $g_{eff} = 6283.1\ rad/sec$, $g_{fo} = 6283.1\ rad/sec$

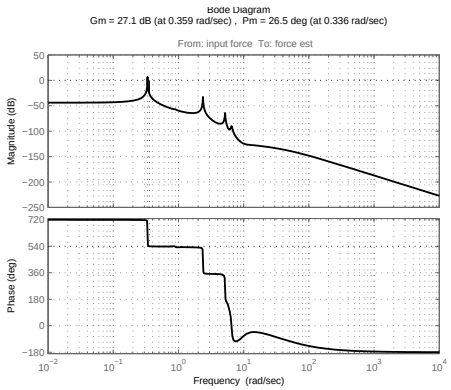

(d) Sensor based control

Figure 6.12: Nyquist stability for the *effort*-based force control versus the force sensor based control for constrained *effort*-force observer gains showing larger stability margins for the sensor based force control system

accessible for measurement. The end-effector is attached to the environment (B) directly without force sensor in between. However, the actual interaction force can be determined from the actuator current and force constant. The experimental results of the force estimation are depicted in Fig. 6.13 and Fig. 6.14 at which the environment was imposing a sinusoidal force with different frequencies at the non-collocated end-effector. In Fig. 6.13 and 6.14 the estimated force obtained through the *effort*-based force observer (Fig. 6.8) are illustrated versus the measured forces from environment. The results show satisfactory estimation results over an acceptable frequency range. Therefore, the estimated forces can be used in realizing the *effort*-based force controller.

Table 6.1: Experimental and simulation parameters

Actuator force constant	k_{fn}	6.43	N/A
Actuator Nominal mass	m_{an}	0.059	kg
Lumped masses	$m_{1,2,3}$	0.019	kg
Identified spring constants	$k_{1,2,3}$	503.96	N/m
Identified viscous damping coefficients	$c_{1,2,3}$	0.262	Ns/m
Reaction force observer gain	g_{reac}	628	rad/s
Disturbance observer gain	g_{dist}	628	rad/s
Force observer gain	g_{fo}	628	rad/s
Low-pass filter gain	g_l	1000	rad/s
Sampling time	T_s	1	ms

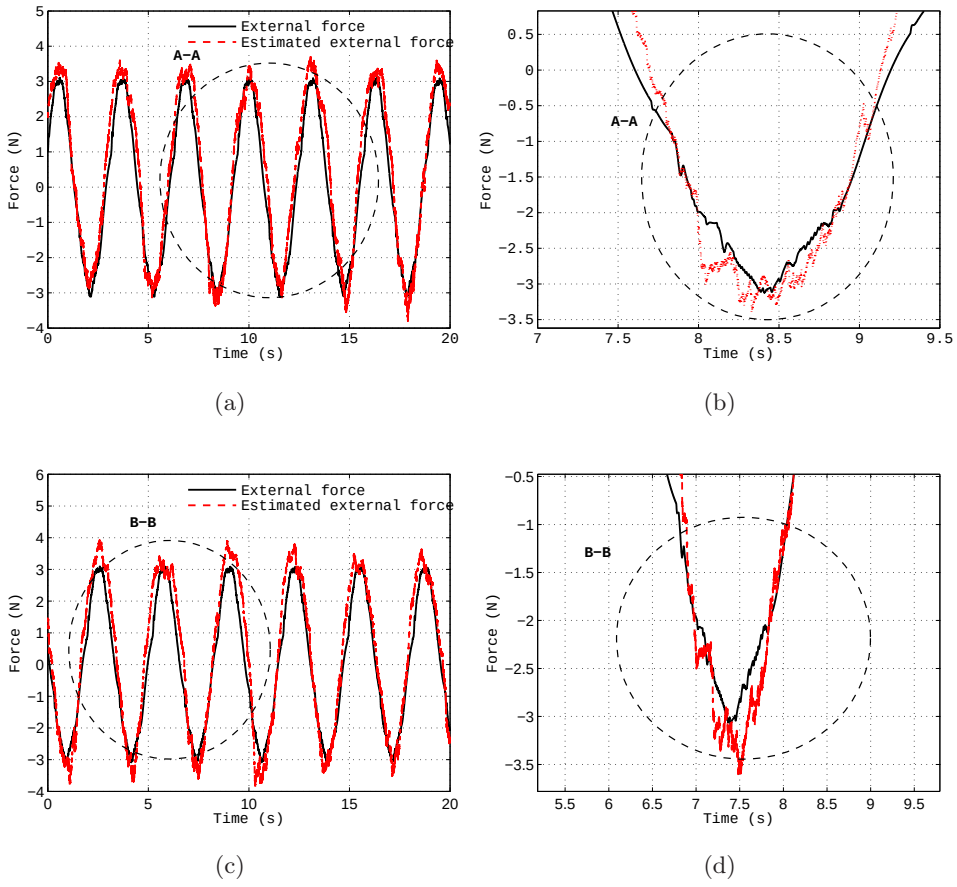

Figure 6.13: *effort*-based force observer experimental results

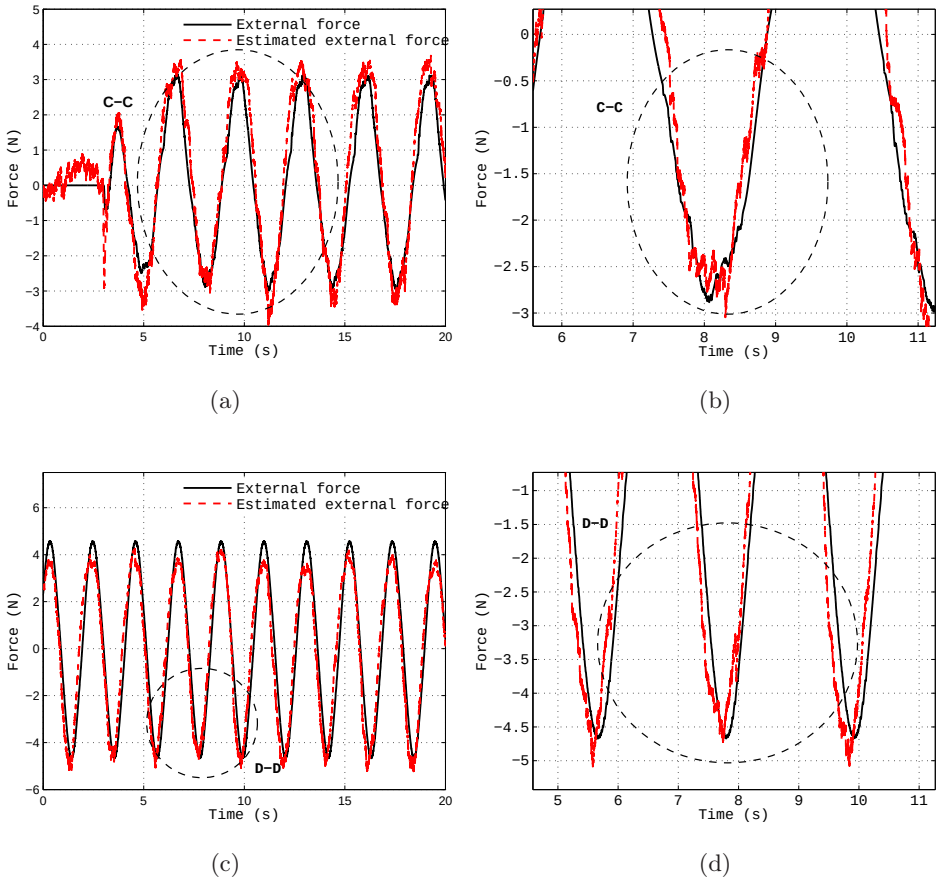

Figure 6.14: *effort*-based force observer experimental results

6.2.3 Summary and discussion

The problems associated with force sensors such as the measurement noise, limited bandwidth due to the physical structure of the sensor and the non-collocation can be avoided through the outlined *effort*-based force observer. This observer differs from the reaction force observer as it doesn't require measuring the *flow* variable of the degree of freedom which interacts with the environment during a force control task. The *effort*-based force observer is rather depending on the feedback-like *effort*-forces in estimating the interaction forces between the robot end-effector and an environment.

It was shown that the frequency response of the *effort*-based force observer based force control can be similar to the sensor based force control frequency response by increasing the observer gains to certain values. This is, however, limited with the bandwidth of the sensor noise. Therefore, phase margin of the *effort*-based force control is less than the phase margin of the ideal sensor based force control. Therefore, theoretically the sensor based observer has better stability than the *effort*-based

force observer. However, the advantages of the *effort*-based force observer appears when the practical limitations outlined in this chapter are taken into consideration.

The *effort*-based state observer has at least 4 degrees of freedom which have to be selected during its design, the *effort*-force observer gains g_{dist} and g_{eff}, the Luenberger-like *effort*-force based state observer vector gain M and the reaction force observer gain g_{fo}. Utilization of higher order observers in order to enhance the performance would increase the number of scaler gains associated with each observer. In addition, to increasing the induced phase lag induced by each of these observer into the overall system. Therefore, the stability and performance analysis outlined in this chapter can be used as a guide line in adjusting these gains and selecting the order of each of these observers.

Chapter 7

Effort Observer based Control of Distributed Systems

WE shall now apply the same formalism to distributed systems that are commonly agreed to be represented with truncated models, perhaps a high or low order representation based on many aspects, i.e., an accurate model is required for control purposes near the crossover frequency and for simulation purposes its enough to capture the essential dynamics within the excitation signal frequency range. Therefore, in the sequel, we shall obtain optimal truncated models for dynamical systems with distributed dynamics based on minimization of the Hankel matrix norm. This is validated by comparing the dynamics of the reduced model to the dynamics of the original. The *effort*-based state observer is then studied in order to overcome problems such as those ones associated with control of flexible manipulators, e.g., limited bandwidth of the strain gauges, the inaccurate kinematical maps between the measurement points and the end-effector and strain gauge measurement noise.

7.1 Optimal Model Reduction in The Hankel Norm

Consider a distributed dynamical system with inaccessible state variables and outputs excited via a single input with r state variables that are accessible for measurement, i.e., its $(\infty - r)$ state variables are not available for measurement. Therefore, we seek to represent a general class of dynamical systems with infinite-dimensional state space realization. After obtaining this infinite-dimensional representation, a higher order model can be easily obtained by assigning some constrains on the bandwidth of the input excitation signal which is the case in most of the physical systems. Hereafter, the optimal model reduction is performed in the Hankel norm [Zhou 1993]-[Kung 1981].

7.1.1 Euler-Bernoulli beam

Flexible beam is modeled using the following partial differential equation [Pal 1988],

$$EIy_{xxxx}(x,t) + ky_t(x,t) + \rho Ay_{tt}(x,t) = \tau(x,t) \tag{7.1}$$

where E, I, ρ, A and k are modulus of elasticity, Inertia, density, cross section area and damping coefficient of the beam respectively. $\tau(x,t)$ is the external applied

force while $y(x,t)$ is the beam's lateral displacement. The slope of the beam can be written as follows

$$\theta(t,x) = \frac{\partial y(x,t)}{\partial x} \tag{7.2}$$

and the simple beam equation is

$$\frac{\partial \theta(x,t)}{\partial x} = \frac{-1}{EI} \tag{7.3}$$

the bending moment is

$$\sigma(x,t) = \frac{\partial M(x,t)}{\partial x} \tag{7.4}$$

Therefore, Newton law can be written as follows

$$\frac{\partial \sigma(x,t)}{\partial x} = \rho \frac{\partial y(x,t)}{\partial t^2} + K \frac{\partial y(x,t)}{\partial t} + \rho g \tag{7.5}$$

that can be written as a matrix differential equation

$$\frac{\partial \mathbf{q}}{\partial x} = F_o + F_1 \frac{\partial \mathbf{q}}{\partial t} + F_2 \frac{\partial^2 \mathbf{q}}{\partial t^2} + u(x,t) \tag{7.6}$$

where $\mathbf{q}$ is the following vector

$$\mathbf{q} \triangleq \begin{bmatrix} y & \theta & m & \sigma \end{bmatrix}^{\mathrm{T}} \tag{7.7}$$

where F_o, F_1 and F_2 are matrices that include beam parameters, taking the Laplace transform of (7.6) we obtain

$$\frac{dQ(x,s)}{dx} = (F_o + F_1 s + F_2 s^2) Q(x,s) + U(x,s) \tag{7.8}$$

$$F_o = \begin{bmatrix} 0 & 1 & 0 & 0 \\ 0 & 0 & \frac{-1}{EI} & 0 \\ 0 & 0 & 0 & 1 \\ 0 & 0 & 0 & 0 \end{bmatrix} \quad , \quad F_1 = \begin{bmatrix} 0 & 0 & 0 & 0 \\ 0 & 0 & 0 & 0 \\ 0 & 0 & 0 & 0 \\ k & 0 & 0 & 0 \end{bmatrix} \quad , \quad F_2 = \begin{bmatrix} 0 & 0 & 0 & 0 \\ 0 & 0 & 0 & 0 \\ 0 & 0 & 0 & 0 \\ \rho & 0 & 0 & 0 \end{bmatrix}$$

solving the previous differential equation (7.8) for $Q(x,s)$ we obtain

$$Q(x,s) = e^{(F_o + F_1 s + F_2 s^2)x} Q(0,s) + \int_o^l e^{(F_o + F_1 s + F_2 s^2)(l-\zeta)} U d\zeta \tag{7.9}$$

The first equation of (7.9) can be used to obtain the following transfer function,

$$\frac{Y(x,s)}{T(s)} = \frac{\beta_1}{s} + \frac{\beta_2}{s + \frac{k}{\rho}} + \sum_{i=o}^{\infty} \frac{\beta_{3_i}}{(s + \frac{k}{\rho})^2 + \frac{\omega_i^2}{4\rho^2}} \tag{7.10}$$

$$\beta_1 = \frac{3x}{kl^3} \ , \ \beta_1 = -\beta_2 \ , \ \beta_{3_i} = \gamma_i Q_i(\lambda)/\rho \ , \ \gamma_1 = \frac{3x}{kl^2}$$

$$\gamma_2 = -\gamma_1 \ , \ \gamma_i = 2[\rho EI(3.928 \pm i\pi)^4 - k^2]/l^2$$

(7.10) represent is an infinite-dimensional linear system representation of the flexible beam which has an equivalent infinite-dimension state space realization. We further consider a limit on the bandwidth of the excitation input signal ($T(s)$). This assumption will allow us to alter the infinite dimensional transfer function representation with a high order representation with dimension n

$$\frac{Y(x,s)}{T(s)} = \frac{\beta_1}{s} + \frac{\beta_2}{s+\frac{k}{\rho}} + \sum_{i=o}^{n} \frac{\beta_{3_i}}{(s+\frac{k}{\rho})^2 + \frac{\omega_i^2}{4\rho^2}} \tag{7.11}$$

which has the equivalent nth order state space representation

$$\Sigma = (A, B, C, D) \tag{7.12}$$

7.1.2 Hankel norm approximation

Given an nth state space realization Σ which is controllable and observable, we seek to find a kth order stable system Σ_k

$$\Sigma_k = (A_k, B_k, C_k, D_k) \tag{7.13}$$

such that the error $\|\Sigma - \Sigma_k\|_{\mathcal{H}}$ is minimal, where the Hankel norm $\|.\|_{\mathcal{H}}$ of a stable system is

$$\|.\|_{\mathcal{H}} = \sup_{0<\|u_-\|_2<\infty} \frac{\|y_+\|_2}{\|u_-\|_2} \tag{7.14}$$

the Hankel norm tells how much energy can be transferred from past inputs u_- into future outputs y_+ through certain system [Krishnan 1988]. In other words, the Hankel operator associated with system Σ is a mapping $\mathcal{H}$ that maps the past inputs to the future outputs of Σ

$$\mathcal{H} : u_{-+} \ \ ; \ \ y_+ = \sum_{k=-\infty}^{-1} h(t-k)u_-(k) \ \ , \ \ t \geq 0 \tag{7.15}$$

where h is the impulse response of the system Σ. Putting (7.15) in matrix form

$$y_+ = \begin{bmatrix} y(0) \\ y(1) \\ y(2) \\ \vdots \end{bmatrix} = \begin{bmatrix} h(1) & h(2) & h(3) & h(4) & \dots \\ h(2) & h(3) & h(4) & h(5) & \dots \\ h(3) & h(4) & h(5) & h(6) & \dots \\ \vdots & \vdots & \vdots & \vdots & \ddots \end{bmatrix} \begin{bmatrix} u(-1) \\ u(-2) \\ u(-3) \\ \vdots \end{bmatrix} \tag{7.16}$$

It can be shown that the impulse response of the system Σ is defined as

$$h(\tau) = \begin{cases} 0 & \text{if} \quad \tau < 0 \\ D & \text{if} \quad \tau = 0 \\ CA^{\tau-1}B & \text{if} \quad \tau > 0 \end{cases}$$

using the definition of the impulse response, it can be shown that (7.16) can be expressed as

$$y_+ = \begin{bmatrix} CB & CAB & CA^2B & CA^3B & \dots \\ CAB & CA^2B & CA^3B & CA^4B & \dots \\ CA^2B & CA^3B & CA^4B & CA^5B & \dots \\ \vdots & \vdots & \vdots & \vdots & \ddots \end{bmatrix} \begin{bmatrix} u(-1) \\ u(-2) \\ u(-3) \\ \vdots \end{bmatrix} \tag{7.17}$$

$$y_+ = \begin{bmatrix} C \\ CA \\ CA^2 \\ \vdots \end{bmatrix} \begin{bmatrix} B & AB & A^2B & \dots \end{bmatrix} \begin{bmatrix} u(-1) \\ u(-2) \\ u(-3) \\ \vdots \end{bmatrix} = PQu_- \tag{7.18}$$

Then, it follows that

$$\mathcal{H} = PQ \tag{7.19}$$

The Hankel singular values of the controllable, observable and stable system Σ are the square roots of the eigenvalues of the matrix PQ, i.e.,

$$\sigma_i(\Sigma) = \sqrt{\lambda_i(PQ)} \tag{7.20}$$

Moreover, the Hankel norm of the system $\Sigma = (A, B, C, D)$ is

$$\|\Sigma\|_{\mathcal{H}} = \sqrt{\lambda_{max}(PQ)} = \sigma_1 \tag{7.21}$$

Therefore, the Hankel Norm is the largest Hankel singular value. We apply this reduction method to system (7.11), the input-output relationship is described using 22 state variables model, each of these state variable represent a displacement or its rate of change. The frequency response of this system is depicted in Fig. 7.1 and the objective is to find a low-order model that preserves the information content shown in the frequency response Fig. 7.1 to an acceptable level of accuracy. In order to show which of the system Σ states are dominant, the Hankel singular values have to be computed. These values are depicted in Fig. 7.2 which suggests that there are seven dominant modes in this system and the contribution of the other modes can be discarded. Therefore, the reduced order model Σ_k we are seeking is of $7th$ order.

As shown in Fig. 7.3, the frequency response of the original system is plotted versus the truncated one. The truncated model captures the information content of the original system below 10 rad/sec. However, the match is poor beneath 10 rad/sec due to the truncation.

Now, we can further proceed by applying the outlined *energy* formalism on the optimal truncated model which represents the optimal representation of the actual system in the sense of Hankel norm.

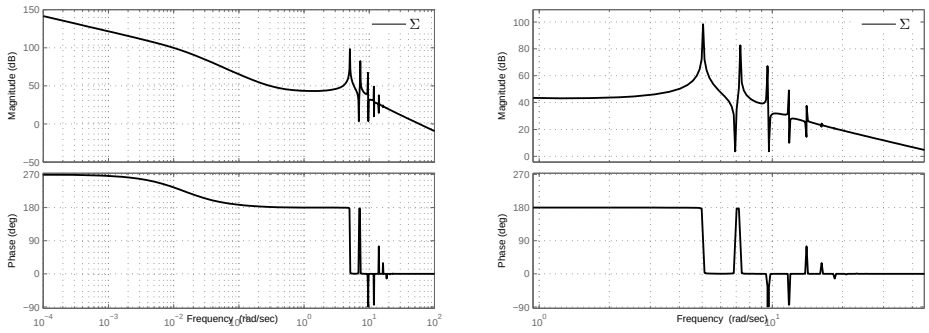

(a) system Σ frequency response (b) magnified plot

Figure 7.1: Frequency response of the original high order system Σ with 22-state variables

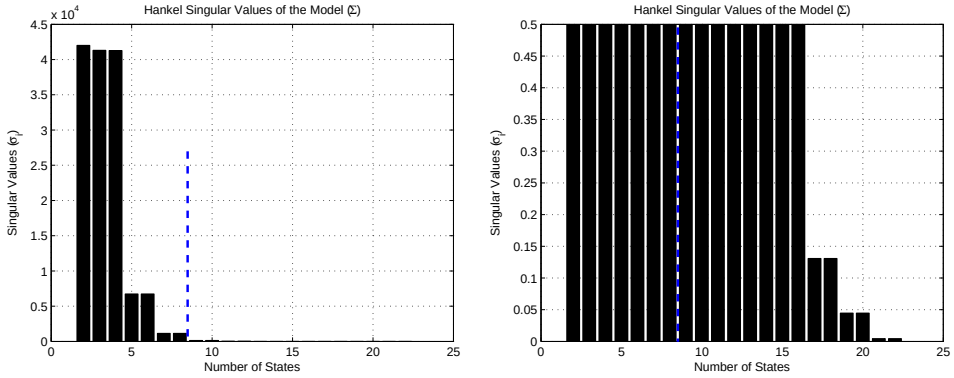

(a) (b) magnified plot

Figure 7.2: Hankel singular values of the high order model Σ.

7.2 Effort based Optimal Control

Since we obtained the following optimal truncated model,

$$\widetilde{x} = A_k\widetilde{x} + B_k u \quad , \quad y = C_k\widetilde{x} + D_k u \tag{7.22}$$

we can proceed to the next step by designing *energy* based state observer in order to estimate the truncated states of the distributed systems we consider in this Chapter.

7.2.1 Effort based state observer

Again, it would natural to apply the same formalism by breaking the optimal truncated model into the standard form presented in Chapter 4 in order to realize the

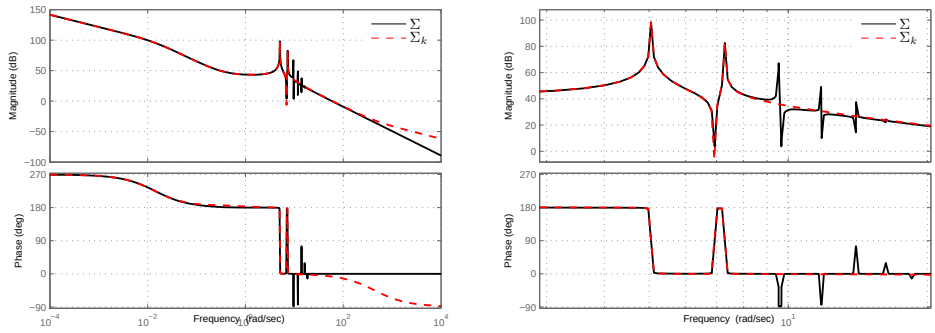

(a) Σ versus Σ_k (b) magnified plot

Figure 7.3: Optimal truncated model versus original system frequency response.

effort-force based state observer. First we have to define the Dirac structure representation which of the *power-conserving* interconnection between the optimally truncated subsystem with inaccessible state variable and the other system with state variables that are accessible for measurement,

$$f^s = e^m = y \quad , \quad f^m = -e^s + u$$

hereafter, the decoupled state space representation can be shown to be,

$$\begin{bmatrix} \dot{\widetilde{x}}^a \\ -- \\ \dot{\widetilde{x}}^p \end{bmatrix} = \left[\begin{array}{c|c} A_k^a & \emptyset \\ -- & -- \\ \emptyset & \emptyset \end{array}\right] \begin{bmatrix} \widetilde{x}^a \\ -- \\ \widetilde{x}^p \end{bmatrix} + \left[\begin{array}{c|c} \emptyset & \emptyset \\ -- & -- \\ \emptyset & A_k^p \end{array}\right] \begin{bmatrix} \widetilde{x}^a \\ -- \\ \widetilde{x}^p \end{bmatrix} + \begin{bmatrix} B_k^a \\ -- \\ \emptyset \end{bmatrix} u$$

$$+ \left[\begin{pmatrix} \emptyset \\ -- \\ B_k^p \end{pmatrix} + \begin{pmatrix} B_k^{eff} \\ -- \\ \emptyset \end{pmatrix} \right] e(\widetilde{\mathrm{x}}^{\mathrm{a}}, \widetilde{\mathrm{x}}^p)$$

therefore,

$$\dot{\widetilde{\mathrm{x}}}^a = A_k^a \widetilde{\mathrm{x}}^a + B_k^a u + B_k^{eff} e(\widetilde{\mathrm{x}}^{\mathrm{a}}, \widetilde{\mathrm{x}}^p) \tag{7.23}$$

$$\dot{\widetilde{\mathrm{x}}}^p = A_k^p \widetilde{\mathrm{x}}^p + B_k^p e(\widetilde{\mathrm{x}}^{\mathrm{a}}, \widetilde{\mathrm{x}}^p)$$

now, we can write the *effort*-force state observer,

$$\dot{\widehat{\widetilde{\mathrm{x}}}} = A_k \widehat{\widetilde{\mathrm{x}}} + B_k u + \mathrm{M}\big(\widehat{e}(u, \widetilde{\mathrm{x}}^a) - e(\widetilde{\mathrm{x}}^a, \widehat{\widetilde{\mathrm{x}}}^p)\big) \tag{7.24}$$

Fig. 7.4 represents the *effort*-based state observer for the truncated model Σ_k of the higher order system Σ which was obtained from a dynamical system with distributed dynamics. We proceed with the same flexible beam example at which 7 truncated state variables are used instead of 22 state variables since the first seven

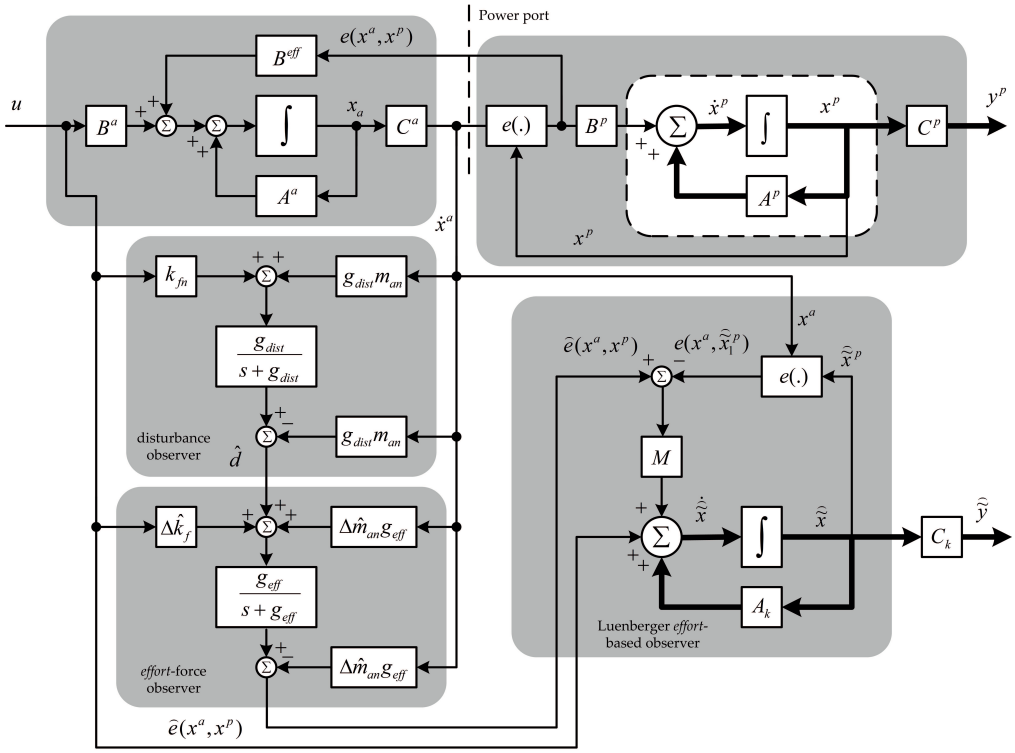

Figure 7.4: *Effort*-force based state observer for the optimal truncated model Σ_k.

Table 7.1: Simulation parameters

Length	L	0.5	m
Thickness	t	0.001	m
Modulus of elasticity	E	200	Gpa
Width	b	0.02	m
Density	ρ	7.83e-1	kg/m^3
effort force observer gain	g_{reac}	628	rad/s
Low-pass filter gain	g_f	628	rad/s

Hankel singular values are dominant as it can be easily shown from Fig. 7.2. First the interconnection between the dynamical system with inaccessible state variables and its single input has to be specified in terms of the Dirac structure in order to be able to model the *effort*-force which is conceptually considered as the single feedback from the dynamical system. The *effort*-force observer has to be then designed in order to estimate this feedback-like force and use it in the realization of the *effort*-based state observer. The procedure of designing the *effort*-based state observer are similar to those studied in Chapter 4.

Simulation results of the *effort*-based state observer are depicted in Fig. 7.5

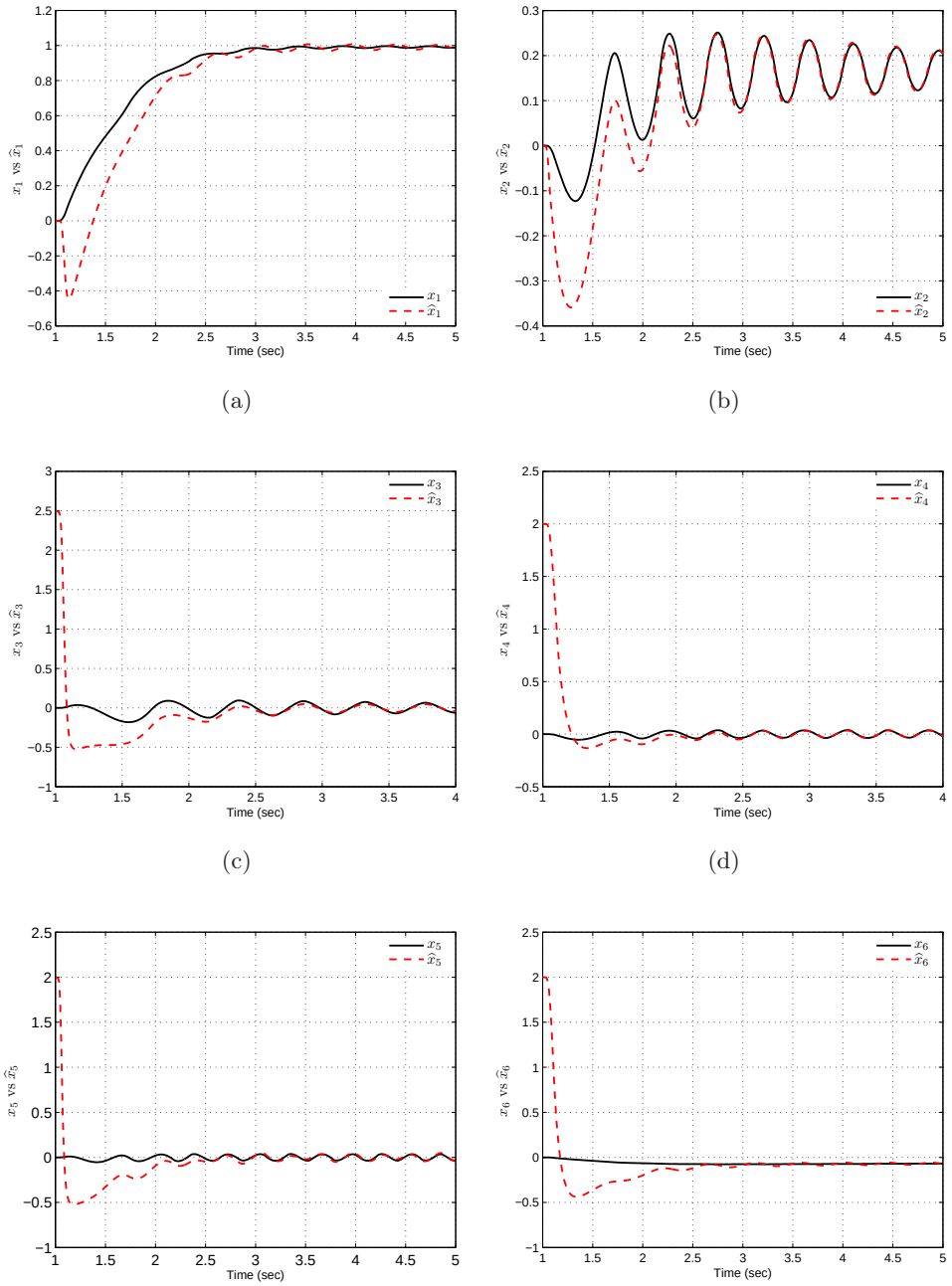

Figure 7.5: Estimated state variables through the *effort*-based state observer versus the actual state variables simulation results.

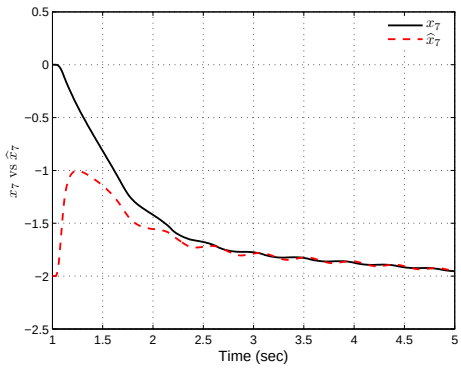

Figure 7.6: Estimated state variables versus actual one.

and Fig. 7.6 where the estimated state variables of the truncated model starts from arbitrary initial conditions in order to examine the robustness of the *effort*-based state observer to the unknown initial conditions. The simulation parameters utilized through out this simulations and throughout the computation of the higher order model of the flexible beam and its optimal truncated model are included in Table. 7.1.

The previous results indicate that, for a system with distributed dynamics such as the flexible beam, one can realize the *effort*-based state observer of its truncated model and therefore can estimate its dominate state variables even in the complete absence of measurements. In addition, the previous results show satisfactory robustness to unknown initial conditions. It is worth noting that due to the truncation which is made based on the Hankel norm minimization between the original system and the reduced order system, the frequency response of the truncated model does not match the original one at frequencies larger than 10 rad/sec. Therefore, we have to avoid exciting the system with frequencies higher than 10 rad/sec as the truncated optimal model does not contain the exact information content of the original system within this frequency range. We can overcome such problem by filtering the control input such that its energy content at this frequency range is zero. This can be done by specifying these frequencies at which the optimal model does not match with the original system then designing band pass-filters accordingly in order to ensure that the control signal will not excite the system in such frequency range [Bhat 1990]-[Bhat 1991].

7.3 Effort based control

Realization of the *effort*-based state observer allows the full observable state variables of the dynamical system to be available. Therefore, it would be nature to devise an optimal control law that requires presence of the system full state vari-

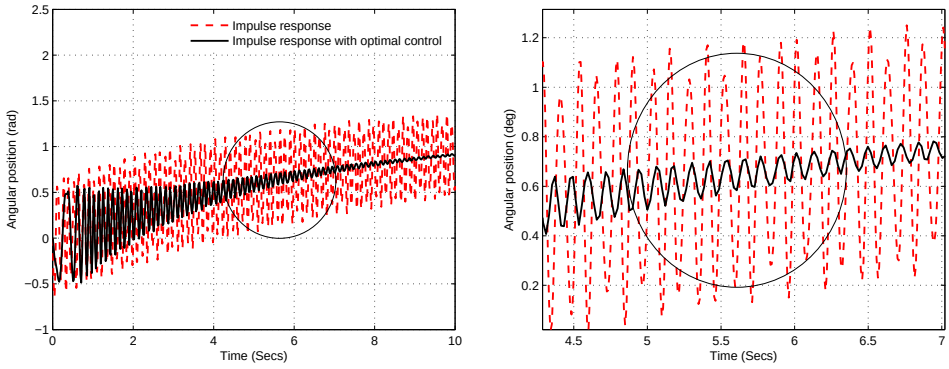

(a) impulse response (b) magnified plot

Figure 7.7: Regulated versus non regulated flexible beam impulse responses.

ables. Selecting the following quadratic performance index

$$\mathbf{J} = \frac{1}{2}[\widehat{\widetilde{\mathbf{x}}}(t_f) - \mathbf{r}(t_f)]^{\mathrm{T}}\mathbf{H}[\widehat{\widetilde{\mathbf{x}}}(t_f) - \mathbf{r}(t_f)] + \int_{t_0}^{t_f} \frac{1}{2}\big[(\widehat{\widetilde{\mathbf{x}}}(t) - \mathbf{r}(t))^{\mathrm{T}}\mathbf{Q}(\widetilde{\mathbf{x}}(t) - \mathbf{r}(t)) + \mathbf{u}^{\mathrm{T}}(t)\mathbf{R}\mathbf{u}(t)\big]dt \tag{7.25}$$

which depends on the truncated estimated states through the *effort*-based state observer (7.24), Q and R are Positive definite symmetric matrices. $\mathbf{r}(t)$ is the time varying reference trajectory. Consequently, the Hamiltonian can be defined as follows

$$\begin{aligned}\mathscr{H}(\widehat{\widetilde{\mathbf{x}}}(t), \mathbf{u}(t), \widehat{\mathbf{p}}(t), t) &= \frac{1}{2} \parallel \widehat{\widetilde{\mathbf{x}}}(t) - \mathbf{r}(t) \parallel^2_{\mathbf{Q}} + \frac{1}{2} \parallel \mathbf{u}(t) \parallel^2_{\mathbf{R}} \\ &\quad + \widehat{\mathbf{p}}^{\mathrm{T}}(t)\mathbf{A}\widehat{\widetilde{\mathbf{x}}}(t) + \widehat{\mathbf{p}}^{\mathrm{T}}(t)\mathbf{B}\mathbf{u}(t)\end{aligned} \tag{7.26}$$

therefore the control low is of the form

$$\mathbf{u}(t) = \mathbf{u}_c^* - \mathbf{R}^{-1}\mathbf{B}^t\mathbf{k}(t)\widetilde{\mathbf{x}}(t) \tag{7.27}$$

where $\mathbf{u}_c^*$ is a feed forward control input and $\mathbf{k}(t)$ is a symmetric matrix that has to satisfy the following Riccati matrix differential equations.

$$\dot{\mathbf{K}}(t) + \mathbf{A}^T\mathbf{K}(t) - \mathbf{K}(t)\mathbf{A} - \mathbf{K}\mathbf{B}\mathbf{R}^{-1}B^t\mathbf{K}(t) + \mathbf{Q} = 0 \tag{7.28}$$

$$\dot{\mathbf{s}} = -[\mathbf{A}^{\mathrm{T}} - \mathbf{K}\mathbf{B}\mathbf{R}^{-1}]\mathbf{s} + \mathbf{Q}\mathbf{r}(t) \tag{7.29}$$

The impulse response of the regulated flexible beam is illustrated in Fig. 7.7 versus the non regulated one which indicates everlasting vibrational behavior in the absence of the regulating control input. Optimal motion control along with the result of the regulated states are depicted in Fig. 7.8 and Fig. 7.9, respectively.

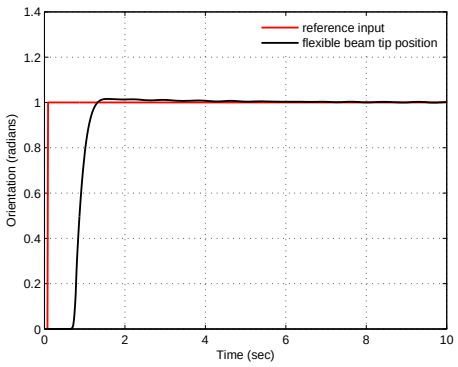

Figure 7.8: *effort*-based optimal control result.

7.3.1 Summary and discussion

The *energy* based state observer can be used in order to estimate the dynamical state variables of systems with continuous dynamics such as flexible robot arms and shafts. First, we assumed that the infinite dimensional state space realization of such systems can be turned into a realization with high order by assuming that there exist a bound on the bandwidth of the excitation signal. Hereafter, the high order model can be used in order to determine the optimal reduced order model through minimizing the Hankel matrix norm. The Hankel norm can be determined through the singular values of the matrix PQ. Then by examining the Hankel matrix singular values we can determine which modes or singular values are dominant.

In the example outlined in this chapter, a flexible beam is modeled to obtain its dynamical model which happened to have an infinite dimensional transfer function representation. Based on the assumption that the excitation signal is bandlimited, a high order model representation is determined which consists of 22-state variables. The Hankel norm minimization is utilized in order to obtain the reduced order model. Then it was shown that the first seven Hankel singular values are dominant, whereas the rest of the singular values can be discarded. Therefore, the optimal truncated model is described with 7-state variables instead of 22-state variables.

As soon as the optimal reduced order model is obtained, we can proceed with the typical procedure of designing *energy* based state observer by breaking down the optimal realization into two state space representations based on subsystem with inaccessible state variables. In the outlined example, the flexible beam is the dynamical subsystem with inaccessible state variables. Then, based on the Dirac structure of the interconnection between the dynamical subsystems with and without available state variable for measurements, a model for the feedback-like *effort*-force is derived and further used in the realization of the *effort*-based state observer. The obtained results showed satisfactory convergence results under unknown initial conditions for most of the estimated state variables.

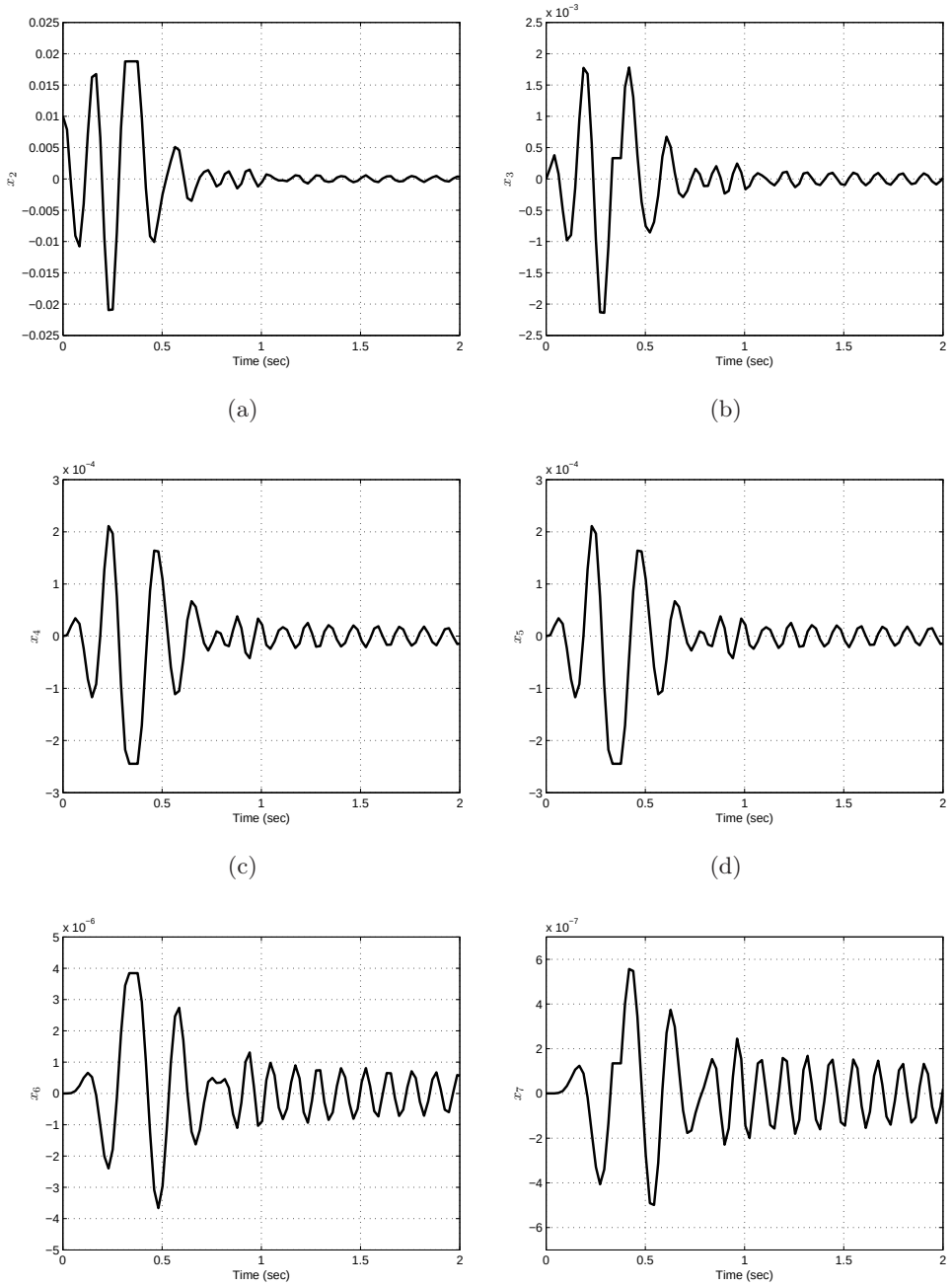

Figure 7.9: Regulated state variables.

Chapter 8

Conclusion

ENERGY exchange between the interconnected dynamical system can be utilized in designing state variables observers as well as control systems. As the *energy* based formalism allows recasting the control problem as finding a dynamical system and an interconnection pattern such that the Hamiltonian overall energy function takes the desired form, it can be also extended to utilize the energy exchange along the interconnected subsystem power ports in the realization of a conceptual feedback-like variables. This feedback-like variables can then be used as basis for the reconstruction of the state variables and the design of state observers.

According to the *energy* based formalism, all the existing state observers regardless to their structure and their state estimation robustness can be categorized as *flow*-based state observer due to their dependency on the *flow* variables in their design. In this observers category, *flow* variables have to be available for measurement then injected onto the observer structure in order to enforce desired estimation error dynamics. Due to the dependency of these observer on the *flow* variables measurements, control and state estimation of a class of dynamical system with inaccessible state variables and outputs can not be realized. Therefore, the dual space of the *flow* variables space, i.e., the *effort* variable space is utilized in the design of state observers when the *flow* variables are not available for measurement. This gives us the ability to categorize state observers into: *flow* based and *effort*-based state observers. The first depend on the availability of *flow* variables for measurements, whereas the second depends on the ability to estimate their dual variables.

In general, the *energy* based formalism allows studying complex linear and nonlinear systems by decomposing them into simpler subsystems which, upon the interconnection, adds up their energies to determine the behavior of the full system. We further decompose the system into two portions, one with and without available state variables for measurements. The *power-conserving* interconnection between these two subsystem can be used to realize a natural feedback from this subsystem with inaccessible state variables on the other subsystem with the accessible state variables. Therefore, in the complete absence of a dynamical subsystem state variables measurements, the *power conserving* interconnection provides a natural feedback through the power port of these systems which can be used as basis to construct state observers.

It was shown that for any *power-conserving* interconnection, we cannot impose both *effort* and *flow* variables at a time, the interconnection is, however, in feedback which means that if two subsystems are in a *power-conserving* interconnection, the

output *flow* variable of the first system acts as an input to the second, while the output *effort* of the second acts as an input to the first subsystem. And it was shown that this is due to the dimension of the Dirac structure that is equal to the dimension of the *flow* variables space or its *effort* variables dual space. This indicates that for any *power-conserving* interconnection between dynamical subsystem, there is always energy exchange between these two subsystems in terms of *flow* and *effort* variables. The specific nature of these variables can be determined upon the nature of power being exchanged between these subsystems. In other words, if electrical power is being exchanged between the dynamical subsystems, spaces of *effort* and *flow* variables are the spaces of voltage and current variables, respectively. Similarly, if mechanical power is being exchanged along the power port of the *power-conserving* interconnection, the spaces of *effort* and *flow* variables are the spaces of generalized forces and generalized velocities, respectively.

The previous analysis indicates that even in the complete absence of the state variables from a dynamical subsystem, its *power-conserving* interconnection with other subsystem guarantee that there exist a natural feedback in terms of *effort* or *flow* variables.

- *Effort*-based State Observer

Effort-based state observer is designed for wide classes of dynamical system with linear and Quasi-nonlinear dynamics. In addition, for dynamical systems with non-linear dynamics, a transformation can be carried out to have them represented in a Quasi-nonlinear form. Therefore, the class of dynamical system we consider is fairly general. The *effort*-based state observer is designed for a dynamical subsystem with inaccessible state variables by estimating its natural feedback (*effort* variable) through the *power-conserving* interconnection with another dynamical system. The estimated *effort* variables are then injected onto the observer structure in order to enforce desired estimation error dynamics.

Due to the dependence of the feedback-like forces utilized in the realization of the *effort*-based state variable on the definition of the Dirac structure. The error dynamics is not trivial it is rather depending on the Dirac structure representation of the interconnected subsystems. However, the Dirac structure representations between most of the interconnected dynamical subsystems are few. Therefore, the error dynamics can be derived for each specific case based on the Dirac structure definition. It was shown that for system with linear dynamics and with a Dirac structure between interconnected subsystems in terms of energy storage element and energy dissipation element that, if the matrix $A + \mathrm{M}\big(c\mathrm{L}_2 + k\mathrm{L}_1\big)$ was Hurwitz, the estimation error will converge to zero for any initial error vector $\widetilde{\mathrm{x}}(0)$, i.e., the estimated states $\widehat{\mathrm{x}}$ will converge to x regardless to the initial value of the estimated and actual states $\widehat{\mathrm{x}}(0)$ and $\mathrm{x}(0)$, respectively. The experimental results showed robustness over parameter deviations and unknown initial conditions. However, the reconstruction time in the presence of parameter deviation and unknown initial conditions is longer.

The *effort*-based state observer is designed for dynamical systems with Quasi-nonlinear dynamics for two cases at which the *effort* feedback-like signals are described with linear and nonlinear functions. For these cases the error dynamics is derived and used to obtain necessary and sufficient conditions for the estimation error asymptotic stability. The necessary and sufficient conditions are then represented in the form of linear matrix inequality which can be solved as an optimization problem in order to obtain the optimum *effort*-based state observer gain vector that provides asymptotic stability of the estimation error for larger range of robustness and estimation stability.

The observer is implemented twice for a cart pendulum and single-link robot manipulator in order to show the effect of the nonlinear and linear *effort* mapping in the estimation error dynamics, respectively. Estimation robustness for unknown initial conditions was also investigated and the observer showed satisfactory asymptotic stability.

In general, the *effort*-based state observer has at least three degrees of freedom since it consists of three observers in cascade, two *effort*-force observers and a Luenberger-like *effort*-based state observer. The associated scaler and vector gains of the observer must be selected such that the reconstruction of the state variables is twice faster than the control system. It is worth noting that the order of these observers associated with the overall *effort*-based state observer affects the accuracy and the speed of the estimated states reconstruction. Therefore, this trade-off must be considered while designing the *effort*-based state observer.

Due to the structure of the *effort*-based state observer which consists of three observer in cascade, the phase margin of the observer based control system is less than the phase margin of the sensor based one. This is due to the amount of phase lag induced by each single observer associated with the overall *effort*-based state observer. Therefore, the sensor based control system turned out to be more stable than *effort*-based observer control system. Experimentally, these two controller were utilized to position a non-collocated point along a dynamical system with three degrees of freedom. The experiment was performed for similar controller gain and experimental parameter and settings. Performance of the sensor based control system showed faster settling time, whereas oscillatory response was obtained with larger settling time in the case of the *effort*-based state observer based control system.

Necessary and sufficient conditions for observability of state variables of a dynamical system with inaccessible state variables from the incident *effort* variables were analyzed. The system matrix of the dynamical system must have distinct eigenvalues in order to be able to observer the dynamical state variables from the *effort* variables obtained from the power port of the interconnection. The observability in this case is not defined by the pair (A, C), it is rather defined by the state matrix and the *effort*-force pair (A, e).

The *effort*-based state observer is fairly general, if a transformation $z = T(x)$ of the dynamical system with the form $f(x, u)$ to the form $\mathbf{A}z + \Phi(z, u)$ exists. Then the necessary and sufficient conditions for the estimation error asymptotic stability

in the form of linear matrix inequality can be used in order to design the observer vector and scaler gains for this general class of dynamical systems.

- *Effort*-based State Observer based Control System

The *effort*-based state observer provides estimates of the full observable states. Therefore, it would be natural to devise controllers such as state feedback controllers and optimal controllers which depends on the presence of full states for linear systems. A state feedback controller along with additional control input to suppress disturbances and for the attainment of robustness is realized based on the estimated states. For the same controller parameters the sensor based controller showed better performance over the observer based controller in terms of settling time due to the larger phase margin of the sensor based controller.

Due to the presence of the estimated full states, the optimal control system is realized with a quadratic performance index which represents the energy content of the system. This controller is compared with a regular PID controller in controlling a dynamical system with multiple degrees of freedom along with actively suppressing its residual vibration. Both controllers were realized based on the estimated states through the *effort*-based state observer. As it was expected, the phase portrait of each degree of freedom indicated that the *effort*-based state observer based optimal controller precisely position a specific degree of freedom to the pre-specified reference without residual vibration. In addition, the experimental result of this optimal controller proved the validity and possibility of realizing the optimal control law through the *effort*-based state observer. Nevertheless, the superior performance shown experimentally of the *effort*-based state observer based optimal control system does not give any information about the robustness and the stability margin of the control system.

Robustness and stability margins are compared for both control systems that are based on sensor measurement and the estimated states of the *effort*-based state observer. The phase margin of the sensor based controller is larger than the observer based one. Phase margin in general shows how much time delay in the open loop can the control system tolerate. It is intuitively clear that due to the structure of the *effort*-based state observer that each single observer induces certain amount of phase lag. Therefore, the phase margin of the observer based control system is less than sensor based control system.

- *Effort*-based force control

The *effort*-based force observer provides a comprehensive solution for many problems associated with both force sensors and force observers. Although force observer avoid most of the problems associated with force sensors, the *flow* variable measurement of the degree of freedom in contact with the environment has to be made. Therefore, in the absence of this measurement, the force observer can not be realized and the force control system has to rely on the problematic force sensors.

The well-known force observer relies on measuring the *flow* variable, whereas the *effort*-based force observer alters the *flow* variable measurement with the estimated incident *effort* variable. Therefore, the degree of freedom (end effector in general) in contact with the environment can be kept free from any attached sensors for force measurement or for *flow* variable measurement. The structure of the *effort*-based force observer consists four observers in cascade, two *effort*-force observers at the power port of the interface plane of the dynamical subsystems, a Luenberger-like *effort*-based state observer and a conventional force observer. Therefore, the *effort*-based force observer has at least four degrees of freedoms that affects the convergence of the estimated interaction forces with the environment to the actual ones.

Robustness and stability margins of the force control system based on force sensor is compared with the observer based force control system. Similar to the motion control system, the stability margin in terms of phase margin of the sensor based control system turned out to be larger than the stability margin of the observer based force control system. This result matches with the previous result and it emphasizes the importance of designing the *effort*-based state observer and the *effort*-based force observer such that the their induced phase lag does not cause instability to the overall control system.

It was shown that sensitivity of the reaction force observer to micro scale interaction forces with the environment are affected by the resolution of the position of velocity sensor used to measure the *flow* variable of the degree of freedom in contact with the environment. However, due to the sensor noise, the signal to noise ratio was close to 1.5 while estimating micro scale interaction forces with the environment. This indicates the difficulty of implementing the reaction force observer for applications such as micromanipulation and micro assembly due to sensor noise. On the other hand, the *effort*-based force observer does not require measuring the *flow* variables of the degree of freedom in contact with the environment it rather depends on the feedback-like *effort*-force estimates.

The *effort* or *energy* based force observer provides excellent match to the force sensor in certain frequency range. Therefore, utilization of this observer allows avoiding majority of force sensors and reaction force observers related problems.

- *Effort*-based Control of Distributed Systems

It was shown that the *effort*-based state observer can be further utilized to estimate state variables of systems with distributed dynamics such as flexible robot arms and manipulators. These systems have infinite dimensional transfer function realization. we assumed that the excitation signal is bandlimited in order to obtain a high order representation instead of the infinite dimensional representation. The high order representation is truncated to its optimal reduced order representation by minimizing the Hankel norm of the system.

The Hankel singular values were utilized in order to decide about the dominant states that has to be included in the optimal model and the states that have to be

discarded. Then the frequency response plots are used to compare the behavior of the original system versus the optimal truncated one. The gains associated with the *effort*-force observer turned out to have a large impact on the accuracy of the optimal representation. It was shown that larger gains result in more accurate representation of the system dynamics in terms of frequency response. However, we have to consider the performance and stability tradeoffs which limits the selection of the *effort*-based observer gains to certain values.

The frequency response of the distributed system optimal truncated model showed exact match at certain frequency ranges and poor match at other ranges. However, it was shown that most of the dynamics can be accurately modeled with the optimal truncated model. However, due to the poor match between the optimal model and the exact system in some other frequency regions, we suggest not to excite the dynamical system within these frequency ranges. This can be accomplished by removing the control input energy content at these particular frequencies by band-pass filters, for example.

Effort-based state observer is designed to estimate the truncated states of the distributed system. The distributed system is conceptually assumed to have inaccessible state variables and outputs but it is in *power conserving* interconnection with another dynamical subsystem, namely the actuator, from which measurements can be taken. The estimated states showed satisfactory convergence to the actual ones in finite time. In addition robustness of the *effort*-based state observer is analyzed under unknown initial conditions and parameter deviations.

The estimated states through the *effort*-based state observer used to realize the optimal control law that minimizes the energy content within the distributed system. An Euler-Bernoulli beam example was studied in order to illustrate the procedures, starting from the dynamical equation of this distributed system till the realization of the *effort*-based state observer based optimal control law. Based on the assumption that the excitation signal is bandlimited, the infinite dimensional Euler-Bernoulli beam is represented wit a high order model with 22-state variables. This higher order model is then used to obtain an optimal truncated model with 7-state variables based on minimizing the Hankel norm. It was shown that the first 7 Hankel singular values are dominant, whereas the rest of the singular values can be discarded. This optimal truncated model is then used in the design of the *effort*-based state observer.

The merits of the proposed *effort*-based state observer for systems with distributed dynamics is the ability to keep these systems free from any attached sensor and measurements while estimating their truncated state variables from measurements taken from their power ports with other dynamical subsystems, namely their actuators.

Thesis Publications

- ***Articles***

- **Islam S. M. Khalil** and Asif Sabanovic, "Action-reaction state observer for single input dynamical systems with compliance ," *IEEE Trans. Ind Electron.*, Accepted for Publication.

- **Islam S. M. Khalil** and Asif Sabanovic, "Sensorless residual vibration suppression of flexible systems," *IEEE Trans. Electric Machines.*, In Review.

- **Islam S. M. Khalil** and Asif Sabanovic "Action-reaction based motion control-Microsystems applications", *IEEE/ASME Trans. Mechatronics*, In Review.

- **Islam S. M. Khalil**, Emrah. D. Kunt and Asif Sabanovic "A novel algorithm for sensorless motion control of flexible structures," *Turkish Journal of Electrical Engineering & Computer Sciences.*, vol. 18, no. 5, pp. 799-817, Dec. 2010.

- **Islam S. M. Khalil**, Emrah. D. Kunt and Asif Sabanovic "Action-reaction based parameters identification and states estimation," *Turkish Journal of Electrical Engineering & Computer Sciences.*, vol. 19, no. 5, pp. 1-10, Dec. 2011.

- **Islam S. M. Khalil** and Asif Sabanovic "Sensorless wave based control of flexible structures using actuator as a single platform for estimation and control," *International Review of Automatic Control.*, vol. 2, no. 1, pp. 83-90, Jan. 2009.

- B. Celebi, G. Cevik, B. Mehmet, **Islam S. M. Khalil** and Asif Sabanovic "Motion control and vibration suppression of flexible lumped systems via sensorless LQR control," *Automatika Journal for Control, Measurement, Electronics, Computing and Communications.*, vol. 51, no. 4, pp. 313-324, Oct. 2010.

- **Islam S. M. Khalil** and Asif Sabanovic "Motion control for dynamical system with inaccessible outputs," *ASME J. Dyn. Syst., Meas. Control*, In Review

- **Islam S. M. Khalil** and Asif Sabanovic "A novel Action reaction based motion control for microsystems applications," *Journal of Micro-Nano Mechatronics*, In Review

- E. D. Kunt, A. T. Naskali, **Islam S. M. Khalil** and Asif Sabanovic "Design and development of workstation for microparts manipulation and assembly," *Turkish Journal of Electrical Engineering & Computer Sciences.*, vol. 19, no. 5, pp. 1-10, Dec. 2011.

- ***Papers in Conference Proceedings***

- **Islam. S. M. Khalil** and Asif Sabanovic, "Sensorless action-reaction-based residual vibration suppression for multi-degree-of-freedom flexible systems," in *Proc IEEEInt. Conf. Industrial Technology, IECON'10-Phoenix*, pp. 1627-1632, Nov. 2010.

- **Islam. S. M. Khalil**, Ahmet. O. Nargiz and Asif Sabanovic, "A novel state observer for dynamical systems with inaccessible outputs,"in *Proc IEEEInt. Conf. on Mechatronics, ICM'11-Istanbul*, Apr. 2011.

- **Islam. S. M. Khalil**, B. Celebi, G. Cevik, B. Mehmet and Asif Sabanovic, "Optimal motion control and vibration suppression of flexible systems with inaccessible outputs,"in *Proc IEEEInt. Conf. on Mechatronics, ICM'11-Istanbul*, Apr. 2011.

- **Islam. S. M. Khalil** and Asif Sabanovic, "Action-reaction based motion and vibration control of multi-degree-of freedom flexible systems," in *Proc IEEEInt. Conf. Advanced Motion Control, AMC'10-Nagaoka*, Mar. 2010, pp. 577-582.

- **Islam. S. M. Khalil** and Asif Sabanovic, "Action-reaction based parameters identification and states estimation of flexible systems," in *Proc IEEEInt. Conf. Industrial Technology, ISIE'10-Pari*, July. 2010, pp. 46-51.

- **Islam. S. M. Khalil** and Asif Sabanovic, "Estimation based control of flexible system-sensorless wave based technique," in *Proc IEEEInt. Conf. Emerging Technologies & Factory Automation, ETFA'09-Mallorca*, Sept. 2009, pp. 1-6.

- **Islam. S. M. Khalil** and Asif Sabanovic, "Sensorless torque estimation in multi-degree-of-freedom flexible system," in *Proc IEEEInt. Conf. Industrial Technology, IECON'09-Porto*, Nov. 2009, pp. 2354-2359.

- **Islam. S. M. Khalil**, A. T. Naskali and Asif Sabanovic, "Force control in multi-degree-of-freedom flexible systems-sensorless technique," in *Proc IEEEInt. Conf. Computational Intelligence in Robotics & Automation, CIRA'09-Daejeon*, Dec. 2009, pp. 199-204.

- **Islam. S. M. Khalil**, A. T. Naskali and Asif Sabanovic, "On fraction order modeling and control of dynamical systems," in *Proc 2nd Intr. Conference on Intelligent Control Systems and Signal Processing, ICON'09-Istanbul*, Sept. 2009.

- **Islam. S. M. Khalil**, E. D. Kunt and Asif Sabanovic, "Estimation based PID controller-sensorless wave based technique," in *Proc 2nd Intr. Conference on Intelligent Control Systems and Signal Processing, ICON'09-Istanbul*, Sept. 2009.

- **Islam. S. M. Khalil**, E. Golubovic and Asif Sabanovic, "High precision motion control of parallel robots with manufacturing tolerances and imperfections,"in *Proc IEEEInt. Conf. Emerging Technologies & Factory Automation, ETFA'10-Bilbo*, Sept. 2010.

- Celebi, G. Cevek, B. Mehmet, **Islam. S. M. Khalil** and Asif Sabanovic, "Motion control and vibration suppression of flexible systems via sensorless LQR,"in *Proc IEEEInt. Conf. Emerging Technologies & Factory Automation, ETFA'10-Bilbo*, Sept. 2010.

- E. Globovic, **Islam. S. M. Khalil** and Asif Sabanovic, "Laser autofocusing: a sliding mode approach," in *Proc IEEEInt. Conf. Industrial Technology, IECON'10-Phoenix*, pp. 1627-1632, Nov 2010.

- **Islam. S. M. Khalil**, E. Globovic, A. Kamadan and Asif Sabanovic, "High precision motion control of parallel robots," in *Proc IFAC. Conf. Automatic Control Conference, TOK'11-Istanbul*, Oct. 2011.

- G. Cevek, Celebi, B. Mehmet, **Islam. S. M. Khalil** and Asif Sabanovic, "Motion control and vibration suppression of flexible system via LQR," in *Proc IFAC. Conf. Automatic Control Conference, TOK'11-Istanbul*, Oct. 2011.

- **Islam. S. M. Khalil** and Asif Sabanovic, "Algilayicisiz dalga tabanli parametre sezimi ve konum kestirimi," in *Proc IFAC. Conf. Automatic Control Conference, TOK'09-Istanbul*, Oct. 2009.

- **Islam. S. M. Khalil** and Asif Sabanovic, "Kestirim ve denetim icin eyleyicinin tek platform olarak kullanildigi, esnek yapilar icin algilayicisiz Dalga tabanli denetim," in *Proc IFAC. Conf. Automatic Control Conference, TOK'08-Istanbul*, PP. 725-730, Oct. 2009.

Appendix A

Experimental Procedures

A.1 Effort Force Estimation

The workstation depicted in Fig. A.1 consists of two manipulator arms to support a flexible biological cell similar to the one depicted in the left bottom corner of Fig. A.1. A needle with 50 nm diameter driven via a direct drive actuator is interacting with the biological cell in order to investigate the precision and sensitivity to sensor noise during a micro scale interaction. The experimental setup consists of a single degree of freedom slave robot that interacts with the biological cell, this slave is bilaterally controlled via a single degree of freedom master robot. Forces and velocities between the master and slave robots are scaled in order to guarantee safe interaction with the delicate object. The optical position encoders utilized in this experiment are of 1 μm resolution. Diameter of the Biological cells utilized in estimating the *effort*-forces are in the range of 500 to 1000 μm.

The experimental results outlined in Chapter 3 aims to illustrates how to estimate the *effort*-forces through the power ports of the interacting physical systems. In addition, Sensitivity to micro scale forces is experimentally evaluated. Estimation of the *effort*-forces requires determination of disturbance forces first. This can be done by designing the observer outlined in Chapter 3 based on the nominal parameter of the plant along with measuring the *flow* variable of a particular degree of freedom. Experimentally, the *flow* variable is obtained through differentiating the position encoder signal through a low-pass filet with cut-off frequency g_l as depicted in Table. A.1. The *flow* variable along with the supplied input. In order to decouple the *effort*-force from the disturbance force, the actuator force ripple and self-varied mass forces have to be determined and subtracted from the disturbance force. This requires identifying the parameter deviations from their actual values. The identified parameters can then be used in the realization of the feedback-like *effort*-forces. Experimentally, first order disturbance and *effort*-force observers were utilized with the gains included in Table. A.1.

Validity of the *effort*-force observer is experimentally demonstrated by comparing the estimated *effort*-force with the actual ones based on measurements and the Dirac structure that is assumed to be known beforehand. This comparison indicates that the *effort*-force observer satisfactory estimates the actual *effort*-forces along the power ports of the interconnected physical systems.

In the experimental setup depicted in Fig. A.1, the interconnection occurs between the needle and the flexible biological cell. Throughout the thesis, interconnections along systems with lumped dynamics were considered. In this case, the

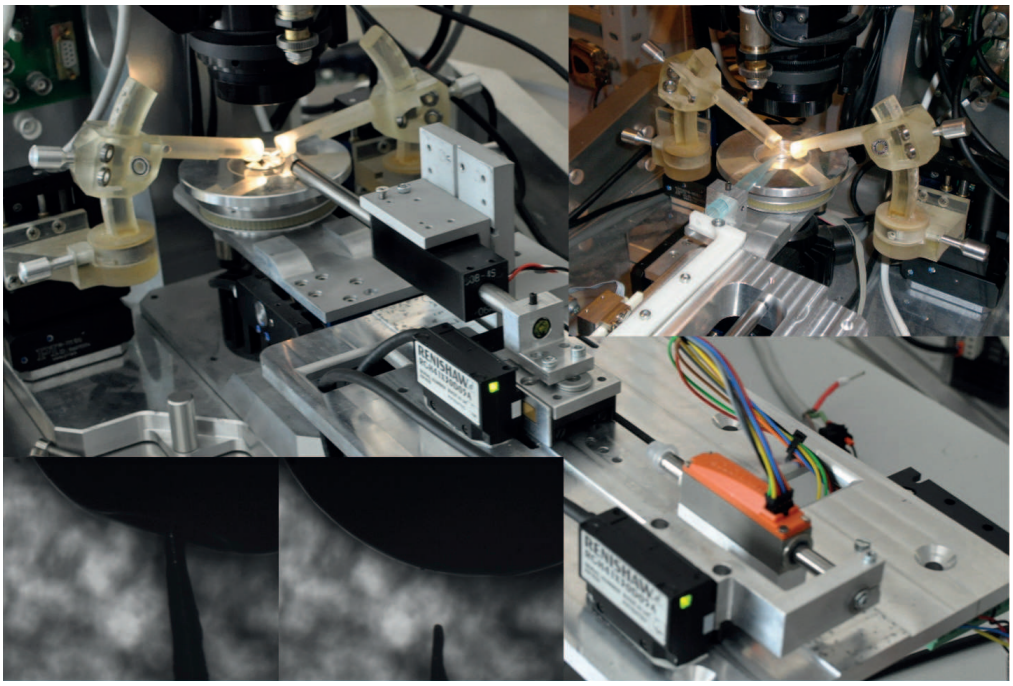

Figure A.1: *Effort*-force based state observer experiment on a micro system workstation.

interconnection occurs between the different energy storage element and energy dissipation elements.

A.2 State Estimation Experimental Setup

The experimental setup utilized in examining the performance of the *effort*-based state observer should possess multiple degrees of freedom in order to allow estimating several state variables. The actual state variables of each degree of freedom should be also measured in order to compare the estimated with the actual state variables. Therefore, the experimental setup includes a lumped mass spring system with three degrees of freedom connected to an actuator via an energy storage element and energy dissipation element. The lumped dynamics allows attaching position encoder to each degree of freedom, which in turn allows comparing the estimated states with the precisely measured ones.

As depicted in Fig. A.2, the experimental setup consists of a linear actuator attached via an energy storage element to a three degree of freedom flexible lumped system. This system is incorporated with a microsystems workstations that is mounted on a vibration isolation table. Although many sensors are attached to the dynamical system, only single sensor is utilized in the realization of the state observer and the control system. The rest of the sensors are used for verification purpose through comparing the actual with the estimated state variables.

Table A.1: Experimental parameters

Master force constant	k^n_{fm}	6.43	N/A
Master nominal mass	m^n_m	0.059	kg
Master *effort*-force observer gain	g^m_{eff}	62.8	rad/s
Master disturbance observer gain	g^m_{dis}	315	rad/s
Slave disturbance observer gain	g^s_{dist}	628	rad/s
Sampling time	T_s	1	ms
Low pass filter gain	g_l	1884	rad/s
Master mass deviation	Δm_m	0.0055	kg
Master force constant deviation	Δk_{fm}	6.32	N/A
Master viscous friction constant	b_m	0.065	Ns/m

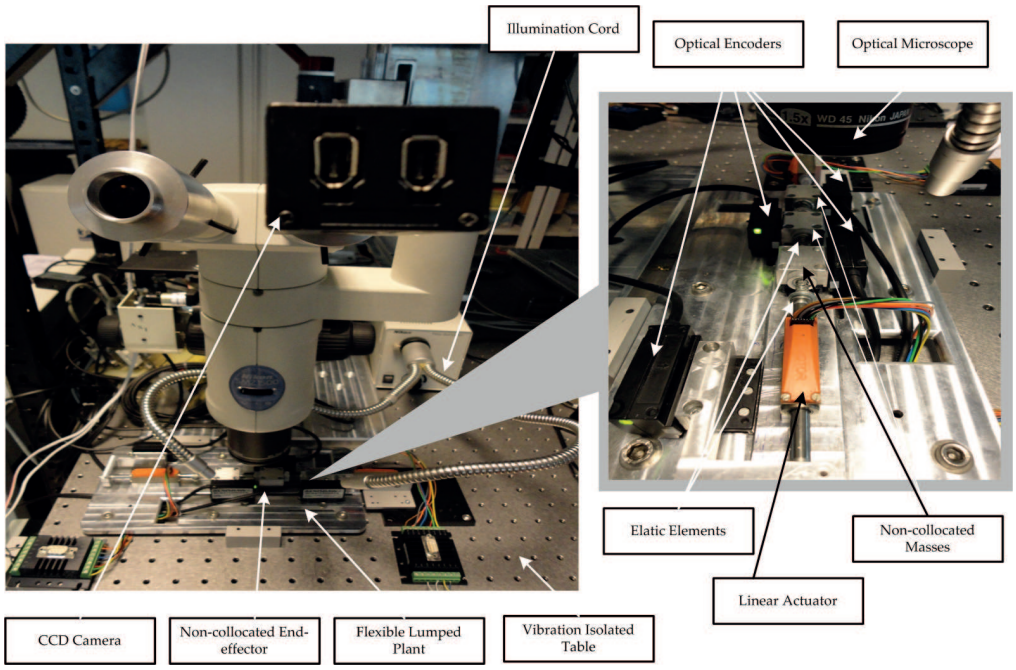

Figure A.2: State estimation experimental setup.

Experimentally, to realize the *effort*-based state observer, the *flow* variable of the actuator has to be measured. This is done through differentiating the position encoder signal through a low-pass filter with cut-off frequency 628 rad/s, in addition the nominal model of the plant is assumed to be known beforehand. Therefore, the entire *energy* based state observer is based on this single measurement from the whole system.

Appendix B

Decoupled State Space Representation

In order to show how to represent the linear state space representation such that the available state for measurement are decoupled from the other unavailable state for measurements, the inaccessible state variables have to be separated from the ones that we can measure. Then based on this separation, the entire dynamical system can be decoupled into two subsystems with accessible and inaccessible state variables. Afterwards, the Dirac structure of the interconnection between these two dynamical subsystems has to be defined to reveal the incident natural feedback-like *effort*-forces from the dynamical subsystem with inaccessible state variables on the other subsystem with accessible state variables.

B.1 Dynamical System with 2 Degrees of Freedom

We consider the dynamical system illustrated in Fig. B.1, its state space representation can be written in the following form,

$$\begin{bmatrix} \dot{x}_1 \\ \dot{x}_2 \\ \dot{x}_3 \\ \dot{x}_4 \end{bmatrix} = \begin{bmatrix} 0 & 1 & 0 & 0 \\ -\frac{k}{m_1} & -\frac{c}{m_1} & \frac{c}{m_1} & \frac{k}{m_1} \\ 0 & 0 & 0 & 1 \\ \frac{k}{m_1} & \frac{c}{m_1} & -\frac{k}{m_1} & -\frac{c}{m_1} \end{bmatrix} \begin{bmatrix} x_1 \\ x_2 \\ x_3 \\ x_4 \end{bmatrix} + \begin{bmatrix} 0 \\ -\frac{1}{m_1} \\ 0 \\ 0 \end{bmatrix} u \tag{B.1}$$

upon the following Dirac structure representation,

$$f^s = e^m = y \quad , \quad f^m = e^s - e^d + u \tag{B.2}$$

the previous state space representation can be represented in the following form,

$$\begin{bmatrix} \dot{x}_1 \\ \dot{x}_2 \\ \dot{x}_3 \\ \dot{x}_4 \end{bmatrix} = \begin{bmatrix} 0 & 1 & 0 & 0 \\ 0 & 0 & 0 & 0 \\ 0 & 0 & 0 & 0 \\ 0 & 0 & 0 & 0 \end{bmatrix} \begin{bmatrix} x_1 \\ x_2 \\ x_3 \\ x_4 \end{bmatrix} + \begin{bmatrix} 0 & 0 & 0 & 0 \\ 0 & 0 & 0 & 0 \\ 0 & 0 & 0 & 1 \\ 0 & 0 & 0 & 0 \end{bmatrix} \begin{bmatrix} x_1 \\ x_2 \\ x_3 \\ x_4 \end{bmatrix} + \begin{bmatrix} 0 \\ -\frac{1}{m_1} \\ 0 \\ 0 \end{bmatrix} u + \tag{B.3}$$

$$\begin{bmatrix} 0 & 0 & 0 & 0 \\ -\frac{k}{m_1} & -\frac{c}{m_1} & \frac{c}{m_1} & \frac{k}{m_1} \\ 0 & 0 & 0 & 0 \\ 0 & 0 & 0 & 0 \end{bmatrix} \begin{bmatrix} x_1 \\ x_2 \\ x_3 \\ x_4 \end{bmatrix} + \begin{bmatrix} 0 & 0 & 0 & 0 \\ 0 & 0 & 0 & 0 \\ 0 & 0 & 0 & 0 \\ \frac{k}{m_1} & \frac{c}{m_1} & -\frac{k}{m_1} & -\frac{c}{m_1} \end{bmatrix} \begin{bmatrix} x_1 \\ x_2 \\ x_3 \\ x_4 \end{bmatrix}$$

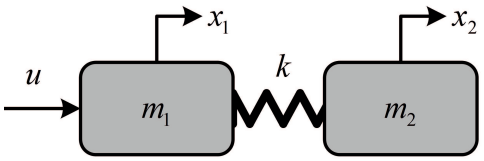

Figure B.1: Dynamical system with 2 degrees of freedom.

here we assume that the Dirac interconnection between the dynamical subsystems is defined by an energy storage element and energy dissipation element, then we attempt to separate the *effort*-force from the system matrices as follows,

$$\begin{bmatrix} \dot{x}_1 \\ \dot{x}_2 \\ \dot{x}_3 \\ \dot{x}_4 \end{bmatrix} = \begin{bmatrix} 0 & 1 & 0 & 0 \\ 0 & 0 & 0 & 0 \\ 0 & 0 & 0 & 0 \\ 0 & 0 & 0 & 0 \end{bmatrix} \begin{bmatrix} x_1 \\ x_2 \\ x_3 \\ x_4 \end{bmatrix} + \begin{bmatrix} 0 & 0 & 0 & 0 \\ 0 & 0 & 0 & 0 \\ 0 & 0 & 0 & 1 \\ 0 & 0 & 0 & 0 \end{bmatrix} \begin{bmatrix} x_1 \\ x_2 \\ x_3 \\ x_4 \end{bmatrix} + \begin{bmatrix} 0 \\ -\frac{1}{m_1} \\ 0 \\ 0 \end{bmatrix} u \quad \text{(B.4)}$$

$$+ \begin{bmatrix} 0 \\ \frac{1}{m_1} \\ 0 \\ 0 \end{bmatrix} \begin{bmatrix} -k & -c & k & c \end{bmatrix} \mathrm{x} + \begin{bmatrix} 0 \\ 0 \\ 0 \\ \frac{1}{m_1} \end{bmatrix} \begin{bmatrix} k & c & -k & -c \end{bmatrix} \mathrm{x}$$

that is of the following form

$$\begin{bmatrix} \dot{\mathrm{x}}^a \\ -- \\ \dot{\mathrm{x}}^p \end{bmatrix} = \begin{bmatrix} \mathrm{A}^a & | & \emptyset \\ -- & | & -- \\ \emptyset & | & \emptyset \end{bmatrix} \begin{bmatrix} \mathrm{x}^a \\ -- \\ \mathrm{x}^p \end{bmatrix} + \begin{bmatrix} \emptyset & | & \emptyset \\ -- & | & -- \\ \emptyset & | & \mathrm{A}^p \end{bmatrix} \begin{bmatrix} \mathrm{x}^a \\ -- \\ \mathrm{x}^p \end{bmatrix} + \begin{bmatrix} \mathrm{B}^a \\ -- \\ \emptyset \end{bmatrix} u$$

$$+ \left[\begin{pmatrix} \emptyset \\ -- \\ \mathrm{B}^p \end{pmatrix} + \begin{pmatrix} \mathrm{B}^{eff} \\ -- \\ \emptyset \end{pmatrix} \right] e(\mathrm{x}^{\mathrm{a}}, \mathrm{x}^p) \quad \text{(B.5)}$$

B.2 Dynamical System with 3 Degrees of Freedom

we further consider a dynamical system with three degrees of freedom, which consists of two dynamical subsystems, one of which has accessible state variables, whereas the state variables of the other degrees of freedom are not available for measurements.

the state space representation of this system can be written as follows

$$\begin{bmatrix} \dot{x}_1 \\ \dot{x}_2 \\ \dot{x}_3 \\ \dot{x}_4 \\ \dot{x}_5 \\ \dot{x}_6 \end{bmatrix} = \begin{bmatrix} 0 & 1 & 0 & 0 & 0 & 0 \\ -\frac{k}{m1} & -\frac{c}{m1} & \frac{k}{m1} & \frac{c}{m1} & 0 & 0 \\ 0 & 0 & 0 & 0 & 1 & 0 \\ \frac{k}{m1} & \frac{c}{m1} & -\frac{2k}{m1} & -\frac{2c}{m1} & \frac{k}{m1} & \frac{c}{m1} \\ 0 & 0 & 0 & 0 & 0 & 1 \\ 0 & 0 & -\frac{k}{m1} & \frac{k}{m1} & \frac{k}{m1} & -\frac{k}{m1} \end{bmatrix} \begin{bmatrix} x_1 \\ x_2 \\ x_3 \\ x_4 \\ x_5 \\ x_6 \end{bmatrix} + \begin{bmatrix} 0 \\ \frac{1}{m_1} \\ 0 \\ 0 \\ 0 \\ 0 \end{bmatrix} u \quad \text{(B.6)}$$

upon the following Dirac structure representation,

$$f^s = e^m = y \quad , \quad f^m = e^s - e^d + u \quad \text{(B.7)}$$

the previous state space representation can be represented in the following form,

$$\dot{\mathrm{x}} = \begin{bmatrix} 0 & 1 & 0 & 0 & 0 & 0 \\ 0 & 0 & 0 & 0 & 0 & 0 \\ 0 & 0 & 0 & 0 & 0 & 0 \\ 0 & 0 & 0 & 0 & 0 & 0 \\ 0 & 0 & 0 & 0 & 0 & 0 \\ 0 & 0 & 0 & 0 & 0 & 0 \end{bmatrix} \mathrm{x} + \begin{bmatrix} 0 & 0 & 0 & 0 & 0 & 0 \\ \frac{-k}{m1} & \frac{-c}{m1} & \frac{k}{m1} & \frac{c}{m1} & 0 & 0 \\ 0 & 0 & 0 & 0 & 0 & 0 \\ 0 & 0 & 0 & 0 & 0 & 0 \\ 0 & 0 & 0 & 0 & 0 & 0 \\ 0 & 0 & 0 & 0 & 0 & 0 \end{bmatrix} \mathrm{x} + \begin{bmatrix} 0 \\ \frac{1}{m_1} \\ 0 \\ 0 \\ 0 \\ 0 \end{bmatrix} u + \quad \text{(B.8)}$$

$$\begin{bmatrix} 0 & 0 & 0 & 0 & 0 & 0 \\ 0 & 0 & 0 & 0 & 0 & 0 \\ 0 & 0 & 0 & 0 & 0 & 0 \\ \frac{k}{m1} & \frac{c}{m1} & \frac{-k}{m1} & \frac{-c}{m1} & 0 & 0 \\ 0 & 0 & 0 & 0 & 0 & 0 \\ 0 & 0 & 0 & 0 & 0 & 0 \end{bmatrix} \mathrm{x} + \begin{bmatrix} 0 & 0 & 0 & 0 & 0 & 0 \\ 0 & 0 & 0 & 0 & 0 & 0 \\ 0 & 0 & 0 & 0 & 0 & 0 \\ 0 & 0 & -\frac{k}{m1} & \frac{-k}{m1} & \frac{k}{m1} & \frac{k}{m1} \\ 0 & 0 & 0 & 0 & 0 & 0 \\ 0 & 0 & \frac{k}{m1} & \frac{k}{m1} & \frac{-k}{m1} & \frac{-k}{m1} \end{bmatrix} \mathrm{x}$$

Again we consider that the interconnection between the dynamical subsystems is defined via a Dirac structure which describes an anergy storage and dissipation elements, this allows putting the previous equations in the following form

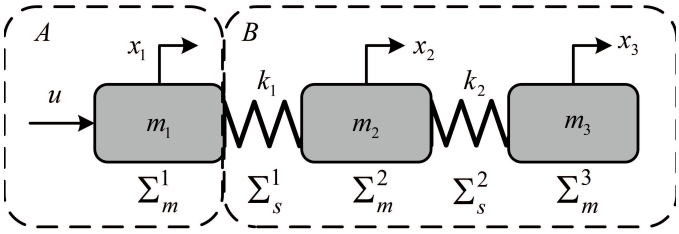

Figure B.2: Block diagram representation of the dynamical system with 3 DOF.

$$\dot{\mathrm{x}} = \begin{bmatrix} 0 & 1 & 0 & 0 & 0 & 0 \\ 0 & 0 & 0 & 0 & 0 & 0 \\ 0 & 0 & 0 & 0 & 0 & 0 \\ 0 & 0 & 0 & 0 & 0 & 0 \\ 0 & 0 & 0 & 0 & 0 & 0 \\ 0 & 0 & 0 & 0 & 0 & 0 \end{bmatrix} \mathrm{x} + \begin{bmatrix} 0 & 0 & 0 & 0 & 0 & 0 \\ 0 & 0 & 0 & 0 & 0 & 0 \\ 0 & 0 & 0 & 0 & 0 & 0 \\ 0 & 0 & -\frac{k}{m1} & \frac{-k}{m1} & \frac{k}{m1} & \frac{k}{m1} \\ 0 & 0 & 0 & 0 & 0 & 0 \\ 0 & 0 & \frac{k}{m1} & \frac{k}{m1} & \frac{-k}{m1} & \frac{-k}{m1} \end{bmatrix} \mathrm{x} + \begin{bmatrix} 0 \\ \frac{1}{m_1} \\ 0 \\ 0 \\ 0 \\ 0 \end{bmatrix} u + \tag{B.9}$$

$$\begin{bmatrix} 0 \\ \frac{1}{m_1} \\ 0 \\ 0 \\ 0 \\ 0 \end{bmatrix} \begin{bmatrix} -k & -c & k & c & 0 & 0 \end{bmatrix} \mathrm{x} + \begin{bmatrix} 0 \\ 0 \\ 0 \\ \frac{1}{m_1} \\ 0 \\ 0 \end{bmatrix} \begin{bmatrix} k & c & -k & -c & 0 & 0 \end{bmatrix} \mathrm{x}$$

that is of the following form

$$\begin{bmatrix} \dot{\mathrm{x}}^a \\ -- \\ \dot{\mathrm{x}}^p \end{bmatrix} = \begin{bmatrix} \mathrm{A}^a & | & \emptyset \\ -- & | & -- \\ \emptyset & | & \emptyset \end{bmatrix} \begin{bmatrix} \mathrm{x}^a \\ -- \\ \mathrm{x}^p \end{bmatrix} + \begin{bmatrix} \emptyset & | & \emptyset \\ -- & | & -- \\ \emptyset & | & \mathrm{A}^p \end{bmatrix} \begin{bmatrix} \mathrm{x}^a \\ -- \\ \mathrm{x}^p \end{bmatrix} + \begin{bmatrix} \mathrm{B}^a \\ -- \\ \emptyset \end{bmatrix} u$$

$$+ \left[\begin{pmatrix} \emptyset \\ -- \\ \mathrm{B}^p \end{pmatrix} + \begin{pmatrix} \mathrm{B}^{eff} \\ -- \\ \emptyset \end{pmatrix} \right] e(\mathrm{x}^{\mathrm{a}}, \mathrm{x}^p) \tag{B.10}$$

Bibliography

[Ahrens 2009] J. H. Ahrens and H. K. Khalil. *High-gain observer in the presence of measurement noise: a switched-gain appraoch.* Automatica, vol. 45, pages 936–943, 2009. (Cited on pages 9, 16 and 79.)

[Aldeen 1999] M. Aldeen and H. Trinh. *Reduced-order linear functional obsever for linear systems.* IEE Proc. Control Theory Appl, vol. 146, no. 5, pages 399–405, 1999. (Cited on page 10.)

[Alici 2005] G. Alici and B. Shirinzadeh. *A systematic technique to estimate positioning error for robot accuracy improvement using laser interfrometry based sensing.* Mech. Mach. Threoy, vol. 40, no. 8, pages 879–906, 2005. (Cited on page 12.)

[Anderson 1989] R.J. Anderson and M.W. Spong. *Bilateral control of teleoperators with time delay.* Automatic Control, IEEE Transactions on, vol. 34, no. 5, pages 494 –501, may 1989. (Cited on page 13.)

[Ball 2008] A.A. Ball and H.K. Khalil. *High-gain observers in the presence of measurement noise: A nonlinear gain approach.* In Decision and Control, 2008. CDC 2008. 47th IEEE Conference on, pages 2288 –2293, dec. 2008. (Cited on page 9.)

[Bazaei 2011] A. Bazaei and M. Moallem. *Improving Force Control Bandwidth of Flexible-Link Arms Through Output Redefinition.* Mechatronics, IEEE/ASME Transactions on, vol. 16, no. 2, pages 380 –386, april 2011. (Cited on page 98.)

[Bhat 1990] S. P. Bhat and D. K. Miu. *Precise point-to-point positioning control of flexible structures.* ASME J. Dyn. Syst., Meas. Control, vol. 112, pages 667–674, 1990. (Cited on page 121.)

[Bhat 1991] Sudarshan P. Bhat and Denny K. Miu. *Experiments on Point-to-Point Control of a Flexible Beam using Laplace Transform Technique - Part II : Closed-Loop.* In American Control Conference, 1991, pages 2455 –2460, june 1991. (Cited on page 121.)

[Bor-Sen 1989] Chen Bor-Sen and Lo Chi-Ho. *Necessary and sufficient conditions for robust stabilization of an observer-based compensating system suffering nonlinear time-varying perturbation.* Automatic Control, IEEE Transactions on, vol. 34, no. 8, pages 899 –900, aug 1989. (Cited on page 56.)

[Bullinger 1997] E. Bullinger and F. Allgower. *An adaptive high-gain observer for nonlinear systems.* In Decision and Control, 1997., Proceedings of the 36th IEEE Conference on, volume 5, pages 4348 –4353 vol.5, dec 1997. (Cited on page 9.)

[Celebi 2010] B. Celebi, G. Cevik, B. Mehmet, I. S. M. Khalil, E. D. Kunt and A. Sabanovic. *Motion control and vibration suppression of flexible lumped systems via sensorless LQR control.* Automatika, Journal of Control, measurement, electronics, computing and communications, vol. 51, no. 5, pages 313–324, 2010. (Cited on page 13.)

[Cervera 2006] J. Cervera, A. J. Van der Schaft and A. Banos. *Interconnection of port-Hamiltonian systems and composition of Dirac structures.* Automatica, pages 1–14, 2006. (Cited on pages 13 and 28.)

[Choi 1999] Byeong-Kap Choi, Chong-Ho Choi and Hyuk Lim. *Model-based disturbance attenuation for CNC machining centers in cutting process.* Mechatronics, IEEE/ASME Transactions on, vol. 4, no. 2, pages 157 –168, jun 1999. (Cited on page 11.)

[Corless 1998] M. Corless and F. J. Tu. *State and input estimation for a class of uncertain systems.* Automatica, vol. 34, no. 6, pages 757–764, 1998. (Cited on page 11.)

[Darouach 2000] M. Darouach. *Existence and design of functional observers for linear systems.* Automatic Control, IEEE Transactions on, vol. 45, no. 5, pages 940 –943, may 2000. (Cited on page 10.)

[der Schaft 2002] A. J. Van der Schaft and J. Cervera. *Composition of dirac structures and control of port-hamiltonian systems.* In Proceedings of the IEEEInt. Symp. on Mathematical Theory of Networks and Systems, pages 1–13, South Bend, 2002. IEEE. (Cited on page 20.)

[Esfandiari 1992] E. Esfandiari and H. K. Khalil. *Ouput feedback stabilization of fully linearizable systems.* INT. J. Control, vol. 56, no. 5, pages 1007–1037, 1992. (Cited on page 9.)

[Fernando 2010] T.L. Fernando, Hieu Minh Trinh and L. Jennings. *Functional Observability and the Design of Minimum Order Linear Functional Observers.* Automatic Control, IEEE Transactions on, vol. 55, no. 5, pages 1268 –1273, may 2010. (Cited on page 10.)

[Han 1995] J. Han. *A class of extended state observer for uncertain systems.* Control and Decision, vol. 1, no. 1, pages 85–88, 1995. (Cited on page 10.)

[Hao 2007] Jin Hao, Chen Chen, Libao Shi and Jie Wang. *Nonlinear Decentralized Disturbance Attenuation Excitation Control for Power Systems With Nonlinear Loads Based on the Hamiltonian Theory.* Energy Conversion, IEEE Transactions on, vol. 22, no. 2, pages 316 –324, june 2007. (Cited on page 36.)

[Hermann 1977] R. Hermann and A. Krener. *Nonlinear controllability and observability.* Automatic Control, IEEE Transactions on, vol. 22, no. 5, pages 728 – 740, oct 1977. (Cited on page 75.)

[Hou 1999] M. Hou, A.C. Pugh and P.C. Muller. *Disturbance decoupled functional observers.* Automatic Control, IEEE Transactions on, vol. 44, no. 2, pages 382 –386, feb 1999. (Cited on page 10.)

[Hung 2007] Shao-Kang Hung, En-Te Hwu, Mei-Yung Chen and Li-Chen Fu. *Dual-Stage Piezoelectric Nano-Positioner Utilizing a Range-Extended Optical Fiber Fabry ndash;Perot Interferometer.* Mechatronics, IEEE/ASME Transactions on, vol. 12, no. 3, pages 291 –298, june 2007. (Cited on page 12.)

[Katsura 2005] S. Katsura and K. Ohnishi. *Force Servoing by Flexible Manipulator Based on Resonance Ratio Control.* In Industrial Electronics, 2005. ISIE 2005. Proceedings of the IEEE International Symposium on, volume 4, pages 1343 – 1348, 20-23, 2005. (Cited on page 100.)

[Katsura 2006] S. Katsura, Y. Matsumoto and K. Ohnishi. *Analysis and experimental validation of force bandwidth for force control.* Industrial Electronics, IEEE Transactions on, vol. 53, no. 3, pages 922 – 928, june 2006. (Cited on page 98.)

[Khalil 2009a] I. Khalil, E.D. Kunt and A. Sabanovic. *Sensorless torque estimation in multidegree-of-freedom flexible systems.* In Industrial Electronics, 2009. IECON '09. 35th Annual Conference of IEEE, pages 2354 –2359, nov. 2009. (Cited on page 13.)

[Khalil 2009b] I.S.M. Khalil, E.D. Kunt and A. Sabanovic. *Estimation based control of flexible systems-sensorless wave based technique.* In Emerging Technologies Factory Automation, 2009. ETFA 2009. IEEE Conference on, pages 1 –6, sept. 2009. (Cited on page 13.)

[Khalil 2009c] I.S.M. Khalil, A.T. Naskali and A. Sabanovic. *Force control in multi-degree-of-freedom flexible systems x2014; Sensorless technique.* In Computational Intelligence in Robotics and Automation (CIRA), 2009 IEEE International Symposium on, pages 199 –204, dec. 2009. (Cited on page 13.)

[Khalil 2010a] I. S. M. Khalil, E. D. Kunt and A. Sabanovic. *A novel algorithm for sensorless motion control of flexible structures.* Turkish Journal of Electrical Engineering and Computer Sciences, vol. 18, no. 5, pages 1–19, 2010. (Cited on page 13.)

[Khalil 2010b] I.S.M. Khalil and A. Sabanovic. *Action-reaction based parameters identification and states estimation of flexible systems.* In Industrial Electronics (ISIE), 2010 IEEE International Symposium on, pages 46 –51, july 2010. (Cited on page 41.)

[Khalil 2010c] I.S.M. Khalil and A. Sabanovic. *Sensorless action-reaction-based residual vibration suppression for multi-degree-of-freedom flexible systems.* In IECON 2010 - 36th Annual Conference on IEEE Industrial Electronics Society, pages 1633 –1638, nov. 2010. (Cited on page 13.)

[Khalil 2011] I. S. M. Khalil and A. Sabanovic. *Action reaction state observer for single input dynamical systems with compliance.* IEEE Trans. Ind Electron, 2011. (Cited on page 14.)

[Kirk 1970] Donald E. Kirk. Optimal control theory an introduction. Dover Publications, Mineola, New York, 1970. (Cited on page 90.)

[Kobayashi 2007] H. Kobayashi, S. Katsura and K. Ohnishi. *An Analysis of Parameter Variations of Disturbance Observer for Motion Control.* Industrial Electronics, IEEE Transactions on, vol. 54, no. 6, pages 3413 –3421, dec. 2007. (Cited on page 11.)

[Krener 1985] A. J. Krener and W. Respondek. *Nonlinear observers with linearizable error dynamics.* SIAM J. Control Optim, vol. 23, no. 2, pages 199–216, 1985. (Cited on page 10.)

[Krishnan 1988] H. Krishnan and M. Vidyasagar. *Control of a single-link flexible beam using a Hankel-norm-based reduced order model.* In Robotics and Automation, 1988. Proceedings., 1988 IEEE International Conference on, pages 9 –14 vol.1, apr 1988. (Cited on page 115.)

[Kung 1981] S. Kung and D. Lin. *Optimal Hankel-norm model reductions: Multivariable systems.* Automatic Control, IEEE Transactions on, vol. 26, no. 4, pages 832 – 852, aug 1981. (Cited on page 113.)

[Liaw 2009] Hwee Choo Liaw and B. Shirinzadeh. *Neural Network Motion Tracking Control of Piezo-Actuated Flexure-Based Mechanisms for Micro-/Nanomanipulation.* Mechatronics, IEEE/ASME Transactions on, vol. 14, no. 5, pages 517 –527, oct. 2009. (Cited on page 12.)

[Liou 1972] C. T. Liou, W. A. Weigand and H. C. Lim. *Optimal output feedback control for systems with inaccessible state variables.* INT. J. Control, vol. 15, no. 1, pages 129–141, 1972. (Cited on page 9.)

[Luenberger 1964] David G. Luenberger. *Observing the State of a Linear System.* Military Electronics, IEEE Transactions on, vol. 8, no. 2, pages 74 –80, april 1964. (Cited on page 10.)

[Luenberger 1971] D. Luenberger. *An introduction to observers.* Automatic Control, IEEE Transactions on, vol. 16, no. 6, pages 596 – 602, dec 1971. (Cited on page 10.)

[Macchelli 2002a] A. Macchelli, S. Stramigioli, A. J. Van der Schaft and C. Melchiorri. *Consideration on the zero-dynamics of port hamiltonian systems and applications to passive implementation of sliding mode control.* In Proceedings of the 15th IFAC World Congress on Automatic Control. IFAC, 2002. (Cited on pages 12, 14 and 15.)

[Macchelli 2002b] A. Macchelli, S. Stramigioli, A. van der Schaft and C. Melchiorri. *Scattering for infinite dimensional port Hamiltonian systems.* In Decision and Control, 2002, Proceedings of the 41st IEEE Conference on, volume 4, pages 4581 – 4586 vol.4, dec. 2002. (Cited on pages 12 and 15.)

[Macchelli 2003] A. Macchelli and C. Melchiorri. *Control by interaction of the timoshenko beam.* In Proceedings of the 2nd IFAC Workshop on Lagrangain and Hamiltonian Methods for Nonlinear Control. IFAC, 2003. (Cited on page 11.)

[Mayne 1997] D. Q. Mayne, E. W. Grainger and G. C. Goodwin. *Nonlinear filter for linear signal models.* IEE Proc. Control Theory Appl, vol. 144, pages 281–286, 1997. (Cited on page 16.)

[Murakami 1993a] T. Murakami and K. Ohnishi. *Observer-based motion control-application to robust control and parameter identification.* In Motion Control Proceedings, 1993., Asia-Pacific Workshop on Advances in, pages 1 –6, jul 1993. (Cited on page 11.)

[Murakami 1993b] T. Murakami, F. Yu and K. Ohnishi. *Torque sensorless control in multidegree-of-freedom manipulator.* Industrial Electronics, IEEE Transactions on, vol. 40, no. 2, pages 259 –265, apr 1993. (Cited on page 11.)

[Murdoch 1974] P. Murdoch. *Further comments on "Observer design for a linear functional of the state vector".* Automatic Control, IEEE Transactions on, vol. 19, no. 5, pages 620 – 621, oct 1974. (Cited on page 10.)

[Niemeyer 1991] G. Niemeyer and J.-J.E. Slotine. *Stable adaptive teleoperation.* Oceanic Engineering, IEEE Journal of, vol. 16, no. 1, pages 152 –162, jan. 1991. (Cited on page 13.)

[O'Connor 1998] W. J. O'Connor. *Position control of flexible robot arms using mechanical waves.* ASME J. Dyn. Syst., Meas. Control, vol. 120, no. 3, pages 334–339, 1998. (Cited on page 13.)

[O'Connor 2003] W. J. O'Connor. *A gantry crane problem solved.* ASME J. Dyn. Syst., Meas. Control, vol. 125, no. 4, pages 569–576, 2003. (Cited on page 13.)

[O'Connor 2007a] W.J. O'Connor. *Theory of Wave Analysis of Lumped Flexible Systems.* In American Control Conference, 2007. ACC '07, pages 4215 – 4220, july 2007. (Cited on page 12.)

[O'Connor 2007b] W.J. O'Connor. *Wave-Based Analysis and Control of Lump-Modeled Flexible Robots.* Robotics, IEEE Transactions on, vol. 23, no. 2, pages 342 –352, april 2007. (Cited on page 12.)

[Ohnishi 1994] K. Ohnishi, N. Matsui and Y. Hori. *Estimation, identification, and sensorless control in motion control system.* Proceedings of the IEEE, vol. 82, no. 8, pages 1253 –1265, aug 1994. (Cited on page 11.)

[Ohnishi 1996] K. Ohnishi, M. Shibata and T. Murakami. *Motion control for advanced mechatronics.* Mechatronics, IEEE/ASME Transactions on, vol. 1, no. 1, pages 56 –67, march 1996. (Cited on pages 11, 36 and 39.)

[Ortega 1999] R. Ortega, A. van der Schaft, B. Maschke and G. Escobar. *Energy-shaping of port-controlled Hamiltonian systems by interconnection.* In Decision and Control, 1999. Proceedings of the 38th IEEE Conference on, volume 2, pages 1646 –1651 vol.2, 1999. (Cited on page 14.)

[Ortega 2001] R. Ortega, A.J. Van Der Schaft, I. Mareels and B. Maschke. *Putting energy back in control.* Control Systems, IEEE, vol. 21, no. 2, pages 18 –33, apr 2001. (Cited on pages 1, 14 and 15.)

[Pal 1988] S. Pal, H.E. Stephanou and G. Cook. *Optimal control of a single link flexible manipulator.* In Robotics and Automation, 1988. Proceedings., 1988 IEEE International Conference on, volume 1, pages 171 –175, apr 1988. (Cited on page 113.)

[Park 1988] Y. Park and J. L. Stein. *Closed-loop, state observer for systems with unknown inputs.* INT. J. Control, vol. 48, no. 3, pages 1121–1136, 1988. (Cited on page 11.)

[Perla 2005] R. Perla and S. Mukhopadhyay. *Observer Design for Lipschitz Nonlinear Systems with State Dependency and Nonlinearity Distribution.* In INDICON, 2005 Annual IEEE, pages 437 – 441, dec. 2005. (Cited on page 67.)

[Raghavan 1994] S. Raghavan and J. K. Hedrick. *Observer design for a class of nonlinear systems.* INT. J. Control, vol. 59, no. 2, pages 515–528, 1994. (Cited on page 11.)

[Rajamani 1995a] R. Rajamani and Y. Cho. *Observer design for nonlinear systems: stability and convergence.* In Decision and Control, 1995., Proceedings of the 34th IEEE Conference on, volume 1, pages 93 –94 vol.1, dec 1995. (Cited on pages 11 and 67.)

[Rajamani 1995b] R. Rajamani and Y. Cho. *Observer design for nonlinear systems: stability and convergence.* In Decision and Control, 1995., Proceedings of the 34th IEEE Conference on, volume 1, pages 93 –94 vol.1, dec 1995. (Cited on page 66.)

[Rajamani 1998] R. Rajamani. *Observers for Lipschitz nonlinear systems.* INT. J. Control, vol. 43, no. 3, pages 397–401, 1998. (Cited on page 11.)

[Rakotondrabe 2009] M. Rakotondrabe, Y. Haddab and P. Lutz. *Development, Modeling, and Control of a Micro-/Nanopositioning 2-DOF Stick x2013;Slip Device.* Mechatronics, IEEE/ASME Transactions on, vol. 14, no. 6, pages 733 –745, dec. 2009. (Cited on page 12.)

[Rundell 1996] A.E. Rundell, S.V. Drakunov and R.A. DeCarlo. *A sliding mode observer and controller for stabilization of rotational motion of a vertical shaft magnetic bearing.* Control Systems Technology, IEEE Transactions on, vol. 4, no. 5, pages 598 –608, sep 1996. (Cited on page 10.)

[Savia 2009] M. Savia and H.N. Koivo. *Contact Micromanipulation x2014;Survey of Strategies.* Mechatronics, IEEE/ASME Transactions on, vol. 14, no. 4, pages 504 –514, aug. 2009. (Cited on pages 12 and 81.)

[Stein 1988] J. L. Stein and Y. Park. *Measurement signal selection and simultaneous state and input observer.* ASME J. Dyn. Syst., Meas. Control, vol. 110, no. 2, pages 151–159, 1988. (Cited on page 11.)

[Stramigioli 2000] S. Stramigioli, A. van der Schaft, B. Maschke, S. Andreotti and C. Melchiorri. *Geometric scattering in tele-manipulation of port controlled Hamiltonian systems.* In Decision and Control, 2000. Proceedings of the 39th IEEE Conference on, volume 5, pages 5108 –5113 vol.5, 2000. (Cited on page 14.)

[Sussmann 1997] H.J. Sussmann and J.C. Willems. *300 years of optimal control: from the brachystochrone to the maximum principle.* Control Systems, IEEE, vol. 17, no. 3, pages 32 –44, jun 1997. (Cited on page 89.)

[Talole 2010] S.E. Talole, J.P. Kolhe and S.B. Phadke. *Extended-State-Observer-Based Control of Flexible-Joint System With Experimental Validation.* Industrial Electronics, IEEE Transactions on, vol. 57, no. 4, pages 1411 –1419, april 2010. (Cited on page 10.)

[Thau 1973] F. E. Thau. *Observing the state of nonlinear dynamical systems.* INT. J. Control, vol. 17, no. 3, pages 471–479, 1973. (Cited on page 10.)

[Tu 1998] F. J. Tu and J. L. Stein. *Modeling error compensation for observer design.* INT. J. Control, vol. 69, no. 2, pages 329–345, 1998. (Cited on page 11.)

[Umeno 1991] T. Umeno and Y. Hori. *Robust speed control of DC servomotors using modern two degrees-of-freedom controller design.* Industrial Electronics, IEEE Transactions on, vol. 38, no. 5, pages 363 –368, oct 1991. (Cited on page 11.)

[Utkin 1992] V. I. Utkin. Sliding-modes in control optimization. Springer-Verlag, Newyork, 1992. (Cited on page 10.)

[Utkin 1999] V. I. Utkin, J. Guldner and J. Shi. Sliding mode control in electromechanical systems. Taylor-Francis, Philadelphia, 1999. (Cited on page 72.)

[van der Shaft 2002] A. J. van der Shaft and B. Maschke. *Hamiltonian formulation of distributed parameter systems with boundary energy flow.* Journal of Geometry and Physics, vol. 42, pages 1–2, 2002. (Cited on pages 14 and 20.)

[Xiao 1989] X. H. Xiao and W. Gao. *Nonlinear observer design by observer error linearization.* SIAM J. Control Optim, vol. 27, no. 1, pages 199–216, 1989. (Cited on page 10.)

[Yao 1997] Bin Yao, M. Al-Majed and M. Tomizuka. *High-performance robust motion control of machine tools: an adaptive robust control approach and comparative experiments.* Mechatronics, IEEE/ASME Transactions on, vol. 2, no. 2, pages 63 –76, june 1997. (Cited on page 11.)

[Yi 1999] Li Yi and M. Tomizuka. *Two-degree-of-freedom control with robust feedback control for hard disk servo systems.* Mechatronics, IEEE/ASME Transactions on, vol. 4, no. 1, pages 17 –24, mar 1999. (Cited on page 11.)

[Zak 1990] S.H. Zak. *On the stabilization and observation of nonlinear/uncertain dynamic systems.* Automatic Control, IEEE Transactions on, vol. 35, no. 5, pages 604 –607, may 1990. (Cited on page 11.)

[Zhang 1990] S.-Y. Zhang. *Generalized functional observer.* Automatic Control, IEEE Transactions on, vol. 35, no. 6, pages 733 –737, jun 1990. (Cited on page 10.)

[Zhou 1993] Kemin Zhou. *Weighted optimal Hankel norm model reduction.* In Decision and Control, 1993., Proceedings of the 32nd IEEE Conference on, pages 3353 –3354 vol.4, dec 1993. (Cited on page 113.)

[Zhu 2002] Fanglai Zhu and Zhengzhi Han. *A note on observers for Lipschitz nonlinear systems.* Automatic Control, IEEE Transactions on, vol. 47, no. 10, pages 1751 – 1754, oct 2002. (Cited on page 71.)

An Energy Based Formalism for State Estimation and Motion Control

Abstract: This work presents an *energy* based state estimation formalism for a class of dynamical systems with inaccessible/unknown outputs and systems at which sensor utilization is costly, impractical or measurements can not be taken. The physical interactions among most of the dynamical subsystems represented mathematically in terms of Dirac structures allow power exchange through the power ports of these subsystems. Power exchange is conceptually considered as information exchange among the dynamical subsystems and further utilized to develop a natural feedback-like information from a class of dynamical systems with inaccessible/unknown outputs. The feedback-like information is utilized in realizing state observers for this class of dynamical systems. Necessary and sufficient conditions for observability are studied. In addition, estimation error asymptotic convergence stability of the proposed *energy* based state variable observer is proved for systems with linear and nonlinear dynamics. Robustness of the asymptotic convergence stability is analyzed over a range of parameter deviations, model uncertainties and unknown initial conditions. The proposed *energy* based state estimation formalism allows realization of the motion and force control from measurements taken from a single subsystem within the entire dynamical system. This in turn allows measurements to be taken from this single subsystem, whereas the rest of the dynamical system is kept free from measurements. Experiments are conducted on dynamical systems with single input and multiple inaccessible outputs in order to verify the validity of the proposed *energy* based state estimation and control formalism.

Keywords: Energy based formalism, *effort*-based state observer, systems with inaccessible state variables, motion control